Investigating the mechanisms underlying Mesenchymal-to-Epithelial Transitions in the *Drosophila melanogaster* embryonic midgut

Eddie Shohei Kan

University of Sheffield, School of Biosciences

Submitted for the degree of Doctor of Philosophy

September 2023

Summary

The terms epithelial-to-mesenchymal transition (EMT) and mesenchymal-to-epithelial transition (MET) describe reversible changes in cell phenotype and behaviour between mesenchymal and epithelial states. EMT/MET is required during development and gives rise to cells with intermediate phenotypes that show functionally important behaviours such as collective migration. This plasticity between epithelial and mesenchymal cell states is also implicated in pathological processes such as cancer metastasis. Thus, investigating the mechanisms underlying EMT/MET may help lead to therapeutics for cancer or in regenerative medicine.

Studies examining MET are far fewer than those examining EMT. This is particularly true in the context of *in vivo* cancer models, where it remains difficult to observe cells undergoing MET. Thus, I have leveraged the *Drosophila* embryonic midgut as a model system to study MET.

Previous studies examining embryonic midgut MET showed that the underlying visceral muscle provides an external cue required for MET. The role of external cues during MET has also been noted in the contexts of development and cancer. Understanding how these external cues regulate MET may provide insight into common principles underlying MET, an area that is still poorly understood.

In this project, I aimed to 1) characterise midgut MET at the cellular and molecular level, 2) use single cell RNA sequencing (scRNAseq) to identify potential genes contributing to midgut MET and 3) explore the mechanisms by which the visceral muscle provides an external cue. I have shown that the contact with the visceral muscle is specifically required for midgut MET. The absence of the visceral muscle leads to a failure of MET, disrupting the reestablishment of apicobasal polarity, tubulin remodelling and the cell shape changes required to form a columnar epithelium. I identified Sema1a and Otk as a potential receptor-ligand pair that mediates interactions between the midgut and the visceral muscle that drives midgut MET.

Table of Contents

Key Abbreviations

AMG	-	Anterior midgut
aPKC	-	Atypical Protein Kinase C
ATAC	-	Assay for Transposase-Accessible Chromatin
Baz	-	Bazooka
Crb	-	Crumbs
Ecad	-	E-cadherein
ECM	-	Extracellular Matrix
EMP	-	Epithelial-Mesenchymal Plasticity
EMT	-	Epithelial-to-Mesenchymal Transition
EMT-TF	-	EMT Transcription Factor
FasIII	-	Fasciclin III
Fra	-	Frazzled
ICP	-	Interstitial cell Precursors
Lgl	-	Lethal Giant larvae
Mad	-	Mothers against decapentaplegic
MET	-	Mesenchymal-to-Epithelial Transition
Net	-	Netrin
Otk	-	Off track
PlexA	-	PlexinA
PMEC	-	Primary Midgut Epithelial Cells
PMG	-	Posterior midgut
pSJ	-	pleated septate junctions
scRNAseq	-	Single cell RNA sequencing
Sema1a	-	Semaphorin 1a
Sna	-	Snail
Srp	-	Serpent
sSJ	-	Smooth Septate Junctions
Tin	-	Tinman
Tor	-	Torso
Twi	-	Twist
Ush	-	U-shaped
Wb	-	Wingblister (laminin chain $\alpha_{1,2}$)

Chapter 1. Introduction

1.0 Introduction to EMT and MET

Epithelial-mesenchymal plasticity describes the capacity for cells to change from a stationary epithelial phenotype to a migratory mesenchymal phenotype, or vice versa. This process of shifting phenotypes is called Epithelial-mesenchymal transition (EMT) and mesenchymal-epithelial transition (MET) (Kalluri and Weinberg, 2009; Nieto et al., 2016; Yang et al., 2020). Both EMTs and METs are crucial in development, underlying the migration and organization of cells during embryogenesis (Pei et al., 2019; Plygawko et al., 2020; Thiery et al., 2009). Similar processes underlie tissue repair in adults (Nieto et al., 2016; Shaw and Martin, 2016). However, both EMT and MET are also implicated in pathogenic processes, including organ fibrosis, cancer progression and metastatic dissemination of tumour cells (Derynck and Weinberg, 2019; Dongre and Weinberg, 2019). Thus, investigating the mechanisms underlying this plasticity between epithelial and mesenchymal cell states, referred to as epithelial-mesenchymal plasticity (EMP), may reveal new targets to prevent or treat cancer, or for regenerative medicine.

When first described (Greenburg and Hay, 1982), EMT and MET was considered to be a binary decision, mediating the transformation between the two distinct states (Hay and Zuk, 1995). It is now widely accepted that EMTs and METs more often gives rise to a variety of intermediate phenotypes, via a process known as partial-EMT/METs (Yang et al., 2020). Partial-EMTs/METs gives rise to mesenchymal-like cells that retain some epithelial features such as cell-cell adhesion (Figure 1). These cells with intermediate phenotypes can demonstrate interesting and functionally important behaviours such as collective migration. Collective migration is central in many developmental processes (Scarpa and Mayor, 2016) such as in neural crest cell migration (Theveneau and Mayor, 2012) and angiogenesis (Costa et al., 2016) but has also been observed in cancer metastasis.
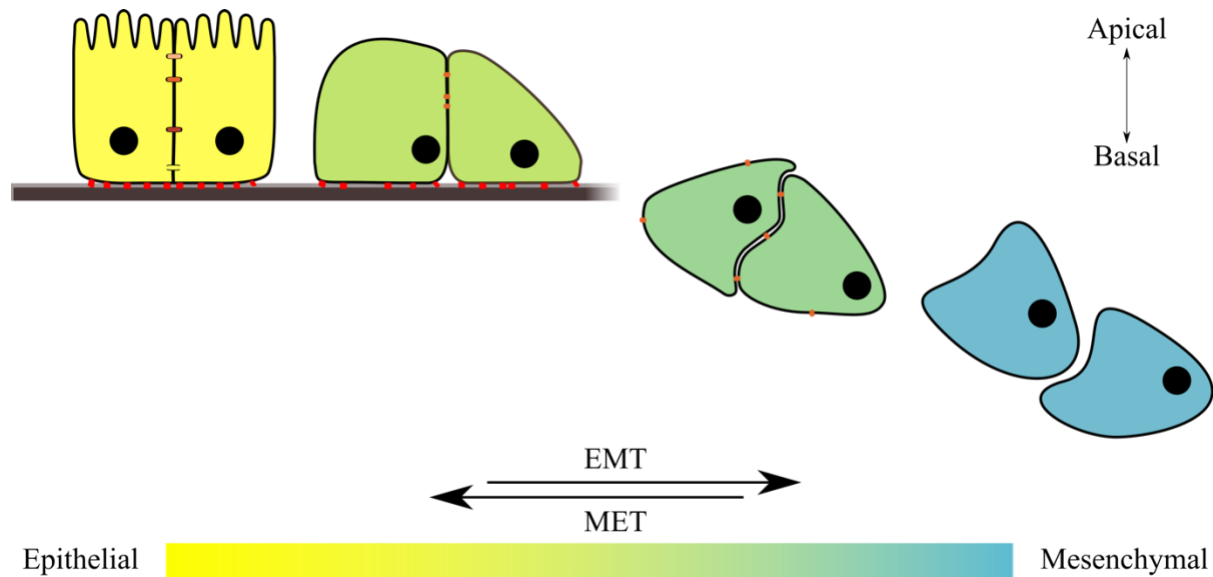
Figure 1. EMT and MET gives rise to cells with intermediate phenotypes. Epithelial cells demonstrate apical-basal polarity and form a monolayer of columnar cells. These cells adhere to neighbouring cells via junctions and the underlying basement membrane. Mesenchymal cells demonstrate front-rear polarity, migrate individually. Cells with intermediate phenotypes can manifest in several different ways such as giving rise to a multi-layered epithelium or undergoing collective migration.
Figure from Plygawko, Kan, and Campbell 2020.

1.1 Characteristics of Epithelial cells

Epithelial cells demonstrate apical basal polarity, cell-cell adhesions, and cell-matrix adhesions. Polarity complexes, lateral adhesions and basal adhesions are regulated in a synchronous manner to establish and maintain these epithelial traits. During EMT, these key aspects are disrupted to promote a shift to mesenchymal phenotype. Here, I will introduce the current understanding of the mechanisms underlying the establishment and maintenance of epithelial organisation. Understanding the architecture of epithelial cells and the mechanisms underlying its formation and maintenance are critical to understanding how EMT is induced.

1.1.1 Apicobasal polarity

Apicobasal polarity is required for the establishment and maintenance of epithelial organisation. Polarity is essential to define the apical, lateral and basal domains, which subsequently define the position of the junctions that form between neighbouring epithelial cells and the underlying ECM (Buckley and St Johnston 2022). These junctions are vital to the

5

integrity and organisation of the epithelia, as well as its biological function. For example, occluding junctions, namely the tight junctions in vertebrates and septate junctions in invertebrates, maintain the barrier function of the epithelia, preventing diffusion across the epithelia (Garcia et al., 2018). Adherens junction play a major role in initiating and stabilising cell adhesion between neighbouring cells (Harris and Peifer, 2004). Dysregulation of apicobasal polarity can disrupt the positioning and formation of these junctions, which leads to the collapse of epithelial organisation (Harris and Peifer, 2004; McGill et al., 2009).

Classic polarity factors can be divided into 2 main groups: complexes that define the apical domains or the basolateral domains (Chen and St Johnston, 2022). Key apical polarity factors include members of the Crumbs (Crb) and Par complex. Key basolateral polarity factors consist of members of the Scribble complex (Table 1). These polarity factors demonstrate antagonistic interactions, excluding one another from co-localising. For example, Atypical protein kinase C (aPKC) antagonises the Scribble complex member Lethal giant larvae (Lgl) (Bailey and Prehoda, 2015) and Par-3/Bazooka (Baz) (Morais-de-Sá et al., 2010) via phosphorylation to define the lateral and sub-apical domains respectively (Hong, 2018). These types of antagonistic interactions help position the complexes required to form junctions that establish epithelial organisation.

Complex	Human/Drosophila Names	Localisation
Crumbs	Crumbs (Crb)	Apical
	Protein associated with LIN7 1 (Pals1)/Stardust (Std)	
	Patj	
Par	Par3/Bazooka (Baz)	Apical
	Par6	
	atypical Protein Kinase (aPKC)	
Scribble	Scribble (Scrib)	Basolateral
	Discs Large (Dlg)	
	Lethal Giant Larvae (Lgl)	

Table 1. Classic Polarity factors. Polarity proteins have largely been discovered in *C. elegans* or *Drosophila*. As such some of the names reflect this. For example, Par proteins were found in a screen for *C. elegans* embryos with a partitioning defect (Nance and Zallen, 2011). Similarly, mutations in Dlg causes an overgrowth phenotype in *Drosophila* imaginal discs (Hough et al., 1997).

It should be noted that the mechanisms underlying apicobasal polarity do vary between different contexts. For example, regulatory mechanisms underlying polarity in vertebrates are typically more complex and may be redundant; loss of one polarity factor does not typically result in collapse of polarity (Choi et al., 2019), as seen in more simpler organisms such as *Drosophila* (Bilder and Perrimon, 2000; Tepass and Knust, 1993) or *Caenorhabditis elegans* (Hung and Kemphues, 1999). Furthermore, it appears that distinct mechanisms can govern polarity even within a single species. For example, the *Drosophila* adult midgut epithelium is unique in that it has an apical septate junction, similar to in vertebrate epithelia (Chen et al., 2018). This is in contrast to a typical epithelium in the *Drosophila*, such as the embryonic epidermal layer, in which the adherens junctions are positioned apically to the septate junctions. This difference in the position of the junctions implies that the mechanisms that define polarity between the two tissues are distinct from one another. Despite these differences, the complexes underlying epithelial polarity appear to be largely conserved in invertebrates and vertebrates (Izumi et al., 1998; Lin et al., 2000).

<u>1.1.2 Lateral Junctions</u>

As briefly described earlier, the two main types of lateral junctions include occluding junctions and adherens junctions.

Tight junctions: Tight junctions are the occluding junctions in vertebrates (Furuse and Takai, 2021). They are more apically positioned compared to the adherens junction on the lateral membrane. They are composed of 2 main transmembrane proteins: claudins and occludins (Garcia et al., 2018). Claudins have two main functions; they mediate adhesion between cells and mediates paracellular transport, acting as a selective barrier for ion transport across the epithelia (Angelow et al., 2008). Occludins may play a role in preventing the paracellular transport of large macromolecules (Al-Sadi et al., 2011) but whether it is essential for tight junction function is controversial (Bamforth et al., 1999; Saitou et al., 1998). Claudins and occludins form the tight junction strands, which encircle epithelial cells. The strands from neighbouring cells then bind to one another, closing the paracellular space between the two cells and forming a selective barrier in its place (Piontek et al., 2020).

The formation and function of tight junctions appears to require ZO-1, a member of the membrane-associated guanylate kinase homologs (MAGUK) family. It has been shown that ZO-1 is essential for tight junction formation (Rodgers et al., 2013), mediating links to the cortical actin cytoskeleton (Fanning et al., 1998). ZO-1 appears to orchestrate this through phase separation (Beutel et al., 2019); ZO-1 drives the localisation of key tight junction-related proteins, such as claudins and actin, to the site of tight junction formation. It has been proposed that phase separation then allows claudins to be concentrated in high enough concentration to drive its polymerisation, a process required for tight junction strand formation. This phase separation appears to facilitate the recruitment of other key adaptor proteins and transcription factors , such as cingulin (Beutel et al., 2019), an adaptor protein responsible for linking tight junctions to actin and microtubules (Yano et al., 2018). Transcription factors ZONAB and YAP were also found to be concentrated by phase separation of ZO-1 (Beutel et al., 2019), linking tight junction formation to cell proliferation and cell size.

Septate Junctions: Septate junctions are the invertebrate equivalent of vertebrate tight junctions. Their formation and composition has been studied extensively in *Drosophila* (Furuse and Izumi, 2017). There are two types of septate junctions in *Drosophila*: Pleated and Smooth. These junctions are named after their appearance when cross-sections of the junctions are examined via electron microscopy. When cross-sections of cells are examined, both septate junctions form ladder-like structures that span across the membrane of neighbouring cells. The difference in appearance is likely a result of differences in protein composition of the junctions. The two types of septate junctions are found in distinct tissue types. Pleated septate junctions (pSJ) are found in ectoderm-derived tissues such as the epidermis, while smooth septate junction (sSJ) mostly form in endoderm-derived tissue such as the midgut and Malpighian tubules (Tepass and Hartenstein, 1994a). Functional differences between the two types of junctions have not been identified (Furuse and Izumi, 2017).

The composition of the pleated septate junction has been extensively characterised and are reviewed in (Jonusaite et al., 2016). These include 15 transmembrane proteins specific to the pSJ complex. These include members of the claudin family, various cell adhesion molecules such as Neurexin IV and subunits of the Na+,K+-ATPase. In contrast, far fewer members of sSJ proteins have been characterised. The four key sSJ proteins have been identified so far include Snakeskin (Yanagihashi et al., 2012), Mesh (Izumi et al., 2012), Tsp2a (Izumi et al., 2016) and Hoka (Izumi et al., 2021). All are required for barrier function and smooth septate junction formation. The correct localisations of Snakeskin, Mesh and Tsp2a are co-dependent on each other. This suggests that they form a complex together and likely form the core complex of smooth septate junction proteins. Hoka also forms complexes with the three other proteins but likely plays a role in the initial assembly and apical localisation of smooth septate junction proteins in stage 15-16 embryos (Izumi et al., 2021). Studies in the Malpighian tubules (Beyenbach et al., 2020; Jonusaite et al., 2020) suggest that smooth septate junction formation play a role in epithelial integrity. Additionally, smooth septate junctions were shown to have a critical role in controlling paracellular transport of ion and macromolecules; loss of smooth septate junctions led to renal failure (Jonusaite et al., 2020).

Mechanisms underlying pSJ formation show some similarities to the mechanism underlying sSJ formation. Studies using the lateral epidermis showed that pSJ junction proteins formed a core complex, not unlike the core complex seen in sSJs. Formation of the core complex was also shown to be co-dependent, such that loss of one member appeared to affect the stability of the complex. This core pSJ complex included Coracle (cora), a key FERM domain protein, and Neurexin IV. Loss of Dlg affected localisation of the pSJ core complex, but not its assembly, suggesting that Dlg plays a role in the localisation of the pSJ. Intriguingly, both Cora and Dlg are found in both sSJs and pSJs. It was previously shown that mutants for *dlg* causes extension of the sSJ towards the lateral membrane (Izumi et al., 2012), perhaps indicative that Dlg also plays a conserved role to localise both types of septate junctions. In contrast, Coracle (Cora), together with Neurexin IV, Na+,K+-ATPase and Yurt, has been shown to play a role in the maintenance of polarity (Laprise et al., 2009), rather that its establishment. Given that Neurexin IV and Na+,K+-ATPase are pSJ-specific proteins (Jonusaite et al., 2016), this may suggest that the function of Cora to maintain polarity is specific to pSJs.

sSJ are critical for barrier function but may also act as part of an important mechanism underlying tissue homeostasis. Disrupting septate junction formation in the adult *Drosophila* midgut by knocking down Ssk and Mesh increased proliferation in enterocytes and enteroblasts. It was found that membrane-bound septate junction proteins repressed Yorkie, regulating proliferation. Increased proliferation was also observed in neighbouring interstitial stem cell population, which normally do not have septate junctions (Chen et al., 2020; Izumi et al., 2021). These observations suggested that an external signal was driving interstitial stem cell proliferation. This was indeed the case; the growth factor Upd3, found downstream of Yorkie signalling, could be expressed by the enterocytes and enteroblasts to drive proliferation of the interstitial stem cells. As membrane-bound septate junction proteins in enteroblasts and enterocytes repressed Yorkie, disrupting smooth septate junction formation activated Yorkie, induced expression of Upd3 and induced proliferation of the neighbouring interstitial stem cell population. Thus, maintenance of smooth septate junctions were implicated with regulation of stem cell-mediated midgut homeostasis (Chen et al., 2020). It is likely that this link between septate junction integrity and proliferation mediates a functional mechanism that drives proliferation upon injury or tissue damage (Chen et al., 2020).

Adherens Junctions: Adherens junctions exist in all epithelial cells, although where it is positioned along the lateral membrane can vary (Buckley and St Johnston, 2022). Adherens junctions are primarily composed of cadherins and nectins (Meng and Takeichi, 2009). Both cadherins and nectins function to maintain cell-cell adhesion and recruit adaptor proteins that mediate several different functions, including actin cytoskeleton remodelling and intracellular signalling (Meng and Takeichi, 2009).

Members of the cadherin family are defined by cadherin repeats, a conserved extracellular subdomain. This domain is responsible mediating homophilic interactions with a neighbouring cell in a calcium sensitive manner (Perez and Nelson, 2004). The link between cadherins and the actin cytoskeleton is mediated by catenins, a family of adaptor proteins. E-cadherin (Ecad)/β-catenin (armadillo) is one such pair that is important for maintaining cell-cell adhesions. Ecad/β-catenin recruits and interacts with α-catenin, although the precise mechanisms for this interaction appears to be controversial (Desai et al., 2013; Drees et al., 2005; Yamada et al., 2005). α-catenin binds to various actin-binding proteins such as formin (Kobielak et al., 2004) and EPLIN (Abe and Takeichi, 2008). Formin and EPLIN appear to be necessary for the initial polymerisation and maintenance of actin filaments respectively and are required for cadherins to mediate adhesion (Abe and Takeichi, 2008; Kobielak et al., 2004). Actin remodelling is required at sites of cadherin-mediated adhesion to drive cell adhesion and the sealing of membranes between two neighbouring cells (Vasioukhin et al., 2000).

Interactions between cadherins and polarity proteins appear to be critical for adherens junction formation. For example, Scribble has been shown to stabilise Ecad/p120 catenin interactions and play a role in regulating Ecad trafficking (Lohia et al., 2012). Furthermore, *Drosophila* Par3 homolog Baz was shown to be required for the formation and maintenance of adherens junctions in the *Drosophila* embryo. While adhesion between cells via apical cadherin-catenin clusters was shown to form independently of Baz, Baz appears to be required to reposition cadherin-catenin clusters to form mature adherens junctions required to maintain epithelial integrity (McGill et al., 2009). Conversely, cadherins may play a role to reinforce polarity through interactions with polarity complexes. For example, Ecad has been shown to maintain the alignment of cell division that occurs in prostate luminal cells, by

anchoring Scribble to the lateral membrane (Wang et al., 2018). Together, these studies provide evidence of a cooperative relationship between cadherins and polarity protein complexes to reinforce polarity.

Members of the nectin family are defined by their immunoglobulin-like domain. Unlike cadherins, nectins can form both homo- and heterophilic interactions (Meng and Takeichi, 2009). Nectins plays several roles in promoting epithelial phenotypes, many of which is mediated by the key adaptor protein Afadin.

With regards to adherens junction formation, Nectin signalling alone can drive the accumulation of weaker non-*trans*-interacting form of Ecad and the recruitment of catenins to the site of cell-cell contact. Upon recruitment of Afadin, Nectin drives the conversion towards the stronger *trans*-interacting form of Ecad, enhancing cell-cell adhesion (Honda et al., 2003; Sato et al., 2006). These two processes occur simultaneously, forming microclusters of Nectin and cadherin adhesion that fuse to form mature adherens junctions. LMO7 (Ooshio et al., 2004) and ADIP (Asada et al., 2003) have been shown to bind to both Afadin and α-catenin, perhaps indicative of a close interaction between Nectins and cadherins.

Nectins also plays a role in positioning tight junctions. Afadin mediates this via recruitment of adaptor protein ZO-1 to Nectin adhesion sites (Yokoyama et al., 2001). Furthermore, Par-3, which determines the position of tight junctions, has been shown to directly bind to Nectins in neuroepithelial cells of the mice embryonic forebrain (Takekuni et al., 2003), suggesting that Nectins may also play a role in positioning tight junctions through direct interactions with polarity complexes.

Interactions with a basal extracellular matrix (ECM) is essential for epithelia formation. Typical epithelial cells have hemidesmosomes on their basal side, which facilitate adhesion to the ECM (Walko et al., 2015). The cell-matrix interactions are mediated by adhesion receptors such as integrins (Walko et al., 2015). These adhesion receptors can recruit accessory proteins with a range of functions that act to induce changes in the cell, such as differentiation (Wang et al., 2015) and cell proliferation (Moreno-Layseca and Streuli, 2014). With respect to epithelial cells, basal adhesion to the ECM play a central role in establishing and maintaining polarity (Lee and Streuli, 2014) and remodelling the cytoskeleton (Delon and Brown, 2007). Thus, these adhesion receptors and associated accessory proteins play important roles in mediating the cells response to the external environment and establishing an epithelial phenotype.

Integrins are a key family of adhesion receptors and are a key component of hemidesmosomes. Integrins function as heterodimers of α and β subunits to bind to various ECM proteins such as collagen, fibronectin or laminins (Kechagia et al., 2019). The different combinations of heterodimers can determine its affinity for specific ECM proteins (Campbell and Humphries, 2011). Additionally, it appears that different heterodimers can induce different signalling pathways; c-Src has been found to be a $\alpha_v\beta3$ heterodimer-specific accessory protein despite the fact that both $\alpha_5\beta_1$ and $\alpha_v\beta_3$ heterodimers can bind to fibronectin, demonstrating that different heterodimers associated with the same ECM molecule can recruit different accessory proteins, which consequently can lead to differences in downstream signalling (Huveneers et al., 2007; Morgan et al., 2009). Furthermore, different integrin heterodimers are able to promote differentiation of embryonic stem cells into specific lineages (Wang et al., 2015), demonstrating functional differences between the heterodimers. Thus, it appears that cells can raise different responses based on external cues, determined by the composition of the ECM; and internal cues, determined by the types of integrin heterodimers expressed.

Talin is an essential accessory protein recruited by integrins. Talin acts to promote integrin signalling in a process called "inside-out" activation of integrins. Talin recruited to an ECM-bound integrin changes the conformation of integrin and thus activating it and promoting its

binding affinity to the ECM (Klapholz and Brown, 2017). Talin bound to an ECM-bound integrin can simultaneously recruit adjacent integrins to the adhesion site and promote ligand binding to them. Thus, Talin can both activate and cluster integrins to mediate maturation of cell-matrix adhesions. Upon actin-binding, Talin undergoes a conformational change that allows it to recruit various accessory proteins (Klapholz and Brown, 2017). These accessory proteins mediate the multitude of signalling factors downstream of integrins, such as cytoskeleton remodelling and adhesion (Lu et al., 2022).

Studies have shown that integrins and ECM proteins play important roles both in initiating a basal cue to orient polarity in epithelial cells, and also in remodelling the surrounding ECM to further reinforce basal cues. Studies *in vitro* using Madin–Darby canine kidney (MDCK) epithelial cysts (O'Brien et al., 2001; Yu et al., 2005) revealed an autocrine signalling mechanism involving Rac1 and laminins. Collagen-bound $\beta 1$ integrins were shown to activate Rac1 signalling, which upon activation drove extracellular laminin assembly. Cysts deficient in Rac1 showed mis-assembly of laminin on the cyst surface. These cysts with deficient Rac1 failed to polarise but could be rescued by embedding them in ECMs with exogenous laminin. However, cysts embedded in ECMs rich in collagen IV or fibronectin did not rescue the polarity defect, demonstrating a specificity for the role of laminins in orienting apicobasal polarity. Separate work using MDCK epithelial cysts identified that laminin-binding integrin heterodimer $\alpha_6\beta_4$, together with collagen-binding integrin heterodimer $\alpha_2\beta_1$, played a central role in initiating a basal cue via Rac1 signalling (Myllymäki et al., 2011). Taken together, these studies demonstrate that integrin-ECM interactions not only provide an initial basal cue orientating polarity, but also a mechanism for cells to be able to remodel their environment to reinforce polarity.

1.2 Hallmarks of EMT

As discussed, epithelial cells demonstrate apicobasal polarity, form junctions with neighbouring cells and are adherent to a basal surface, typically to an extracellular matrix (Buckley and St Johnston, 2022; Yang et al., 2020). Establishment and maintenance of apicobasal polarity and cellular junctions is a complex interdependent process and it is these processes that are disrupted during EMT. This transition is driven by transcriptional changes, regulated by a group of transcription factors called EMT-transcription factors (EMT-TFs). The two key hallmarks of EMT are the loss of apicobasal polarity and the disassembly of cellular junctions. Additionally, this shift in phenotype driven by EMT-TFs are typically accompanied by the acquisition of migratory behaviours (Campbell and Casanova, 2015; Shtutman et al., 2006; Thiery et al., 2009). Expression of EMT-TFs are also associated with the acquisition of oncogenic qualities such as proliferation (Qiu et al., 2000; Williams et al., 2017).

Studies in developmental models have identified a number of transcription factors that drive EMT. A list of core EMT-transcription factors (EMT-TFs) include members of the Snail, Zeb and Twist families. They have been found to regulate the changes in gene expression required for cells to undergo EMT (Lim and Thiery, 2012; Yang et al., 2020) and to be responsible for driving EMT in disease settings as well (Antony et al., 2019; Thiery et al., 2009; Yang et al., 2020). It should be noted that EMT-TFs typically have other non-EMT related functions in development. For example, Snail (Sna) drives mesoderm fate in *Drosophila* (Leptin, 1991) and but also functions as an EMT-TF in many developmental (Carver et al., 2001; Dale et al., 2006; Weng and Wieschaus, 2016; Wu and McClay, 2007) and disease settings (Batlle et al., 2000; Campbell et al., 2019; Tran et al., 2014). While the mechanisms by which EMT-TFs drive EMT tend to be highly contextual (Lim and Thiery, 2012; Stemmler et al., 2019), they are widely conserved and are considered a central part of the regulatory mechanisms underlying EMT (Yang et al., 2020).

Transcription Factor	Type	Studies demonstrating transcriptional repression of Ecad	Roles in Development
Snai1 (Snail)	Zinc Finger	(Batlle et al., 2000; Cano et al., 2000)	• Mesenchymal differentiation (Leptin, 1991); • Somitogenesis (Dale et al., 2006); • Bone morphogenesis (Chen and Gridley, 2013)19/12/2023 11:35:00
Snai2 (Slug)	Zinc Finger	(Hajra et al., 2002)	• Bone morphogenesis (Chen and Gridley, 2013)
Zeb1	Zinc Finger	(Aigner et al., 2007)	• Skeletal patterning (Takagi et al., 1998) • Smooth muscle differentiation (Nishimura et al., 2006)
Zeb2 (SIP1)	Zinc Finger	(Comijn et al., 2001)	• Neuroectoderm differentiation
Twist1	bHLH	(Yang et al., 2004)	• Neural tube formation (Chen and Behringer, 1995) • Mesenchymal differentiation (Leptin, 1991)

Table 2. Core EMT-TFs. All of the core EMT-TFs transcriptionally repress of Ecad. They also play important roles in development, some independent of their ability to drive EMT. For example, Twist and Snail both drive expression of mesenchymal genes (Leptin, 1991). It should be noted that the list of core EMT-TFs is not a comprehensive list; other EMT-TFs have been identified. Adapted from Yang et al. 2020; Stemmler et al. 2019.

A key common function of the core EMT transcription factors is to drive the breakdown of intercellular adhesion between epithelial cells, typically via the downregulation of Ecad. All of the core EMT-TFs have been shown to be direct transcriptional repressors of Ecad (Table 2). Thus, expression of these EMT-TFs drives the breakdown of adherens junctions and the subsequent loss of epithelial integrity. In many contexts, expression of EMT-TFs is also associated with cell motility and increased invasive capacity (Yang et al., 2020).

One example of how downregulation of Ecad drives EMT is the breakdown of the membrane bound Ecad/ β-catenin complex. While membrane-bound β-catenin plays a central role in adhesion, β-catenin is also associated with Wnt signalling (Bienz, 2005). Cytoplasmic β-catenin can localise to the nucleus to bind TCF, a transcriptional co-activator of downstream Wnt genes. This switch between membrane-bound β-catenin to cytoplasmic β-catenin has been shown to drive EMT in both disease and developmental contexts (Kim et al., 2019; Li et

al., 2020; Liebner et al., 2004; Mylavarapu et al., 2019; Sanchez et al., 2021), highlighting that adherens junction stability is central to the maintenance of epithelial phenotype. The mechanisms underlying this switch between catenin as an adhesion molecule or as a signalling molecule are complex and are reviewed in (Gammons and Bienz, 2018).

While repressing transcription of Ecad is a common hallmark of EMT, it is important to note that EMT is not simply a consequence of transcriptional repression of Ecad. This is evident in the embryonic *Drosophila* midgut. Serpent (Srp), a GATA-factor, was identified in the *Drosophila* embryo as an EMT-TF that drives the disassembly of adherens junctions through the delocalisation of Ecad protein, without affecting Ecad at the transcriptional level. The key mechanism through which Srp drives EMT, instead appears to be through the inhibition of *crb* transcription; this disturbs apicobasal polarity and results in the loss of Ecad at the junctions (Campbell et al., 2011). Furthermore, this non-junctional Ecad was shown to be play an active role during the subsequent migration of the embryonic *Drosophila* midgut cells, mediating transient adhesion of the non-epithelial cells with the rest of the midgut cells, coordinating their collective migration (Campbell and Casanova, 2015). This demonstrates that Ecad is not simply an epithelial characteristic that is switched off during EMT but can in fact can be dynamically regulated to mediate migratory cell behaviours. Additionally, studies *in vitro* using experimentally- driven EMT in mammary epithelial cells (EpH4) showed that endocytosis and lysosomal degradation of Ecad occurs prior to transcriptional repression, suggesting that EMT can initiate the breakdown of adherens junctions prior to transcriptional repression of Ecad (Janda et al., 2006). This illustrates that transcription repression of Ecad does not necessarily initiate EMT; and that alternative regulatory mechanisms independent of transcriptional repression of Ecad may also act as a driving force. Put together, these studies suggest that transcriptional repression of Ecad does not fully explain the cellular changes that occur during EMT.

In line with this, EMT-TFs can also mediate EMT by interacting with polarity complexes directly. For example, Snail (Sna) and Zeb1 have been shown to disrupt junction formation by repressing transcription of *crb* (Aigner et al., 2007; Whiteman et al., 2008). In contrast, aPKC has also been shown to be able to promote Snai1 degradation by phosphorylating Snai1 (Jung et al., 2019), which may suggest an inverse role in which polarity complexes can regulate EMT-

TF activity. These examples show the antagonistic interactions between polarity proteins and EMT-TFs, illustrating the different mechanisms that controls whether cells maintain an epithelial state or transition to a mesenchymal state.

EMT-TFs are also associated with activation of genes involved in ECM remodelling and migration, such as matrix metalloproteinases (MMPs) (Scott et al., 2019). All classic EMT-TFs have been associated with upregulation of MMP family members; studies in cancer cell lines have shown that repression of these MMPs leads to an attenuated invasion phenotype (Bae et al., 2013; Jordà et al., 2005; Joseph et al., 2009; Khales et al., 2020; Miyoshi et al., 2004; Yalim-Camci et al., 2019). MMPs have a range of functions in both disease and development; MMPs facilitate delamination of epithelial cells through degradation of the cell-matrix or cell-cell junctions. MMPs can also stimulate EMT via the degradation of ECM proteins into fragments with active roles in signalling, the cleavage of cell-surface receptors and the processing of growth factors (Page-McCaw et al., 2007; Radisky and Radisky, 2010). However, it should be noted these pro-EMT activities of MMPs are often context specific (Radisky and Radisky, 2010) and reflect an intersection between the effects of MMP activity and ECM composition on EMP.

In summary, EMT is a multifaceted process involving loss of junctions, loss of apical-basal polarity and increased motility. As such, it is widely agreed upon that EMP should be characterised by changes in gene expression of numerous molecular markers together with descriptions of changes in cellular phenotypes (Yang et al., 2020).

1.3 EMP in Cancers

EMP is considered a critical characteristic of cancer cells that mediates metastasis (Yang et al., 2020). Metastatic cancers are responsible for the majority of cancer deaths (Chaffer and Weinberg, 2011) and thus represents an area of critical research. EMT is associated with the early stages of cancer progression, facilitating escape from the primary tumour and intravasation. Expression of EMT-TFs is also associated with the acquisition of stemness, the ability to seed tumours (Dongre and Weinberg, 2019). Intermediate cell states that manifest in collective migration appear to facilitate survival during circulation (Saxena et al., 2020). Finally, colonisation at a secondary site appears to be enabled by MET. Understanding how EMP contributes to cancer progression may help identify drug targets to develop therapeutics that prevent cancer metastasis (Yang et al., 2019).

There is extensive literature examining the role of EMT in cancers. The increase in motility and the ability to degrade the extracellular matrix acquired during EMT promote cell dissemination from primary tumours (Derynck and Weinberg, 2019). Consistent with this, experimental models show that expression of EMT-TFs, such as Sna and Twi, can drive metastasis (Tran et al., 2014; Tsai et al., 2012). Furthermore, metastatic primary tumour cells undergoing EMT in a physiological disease state have been described (Beerling et al., 2016), providing evidence of EMT during metastasis *in vivo*.

Cancer cell EMT is also often associated with the gain of stemness. These cancer cells display stem-cell like properties, such increased proliferation, and acquire the ability to seed tumours; these are dubbed cancer stem cells (CSC). It is possible that EMT is accompanied by stem-cell like behaviours which promote self-renewal and therefore, the progression of tumour formation (Martin-Belmonte and Perez-Moreno, 2012; Shibue and Weinberg, 2017). This stemness may facilitate survival and underlie the capacity for the cells to adapt to secondary sites.

While the role for EMT during the initiation of metastasis has been made clear, the role of MET during the subsequent stage of metastasis is not fully clarified. Several lines of evidence demonstrate that MET is required to mediate subsequent metastatic colonisation (Williams

et al., 2019). In contrast to mesenchymal disseminated tumour cells (Beerling et al., 2016), distant secondary tumours are often epithelial, suggesting that these cells undergo MET (Beerling et al., 2016; Williams et al., 2019). Additionally, multiple models have shown that there is a requirement for MET during secondary tumour formation and proliferation. Crucially, decreased tumour formation is observed in experimental models in which cells are prevented from undergoing MET (Ocaña et al., 2012; Tsai et al., 2012). Thus, EMP and the plasticity to go between epithelial and mesenchymal states appears to be a critical aspect of metastatic potential.

How this cancer cell MET is regulated is still an active field of research (Shibue and Weinberg, 2017). Unlike EMT, there does not appear to be any conserved transcription factor that drives the process. Rather, MET occurs when EMT-TFs are downregulated. Some evidence suggests that specific environmental cues promote cancer MET.

In mice models with breast tumours that form metastases in the lung, the secretion of Versican, an ECM chondroitin sulfate proteoglycan, by a subpopulation of myeloid cells from the bone marrow, was shown to promote tumour formation and MET (Gao et al., 2012). These myeloid cells were found to specifically migrate to the lungs prior to metastasis; myeloid cells did not appear to migrate to primary tumours in the breast. Knockdown of Versican in these myeloid cells attenuated tumour growth. The tumours that did form in the absence of Versican expressed high levels of vimentin and low levels of Ecad, indicative of failure to undergo MET. Furthermore, human breast cancer cell lines grown in media conditioned by Versican-secreting myeloid cells isolated from the mice showed increased proliferation and acquired epithelial phenotypes, demonstrating that Versican can MET via paracrine signalling. Versican appeared to drive MET by disrupting the TGFβ/Smad2 pathway and Sna expression, both of which contribute to EMT. Intriguingly, expression of Versican does not appear to be a cue mediating migration of the tumour cells to the lungs. Upon injection of breast cancer cells in the tail vein of severe combined immunodeficiency (SCID) mice without tumours, breast cancer cells engineered to express Versican showed greater load of metastases compared to control. Importantly, these metastases still formed in the lungs, suggesting that increased Versican expression in the pre-metastatic lungs is not a

prerequisite for preferential lung metastasis. This demonstrates Versican does not determine the site of metastasis but rather the potential for metastatic progression (Gao et al., 2012).

A similar example demonstrating the role of the environmental cues was observed in mice studies of bone metastasis (Esposito et al., 2019). Cancer cell MET during the formation of bone metastases was shown to be mediated by the receptor E-selectin, which is expressed in the bone vascular niche. In the context of the bone metastasis model, E-selectin was shown to bind to Glg1 with a terminal sialyl Lewis X or A (sLeX/A) tetrasaccharides, with formation of sLeX/A requiring α1-3 fucosyltransferases (Fut) 3 and 6. Although E-selectin was not essential for metastasis formation, it appeared to promote bone metastasis growth by inducing an MET. Upon injection of bone-tropic breast cancer cell lines SUM159-M1a or the BM2 subline of MDA-MB-231 into WT or E-selectin knockout non-obese diabetic (NOD)/SCID background mice, the absence of E-selectin attenuated bone metastasis growth, but not primary tumour growth. Additionally, injecting SUM159-M1a engineered to express Fut3 and Fut6 respectively into the mammary fat pad of NOD/SCID mice showed that Fut3 and Fut6 expression promoted bone metastasis, but not primary tumour growth, further demonstrating that E-selectin binding plays a role specifically during metastasis. In-vitro experiments with both BM2 and M1a lines demonstrated that E-selectin coated plates were sufficient to induce a shift toward epithelial phenotypes and significant changes in gene expression, indicative of a MET (Esposito et al., 2019).

These studies suggest that environmental cues drive MET. However, it should be noted that in both of these examples, the key experiments demonstrating that these cues actually drive MET, rather than just contribute to it, were conducted *in vitro*. Thus, how these external cues influence cancer cell MET *in vivo* is still not well understood. Studying cells undergoing MET appears to be a major challenge, due to challenges of detecting these cells. Cells that undergo EMT and MET make up a small subset of cells (Beerling et al., 2016). Furthermore, studying the actual process of MET during tumour formation is made difficult due to the challenges of predicting sites of colonisation and the subsequent imaging of these processes.

1.4 Understanding of MET from development.

As described above, two common traits observed in cancer MET appears to be that it requires downregulation of EMT-TFs and the presence of external cues from its environment. Evidence from developmental models appears to suggest that MET does not lead to a reversal of phenotypes to the initial epithelial state (reviewed in Plygawko et al, 2020). Instead, MET appears to drive cells towards an epithelial state distinct from the initial state. It is therefore possible that it is the combination of internal signals mediating MET and external signals from a neighbouring tissue that permits the acquisition of a distinct epithelial phenotype (Plygawko et al., 2020). However, despite the fact that MET occurs in a range of developmental processes, studies examining the molecular mechanisms underlying MET are somewhat limited (Plygawko et al., 2020). Here, I describe two developmental processes in which MET plays a central role: nephrogenesis and somitogenesis. In both example, cells undergo EMT, collective migration and MET in sequence. Considering the different contexts in which MET occurs, may help identify general conserved mechanisms governing MET.

Nephrogenesis

MET is central to the formation of nephrons, which is triggered by interactions between the nephron progenitor cells, derived from the metanephric mesenchyme, and the ureteric bud, an epithelial structure that starts to branch off the Wolffian duct. Signalling from the ureteric bud recruits a mass of cells from the metanephric mesenchyme, forming a structure called the cap mesenchyme around the ureteric bud. The cap mesenchyme has a sub-population of mesenchymal progenitor stem cells that proliferate, which gives rise to a transient population of cells called the nephron progenitor cells. These nephron progenitor cells condense at the base of the ureteric bud to form a pretubular aggregate (Yang et al., 2013), which undergoes MET to form the renal vesicle, comma shaped body and S-shaped body in sequence, eventually forming a continuous lumen. This forms the collecting duct of the kidney. Nephrogenesis is followed by glomerulogenesis, which leads to the formation of a functional kidney (Chambers and Wingert, 2020; Kuure et al., 2000).

External signals from the ureteric bud mediated by Wnt9b permits the nephron progenitor cells to undergo MET. Loss of Wnt9b does not disrupt early ureteric bud formation or the

metanephric mesenchyme, it does disrupt branching growth of the nephron, indicative of a specific failure to induce the epithelisation required for renal vesicle formation. Wnt9b appears to mediate MET by inducing the metanephric mesenchyme to express Wnt4 (Carroll et al., 2005), an autoinducer of MET (Stark et al., 1994). Experimentally induced Wnt4 was sufficient to drive MET in the absence of Wnt9b, positioning Wnt4 as a downstream effector of Wnt9b signalling. Additionally, it suggests that Wnt4 expression in the metanephric mesenchyme initiates signalling cascades required for the formation of the renal vesicle (Carroll et al., 2005).

Six2, a homeodomain transcription factor involved downstream of Wnt9b signalling (Kobayashi et al., 2008), shows some similarities with the core EMT-TFs and plays a central role in regulating nephron formation. During normal development, Six2 is expressed in the metanephric mesenchyme and is lost during epithelialisation. Six2-null mice showed ectopic and premature formation of renal vesicles, as well as an expansion in the region of Wnt4 expression (Self et al., 2006). This suggests that Six2 functions to maintains mesenchymal phenotypes via the repression of Wn4. Six2 also appears to functions to promote stemness; Six2-positive cells in the cap mesenchyme can differentiate into all cell types present of the nephron (Kobayashi et al., 2008). Further evidence of this link between Six2 and stemness can be observed in mice models of breast cancer (Wang et al., 2014); Six2 was shown to drive repression of Ecad via methylation of the Ecad promoter site and upregulation of Zeb2. Together, this shows that Six2 is required to maintain a mesenchymal phenotype and to maintain stemness, both of which are common features of EMT-TFs.

The core EMT-TF Sna is also downregulated during kidney formation. The mesoderm expresses Sna early during development and this is maintained in the metanephric mesenchyme. However, during epithelialisation of the metanephric mesenchyme, Sna is downregulated. This downregulation is accompanied by the upregulation of cadherin-16, a kidney specific cadherin, and is likely to play a role in promoting lateral cell adhesion during epithelialisation. Additionally, activation of Sna in adult transgenic mice kidneys was shown to repress cadherin-16 and drive EMT, suggesting a role for Sna in EMP throughout kidney development and disease (Boutet et al., 2006).

Following the downregulation of Six2 and Sna, the mesenchymal nephron progenitor cells undergo MET to form the renal vesicles. Formation of the renal vesicle from the pretubular aggregate requires *de novo* lumen formation; the apical domains have to be defined within the mesenchymal mass prior to epithelialisation. This process appears to involve the Par complexes; Par3 enriched membrane domains were found in precursors of the renal vesicle and were localised apically in mature renal vesicles (Yang et al., 2013). The regulation of Par complex formation required afadin, which was shown to also play a role in recruit R-cadherin and actin at the apical junction (Yang et al., 2013). Together, this demonstrates the role for afadin to define and establish the apical domains during MET to form the renal vesicle. This implicates nectins and tight junction formation as processes that play central roles in nephron MET.

In summary, nephron formation demonstrates several conserved characteristics of an MET. Nephron formation requires environmental cues, mediated by external Wnt9b from the ureteric bud to drive a signalling cascade that drives MET. As part of this cascade, Sna and Six2 appear to act as EMT-TFs, both of which are downregulated during MET of the metanephric mesenchyme. Downregulation of Sna also appears to be required for the expression of a kidney-specific cadherin, contributing to MET. While it is unclear whether these external cues specifically help orient apicobasal polarity of the renal vesicles, afadin has been shown to organise the apical domain required for *de novo* lumen formation.

Somitogenesis

MET plays a central role in the formation of somites, a transient circular structure with an outer layer of epithelial cells that surround a central population of mesenchymal cells. Somitogenesis is a process conserved in all vertebrates, in which the two strips of paraxial mesoderm on either side of the extending neural tube undergo MET in a controlled manner. Somites form in pairs flanking the neural tube, in a sequential manner, starting from the anterior to the posterior. In each developing somite, the posterior membrane neighbouring the presomitic mesoderm forms last, forming distinct segments separated by an intersomitic gap (Baker et al., 2006). The patterning and segmentation of the somite is determined by a clockwork-wavefront mechanism (Baker et al., 2006; Niwa et al., 2011). These somites go on to form the precursors of axial bones and skeletal muscles (Takahashi et al., 2005).

Downregulation of Sna is required for somite MET and epithelialisation. Sna is precisely controlled during somitogenesis by FGF and Wnt signalling pathways, leading to oscillating expression of Sna within the mesenchymal presomitic mesoderm (Dale et al., 2006). Regions in which FGF and Wnt are simultaneously downregulated results in the loss of Sna expression. This allows for MET to occur, leading to epithelialisation of the presomitic mesoderm and subsequent segmentation. Additionally, ectopic overexpression of Sna inhibits MET and blocks segmentation (Dale et al., 2006), demonstrating that this downregulation of Sna is required for MET.

The surface ectoderm appears to play the role of an external cue during somitogenesis MET. In the absence of any ectoderm, the presomitic mesoderm does not undergo MET (Correia and Conlon, 2000). It was found that surface ectoderm cells that overlap the developing somites secrete Wnt6, which drives expression of the bHLH transcription factor Paraxis in the presomitic mesoderm (Linker et al., 2005; Schmidt et al., 2004). Paraxis appears to drive the expression of many genes required during somite MET, including those that play roles in cytoskeleton remodelling, ECM remodelling, cell-cell adhesion, and cell-matrix adhesion. It should be noted that Paraxis also regulated transcription factors known to play roles in patterning and cell fate decisions, highlighting that Paraxis is also involved in regulating more than just MET alone (Barnes et al., 1996; Leimeister et al., 2000; Rowton et al., 2013). Aside from its role to drive Paraxis, Wnt6 is also likely to provide basal cue that helps orient the polarity of the somite undergoing MET (Takahashi et al., 2005).

Put together, somitogenesis shows characteristics conserved in other METs. As in other examples, downregulation of EMT-TF Sna is required for somite MET. Furthermore, the overlying ectoderm provides an external cue, driving transcriptional changes via Paraxis and providing a basal cue to help orient somites. This cue provided by the ectoderm appears to be another example of how the external environment can drive MET.

1.5 Leveraging the Drosophila embryonic midgut to study MET.

As discussed, studies that explore the mechanisms underlying MET are far fewer than those examining mechanisms underlying EMT. It appears that characterising cells during MET using *in vivo* cancer models continues to be a challenge. In this regard, the *Drosophila* embryonic midgut provides an excellent developmental system that is amenable to both genetic transformation and imaging techniques to study MET. The *Drosophila* embryonic midgut undergoes EMT, collective migration and MET in quick succession as part of embryogenesis (Figure 2). This forgoes the need for any experimental intervention to study the mechanisms underlying physiological EMP.

Drosophila is a well-established developmental model organism. The mechanisms underlying the establishment of polarity and formation of cellular junctions have been studied extensively in *Drosophila*, providing a foundation to explore how MET re-establishes polarity and forms junctions. Furthermore, the mechanisms underlying polarity in *Drosophila* are simpler than that of vertebrate systems (Buckley and St Johnston, 2022), which may make for better model to identify genes that disrupt polarity, and thus a better model to understand the mechanisms underlying MET.

Previous work from the Campbell lab has already established the principal midgut epithelial cells from the posterior midgut (PMG) primordium as a model system to study for EMT and collective migration. In stage 10 embryos, the three distinct endoderm populations form: the principle midgut epithelial cells (PMECs), interstitial cell precursors (ICPs) and adult midgut precursors (AMPs) (Tepass and Hartenstein, 1995, 1994b). AMPs and ICPs make up a subpopulation of endoderm cells that remain mesenchymal throughout embryogenesis. The rest of the cells make up the PMECs, and while all of the midgut cells undergo EMT and migrate together in an organised coordinated fashion, only the PMECs undergo MET and re-epithelise.
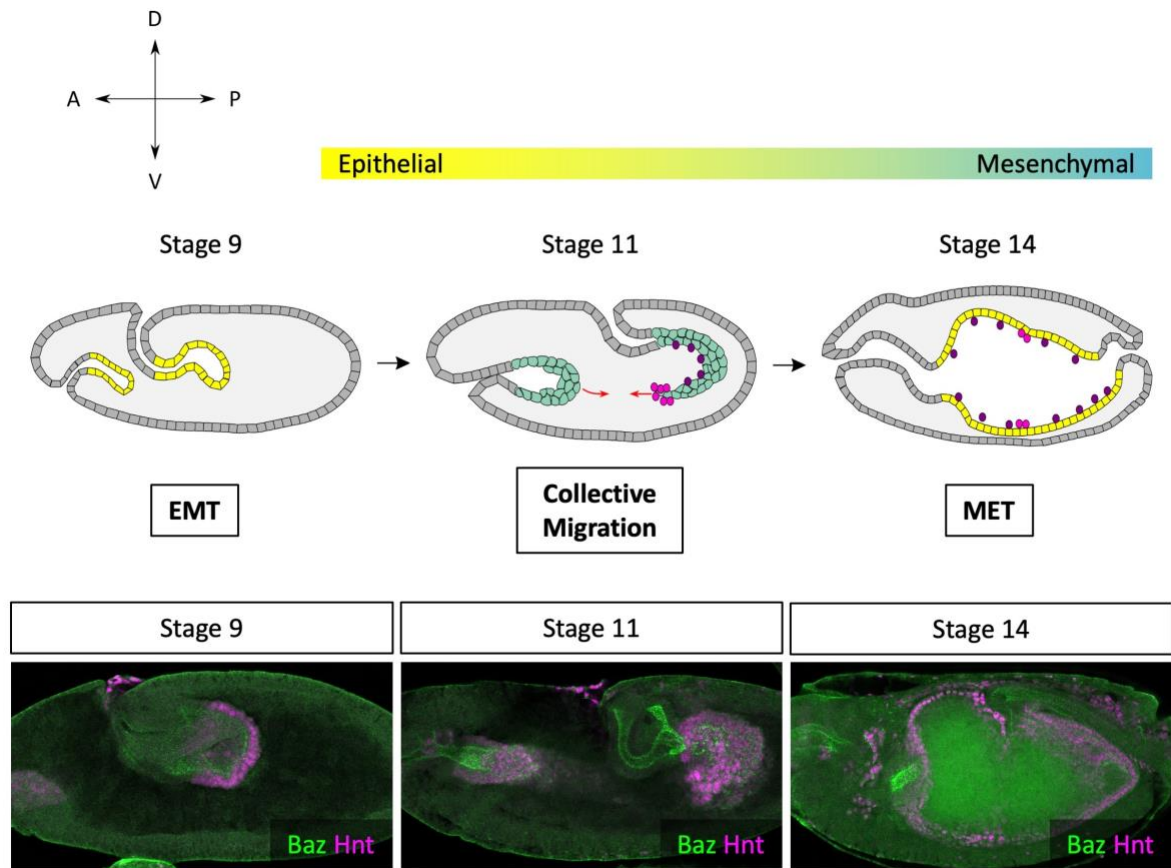
Figure 2. *Drosophila* Embryonic midgut as a model to study EMP.

The midgut undergoes EMT, collective migration and MET. In stage 9 embryos, the PMECs are epithelial (coloured yellow). As the midgut undergoes EMT, it becomes more mesenchymal (green) and starts to migrate towards the posterior. At stage 11, upon reaching the posterior end of the embryo, the posterior midgut (PMG) primordium migrates ventrally and back towards the anterior and forms a bilobed forked structure that fuse with the similarly shaped anterior midgut primordium (AMG). Upon fusion, the midgut extends laterally to close around the yolk and forms a tube. At stage 14, the PMECs regains its epithelial state (yellow). ICPs are in pink, and AMPs are in purple.

EMT of the PMG is driven by a single EMT-TF, Srp (Reuter, 1994; Campbell et al., 2011). In contrast, the anterior midgut (AMG) cells also express Sna, making it more complicated to elucidate molecular and cellular targets downstream of each of the EMT-TFs (Reuter and Leptin, 1994). The fact that all processes downstream of PMG EMT and migration is controlled by Srp alone makes the PMG a simpler and thus more tractable model to study the downstream processes that occur during both EMT and MET.

A recent study from the Campbell Lab (Pitsidianaki et al., 2021) showed that while downregulation of an EMT-TF is required, it is not sufficient for MET to take place in the midgut in the *Drosophila* embryo; midgut-MET requires additional external cues, mediated by the ECM and the underlying visceral muscle. This is in line with the previously discussed evidence in cancer and developmental systems suggesting that MET can be driven by external cues. Thus, the embryonic midgut also provides an opportunity to examine how external cues promote MET. In combination with single cell sequencing data capturing the transcriptional changes throughout midgut development, the model can be used study midgut EMP and to examine how these precisely timed and coordinated changes in cell phenotype are regulated throughout midgut development with respect to both cell-intrinsic gene expression and external cues.

1.6 Collective migration and MET in the Drosophila embryonic midgut.

Here I review the known mechanisms underlying cell migration and MET in the *Drosophila* embryonic midgut. A key cell-intrinsic factor mediating migration and MET is the regulation of EMT-TF Srp. With respect to external cues, two mechanisms by which visceral muscle provides an external cue for midgut morphogenesis have been explored to-date. One is mediated by the secretion of laminins (Pitsidianaki et al., 2021). The other is mediated by Netrin, a secreted chemokine (Pert et al., 2015). Given the close link between the midgut migration and MET, understanding the underlying mechanisms of both processes will be required to investigate how the mesenchymal cells organise to form the epithelia.

Srp – Primary EMT-TF of the embryonic PMG:

At stage 9, prior to EMT, the cells in the PMG are columnar and have apical adherens junction (Tepass and Hartenstein, 1994a). As a key component of adherens junctions, Ecad is tightly apically localised at this stage. Crb, Stardust (Sdt), Stranded-at-second (Sas), and Par complex proteins aPKC and Baz are also apically localised (Campbell et al., 2011). In wildtype embryos, EMT is initiated at stage 10, upon which cells of the PMG start to round up and form a mesenchymal mass (Campbell et al., 2011). By stage 11, adherens junctions are disassembled, and Ecad and the Par complex proteins are no longer apical localised.

The expression of GATA-factor Srp, the *Drosophila* ortholog of human GATAs 4 and 6, is critical for EMT (Campbell et al., 2011). In *srp* mutants, the PMG maintains apical Ecad at stage 10 and is unable to undergo EMT, demonstrating that Srp acts as the upstream EMT-TF responsible for the changes in junctional organisation that occurs. Analysis of Srp binding sites demonstrated that Srp mediated transcriptional repression of *crb*, *std* and *SAS,* but not *baz* or *aPKC.* This is in line with the complete loss of Crb, Std and SAS protein expression in midgut cells in stage 11 embryos. In contrast, although Ecad and the Par complex proteins are no longer apically localised, their expression is maintained throughout stage 11 and onwards.

Unlike typical core EMT-TFs such as Sna, Srp in the midgut does not repress Ecad. Instead, Srp was shown to drive loss of junctional Ecad via transcriptional repression of *crb*. While apical Ecad is maintained in *srp* mutants, Ecad is delocalised from the apical domain in double

mutants of *srp* and *crb*. This demonstrates that loss of Crb disrupts junctional Ecad. Furthermore, in contrast to the complete failure of EMT in *srp* mutants, double mutants of *srp* and *crb* appeared to undergo EMT, demonstrating that disruption of junctional Ecad mediated by Srp induced repression of *crb* is a crucial aspect of PMG EMT (Campbell et al., 2011). This agrees with the known function of Crb to aid in the formation and maintenance of adherens junctions (Tepass, 1996). Put together, Srp functions as an EMT-TF, driving loss of apical polarity and loss of junctional Ecad that occurs during PMG EMT.

Although junctional Ecad is lost at stage 10, expression of Ecad, Baz and aPKC expression is maintained throughout EMT and migration. It was suggested that these act in conjunction to form sAJs to mediate adhesion during migration (Campbell et al., 2011). However, very few sAJs were found in migrating cells by EM analysis. Instead, Ecad was shown to localise to short-lived punctate spots on the membrane that appeared to mediate adhesion. In the absence of Ecad, large gaps between the migrating cells were observed, suggesting that Ecad functions to maintain membrane adhesion between midgut cells without forming any junctions visible by electron microscopy (Campbell and Casanova, 2015).

Downregulation of Srp occurs at stage 11. Following this, midgut cells of stage 12 embryos undergoing MET regain epithelial organisation and apical localisation of Ecad and Baz (Pitsidianaki et al., 2021). This process is analogous to examples of MET discussed above, where downregulation of an EMT-TF is required for MET to occur. Moreover, sustaining Srp expression in the PMG disrupted MET, further demonstrating that downregulation of Srp is essential for PMG MET (Campbell et al., 2011). However, it has also been demonstrated that this downregulation of Srp is not sufficient to drive MET; in the embryos lacking mesodermal cells, Srp is downregulated in midgut cells as in wildtype, but MET does not occur and the cells remain in a mesenchymal state through embryogenesis (Pitsidianaki et al., 2021).

Interaction with the muscle

Observations in various mutants which affect mesoderm development indicate that contact between the midgut and muscle is essential for both midgut migration and MET. Observations in strong *twi* allele mutant *twi*^{1D96} and *sna* and *twi, sna* double mutants that lack mesoderm entirely, both the AMG and PMG do not migrate; while both the AMG and PMG are internalised, they remain as large mesenchymal clusters at opposing ends of the embryo, indicative of a failure to migrate or differentiate (Reuter et al., 1993).

Given that the midgut is in direct contact with the visceral muscle after stage 10 throughout migration and MET (Reuter et al., 1993; Wolfstetter et al., 2009), it was proposed that the visceral muscle plays a specific role to provide a basal substrate for the midgut cells to migrate along (Reuter et al., 1993). In mutants deficient for *tin* that lacked the visceral muscle, the AMG and PMG did not form bilobate structures and demonstrated a significant delay in migration such that the guts did not fuse at stage 13, suggesting a role for the visceral muscle in mediating migration (Reuter et al., 1993).

In addition to its role in migration, the visceral muscle has been proposed to play a role in driving MET. In *tinman*^{EC40} *(tin)* mutant embryos, it was reported that a few small remnant clusters of visceral muscle remained. In these *tin*^{EC40} mutants, only small islands of midgut cells that came into contact with the mesodermal cells formed an epithelial layer (Tepass and Hartenstein, 1994b), suggesting a specific role for the visceral mesoderm for MET. Put together, these observations suggest that the visceral muscle provides the external cue that contributes to migration and MET.

The visceral muscle of the hindgut also appears to be capable of supporting midgut MET. In *torso*^{421} *(tor)* mutant embryos, the midgut visceral muscle is completely absent and the posterior midgut fails to invaginate and shows significant morphological defects (Tepass and Hartenstein, 1994b). However, in these mutants, a small proportion of midgut cells are able to interact with the hindgut visceral muscle and those that do form epithelial layers. The hindgut visceral muscle is thought to be distinct from that of the midgut visceral muscle – for example the midgut visceral mesoderm uniquely expresses Fasciclin III (Tepass and Hartenstein, 1994b). Despite this difference, contact between the hindgut mesoderm and

midgut cells was able to drive MET. This may be interpreted to suggest that the midgut does not specifically require contact with the midgut visceral muscle, and that the cues which drive MET are present in all types of visceral muscle (Tepass and Hartenstein, 1994b).

Integrins and Laminins mediate interactions with the visceral muscle for migration.
Integrins and laminins are major players that facilitate cell-matrix contacts between tissues and an underlying ECM in other systems (Yu et al., 2005) and in different tissues in *Drosophila* (Urbano et al., 2011, 2009). Several papers documenting the various phenotypes in mutants for integrins and laminins have revealed their roles in midgut migration and MET.

Four integrin subunits expressed in the midgut are known to play key roles during midgut morphogenesis: αPS1, αPS3, βPS and βv (Devenport and Brown, 2004; Martin-Bermudo et al., 1999). These integrin subunits form dimers of one α and β subunit each to form functional receptors. Meanwhile, Laminins in *Drosophila* are encoded by four genes; Laminin subunits $\alpha_{1,2}$, $\alpha_{3,5}$, β and γ are encoded by the genes *wingblister* (*wb*), *Laminin A* (*LanA*), *Laminin B1* (*LanB1*) and *Laminin B2* respectively. Laminins form trimers made up of one α-, β-, γ-subunit each (Fessler et al., 1987). Thus, *Drosophila* only has 2 different heterotrimers; Heterotrimer LamininW consists of the $\alpha_{1,2}$, β, γ subunits while Heterotrimer LamininA consists of the $\alpha_{3,5}$, β, γ subunits (Fessler et al., 1987; Martin et al., 1999).

In embryos mutant for the two integrin β subunits, there is a complete absence of integrin heterodimers. In these mutants that lack functional integrin receptors, a failure to initiate migration was observed. Importantly, this failure to migrate was observed despite the presence of an intact visceral mesoderm at stage 12 (Devenport and Brown, 2004). In these embryos, the AMG and PMG primordium remained clustered and did not fuse. Similarly, in embryos mutant for *LanB1*, in which neither Laminin heterotrimers are able to assemble (Urbano et al., 2009), midgut migration was slower, demonstrated less directional persistence, and was less coordinated. (Pitsidianaki et al., 2021). Together, this suggests that both integrins and laminins are required for midgut migration.

Of the two β integrin subunits, βPS was shown to play a more important role in the migration. In the absence of βPS, midgut migration was delayed but the AMG and PMG primordium

fused at a later stage. In contrast, the absence of βv alone did not appear to cause any phenotype (Devenport and Brown, 2004), suggesting that the βPS alone is able to drive normal migration. As βPS mutants resulted in defects in muscle organisation, the role of βPS integrin independent of muscle organisation was examined. Upon driving βPS under a mesoderm-specific driver, aberrant muscle phenotypes were rescued but did not rescue the strong delays in midgut migration or the presence of cell projections (Martin-Bermudo and Brown, 1999). This demonstrated the requirement of βPS in the midgut for migration. This functional difference between the two β subunits is likely due to the fact that the Bv subunit lacks the cytoplasmic tail found in the βPS subunit that mediates its interaction with Talin, highlighting a key functional difference (Brown et al., 2002; Devenport and Brown, 2004). In line with this, migration in *talin* mutants were comparable to migration in the absence of βPS, suggesting that the role of βPS in migration is dependent on its interaction with Talin (Devenport and Brown, 2004).

Analysis of integrin α subunits involved in migration revealed distinct roles for αPS1 and αPS3. *αPS1* mutants demonstrated a mild delay in midgut migration, while αPS3 had no phenotype. This delay observed was exacerbated in double mutants of *αPS1* and *αPS3*, suggesting that there is interplay between αPS1 and αPS3 in mediating migration. Furthermore, this delay observed in double mutants was comparable to the loss of βPS, suggesting that αPS1 and αPS3 functions together with βPS to mediate midgut migration. Together, this demonstrates that while both αPS1 and αPS3 play roles in migration, αPS1 is comparatively more important. A key distinction between αPS1 and αPS3 was their ability to stimulate expression of integrin target genes such as *teashirt*. This functional difference was suggested to underly the ability of αPS1 to compensate for the absence of αPS3 (Martin-Bermudo et al., 1999). However, a subsequent paper looking at αPS1 and αPS3 localisation indicates that αPS1 is largely basally localised while αPS3 is largely apically localised (Pitsidianaki et al., 2021). This may suggest that this difference in function maybe due to differences in localisation. It would make sense that migration is mediated primarily proteins localised to the basal domain given that with the visceral muscle provides a basal substate upon which the midgut migrates.

Examining localisation of Laminins in wildtype embryos showed that both LanA and Wb were found along the basal membrane of the midgut. Examining localisation of Laminins in mutants

lacking mesodermal derivatives showed that a complete loss of Wb while LanA remained present, indicating that Wb is predominantly expressed in the muscle and that the midgut secretes LanA. Furthermore, it was shown that secretion of LanA by the midgut was disrupted in *wb* mutants, leading to punctae of LanA within the midgut (Pitsidianaki et al., 2021). Put together, this suggested that secretion of Wb by the muscle is required for the secretion of LanA by the midgut. Blocking laminin secretion in either the midgut or visceral muscle using a Sar1 dominant negative construct showed similar defects in migration, suggesting that both Wb from the visceral muscle and LanA from the midgut are required for migration (Pitsidianaki et al., 2021). In agreement with this, both *wb* mutants and *LanA* mutants have similar migration defects to *LanB1* mutants, suggesting that both Laminin W and Laminin A trimers are required for migration (Pitsidianaki et al., 2021). Given these results, it appears that instead of being entirely dependent on the visceral muscle to lay down a basal substrate for migration, the midgut plays an active role in mediating migration by secreting LanA.

Integrins and Laminins mediate interactions with the visceral muscle for MET.

As for migration, both integrins and laminin are vital for MET. In the absence of integrin heterodimers, the midgut PMECs failed to polarise, indicative of a disruption of MET (Devenport and Brown, 2004; Martin-Bermudo et al., 1999). Similarly, in the absence of both Laminin heterotrimers, midgut cells fail to undergo MET; apical localisation of Ecad and Baz are lost, and the basal localisation of βPS integrin is lost.

βPS appears to be critical for interactions between the basal surface of the midgut and the visceral muscle. In βPS mutants, gaps form between the visceral muscle and PMECs, demonstrating a role for βPS in mediating adhesion. In these mutant, basal localisation of talin is also completely lost (Devenport and Brown, 2004) and as such, suggests that βPS-mediated adhesion drives Talin localisation. It is likely that αPS1βPS heterodimers mediate this process, as αPS1 was shown to localise to the basal domain. This is in line with observations in embryos lacking αPS1; in the absence of αPS1 the midgut was unable to polarise and did not form a monolayer. This phenotype resembled Wb mutants, in which the PMECs are unable to repolarise or form a monolayer. Together, this suggested that αPS1βPS heterodimers binding to LamininW trimers secreted by the visceral muscle is required for polarisation. Furthermore, the polarisation defect observed in *wb* mutants was also

comparable to expression of Sar1 dominant negative in the mesoderm, emphasizing the role of the mesoderm in forming the LamininW trimer and driving polarisation.

In contrast to the polarisation defects observed in *wb* mutants, *LanA* mutants have a milder phenotype; in the absence of LamininA, the midgut forms a monolayer with a disordered apical domain, such that βPS is basally localised but apical localisation of both Baz and Ecad are disrupted (Pitsidianaki et al., 2021). A similar phenotype is observed in the absence of αPS3. In both of these mutants, the midgut can still form a columnar epithelium, suggesting that LanA and αPS3 have a role in organising apical polarity. Together, this suggests that αPS3 mediates binding to LamininA trimers. Previous observations have suggested that βv forms a heterodimer with αPS3 (Devenport and Brown, 2004), perhaps suggesting that the interaction between LanA and αPS3βv heterodimer is responsible for organising the apical domain. Crucially, LanA accumulates in the midgut cells when Wb is absent. This places the polarised secretion of LanA by the midgut cells downstream of Wb-driven polarisation of the PMECs. Thus, this secretion of LanA, which appears to drive apical localisation of αPS3, has been proposed to further reinforce apicobasal polarity after the initial cue provided by LanW (Pitsidianaki et al., 2021).

Frazzled and Netrins play roles in migration and MET.
Another mechanism by which the visceral muscle drives MET involves chemotrophic signalling mediated by the secreted ligands Netrin and its receptor Frazzled (Fra) (Pert et al., 2015). In *Drosophila,* there are two Netrin genes, encoded by NetA and NetB respectively, and both netrins are expressed in the visceral muscle. Meanwhile, Fra is expressed in the midgut PMECs. In wild type, Fra is strictly localised to the basal membrane in the midgut while netrins are found in internal puncta within the basal domain of the PMECs, indicative of endocytosis. Fra mutants led to loss of internal netrin puncta, suggesting that Fra mediates this endocytosis. In agreement with this, inhibiting endocytosis via expression of a Rab5 dominant negative in the midgut also resulted in the loss of internal netrin puncta (Pert et al., 2015). Thus, it is clear that netrins from the visceral muscle is internalised by PMECs.

This signalling mediated by Netrins and Fra appears to play a role in midgut migration; in the absence of both netrins, midgut migration is delayed. This delay observed in *netAB* double

mutants could be rescued by expression of either netrins, suggesting that both NetA and NetB are sufficient to support normal midgut migration. On the other hand, Fra mutants exhibit a greater delay compared to *netAB* double mutants, suggesting an additional role for Fra in migration.

Netrins and Fra were also shown to play a role in MET. In *netAB* double mutants, PMECs were rounded and failed to form a single-layered epithelium. Apical localisation of Ecad was also partially affected, with a greater proportion being localised to the lateral membrane. Mutants for Fra demonstrated a similar but milder phenotype, perhaps indicative of a role for Netrins independent to its role as a ligand for Fra during MET or perhaps in muscle development. Compared to wildtype, both *netAB* double mutants and *fra* mutants demonstrated stricter localisation of βPS to the basal side of the midgut. A exaggerated version of this strict basal βPS phenotype was observed upon blocking endocytosis via expression of a Rab5 dominant negative, suggesting that Fra and netrins play a role in βPS endocytosis (Pert et al., 2015).

This link between Fra-Netrin signalling and βPS endocytosis may partially explain various phenotypes observed upon disrupting Fra-Netrin signalling. For example, attenuating integrin endocytosis has previously been shown to cause delayed cell migration *in vitro* (De Franceschi et al., 2016) and thus, delayed migration observed upon disturbing Fra-Netrin signalling could partially be a result of blocking integrin endocytosis. Additionally, the overall tissue morphology of migrating midgut cells in *fra* mutants resembles that of βPS mutants (Martin-Bermudo and Brown, 1999; Pert et al., 2015). In both mutants, the midgut migrated as rounded cluster, as opposed to a wedge-shaped mass observed in wildtype. Furthermore, the fine cell protrusions in the front-most cell found in wildtype were also lost in both mutants. However, it was noted that delays in midgut migration in double mutants of *Fra* and *βPS* were greater compared to single mutants of either gene, suggesting that Fra has an effect on migration independent of integrin endocytosis (Pert et al., 2015).

This additional role of Fra independent of integrin endocytosis may be related to Cheerio/Filamin localisation. Cheerio (Cher) crosslinks actin filaments, anchors actin filaments to the plasma membrane and can act as a mechanosensor (Razinia et al., 2012). Basal localisation of Cher is maintained in the absence of both β integrin subunits (Devenport and

Brown, 2004), but this localisation is partially lost in double mutants of *Fra* and *βPS* (Pert et al., 2015), suggesting that Fra helps localises Cher in an integrin-independent manner. However, Fra does not appear to be the only cue driving basal localisation of Cher; basal Cher is only partially reduced in *fra* mutants (Pert et al., 2015), which may point to other mechanisms that also contribute to Cher localisation.

In summary, βPS appears to play a central role in the basal membrane of the midgut, mediating both adhesion and polarisation via interactions with basal laminin W. Furthermore, βPS also drives basal localisation of Talin, which functions as the major integrin activator and likely other downstream functions of βPS-mediated integrin signalling (Klapholz and Brown, 2017). For example, the establishment of the basal αPS1βPS heterodimer appears to be a prerequisite for organisation of the apical domain, likely mediated by apical αPS3βv. Defects in MET observed upon disrupting Fra and Netrin signalling may be partially a result of its effect on integrin endocytosis, further establishing βPS as a central player in MET. One key aspect of shown to be independent of integrin is the basal localisation of Cher, which may partially be regulated by Fra and Netrin signalling. While the extent to which Cher contributes to midgut MET is not known, basal Cher in the absence of βPS has been shown to be insufficient to mediate MET (Devenport and Brown, 2004). Regardless, it is clear that contact with the visceral muscle plays a key role to provide a basal cue to help orient polarity. In this regard, this system appears to be analogous to the other developmental contexts discussed where the external cue appears initiate MET, e.g Wnt9b from the ureteric bud in Nephrogenesis and Wnt6 from overlying ectoderm in somitogenesis.

1.7 Objectives

The goals of my project were as follows:

1) Chart midgut MET at the cellular and molecular level.

2) Identify mesoderm-dependent molecular mechanisms and signals that drive MET in midgut cells.

3) Use single-cell RNA sequencing (scRNAseq) data to identify transcriptional changes associated with MET and the underlying mechanisms.

Given the difficulties of studying MET *in vivo,* descriptions of changes in cell phenotypes that occur during MET are somewhat limited. To this end, I aimed to characterise and describe wild type migration and MET of the *Drosophila* embryonic PMG cells in detail. So far, methods of quantifying the localisation of proteins have been established but descriptions of cell shape and morphology are limited and brief. Thus, I aimed to quantify aspects of cell morphology at various timepoint throughout MET in an attempt to characterise the various cellular processes that occur within MET. The *Drosophila* embryo is amenable to both high resolution fixed and live imaging, making it possible for the process to be studied at a fine temporal resolution.

The presence of an external cue that drives MET appears to be conserved in various settings. Existing literature specifically points to the visceral muscle as the external cue driving MET. Thus, I set out to explore the role of the visceral muscle and its effects on collective migration and MET.

Finally, the scRNAseq data available in the lab allows for analysis of the transcriptional changes that occurs in specific subsets of both midgut and mesodermal cells during the time windows in which the midgut cells undergo EMT, migration and MET. Using this data, I attempted to identify genes involved in midgut MET. Given the evidence suggesting a role for the visceral muscle in migration and MET, I aimed to identify and screen candidate genes that may mediate interactions between the visceral muscle and the midgut that drive MET. A functional screen of various candidate genes from this data revealed Off-track and Semaphorin 1a as potential receptor ligand interaction mediating signals between the visceral muscle and midgut that drive MET.

Chapter 2. Dissecting the role of somatic and visceral muscle in midgut morphogenesis.

2.0 Introduction

As discussed in the previous chapter (Section 1.6), various studies (Reuter et al., 1993; Tepass and Hartenstein, 1994b) have examined migration and MET in various mesoderm mutants. While it has been suggested that the visceral muscle plays a central role in driving MET for the formation of the midgut epithelium (Tepass and Hartenstein, 1994b), the specific mechanisms underlying this have not been thoroughly explored (Pert et al., 2015; Pitsidianaki et al., 2021). Given the role for visceral muscle in driving MET, I wanted to examine migration and MET in a mutant that lacked visceral muscle. For this, mutants for *biniou* (*bin*) previously identified as a mutant lacking the visceral muscle (Zaffran et al., 2001), provided an opportunity to examine the role of the visceral muscle in midgut morphogenesis. Here, I briefly describe embryonic muscle development, with a focus on the development of visceral muscle and the role of Bin.

The visceral mesoderm is defined by expression of Bagpipe (Bap) and Bin (Zaffran et al., 2001). Between the two, Bin is considered to be the central transcription factor that defines visceral muscle fate; ectopic Bin expression under a general mesoderm driver disrupts somatic muscle differentiation and drives expression of visceral muscle markers (Zaffran et al., 2001). Bin plays an active role in regulating transcription throughout visceral muscle development. Chip-on-chip sequencing revealed 218 different *bin*-bound enhancers (Jakobsen et al., 2007). Of these enhancers, Bin is continuously bound to 47% throughout visceral muscle development. However, it was also shown that Bin binding to enhancers is temporally regulated; 22% and 31% of Bin-bound enhancer regions are bound specifically at stages 10 to 11, and 14 to 15, respectively (Jakobsen et al., 2007). This temporal restriction of Bin binding is likely mediated by co-factors. This dynamic binding to enhancers throughout visceral muscle development enables Bin to drive transcription of various genes in spatially and temporally restricted patterns. For example, Bin was shown to continuously bind to the *bap3.5* enhancer, which drives expression in the foregut and hindgut, demonstrating a regional restriction to the gene expression. In contrast, Bin was shown to bind to the *fd64a* enhancer specifically at stage 12.

This corresponded with the activity of the *fd64a* enhancer, which drives expression within a subset of trunk visceral muscle at stage 13 (Jakobsen et al., 2007). Putting these results together, it appears that while Bin functions throughout visceral muscle development, it is also able to mediate spatially and temporally restricted transcription throughout visceral muscle development.

The visceral mesoderm defined by Bap and Bin differentiates into two distinct muscle types: an inner layer called the circular visceral muscle, and an outer layer called the longitudinal visceral muscle. Although previously thought to be mononuclear, the development of visceral muscle involves the fusion of founder cells to fusion competent myoblasts to form syncytial fibres (Klapper et al., 2002; Martin et al., 2001). Founder cells of the circular visceral muscle are defined by secretion of Jelly belly (Jeb) from the somatic muscle (Lee et al., 2003) and form two rows within trunk visceral mesoderm on either side of the region to be occupied by the midgut (Martin et al., 2001). These circular visceral founder cells fuse with adjacent visceral fusion competent myoblasts that reside within the trunk mesoderm to form syncytial circular visceral muscles (Martin et al., 2001). In contrast, the founder cells of the longitudinal visceral muscle are migratory. They arise within the mesoderm close to the hindgut but migrate along the circular visceral muscle to the trunk mesoderm (Ismat et al., 2010; Macabenta and Stathopoulos, 2019; Urbano et al., 2009). Migration of the longitudinal founder cells occurs during the formation of syncytial circular visceral muscle fibres (Wolfstetter et al., 2009; Zaffran et al., 2001). After migration, the longitudinal visceral muscle founder cells, now adjacent to the visceral fusion competent myoblasts that reside in the trunk mesoderm, are able to fuse to form syncytial longitudinal muscle fibres (Martin et al., 2001).

In wildtype, the migration of midgut cells occurs at the same time as the migration of the longitudinal visceral muscle founder cells. Midgut cells make contact and migrate along the inside of the syncytial circular visceral muscle and unfused fusion competent myoblasts (Wolfstetter et al., 2009). This migration does not appear to require the formation of syncytial fibres; midgut migration occurs normally in mutants for Jeb and its receptor Alk, which lack visceral muscle founder cells and cannot undergo myoblast fusion (Shirinian et al., 2007). In these mutants, the lack of visceral founder cells causes the visceral fusion competent

myoblasts to fuse with the somatic founder cells, resulting in the absence of visceral muscles. Lateral migration of the midgut cells fails in these mutants (Shirinian et al., 2007), supporting the idea that the visceral muscle plays a key role in midgut morphogenesis.

Given that Bin plays a central role in defining the visceral mesoderm, the precursors of both the circular and longitudinal visceral muscle, it was suggested that *bin* mutants would lack both the circular and longitudinal visceral muscle (Zaffran et al., 2001). In line with this, the circular visceral muscle is absent in *bin* mutants, indicated by the absence of tissue expressing circular visceral muscle-specific markers Vimar and Brokenheart (Zaffran et al., 2001). Furthermore, a study using single cell assay for transposase-accessible chromatin with sequencing (scATAC-seq) to track mesoderm lineage trajectory indicated that *bin^R22* mutant cells were unable to differentiate towards a circular visceral muscle lineage (Secchia et al., 2022). While it is clear that the circular visceral muscle is disturbed in *bin* mutants, the existing literature is unclear whether the longitudinal visceral muscle is present in *bin* mutants. Staining *bin^R22* mutant embryos for HLH54F, a key marker of longitudinal visceral founder cells (Ismat et al., 2010), suggested that the number of founder cells are greatly reduced and that those that remain, fail to migrate to regions surrounding the midgut (Zaffran et al., 2001). In contrast, data from the scATAC-seq mesoderm lineage trajectory suggested that differentiation towards the longitudinal visceral muscle lineage was unchanged in *bin^R22* mutants and comparable to wildtype (Secchia et al., 2022). Regardless, description of *bin* mutants suggested that it could be used to dissect out the precise role of the visceral muscle in midgut morphogenesis.

In this chapter, I focus on characterising midgut morphogenesis in wildtype and *bin* mutants to examine the role of the visceral muscle during migration and MET.

2.1 Results

2.1.1 Characterisation of the *bin^R22* mutant

Given the role of the visceral muscle in midgut morphogenesis (Tepass and Hartenstein, 1994b), I wanted to leverage the *bin^R22* to examine midgut morphogenesis in the absence of the visceral muscle. The null allele *bin^R22* carries a mutation within the first exon that introduces a premature stop codon. The resulting polypeptide lacks the Forkhead domain, and thus cannot bind to DNA or induce transcription (Zaffran et al., 2001). In *bin^R22* mutants, the mesoderm is unable to differentiate in to circular visceral muscle and instead said to transformed into somatic muscle (Zaffran et al., 2001). However, there are conflicting descriptions as to the presence of the longitudinal visceral muscle (Secchia et al., 2022; Zaffran et al., 2001). Although the circular visceral muscle appears to be more important during midgut morphogenesis, the possibility that remnant longitudinal visceral muscle in *bin^R22* mutants may contribute to midgut morphogenesis cannot be ruled out. Thus, I examined the visceral muscle in *bin^R22* mutants to confirm the absence of the circular visceral muscle and determine whether the longitudinal visceral muscle was present.

Ig-domain adhesion molecule Fasciclin *III* (FasIII) is specific to the trunk visceral mesoderm surrounding the midgut (Martin et al., 2001; Patel et al., 1987). FasIII staining in stage 13 wildtype embryos shows the presence of the visceral muscle. The muscle at this stage shows a striated pattern, typical of the syncytial circular visceral muscle fibres (Figure 4A, arrowhead). A dorsal view of a stage 13 wildtype embryos shows that the visceral muscle is in close contact with the midgut (Figure 4B). In homozygous *bin^R22* mutants, staining with FasIII reveals a complete absence of visceral muscle (compare Figure 4B and Figure 4C). As FasIII stains both longitudinal and circular visceral muscle (Martin et al., 2001; Patel et al., 1987), this suggested that both the longitudinal and circular visceral muscle was absent.
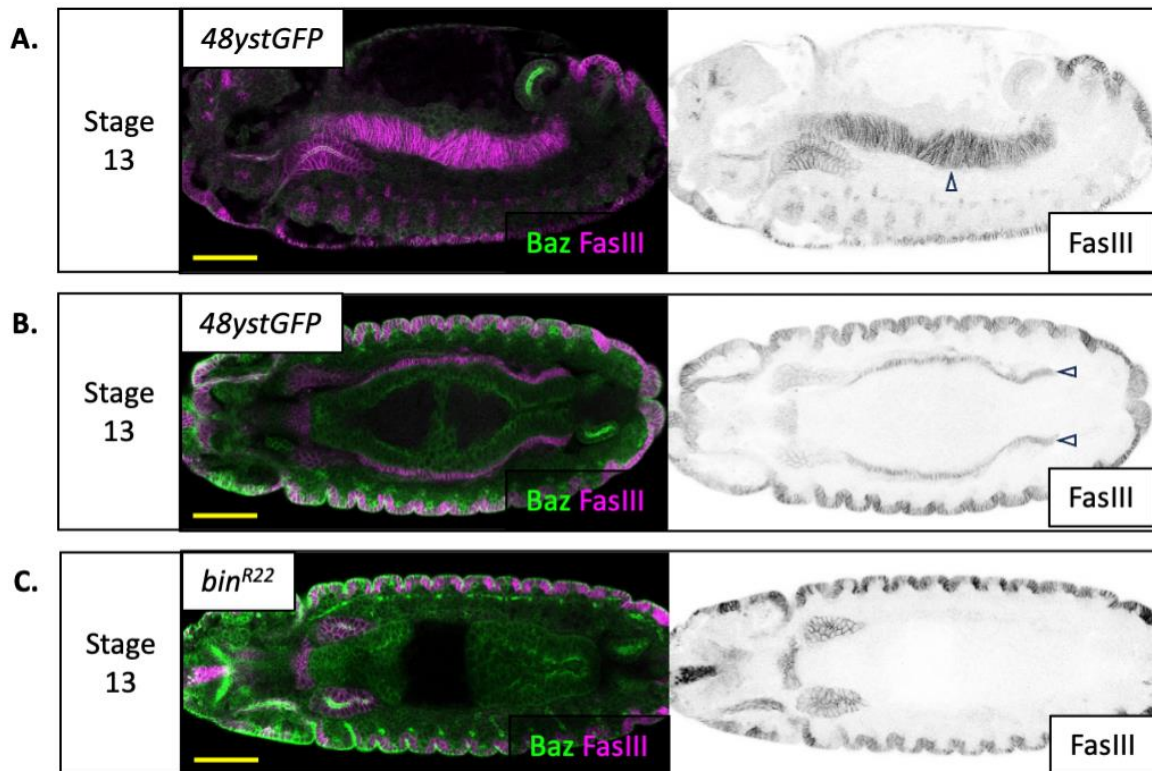
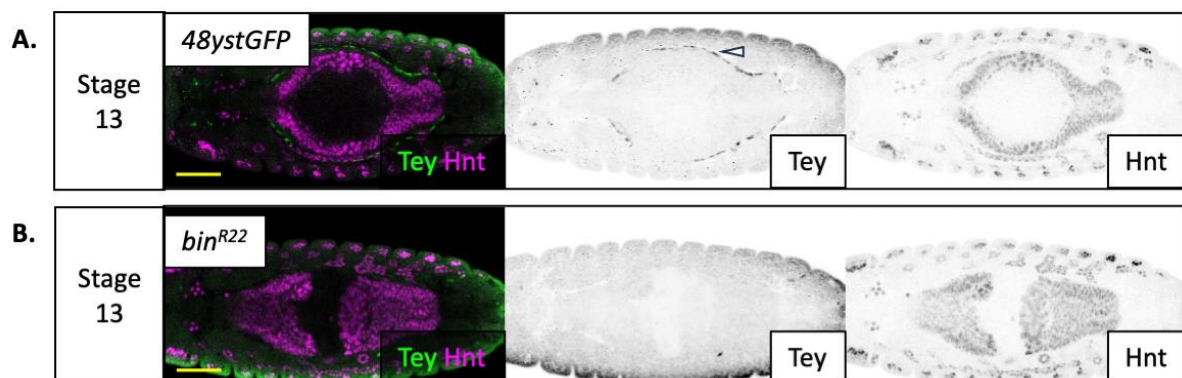**Figure 4. The visceral muscle is absent in homozygous *bin* mutants.**

A. Lateral view of a wildtype (*48ystGFP)* embryo at stage 13. Staining for FasIII (magenta) reveals the striated pattern of the visceral muscle (arrowhead). The midgut is visualised by staining for Bazooka (Baz) (green) which localises to the apical domain of midgut cells after migration.

B. Ventral view of a wildtype embryo at stage 13. FasIII stains reveal two rows of visceral muscle (arrowhead), in close contact with the midgut.

C. Ventral view of homozygous *bin^R22^* mutant at stage 13. Absence of FasIII indicate that the visceral muscle is absent in *bin^R22^* mutants.

All scale bars 50μm. 48ystGFP, N = 18. *bin*, N=12.

To confirm the absence of the longitudinal visceral muscle, I checked for the presence of longitudinal visceral muscle founder cells using Teyrha-Meyrha (Tey) as a marker for (Macabenta and Stathopoulos, 2019). Examining stage 13 wildtype embryos revealed the presence of longitudinal visceral muscle founder cells around the midgut, in a region occupied by the visceral muscle (Figure 5A). In contrast, in stage 13 *bin* mutant embryos, the longitudinal visceral muscle founder cells were entirely absent (Figure 5B). As the founder cells are required for the formation of longitudinal visceral muscle, this indicates that the longitudinal visceral muscle is absent in *bin* mutants. This observation, together with the absence of FasIII-positive tissue around the midgut, indicates that both types of visceral muscle are absent in *bin^{R22}* mutants.

Figure 5. Longitudinal visceral muscle founder cells are absent in homozygous *bin* mutants.

A. Ventral view of a wildtype embryo at stage 13. Tey stains (green) reveal a row of longitudinal visceral muscle founder cells (arrowhead). The nucleus of midgut cells are marked by Hnt stains (Magenta). It appears that the midgut does not make direct contact with the longitudinal visceral muscles.

B. Ventral view of a *bin^{R22}* mutant embryo at stage 13. Absence of Tey (Green) stains indicate that longitudinal visceral muscle founder cells are absent in *bin^{R22}* mutants.

All scale bars 50µm. 48ystGFP, N = 7. *bin*, N= 3.

2.1.2 Dissecting the role of the somatic and visceral muscle during midgut migration.

Having established that *bin* mutants completely lack visceral muscle, I next wanted to examine midgut migration under these conditions. To examine migration, I made movies of live stage 10 embryos with midgut cells labelled with nuclear GFP, at which point the midgut is just starting to initiate migration (Tosi and Campbell, 2019). In previously published work, a fixed speed was subtracted from the observed nucleus migration to compensate for the general embryo-wide movement resulting from germband retraction (Campbell and Casanova, 2015). Instead of this, I came up with an approach that allowed me to measure germband retraction for each embryo. Using the two-photon laser, I created small regions of fluorescence by intentionally causing photodamage (Galli et al., 2014). Using these marks, I was able to track the speed of germband retraction for each embryo and thus, was able to isolate midgut migration dynamics from overall germband retraction (Figure 6A). Photodamaging the embryos did not appear to cause any changes to the speed of germband retraction and was consistent between embryos (see methods). Quantifying migration with movies of stage 10 embryos has been previously used to show uncoordinated migration in Ecad/*shotgun* (*shg*) mutants between PMEC and ICP populations (Campbell and Casanova, 2015). Given this finding, I also measured PMEC and ICPs population separately (Figure 6B, C).

The speed, directional persistence and displacement of cells and the overall length of tracks were examined. Displacement refers to the straight-line distance between the start and end point. The calculations behind each metric are described in Tosi and Campbell, 2019. All four metrics did not show a difference in migration between wildtype and *bin* mutant PMECs (Figure 7A, B) or ICPs (Figure 7C, D). Thus, the data suggests that wildtype and *bin* mutants show the same capacity to undergo migration. The fact that migration is unperturbed in *bin* mutants suggests that collective migration does not specifically require the visceral muscle. Furthermore, given that the *bin* mutants have a similar migratory capacity as wildtype, the results also suggests that the subsequent failure to undergo fusion in *bin* mutants is not likely to be the result of differences in capacity to migrate.
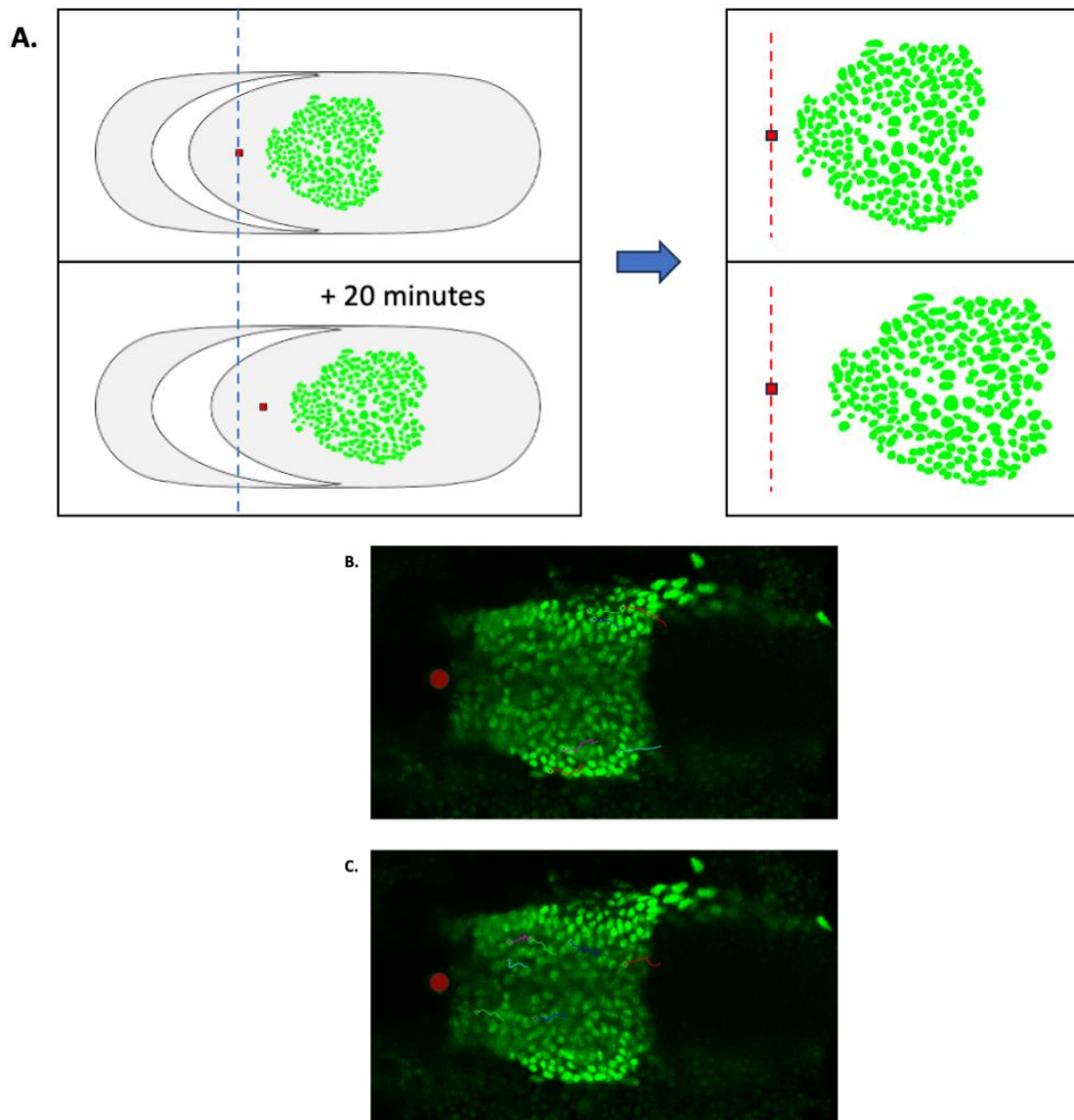
Figure 6. Experimental setup to quantify migration of midgut cells.

A. Schematic demonstrating experimental setup. Red square indicates point of laser ablation. Laser ablations were made adjacent to the midgut to mark the germband. Germband retraction causes overall morphological movement, moving the point of laser ablation relative to the length of the embryo (blue dotted line). However, as the point of laser ablation remains constant relative to the germband (red dotted line), the point can be used as marker to isolate midgut movement from overall morphological movements caused by germband retraction.

B. Exemplar of PMEC tracks. Coloured lines indicate migration tracks. Red circle indicates point of laser ablation.

C. Exemplar of ICP tracks. Coloured lines indicate migration tracks. Red circle indicates point of laser ablation.

A.
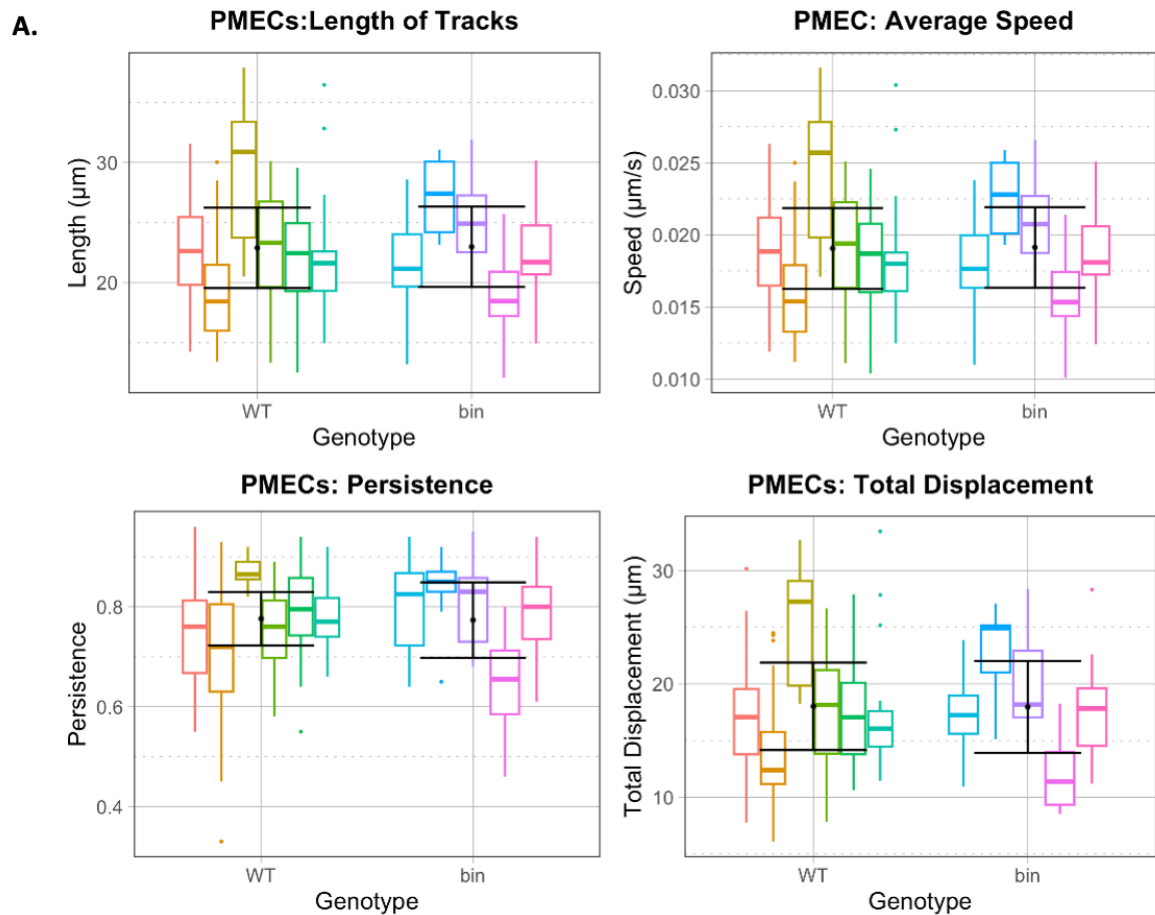
B.

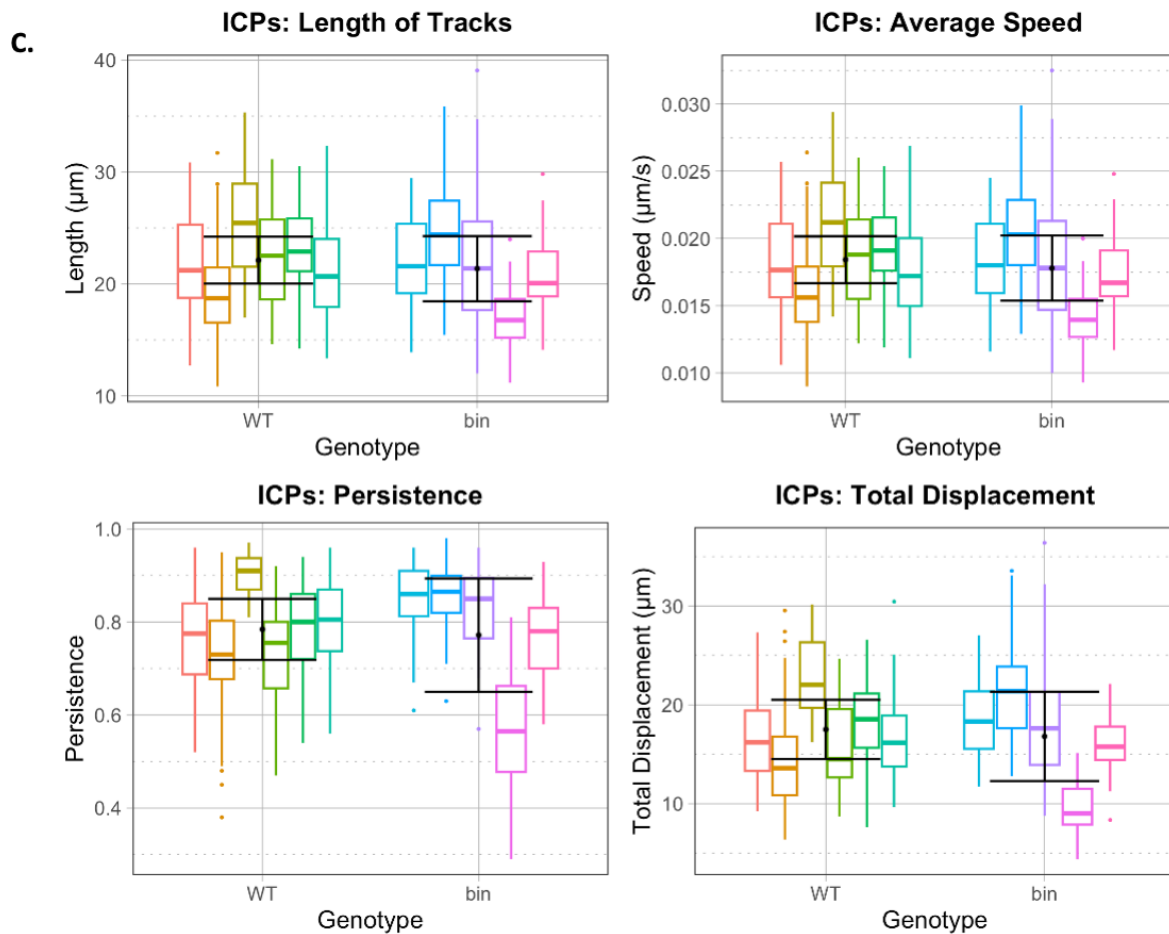| Characteristic	WT, N = 6[1]	bin, N = 5[1]	p-value[2]
Length	22.89	22.98	0.93
Total Displacement	18.02	17.96	0.79
Average Speed	0.0191	0.0191	0.93
Persistence	0.78	0.77	0.54

[1] Mean
[2] Wilcoxon rank sum exact test

Figure 7. Early migration is unchanged in *bin* mutants.

A. Plots describing migration of PMECs. Each box plot corresponds to tracks from a single embryo, showing the distribution of tracks. Black dot plot corresponds to mean of the average values of each embryo. Black error bars are standard deviation. 48ystGFP, N = 6 embryos. *bin*, N= 5 embyros. n for WT tracks: 13 ~ 71, n for *bin* tracks: 9 ~ 36.

B. Summary table of PMEC measurements. Values in the table correspond to the mean of the average values of each embryo. P-value for all four measurement suggests that medians are not shifted, and thus suggest that there is no difference between WT and *bin* mutants.

C.

ICPs: Length of Tracks

ICPs: Average Speed

ICPs: Persistence

ICPs: Total Displacement

D.

| Characteristic	WT, N = 6[1]	bin, N = 5[1]	p-value[2]
Length	22.12	21.37	0.79
Total Displacement	17.52	16.81	0.93
Average Speed	0.0184	0.0178	0.79
Persistence	0.78	0.77	0.79

[1] Mean

[2] Wilcoxon rank sum exact test

Figure 7. Early migration is unchanged in _bin_ mutants.

C. Plots describing migration of ICPs. Each box plot corresponds to tracks from a single embryo, showing the distribution of tracks. Black dot plot corresponds to mean of the average values of each embryo. Black error bars are standard deviation. (48ystGFP, N = 6 embryos. _bin_, N= 5 embryos. n for WT tracks: 42 ~ 112, n for _bin_ tracks: 41 ~ 60)

D. Summary table of ICPs measurements. Values in the table correspond to the mean of the average values of each embryo. P-value for all four measurement suggests that medians are not shifted, and thus suggest that there is no difference between WT and _bin_ mutants.

Given the capacity for the midgut to undergo migration in the absence of visceral muscle, this suggested that the somatic muscle is able to support migration. In light of this, I wanted to examine migration in the absence of both visceral and somatic muscle. It has been previously reported that the midgut fails to form in single mutants of *sna* and *twi* (Reuter et al., 1993). I found that this was also the case in *sna^{18} twi^3* double mutants, which lack all mesodermal cells (Leptin, 1991). Live imaging the posterior midgut of *sna twi* mutant embryos proved to be difficult as the midgut appeared to be positioned more internally than that of wildtype or *bin* mutant embryos. Instead, I examined midgut migration in fixed *sna twi* mutant embryos.

In wildtype stage 11 embryos, the posterior midgut extends towards the posterior and migrates ventrally. In contrast, the posterior midgut in stage 11 *sna twi* mutants appears to remain clustered and fails to migrate (Figure 8A, arrowhead). Absence of Bazooka (Baz), a marker for the apical side of midgut cells, indicates that this cluster of midgut cells is a mesenchymal mass. In wildtype stage 12 embryos, the posterior midgut fuses with the anterior midgut. This does not occur in stage 12 *sna twi* mutants (Compare WT and *sna twi*, Figure 8B). Furthermore, the cluster of posterior midgut cells remains as a mesenchymal mass around the hindgut (Figure 8B, arrowhead), indicative of failure to migrate. This is clearly distinct from the behaviour of midgut cells in wildtype; cell of the posterior midgut extends nearly halfway across the length of the embryo away from the hindgut. However, there are gross morphological phenotypes in *sna twi* mutants, as these embryos fail to undergo germband retraction.
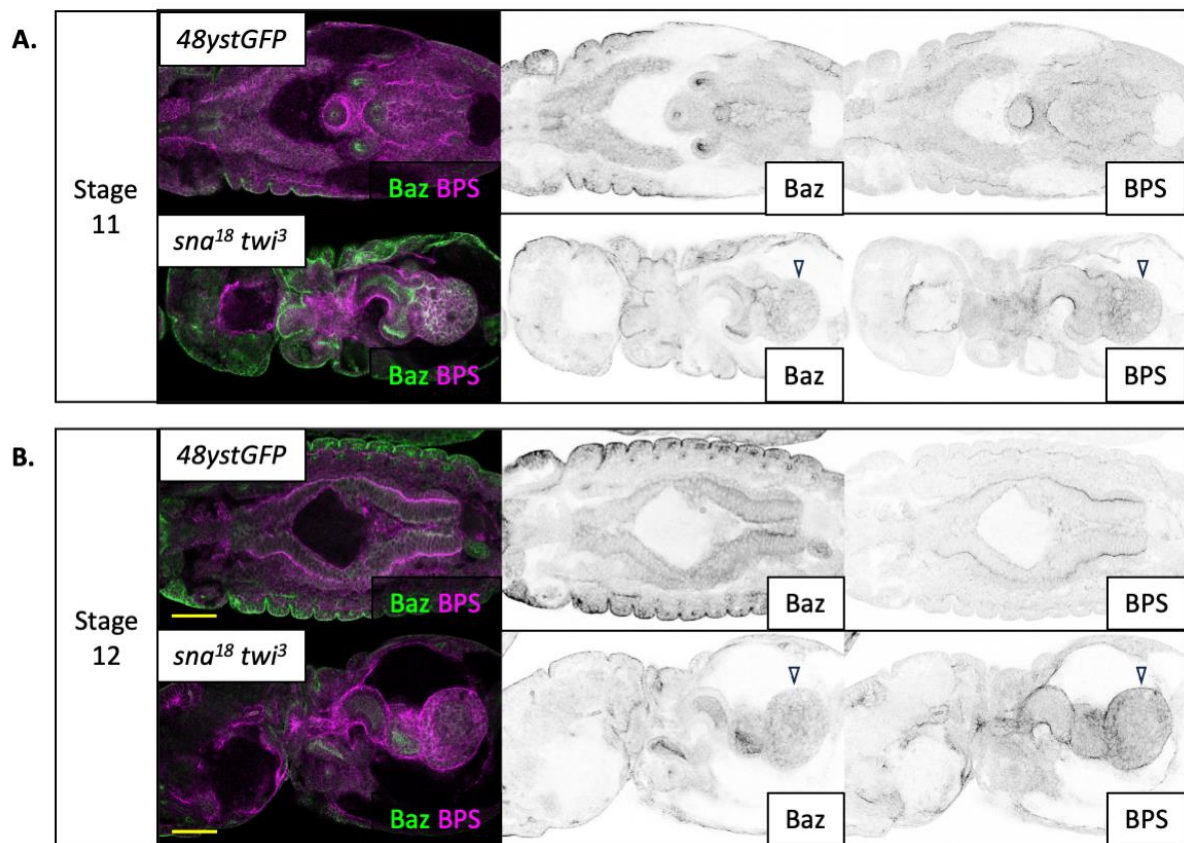
Figure 8. The midgut does not actively migrate in the absence of mesodermal tissue in *sna18 twi3* double mutants.

At stage 11, the wildtype gut undergoes significant migration. The midgut extends towards to posterior, moving ventrally. In comparison, the midgut in sna[18] twi[3] double mutants remains clustered, indicative of failure to migrate (arrowhead). At stage 12, the wildtype midgut fuses. At a comparable stage, the midgut in sna[18] twi[3] double mutants remains clustered at the posterior end of the embryo. It should be noted that staging of sna[18] twi[3] double mutants is difficult due to extensive morphological defects. The hindgut and Malpighian tubule are used to stage sna[18] twi[3] double mutants.

All scale bars 50µm.

Stage 11: 48ystGFP, N = 7 embryos. *sna twi,* N= 11 embryos.

Stage 12: 48ystGFP, N = 22 embryos. *sna twi,* N= 11 embryos.

This failure to undergo germband retraction observed in *sna twi* mutants could be interpreted to suggest that germband retraction is required for midgut migration. To investigate this, I leveraged a *u-shaped* (*ush*) mutant, which fails to undergo germband retraction (Reuter et al., 1993). Crucially, the failure to undergo germband retraction in *ush* mutants is the result of effects on the amnioserosa, such that an key mechanical contraction force that permits germband retraction is lost (Lynch et al., 2013). Thus, any phenotypes observed in *ush* mutants should be independent of gut development.

Examination of embryo morphology firstly confirmed that *ush²* mutant embryos fail to retract their germband (Figure 9A and B). Second, FasIII stains showed that the visceral muscle forms normally (Figure 9A). Midgut migration occurs normally along the visceral muscle (Figure 9A), and subsequent MET also appears normal, indicated by localisation of apical Baz (Figure 9B, arrowhead). Together, this demonstrated that midgut migration is entirely independent of germband retraction. Furthermore, it indicates that the migration phenotypes observed in the *sna twi* mutant are independent of its failure to undergo germband retraction. Observations from the *sna twi* mutant and *ush* mutant together emphasizes the role of the mesoderm in supporting midgut migration.
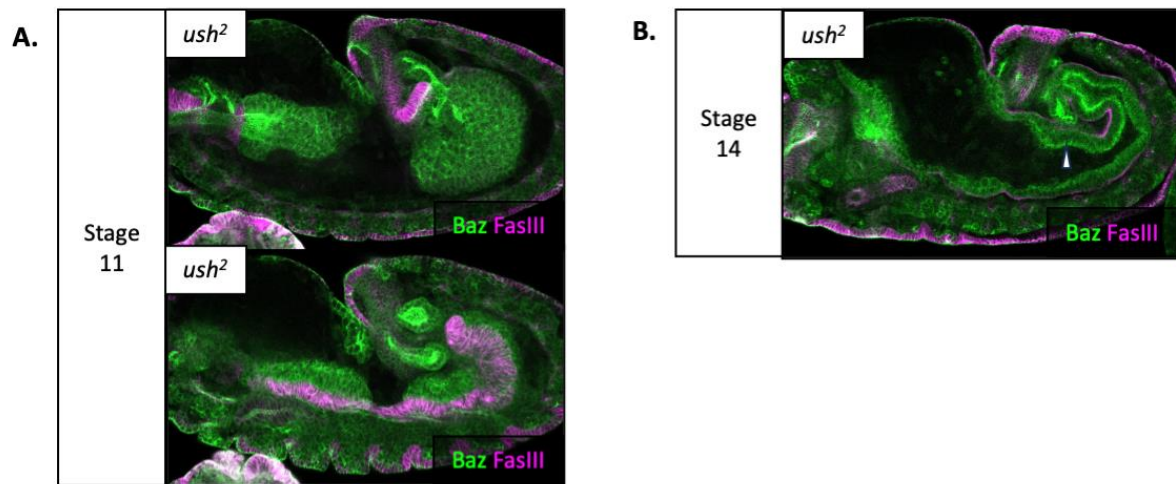
Figure 9. Midgut migration, fusion and MET is independent of germband retraction.

A. Lateral view of stage 11 *ush²* mutant embryo at a central z-stack bisecting the midgut (upper panel) and at a higher z-stack level with the visceral muscle (lower panel). Germband retraction fails to occur. The midgut, stained with Baz (green), appears to migrate normally along the visceral muscle, as labelled by FasIII (magenta). The visceral muscle is intact and striated.

B. Lateral view of stage 14 *ush²* mutant embryo. The AMG and PMG fuse normally and forms an epithelial tube. Furthermore, Baz is apically localised throughout the midgut (arrowhead), demonstrating normal MET.

All scale bars 50µm. Stage 11, N = 8 embryos. Stage 14, N = 6 embryos.

2.1.3 Dissecting the role of the somatic and visceral muscle during MET.

Several studies have noted the epithelialisation of the midgut cells upon contact with the visceral muscle (Reuter et al., 1993; Tepass and Hartenstein, 1994b; Wolfstetter et al., 2009). The integrin βPS appears to be a central part of midgut polarisation, providing a means for the midgut to interact with the major ECM component Laminin (Devenport and Brown, 2004; Pitsidianaki et al., 2021). Together with βPS, the $\alpha_{1,2}$ Laminin chain Wingblister (Wb) secreted by the visceral muscle is thought to play an important role during polarisation of the midgut by providing an initial basal cue (Pitsidianaki et al., 2021).

I therefore examined the localisation of Wb and βPS in *bin* mutants. In wildtype stage 12 embryos, Wb appears to be localised at the interface between midgut cells and the visceral muscle (Figure 10A, white arrowhead). βPS was basally localised in the midgut cells (Figure 10A, blue arrowhead). Surprisingly, Wb was also found at the interface between the midgut and somatic muscle in stage 12 *bin* mutants (Figure 10B, white arrowheads). Furthermore, βPS was also basally localised (Figure 10B, blue arrowhead), although it appeared that there were greater levels of lateral βPS as well (Figure 10B, blue arrow). Basal localisation of βPS suggested that the midgut in *bin* mutants were partially polarised; although βPS localisation was somewhat disrupted, there is a clear difference between basal and lateral domain. Furthermore, βPS stains suggest that there are no gaps between the midgut and the somatic muscle, indicative of adhesion between the two tissues, likely mediated by Wb.

In light of basal polarisation of βPS in the *bin* mutants, I next examined localisation of Talin, a major component of the integrin adhesion complex, which mediates the majority of integrin functions (Klapholz and Brown, 2017). In wild type embryos, Talin localisation appeared to be tightly restricted to the basal membrane (Figure 10C, arrowhead). In contrast, Talin localisation in *bin* mutants appeared to be dispersed (Figure 10C, blue arrow), but retained a basal bias (Figure 10C, white arrowhead). This could suggest a failure to traffic Talin or maintain Talin at the basal membrane.
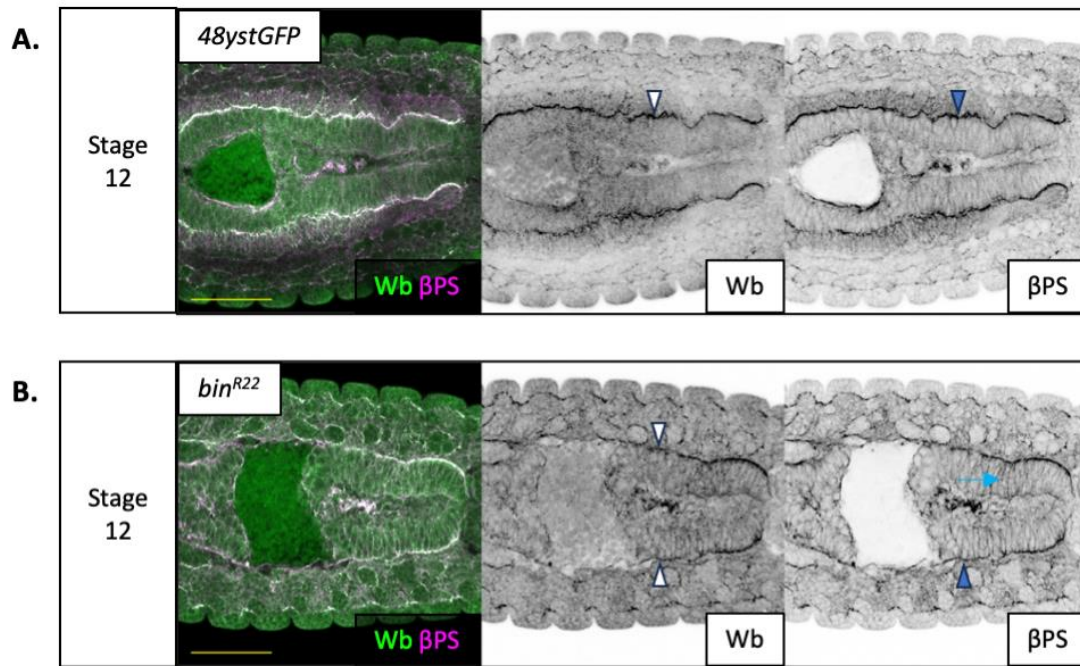
Figure 10. Mislocalisation of proteins in *bin* mutants suggests that the midgut is partially polarised but is unable to organise its apical domain.

A. Ventral view of stage 12 wildtype midgut stained for Wb and βPS. Wb is localised to the interface between the visceral muscle and the midgut (white arrowhead). βPS is polarised to the basal membrane of midgut cells (blue arrowhead).

B. Ventral view of stage 12 *bin* mutant midgut stained for Wb and βPS. Wb is localised to the interface between somatic muscle and the midgut (white arrowhead). βPS is polarised to the basal membrane of midgut cells (blue arrowhead). βPS may also be dispersed laterally (blue arrow). The midgut appears to maintain close contact with the underlying somatic muscle.

All scale bars 50μm.

48ystGFP, N = 6 embyros. *bin*, N = 6 embryos.

Figure 10. Mislocalisation of proteins in *bin* mutants suggests that the midgut is partially polarised but is unable to organise its apical domain.
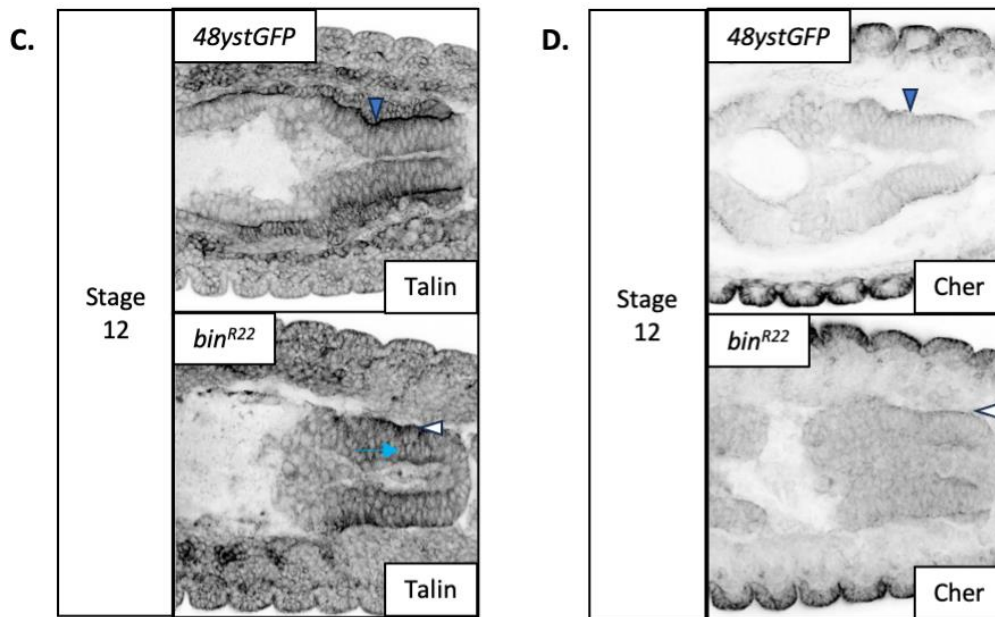
C. Ventral view of stage 12 embryos. Upper panel: Talin is localised to the basal membrane (blue arrowhead). Lower panel: Talin appears much more dispersed in *bin* mutant but retains a basal bias (white arrowhead). Talin also appears to be dispersed in the cytoplasm but also along the lateral membranes (blue arrow). 48ystGFP, N = 4 embryos. *bin,* N = 4 embryos.

D. Ventral view of stage 12 embryos. Upper panel: Cheerio is localised basally in wildtype (blue arrowhead). Lower panel: Localisation of Cher is largely lost, although faint signal appears along the basal membrane (white arrowhead).

All scale bars 50µm.

Talin stain: 48ystGFP, N = 4 embyros. *bin*, N = 4 embryos.

Cher stain: 48ystGFP, N = 14 embyros. *bin*, N = 18 embyros.

Next, I examined localisation of Cher/filamin, previously shown to be basally localised in wildtype midguts in an integrin-independent manner (Devenport and Brown, 2004). As previously reported, I found that Cher was basally localised in midgut cells of a wildtype stage 13 embryo (Figure 10D, arrowhead). However, localisation of Cher was largely lost in *bin* mutants, suggesting that the visceral muscle likely plays a role in its localisation (Figure 10D, compare WT and *bin*).

Previous work has established that organisation of the apical domain occurs downstream of the basal cues provided by Wb (Pitsidianaki et al., 2021). Given the presence of Wb and partial polarisation of the *bin* mutants, I next examined the localisation of Baz and Ecad, both known to be apical in the wildtype midgut (Pitsidianaki et al., 2021). In wildtype stage 13 embryos, both Ecad and Baz were apically polarised (Figure 10 E and F, blue arrowheads). In contrast, in *bin* mutants, the apical localisation of both proteins are lost, indicative of a failure to organise the apical domain (Figure 10E and F, white arrowheads, compare WT and *bin*).

Together, these results suggest that the midgut in *bin* mutants appear to retain some aspects of basal polarisation but fail to organise an apical domain. As previously suggested (Pitsidianaki et al., 2021), Wb at the interface between the midgut and somatic muscle likely facilitates adhesion between the two tissues. This in turn appears to be sufficient for basal localisation of βPS. Similarly, Talin appears to retain a basal bias. However, these basal cues appear to be insufficient to drive the organisation of an apical domain. This suggests that cues from the visceral muscle are critical for organisation of the apical domain. Basal localisation of Cher, previously shown to be independent of integrins, is also lost in *bin* mutants, suggesting that the visceral muscle is required to provide a basal cue that drives Cher localisation.
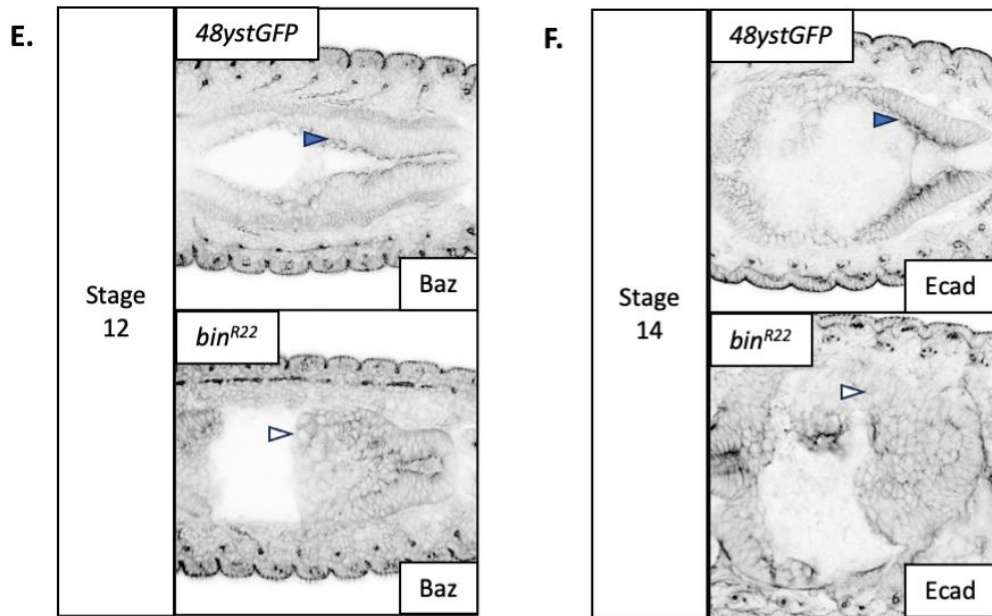
Figure 10. Mislocalisation of proteins in *bin* mutants suggests that the midgut is partially polarised but is unable to organise its apical domain.

E. Ventral view of stage 12 embryos. Upper panel: Baz is localised to the apical membrane (blue arrowhead). Lower panel: Baz appears punctate along the membrane of unpolarised midgut cells. (white arrowhead).

D. Ventral view of stage 14 embryos. Upper panel: Ecad is localised apically in wildtype (blue arrowhead). Lower panel: Localisation of Ecad is largely lost, it appears largely uniform around the membrane (white arrowhead).

All scale bars 50µm.

Baz stain: 48ystGFP, N = 20 embyros. *bin*, N = 12 embryos.

Ecad stain: 48ystGFP, N = 14 embyros. *bin*, N = 9 embryos.

A role for Wb in mediating adhesion of the mesoderm and midgut cells, as well as acting as an initial polarising cue, has been suggested by previous work from the lab (Pitsidianaki et al., 2021). However, MET failed in *bin* mutants despite the fact that Wb was present at the interface between the midgut and somatic muscle. In light of the fact that a βPS retained a basal bias, it was likely that this was mediated by Wb. Thus, I wanted to confirm whether Wb is able to drive basal localisation of βPS. Thus, homozygous *wb^PZ09437* mutant was examined to confirm its functions.

In wildtype embryos, the visceral muscle and the midgut remain in close contact with one another. In contrast to wildtype, *wb* mutants formed visible gaps in between the visceral muscle and the midgut (Figure 11A and B, blue arrows). Furthermore, basal localisation of βPS was completely absent, indicative of the absence of a basal polarising cue (Figure 11A, arrowheads, compare WT and *wb*). In line with previous work, apical localisation of Baz was also lost in these mutants (Figure 11B, compare WT and *wb*). These observations suggest that Wb plays a key role in adhesion and, given that it is a major binding partner for integrins, is also likely required for basal localisation of βPS.

Cher localisation was previously shown to be independent of integrins and also maintained despite gaps between the visceral muscle and the midgut (Devenport and Brown, 2004). I re-examined Cher localisation in *wb* mutants to confirm this. However, in my hands, basal localisation of Cher was largely lost in *wb* mutants (Figure 11C, compare WT and *wb*). Together with the results from *bin* mutants, it appears that Cher localisation is dependent on the presence of the visceral muscle but also requires Wb to be expressed. This could suggest that possible integrin-independent functions of Wb plays a role in mediating cues required for MET.

Reconsidering the *bin* mutants in light of these findings, it is likely that Wb at the interface between the midgut and somatic muscle in *bin* mutants mediates both adhesion and basal localisation of βPS. As such, the *bin* mutant likely represents a phenotype in which basal cues mediated by Wb are present. In other words, the failure to undergo MET observed in *bin* mutants is likely the results of loss of basal cues normally provided by visceral muscle.
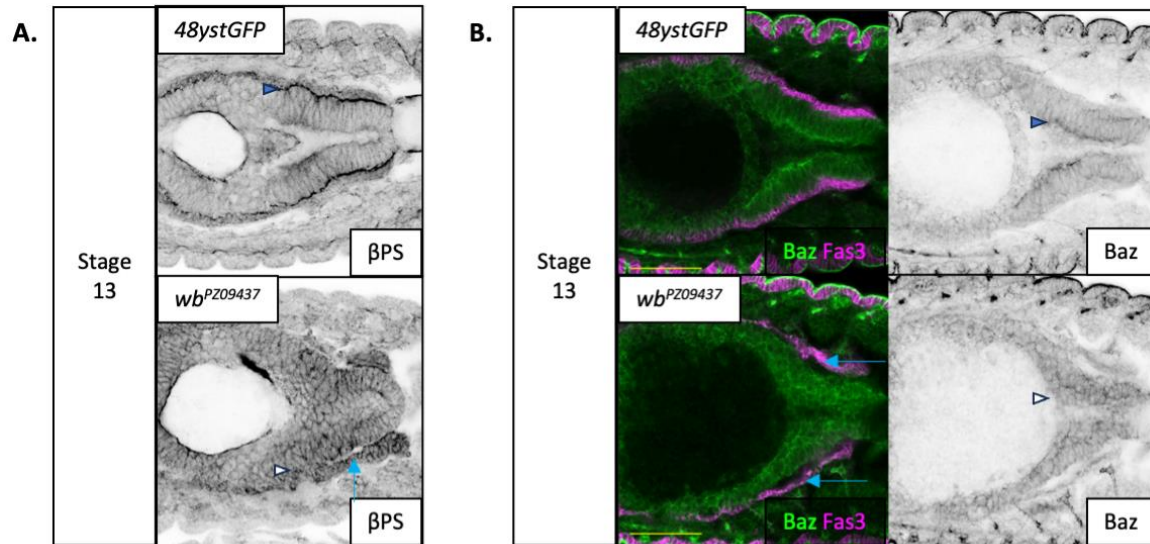
Figure 11. Complete loss of localisation βPS localisation upon detachment of the midgut from the visceral muscle suggests that adhesion mediated by Wb is a prerequisite for MET.

A. Ventral view of stage 13 embryos. Upper panel: βPS is localised to the basal membrane wildtype midguts. Lower panel: Gaps form between the midgut and visceral muscle (blue arrows). βPS localisation is lost in *wb* mutants. The phenotype is distinct from *bin* mutants such that no basal bias remains (compare with Figure 10B). 48ystGFP, N = 18 embryos. *wb*, N = 10 embryos.

B. Ventral view of stage 13 embryos. Upper panel: The midgut is adherent to the visceral muscle. Baz is apically localised (Blue arrowhead). Lower panel: Gaps form between the midgut and visceral muscle (blue arrows). Apical Baz is lost (white arrowhead). 48ystGFP, N = 18 embryos. *wb*, N = 7 embryos.
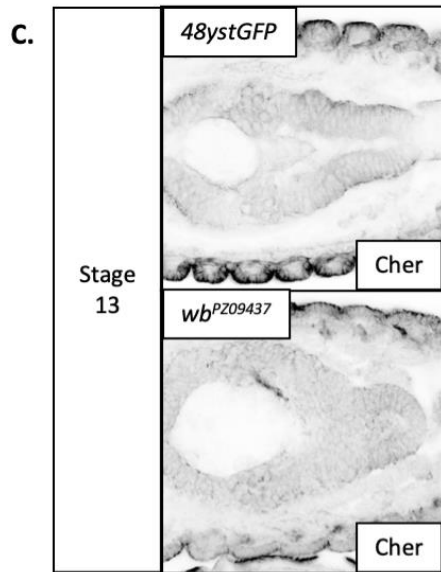
Figure 11. Complete loss of localisation βPS localisation upon detachment of the midgut from the visceral muscle suggests that adhesion mediated by Wb is a prerequisite for MET.

C. Ventral view of stage 13 embryos. Upper panel: Cher is basally localised in wildtype midguts. Lower panel: Cher localisation is lost in *wb* mutants. 48ystGFP, N = 18 embryos. *wb*, N = 10 embryos.

All scale bars 50μm.

2.1.4 Epithelial PMECs exhibit apical-basal microtubule arrays.

The *wb* and *bin* mutants demonstrate failure to undergo MET, likely due to loss of certain contact with the visceral muscle and/or basally localised βPS integrins. Previous work from the lab supports this idea, showing that organisation of the apical domain by αPS3 completely fails in *wb* mutants (Pitsidianaki et al., 2021), indicating that basal cues are required for the organisation of the apical domain that occurs later during MET. Given the importance of basal cues in polarisation, this raises the question as to how loss of basal cues translates into organisation of the apical domain. One such possibility is apical-basally oriented tubulin bundles. Tubulin bundles are known to be critical for intracellular trafficking in epithelial tissues (Müsch, 2004). Thus, the organisation of microtubules in wildtype and mutants were examined.

Staining for alpha-Tubulin in the wildtype midgut shows that epithelial cells have tubulin bundles that extend from the apical domain towards the basal domain (Figure 12, red lines to blue lines). These structures are found both pre-EMT (Figure 12A, stage 8) and post-MET (Figure 12C, stage 13), although the tubulin bundles appear less dense in stage 13 embryos (Figure 12C). It appears that these tubulin bundles are disassembled when the midgut cells transition to a mesenchymal state. Close examination of the stage 10 midgut (Figure 12B, yellow arrowheads) reveals short bars of tubulin within the cells. These are likely the spindle microtubules in dividing cells.

Staining for alpha-Tubulin in *bin* mutants showed an absence of polarised tubules in *bin* mutants. (Figure 13A, compare arrowheads). Additionally, the tubulin structures are much less dense and fainter compared to wildtype, suggesting a defect in tubulin bundling. Given that the midgut cells in *bin* mutants are adherent to the somatic muscle via Wb, the results suggests that adhesion to the somatic muscle is not sufficient to organise tubulin. Instead, it appears that the midgut specifically requires contact with the visceral muscle for tubulin organisation.

Staining for alpha-Tubulin in *wb* mutants showed an absence of polarised tubules (Figure 13B, compare arrowheads). Similar to *bin* mutants, the tubules are much less dense and fainter compared to wildtype. Given that midgut is detached from the visceral muscle in *wb* mutants,

this suggests that the presence of the visceral muscle is not sufficient to drive tubulin organisation but rather that adhesion to the visceral muscle is required for tubulin organisation in the midgut. Putting together the results from *bin* and *wb* mutants suggest that that adhesion specifically to the visceral muscle plays a key role in mediating this process.
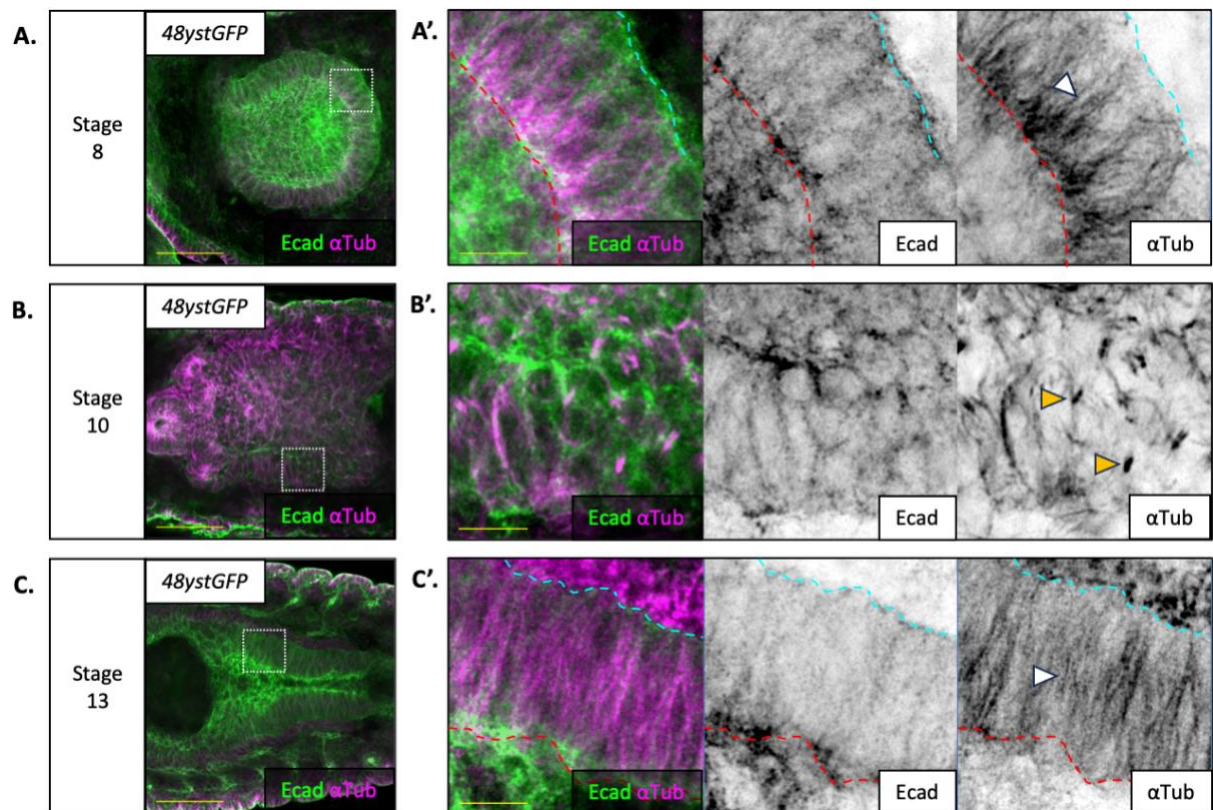
Figure 12. Apical-basal microtubule arrays are disassembled and reassembled during midgut development.

A. Dorsoventral view of a stage 8 embryo. The PMG is epithelial. Ecad is apically localised.

A'. Digital zoom of A. Apicobasal microtubule arrays can be observed (white arrowhead). Red and blue dotted lines indicate the apical and basal domains respectively.

B. Dorsoventral view of stage 10 embryo, showing the midgut undergoing EMT.

B'. Digital zoom of B. Sections of the midgut that have undergone EMT are more mesenchymal, indicated by the loss of apical Ecad and also appear to lose apicobasal microtubule arrays. Short bars within the midgut are likely to be the spindle microtubules that form during cell division (yellow arrows).

C. Dorsoventral view of a stage 13 embryo. The midgut is epithelial.

C'. Digital zoom of C. Apical localisation of Ecad is reacquired. Apical-basal microtubule arrays can be observed (white arrowhead), indicating that these have been reassembled during MET. Red and blue dotted lines indicate the apical and basal domains respectively.

A, B, C: Scale bars 50µm. A', B' C': Scale Bars 10µm

Stage 8, N = 4 embryos. Stage 10, N = 3 embryos. Stage 13, N = 7 embryos.
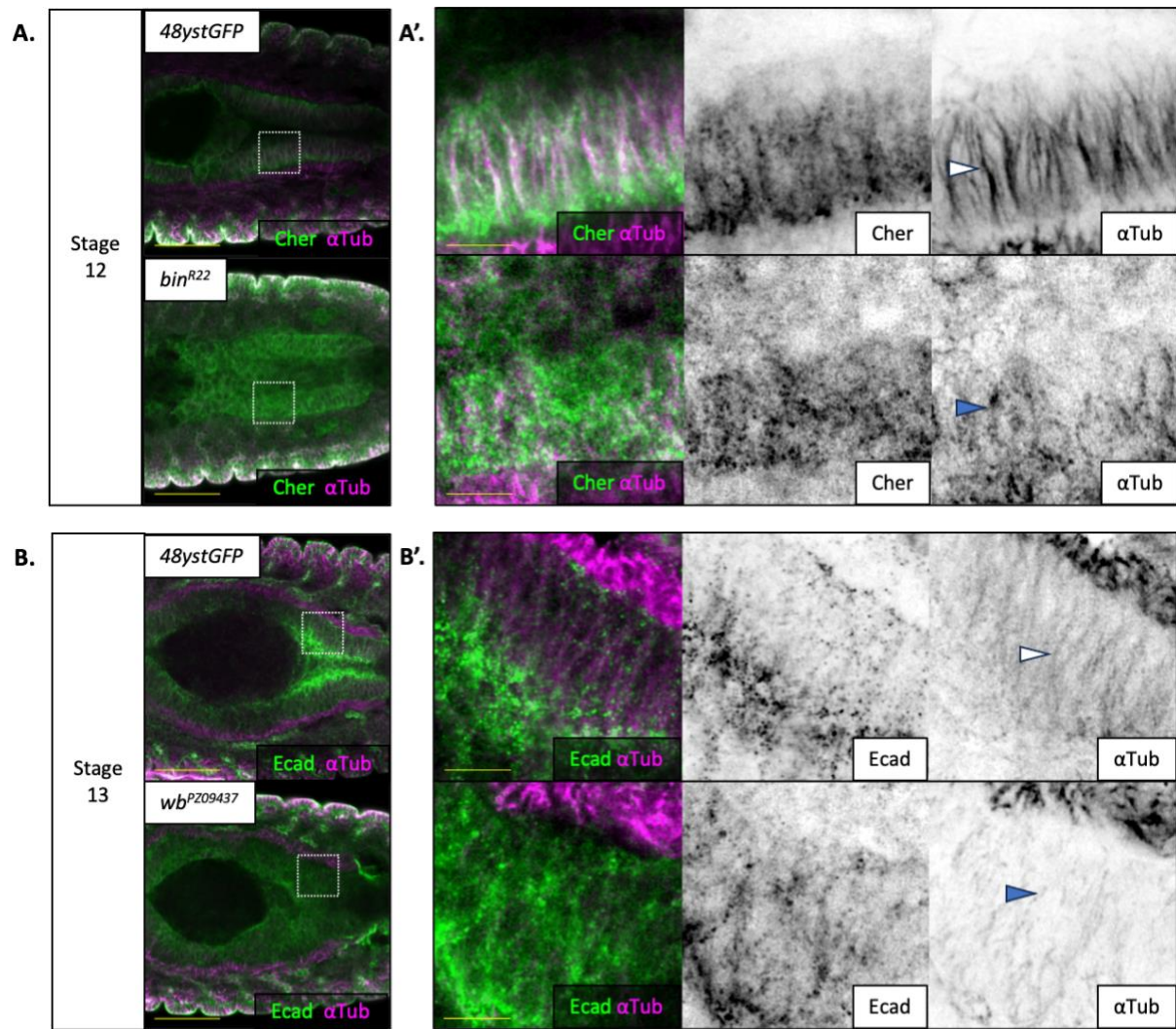
Figure 13. Formation of apical-basal microtubule arrays is disrupted in both *bin* and *wb* mutants.

A. Dorsoventral view of stage 12 embryos.

A'. Digital zooms of A. In wildtype, apical-basal microtubule arrays can be seen (white arrowheads). In *bin* mutants, these microtubule arrays appear to be lost (blue arrowhead).

B. Dorsoventral view of stage 13 embryos.

B'. Digital zooms of B. In wildtype, apical-basal microtubule arrays can be seen (white arrowheads). In *wb* mutants, these microtubule arrays appear to be lost (blue arrowhead).

A, B: scale bars 50µm. A', B': Scale Bars 10µm.

Stage 12 *48ystGFP*, N = 4 embryos. Stage 12 *bin*, N = 3 embryos. Stage 13 48ystGFP, N = 7. Stage 13 *wb,* N = 9.

<u>2.1.5 Characterising and quantification of cell shape reveals gradual changes in cell shape over time during normal MET.</u>

One of the critical outcomes of MET is the change in cell shape from an irregular mesenchymal shape to columnar epithelium. Thus, I aimed to characterise and measure cell shape in wildtype and *bin* mutants across stage 12 and 15 to examine the changes that occur during normal MET and the consequences of disrupting this process. Furthermore, I investigated whether a quantified measure of cell shape could be used as a measure of how epithelial or mesenchymal cells are, which will be referred to as EM state. Being able to quantify EM state would allow for statistical comparisons to be made in other mutants with aberrant MET.

To assess cell shape changes during MET, Resille-GFP (GFP[CG8668-117-2]) and Spider-GFP (gish[Spider]) constructs were used to label the cell membrane. Resille-GFP is a GFP tagged form of CG8668, a membrane protein orthologous to human beta-1,3-galactosyltransferase (Gramates et al., 2022). Spider-GFP is a GFP-tagged form of Gilgamesh (gish), a plasma membrane kinase. Both have been previously used to look at cell shape (Mateos et al., 2020; Reversi et al., 2014). To examine cell shape in wildtype, a fly line with both the Resille-GFP and Spider-GFP constructs was used. It was subsequently found that Resille-GFP alone was sufficient to examine cell shape Furthermore, Spider-GFP appeared to cause more background when studying the midgut, as seen by the signals observed in the yolk. Thus, only the Resille-GFP construct was used to examine cell shape in homozygous *bin* mutants (compare *Resille-GFP; Spider-GFP* vs *Resille-GFP; bin* in Figure 14A vs 14B). Although it should be noted that the cell membrane was labelled in different ways in wildtype and *bin* mutants, the lack of Spider-GFP in *bin* mutant embryos is unlikely to cause any differences in cell shape measurements.

Wildtype cell shape suggests that significant cell shape changes and tissue organisation occur during MET. Examination of the epithelium at stage 12 shows some cells extend throughout the epithelium, indicative of a pseudostratified epithelium (Figure 14A, yellow arrows). Furthermore, examining the cells across z-stacks suggests that many of the cells that initially appear multi-layered are also intact throughout the epithelium, indicating that many cells weave in and out of the z-stack at this stage. In contrast, many more cells stage 13 onwards extend throughout the monolayer in single-z stack images (Figure 14A, yellow arrows),

suggesting that PMECs shift from a pseudostratified epithelium with cells that interweave with one another to a more regular columnar monolayer throughout MET. Given that the midgut cells form a single cluster at stage 10, it appears that the midgut cells shift sequentially from a mesenchymal state, pseudostratified epithelium, and to a columnar monolayer. Given that the formation of a pseudostratified epithelium appears to occur prior to stage 12, earlier stages may be of interest for future experiments for a more comprehensive examination of how these cell shape changes occur. In contrast, there does not appear to be a significant cell shape change in *bin* mutants; cells maintain irregular cell shapes and fail to organise an apical domain (Figure 14B, arrowheads).
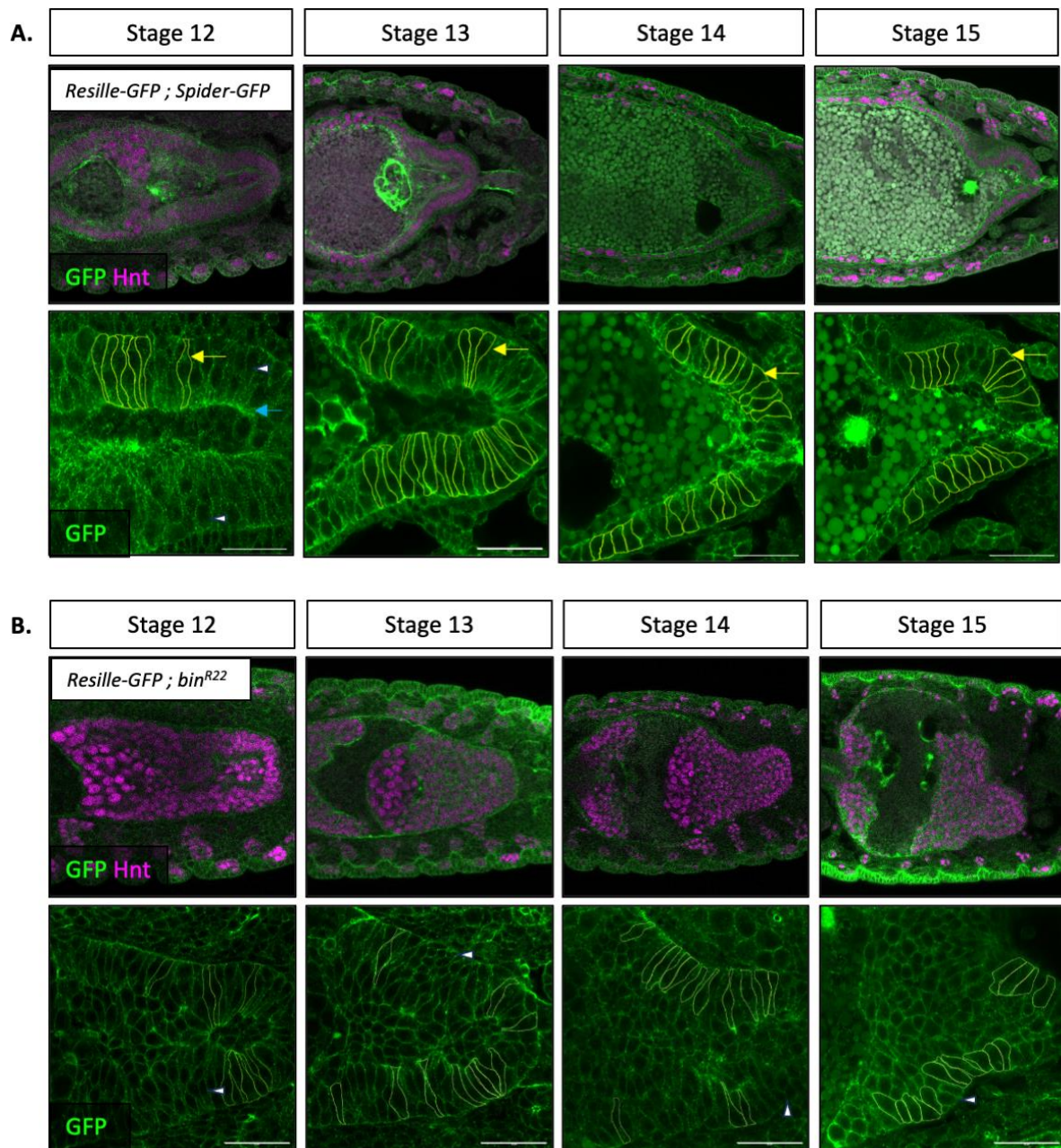
Figure 14. Cell shape changes during MET in wildtype and MET.

A &B. Ventral view of wildtype embryos between stage 12 to 15. Upper panels show overview of the midgut. Lower panels show 63x AiryScan images. All scale bars 20μm.

A. Yellow outline indicates cells used for quantification. Yellow arrows point to cells that extend throughout the epithelium. White arrowheads point to cells that appear multi-layered in stage 12 embryos. Blue arrow points to diffuse GFP signal in stage 12 embryos, possibly indicative of apical trafficking. In wildtype, apical-basal microtubule arrays can be seen (white arrowheads). In *bin* mutants, these microtubule arrays appear to be lost (blue arrowhead).

B. Yellow outline indicates cells used for quantification. White arrowheads point to cells with irregular shapes.

To quantify the images, I needed to create masks by segmenting cell shape from the images captured. In order to segment cells, I initially attempted to use 2D CellPose, a deep learning based segmentation tool trained on image sets from both *in vivo* and *in vitro* experiments (Stringer et al., 2021). Unfortunately, CellPose tended to cut irregular concave-shaped cells into two cells and did not accurately segment along the membrane. Thus, the masks for the following results were drawn manually. The masks were then quantified using ImageJ's in-built Circularity measurements.

The cell shapes of the posterior-most portion of the posterior midgut were quantified, corresponding to the most organised region of the *bin* mutants (Figure 14A and B). This was done as to allow for like-to-like comparisons to be made between the same sub-population of PMECs; the more anterior regions of bin mutants are more unorganised and make it difficult to compare to wildtype. Thus, it should be noted that the changes observed reflect a conservative comparison between wildtype and *bin*.

The circularity of wild type cells indicated that the cells undergo shape change in a gradual manner between stage 12 and 14 (Figure 14C). This corresponds to cell shape changes observed, as the cells are initially elongated at stage 12 but appear to gradually flatten against the visceral muscle (Figure 14A). Cell shape changes appear to plateau at stage 15, which indicates that the bulk of cell shape change occurs between stage 12 and 14. In contrast, *bin* mutants appear to undergo little cell shape changes until a large shift between stage 14 and stage 15 (Figure 14D). Although the quantified data may appear to indicate that difference in cell shape in the *bin* mutant is rescued at stage 15 (Figure 14E, compare stage 15), qualitative observations reveal differences in organisation. Wildtype PMECs form a distinct epithelial monolayer showing an alignment of their apical domains, while *bin* mutant PMECs are multi-layered. The results indicate that wildtype undergoes a series of cell shape changes that does not occur in *bin* mutants. While the method of quantification used can capture differences between two states, it does not appear to be a good measure of EM state; this is best highlighted by the fact that epithelial cells in stage 15 wildtype have a similar circularity with the irregularly shaped cells in stage 15 *bin* mutants.
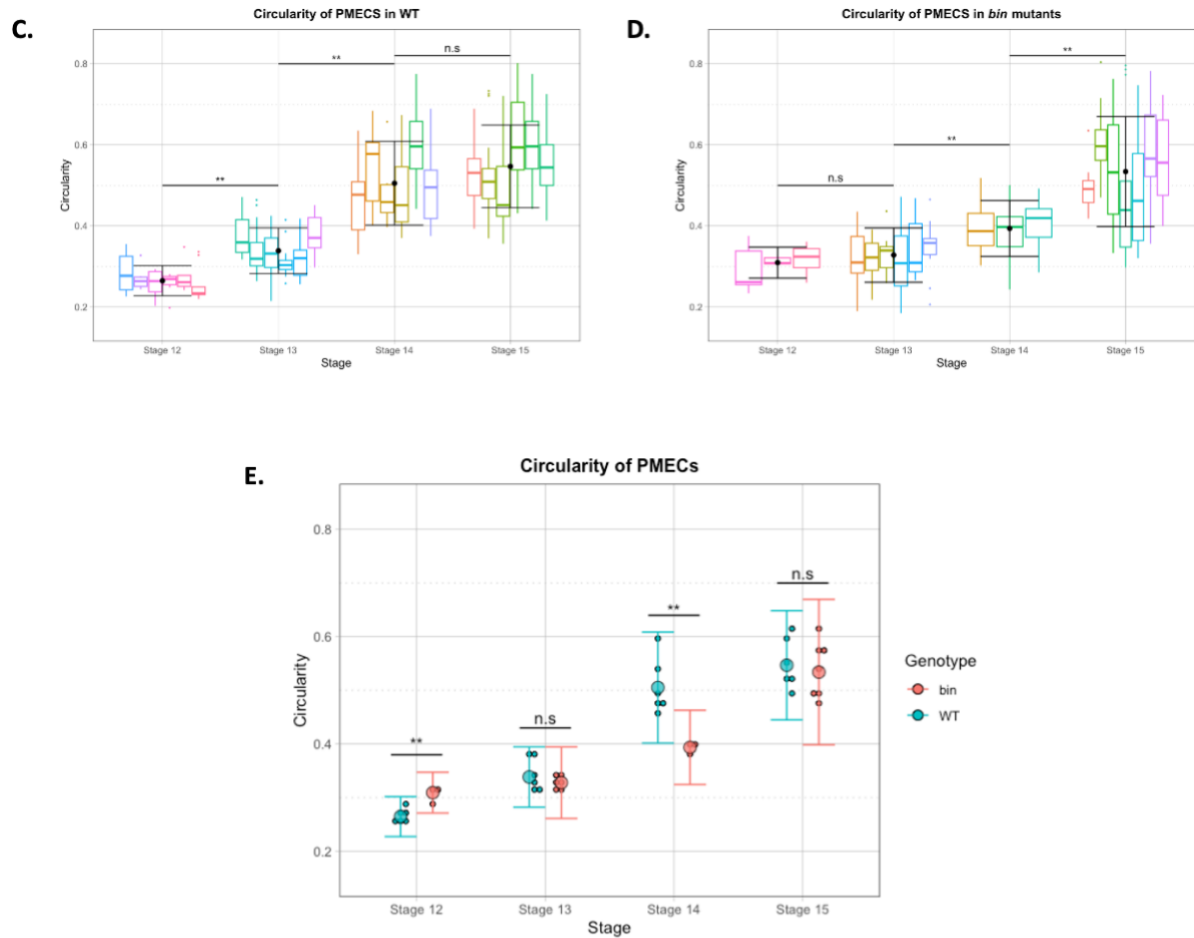
Figure 14. Cell shape change during MET in wildtype and MET.

C, D and E. Circularity of PMECs during MET. A minimum of 6 cells were measured in each embryo.

C and D. Circularity of wildtype (C) and bin (D) PMEC cell shape. Each box plot represents the distribution of cell shapes from one embryo. The black dot represents the average of the mean circularity of each embryo. Error bars are standard deviation.

E. Summary graph showing circularity of wildtype and *bin* mutant PMEC cell shape. Each smaller dot indicates the mean of each embryo. Larger dot indicates average of genotype. Error bars are standard deviation.

Wildtype, N = 5, 6, 6, 6 embryos for stages 12, 13, 14, 15 respectively.

*bin,* N = 3, 6, 3, 6 embryos for stages 12, 13, 14, 15 respectively.

<u>2.1.6 Nuclear shape changes according to EM states but is not a robust qualitative measurement.</u>

Circularity of cell shape did not appear to be a good measure of EM states. An alternative to cell shape may be to use cell nuclei. In agreement with this, in vitro studies have shown that EMT correlates with changes in nuclear shape (Leggett et al., 2016). Thus, I examined nuclear shape change throughout midgut development to see if cell nuclei can be used as a proxy for EM state. Nuclear cell shape was detected in a semi-automated manner using StarDist 2D, an object-detection plugin for star-convex shape priors (Schmidt et al., 2018).

Nuclear shape was quantified using ImageJ's in-built formula for circularity. Single Z-stacks of stage 8, 10 and 13 embryos of flies with the 48y-Gal4 driver expressing nuclear stinger-GFP reporter (48ystGFP) were imaged (Figure 15A). Stage 13 midguts could not be imaged in the same orientation as prior stages; the midgut at stage 13 is positioned ventrally and cannot be imaged from the dorsal side like with stage 8 and 10 midguts. As a result, imaging the gut in the same embryo at the 3 selected stages was not possible. Thus, the data reflects unpaired datasets; each embryo was imaged at a single timepoint.

In wildtype embryos, epithelial cells at stage 8 were less circular compared to mesenchymal cells at stage 10, suggesting a quick, dramatic change in nuclear shape during EMT (Figure 15C). While nuclear shape at stage 13 tended to be less circular than stage 10, these changes were not statistically significant (Figure 15C). The mild differences between stage 10 and 13 in WT suggests that circularity of nuclear shape is a poor indicator of EM states.
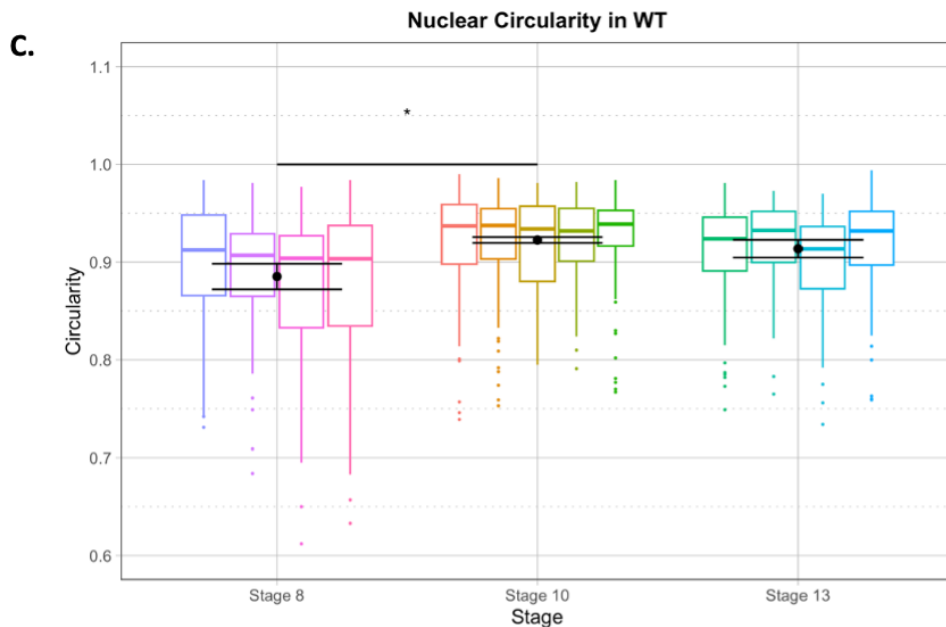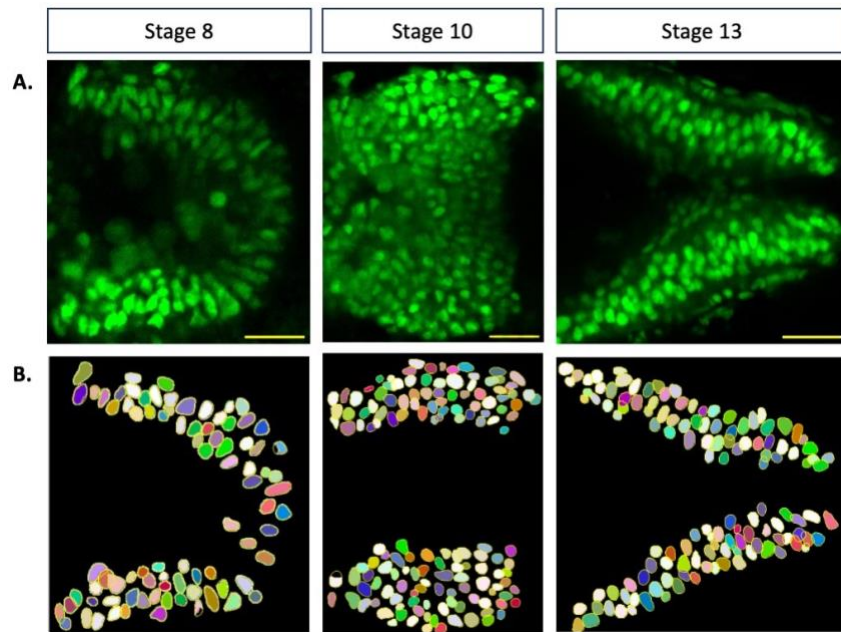
Figure 15. Nuclear shape cannot be used as a proxy to measure EM state.

A. Stardist 2D allows for nuclear shape to be segmented in a semi-automated way. Examples show masks overlayed on top of the microscopy images of the midgut expressing nuclear GFP. Scale bar 20μm.

B. Examples of segmented masks.

C. Nuclear circularity in wildtype. Each boxplot represents the distribution of the values measured in each embryo. Black dots represent the average of the mean circularity measured from each embryo. Asterix indicates significance to 0.05. (Stage 8 vs Stage 10, p = 0.046). N = 4, 5, 4 for stages 8, 10 and 13 respectively.

2.2 Discussion:

The visceral muscle has been considered to be an important basal substrate for midgut migration and MET (Devenport and Brown, 2004; Pitsidianaki et al., 2021; Reuter et al., 1993; Tepass and Hartenstein, 1994b). In this chapter, I aimed to characterise migration and MET in wildtype and *bin*^*R22* mutants to examine the role of the visceral muscle. First, due to conflicting reports regarding the presence of the longitudinal muscle in *bin*^*R22* mutants, I examined FasIII and Tey stains to look for any visceral muscle around the midgut. No tissue positive for either marker was found around the midgut in *bin*^*R22* mutants, confirming that the *bin*^*R22* mutants lack all visceral muscle.

Having established *bin*^*R22* mutants as a mutant that lacked visceral muscle, I examined midgut migration. In wildtype, the midgut makes contact with the circular visceral muscle during migration (Wolfstetter et al., 2009) and thus, was thought to be critical for migration. Additionally, delay or failure of gut fusion, as seen in *bin*^*R22* mutants, was previously used as an indicator for perturbed migration (Pert et al., 2015). Therefore, it was unexpected that there was measurable no difference between wildtype and *bin*^*R22* mutants at stage 10, despite the absence of the visceral muscle.

Critically, this finding suggests that the visceral muscle does not play a role in initiating migration or during early migration. Furthermore, considering that migration fails outright in the absence of all mesoderm, as seen in *sna twi* double mutants, the results also suggests that the somatic muscle, which underlies the midgut in *bin*^*R22* mutants, is sufficient to support the initiation of midgut migration. Finally, the similarity in migratory capacity indicates that *bin*^*R22* mutants and wildtype midgut cells have a comparatively similar intermediate mesenchymal phenotype. In light of this, it can also be concluded that the subsequent failure to undergo midgut fusion and MET in *bin* mutants is not the result of any differences in mesenchymal phenotype at stage 10.

The finding that the visceral muscle does not play a role in collective migration may contradict the finding that Netrins secreted from the visceral muscle contribute to migration (Pert et al., 2015). Differences in the way cell migration was studied may resolve aspects of this

contradiction. Firstly, the method used to quantify migration in *bin* mutants focused on stage 10, focusing on the initiation of migration. In contrast, the methods used to examine the role of Fra-Netrins during migration relied on measuring the gap between the AMG and PMG at stage 12 and 13 as a readout for migration speed. Although the capacity to migrate was unchanged in *bin* mutants at stage 10, later stages of migration may indeed be affected by the absence of the visceral muscle. Thus, without looking at later stages, it is not clear whether PMEC migration at later stages is affected in *bin* mutants. Thus, this apparent contradiction cannot be reconciled without further experiments. Future experiments quantifying midgut migration in *fra* and *netAB* mutants with the same methods used for wildtype and *bin* mutants would help resolve this conflict. Regardless, it seems clear that early midgut migration can be supported by the somatic muscle.

Integrins and laminins are key mediators of MET (Devenport and Brown, 2004; Pitsidianaki et al., 2021). It was previously suggested that the laminin chain Wb plays important roles in mediating adhesion (Pitsidianaki et al., 2021). The visceral muscle is a major contributor of Wb during MET (Pitsidianaki et al., 2021), and thus it was expected that in the absence of the visceral muscle, *bin* mutants would lack basal laminin to adhere to. It was therefore surprising to see Wb at the interface between the midgut and somatic muscle in *bin* mutants. It remains unclear which tissue is responsible for the Wb found at the interface of the two tissues in *bin* mutants. Experiments blocking secretion of Laminins by driving the a Sar1-Dominant Negative construct in either tissue (Pitsidianaki et al., 2021) could help identify which tissue is responsible for Wb secretion.

The importance of Wb for midgut adhesion to a basal substrate confirmed upon examining *wb* mutants; the absence of Wb causes the midgut to detach from the underlying visceral muscle. Furthermore, this loss of adhesion completely disrupts βPS localisation, despite the presence of the visceral muscle. Thus, it appears that adhesion mediated by Wb is a requirement for polarisation. Reconsidering *bin* mutant phenotypes in light of these observations also indicates that adhesion mediated by Wb is not sufficient to drive MET; despite the fact that basal Wb and βPS is maintained in *bin* mutants, basal localisation of Cheerio and the organisation of the apical domain is disrupted, indicative of a failure to drive

MET. Thus, it appears that adhesion to somatic muscle is not sufficient to drive MET, and thus supports the idea that the visceral muscle is specifically required for midgut MET.

It remains unclear what drives localisation of Cher. Published results showed that basal localisation of Cher was retained in mutants for both β integrin subunits, indicating that Cher localisation was independent of integrin mediated signals, as well as adhesion (Devenport and Brown, 2004). Thus, I hypothesised that Cher localisation would be mediated by cues from the visceral muscle. This was also supported by findings that Fra and Netrins play a partial role in the localisation of Cher (Pert et al., 2015). In line with this, Cher localisation was lost in *bin* mutants, and as such suggests that the visceral muscle is required in driving its localisation. However, I also found that Cher localisation was also lost in Wb mutants. If Cher localisation is independent of adhesion, integrin-mediated signals and requires the visceral muscle, the fact that Cher localisation is lost in *wb* mutants despite the presence of the visceral muscle suggests that Cher localisation is downstream of cues mediated by the visceral muscle. This also suggests Cher localisation is dependent on Wb, unrelated to its role in adhesion or integrin signalling. In support of this, laminins play a critical role to organise the basal membrane (Urbano et al., 2009); loss of LanB1 is known to disrupt ECM organisation in stage 17 embryos. Given that LanA is lost from the midgut-muscle interface in in *wb* mutants (Pitsidianaki et al., 2021), the loss of both laminin α chains likely results in the loss of Laminin heterotrimers. Thus, this suggests that the organisation of the basal ECM would be disrupted in *wb* mutants. Put together, this could indicate that specific signals from the visceral muscle, mediated via the ECM, drives localisation of Cher.

Previous work from the lab showed that organisation of the apical domain by βv is downstream of cues provided by Wb (Pitsidianaki et al., 2021). My results suggested that cues driving basal polarisation provided by Wb were maintained in *bin* mutants but failed to organise the apical domain. The failure to translate these basal cues into organisation of the apical domains suggested a breakdown in a functional link between the processes. I hypothesized that tubulins could play a role in this process. Examining tubulin formation in wildtype showed that the midgut cell post-MET reformed polarised tubulin bundles oriented parallel to the lateral membrane. These polarised tubulin bundles were lost in both *wb* and *bin* mutants, suggesting that adhesion to the visceral muscle is required for tubulin

organisation but also that adhesion to the somatic muscle is not sufficient, further emphasising the importance of the visceral muscle. Further experiments will be needed to examine the roles of these microtubules. I attempted to sever microtubules to see whether the formation of apical domains was downstream or upstream to microtubule organisation, but these experiments were inconclusive.

Finally, examining cell shape changes over time revealed a gradual but continuous change in cell shape throughout stages 12 to 15; the epithelium appeared to shift from pseudostratified epithelium to a monolayer. During this shift, cells in the pseudostratified epithelium appeared to straighten their lateral membranes to form more columnar cells. These cell shape changes were lost in *bin* mutants.

Put together, close examination of wildtype and *bin* mutant embryos indicate that MET is a multi-faceted sequential process (Figure 16). Adhesion mediated Wb to a basal substrate appears to be a key initial step required for the localisation of βPS (Figure 16, steps 1 and 2). This is followed by organisation of the apical domain and organisation of tubulin structures (Figure 16, steps 3 and 4); although which comes first is unclear, it appears that both of these processes require cues from the visceral muscle. Basal polarisation of Cher appears to be a parallel process independent of integrin mediated signals, but likely requires an intact ECM and cues from the visceral muscle. It is likely that these mechanisms work together to drive the cell shape changes that occur during MET, enabling the midgut to transform from a pseudostratified epithelium into a more columnar monolayer. The *bin* mutants show that basal cues mediated by Wb is not sufficient for MET and that various aspects of MET appear to specifically require the visceral muscle. Thus, the role of the visceral muscle during MET will be investigated in the following chapters.
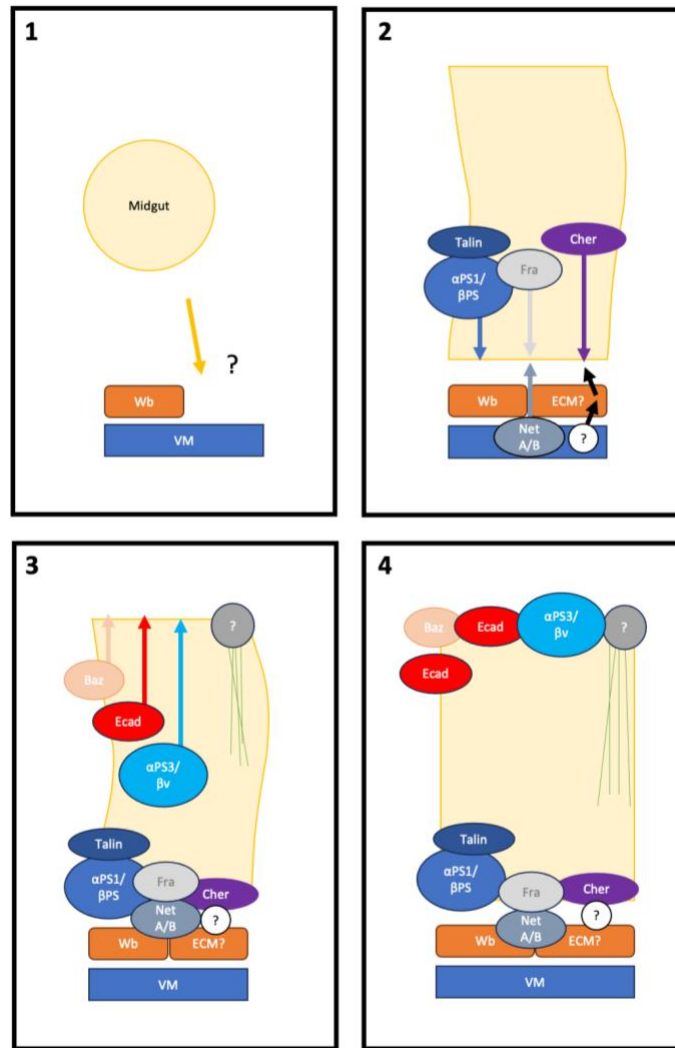
Figure 16. Schematic of processes that occur during MET.

1. Midgut comes into contact with the visceral muscle. Wb likely mediates adhesion of the midgut to the visceral muscle. It is unclear what drives the mesenchymal midgut cell to come into contact with the visceral muscle.

2. Wb at the interface between the visceral muscle and the midgut drives basal polarisation of αPS1βPS integrin dimers. NetAB from the visceral muscle drives basal polarisation of Fra. The mechanisms driving basal polarisation of Cher but is thought to be dependent on cues from visceral muscle that also depend on the organisation of the ECM. The epithelial is a pseudostratified and cell shapes are irregular.

3. Basal cues are thought to drive organisation of the apical domain including apical localisation of Baz and αPS3βv, and apicolateral localisation of Ecad. Organisation of aligned tubulin bundles oriented in an apicobasal manner is also thought to be downstream of basal cues.

4. Cell shape changes continue up until stage 15. Lateral membranes become more linear as the cells adopt a more regular shape to form a columnar monolayer.

Chapter 3. scRNA-seq Analysis reveals potential mechanisms underlying MET.

3.0 Introduction to scRNA-seq

Single cell RNA-sequencing (scRNA-seq) allows for the sequencing of mRNA transcripts within individual cells, and therefore provides an insight into patterns of gene expression, developmental lineage and function of the sampled tissue or organism. For example, scRNA-seq data of the *Drosophila* adult midgut has previously been used to reconstruct lineage trajectories and identify new markers of enteroendocrine (EEs) cells. Furthermore, five neuropeptides previously not known to be expressed by EEs were identified (Hung et al., 2020). Thus, this demonstrates that scRNA-seq can be used to infer information about developmental lineage and function of different cell types.

To construct a scRNA-seq atlas of gene expression in midgut cells and the surrounding tissues during early stages of development, the posterior region of the embryo was dissected from living embryos from four different developmental timepoints were sequenced. The timepoints corresponded to key steps during midgut development: timepoint 1 captured the pre-EMT epithelial state; timepoint 2 captured EMT; timepoint 3 captured migration and MET and timepoint 4 captured the post-MET epithelial state (Figure 1A, bottom schematic). For each timepoint, the dissected posterior region from 100-150 embryos were pooled together. Details regarding the methods for dissection and single cell sequencing have been described in Plygawko et. al, 2024 (in submission) and are also outlined in the methods section. In addition to the wildtype midguts, *bin* mutant midguts at stages 13-14, corresponding to stages post-MET in wildtype were also dissected and sequenced. Embryo dissections and single cell sequence sample preparation were performed by Kyra Campbell.

Unsupervised clustering of the wildtype cells from all four timepoints gave rise to four distinct clusters (Figure 1A, UMAP), corresponding to the endoderm, mesoderm, ectoderm, and germ cells. The different cell populations were identified using known marker genes (Figure 1B) (from Plygawko et. al, 2024, in submission).

Distinct lineages within these clusters were identified using Monocle (Trapnell et al., 2014), a program designed to calculate transcriptional similarity between cells. By ordering cells by transcriptional similarity, the program is able to order cells based on relative progression through a differentiation process. This measure of relative progression was dubbed Pseudotime. Crucially, by calculating Pseudotime across a group of cells, the program is able to detect branching differentiation lineages and thus, identify precursor cells with no input regarding the cell type, its gene expression or collection timepoint. Upon calculating Pseudotime of the wildtype scRNA-seq data, the Pseudotime largely corresponded to the timepoints in which cells were sampled. This suggested that the scRNA-seq data captured the differentiation of cells. The UMAPs in Figure 17 were generated using Seurat and Monocle by Camille Stephan-Otto Attolini.

In this chapter, I leverage the scRNA-seq data to examine transcriptional changes within the PMEC population and the mesoderm population. Using this data, I investigate the expression patterns of genes thought to play a role in MET. From this, I confirm that the mechanisms governing polarity post-MET are distinct from those governing polarity mechanisms pre-EMT. Given that just the visceral, but not the somatic muscle, is capable of supporting MET, I examined for genes specifically upregulated in the circular visceral muscle that are not expressed in the somatic muscle. Finally, I outline an approach used to investigate possible interactions between the visceral muscle and the midgut to identify candidate genes that may play a role in driving MET.
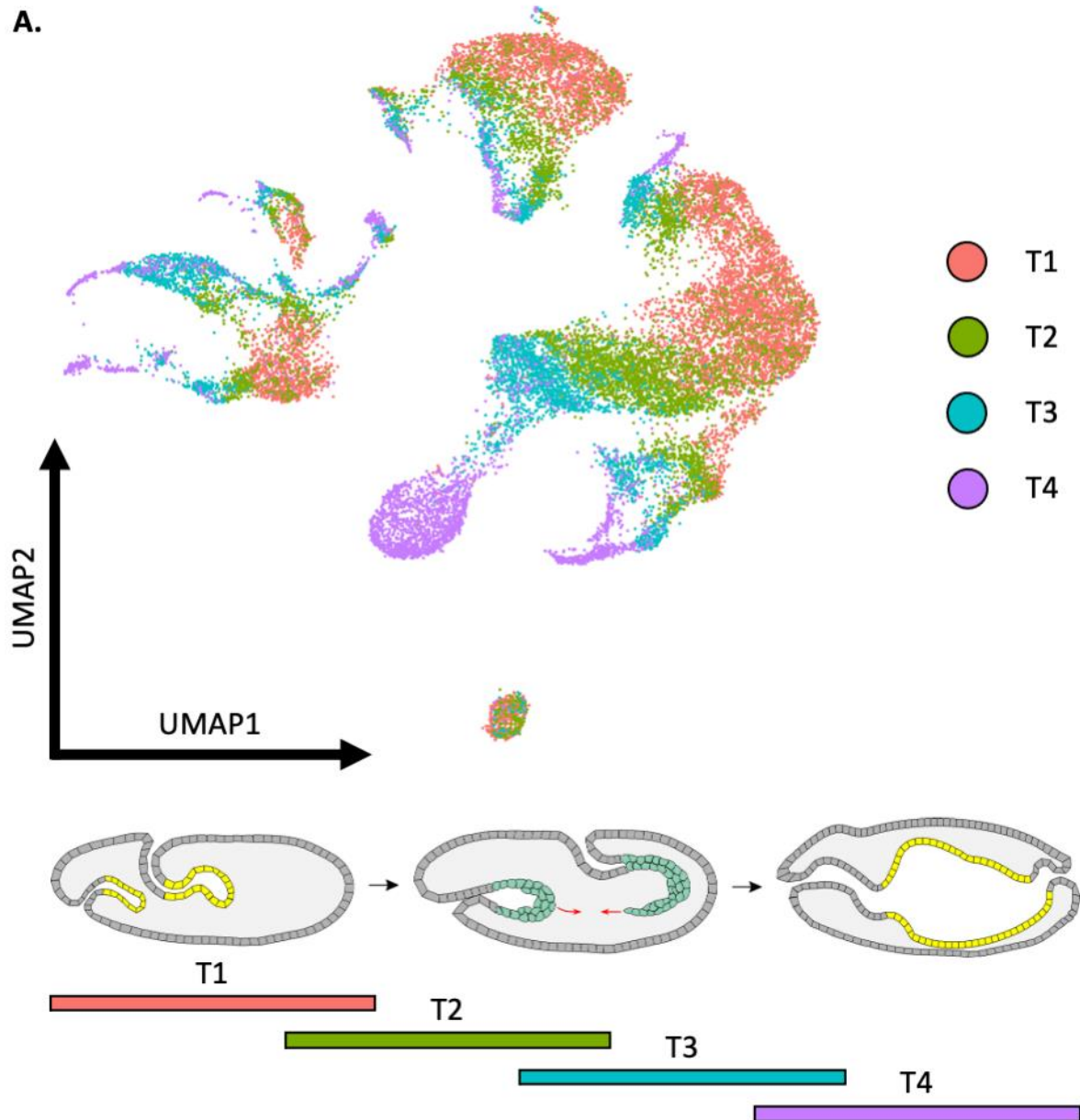
A.

Figure 17. scRNA-seq data of the dissected midguts from embryos at four different timepoints reveals transcriptional changes in the midgut and muscle population throughout development. From (Plygawko et al., 2024).

A. Single cell sequencing data represented on a Uniform Manifold Approximation and Projection (UMAP). Each dot represents a cell. UMAP is coloured according to the timepoints at which the embryos were sampled. Distance within clusters correlate with differences in transcription such that cells closer together within a cluster reflect similar transcriptional state. Distances between clusters do not correlate with differences in transcription.

B.

Figure 17. scRNA-seq data of the dissected midguts from embryos at four different timepoints reveals transcriptional changes in the midgut and muscle population throughout development.
From Plygawko et al., 2024.

B. Clusters labelled using known markers of distinct cell types. The clusters can be divided into four major populations, corresponding to the endoderm, mesoderm, ectoderm, and germ cells. Within these clusters are key sub-populations. For example, the largest of the clusters, which correspond to the endoderm, consist of cells from the midgut and the Malpighian tubules.
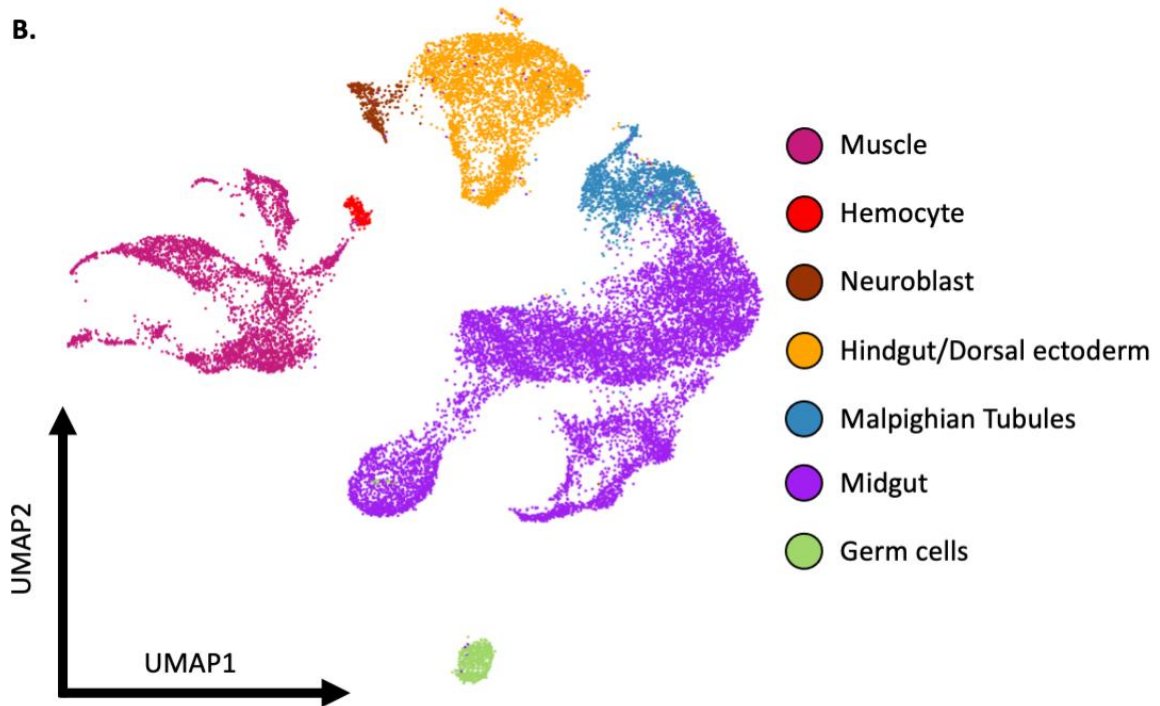
C.
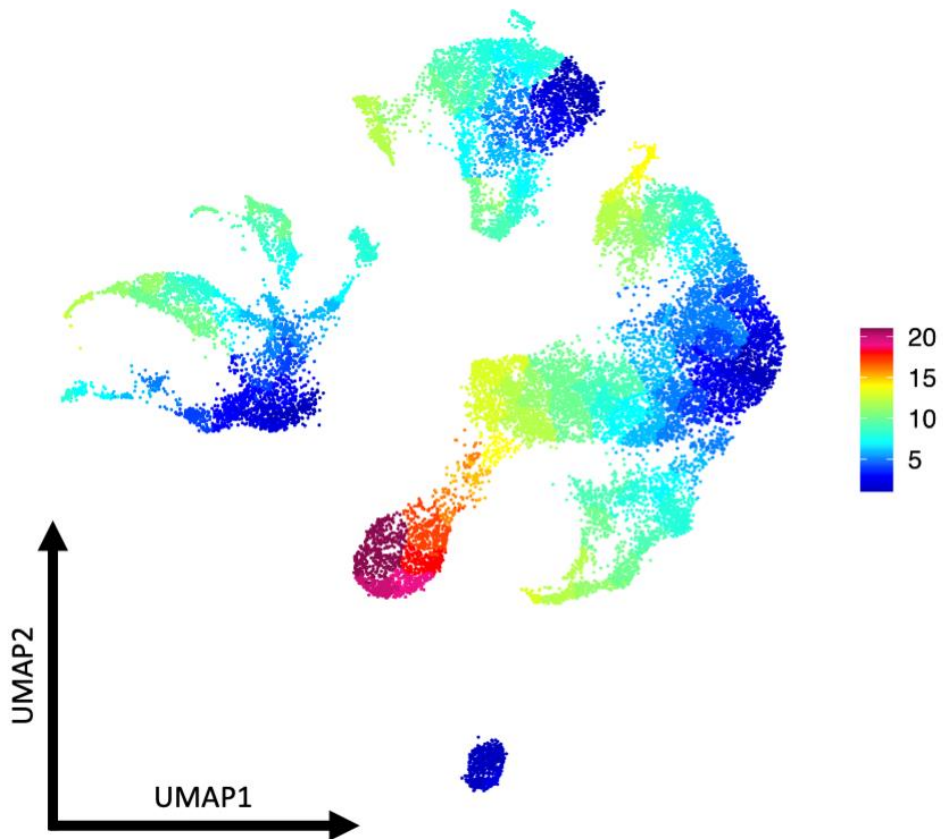
Figure 17. scRNA-seq data of the dissected midguts from embryos at four different timepoints reveals transcriptional changes in the midgut and muscle population throughout development. From Plygawko et al., 2024.

C. Pseudotime plot reveals distinct lineages within clusters. With the exception of germ cells, cells early in development (dark blue) appear to differentiate to give rise to a number of different cell types. The cluster corresponding to the midgut appeared to undergo the greatest amount of transcriptional change.

3.1 Results

3.1.1 Examining PMEC Gene expression.

The midgut population, identified by expression of a combination of marker genes including *hindsight* (*hnt*) and *GATAe*, was extracted from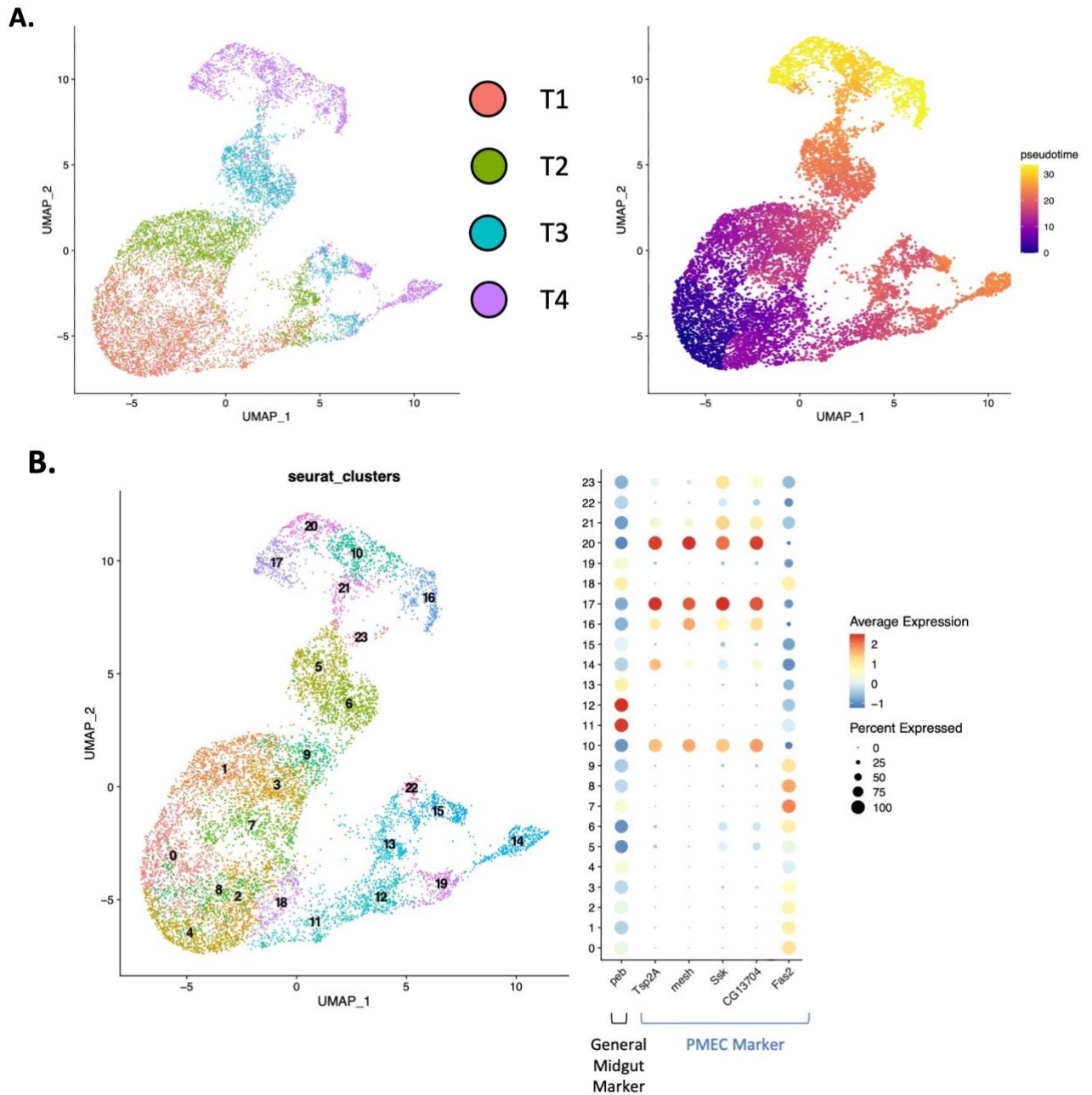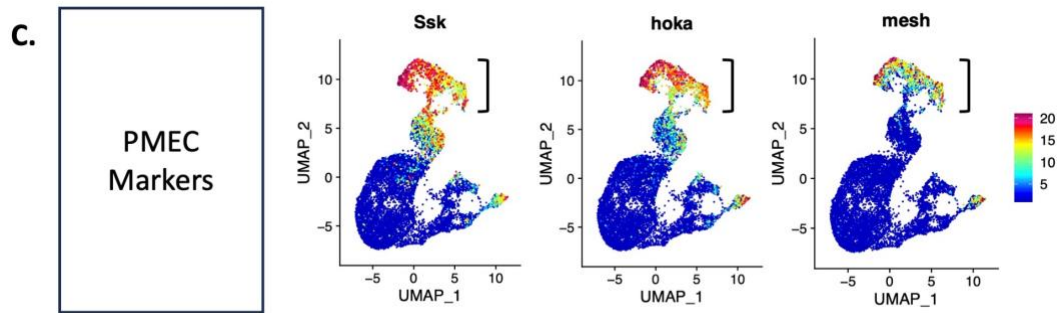 the whole dataset and plotted separately on a UMAP (Figure 18A). The midgut UMAPs and dot plot in Figure 18 were generated using Seurat and Monocle by Camille Stephan-Otto Attolini. Comparing the plots showing sampling timepoint and the calculated Pseudotime shows that they are largely in line with one another (Figure 18A, compare left and right). Given that timepoint 1 and lower pseudotime corresponds with one another, this indicates that the different populations within the midgut likely originates from a single progenitor population. Plygawko et al., 2024 (in publication) demonstrated that four different midgut cell populations could be identified. Of these population, I will focus on PMECs, as they are the only population that undergoes MET (Tepass and Hartenstein, 1994b).

Dotplots of known markers genes (Figure 18B) were generated based on expression within Seurat clusters, another method of unsupervised clustering (Butler et al., 2018). Pebbled/hindsight was used as a general midgut marker to identify the midgut (Yip et al., 1997), and was found to be expressed throughout all midgut cells, albeit at varying levels. Various genes encoding sSJ proteins including *mesh*, *snakeskin* (Ssk) and *hoka* (Izumi et al., 2021) were expressed in clusters 10, 16, 17, and 20 (Figure 18B), corresponding to clusters within cells sampled at T4 (Figure 18C). *Tetraspanin 2A* (*Tsp2A*), known to organise sSJs (Izumi et al., 2021), was also similarly expressed. Given that mature sSJ are only found in PMECs at larval stages (Tepass and Hartenstein, 1994a), these clusters likely correspond to PMEC populations at later stages. *FasII*, which is found along the lateral membrane of PMECs, appears to be strongly expressed in cluster 0, 7 and 8, corresponding to cells collected at T1 (Figure 18B). Thus, the largest lineage within the midgut population appears to reflect the PMECs.

Figure 18. ScRNA-seq data can be used to identify PMECs within the midgut population.

A. UMAP of midgut cells coloured by timepoints (Right) and by Pseudotime (Left).

B. Dot plot of genes expressed in the UMAP, based on expression within clusters. Dot colour corresponds to level of expression while dot size corresponds to the proportion of the population expressing the gene.

All figures adapted from Plygawko et al., 2024, in submission.

Figure 18. ScRNA-seq data can be used to identify PMECs within the midgut population.

C. UMAPs coloured by relative expression level. Labelling with various known markers reveals expression of sSJ proteins in PMECs. Brackets in the *ssk*, *hoka* and *mesh* UMAPs correspond to T4 timepoints.

All figures adapted from Plygawko et al., 2024, in submission.

Identifying the clusters corresponding to the PMECs within the midgut UMAPs allowed for subsequent analysis of the PMECs to examine the transcriptional changes associated with polarity. I used R to examine and analyse the transcriptional changes based on the datasets from the single cell data processed by Camille. SAS and Crb are apically localised pre-EMT and have been shown to be downregulated during EMT (Campbell et al., 2011). Examining *sas* expression within PMECs shows that *sas* is indeed downregulated at early stages of midgut morphogenesis (Figure 19A). Similarly, *crb* is strongly expressed at early stages and downregulated in PMECs prior to migration (Figure 19B). This is in line with reports that Srp drives repression of *crb*.

In contrast to these apical polarity protein, Baz protein has been shown to be continuously expressed throughout EMT and migration (Campbell et al., 2011). This appear to be the case at the RNA level, as *baz* appears to be lost in PMECs during T2 and T3 (Figure 19C). It was unexpected to see downregulation of *baz* at late stages of PMEC differentiation given that Baz remains apically localised in stage 15 midguts post-MET (Pitsidianaki et al., 2021), suggesting that the protein persists after transcription has been turned off. Downregulation of *baz* is interesting in the context of findings that Baz is not expressed in the adult midgut, which may suggest that *baz* is not re-expressed at later stages (Chen et al., 2018). In contrast, expression of *itgbn*, which encodes integrin subunit βv, appears to be is restricted to late stages of PMEC differentiation (Figure 19D). Late expression of *itgbn* coincides with the proposed role for βv to organise the apical domain with αPS3 (Devenport and Brown, 2004; Pitsidianaki et al., 2021). Put together, the patterns of *baz* and *itgbn* expression in PMEC appear to indicate a switch in transcriptional module. It is tempting to suggest that this switch in transcriptional activity indicates shift in function from a mechanism that establishes apical polarity to one that reinforces apical polarity.

Put together, temporally restricted expression of *sas* and *crb* at early stages and *βv* at later stages is indicative of their specific role to organise polarity in the PMECs pre-EMT and post-MET respectively, suggesting that the mechanisms underlying polarity in pre-EMT and post-MET midgut cells are distinct from one another.

To further investigate the common mechanisms underlying polarity pre-EMT and post-MET, I examined genes that were differentially expressed during epithelial and mesenchymal states. To do this, I compared relative gene expression levels in PMECs from timepoint 1, 3 and 4, corresponding to the pre-EMT epithelial state, mesenchymal state, and the post-MET epithelial state respectively. By comparing relative expression levels, I could broadly split gene expression into 9 different trajectories (Figure 19E).

Thresholding for genes showing a log fold change (log$_2$FC) greater than 0.25 (~20% change) only gave a total 16 genes that were specifically upregulated in epithelial cells compared to mesenchymal cells (Figure 19E, Trajectory 7. Genes list in Figure 19F). Within these genes, the polarity protein *lethal giant larvae* (*lgl*) was part of this list. The other terms do not appear to be obviously linked to epithelial biology; running the list through g:Profiler (Kolberg et al., 2023) suggests that the list is enriched in genes associated with metabolism and mitochondrial respiratory chain complex III (Figure 19F). Thus, it appears that there are very few genes that are specifically upregulated midgut cells in both the early pre-EMT epithelial and post-MET epithelial states, when compared to during their migratory stage, which indicates that the re-epithelialisation of PMEC cells post-MET is distinct from the mechanisms underlying formation of the epithelia pre-EMT.
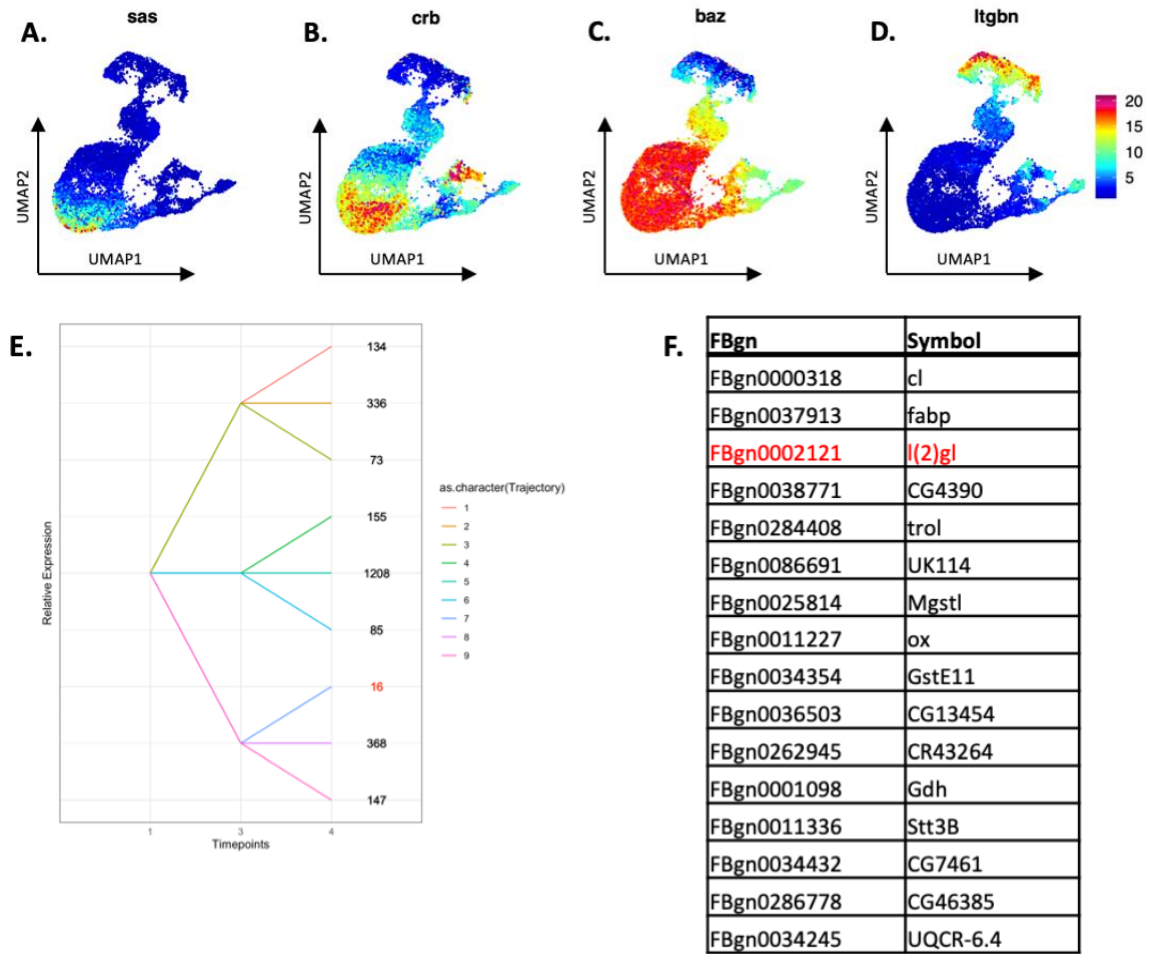
Figure 19. Examining transcriptional patterns in PMECs suggests that epithelial states pre-EMT and post-MET are regulated by distinct mechanisms.

A, B, C, D. Midgut UMAP coloured by relative expression of respective genes.

E. Trajectory of genes in wildtype PMECs. Thresholding differential expression by $\log_2$FC < 0.25 shows only 16 genes that are specifically upregulated at epithelial states (Trajectory 7).

3.1.2 Identifying and validating mesoderm lineages in single cell data

The expression of various mesodermal markers was used to identify the different mesodermal lineages present in the samples (Figure 20A, 20B). Four distinct populations were identified, consisting of the somatic muscle, circular visceral muscle, longitudinal visceral muscle, and the fat body (Figure 20B). The mesoderm UMAP in Figure 20A were generated using Seurat and Monocle by Camille Stephan-Otto Attolini. Dot plot in Figure 20B generated with help from Camille. Subsequent interpretation and analysis of the mesoderm UMAPs was done independently.

Somatic muscle was identified by expression of fusion competent myoblasts markers, which make up the majority of the somatic cell population. Somatic fusion competent myoblasts are defined by expression of Lameduck (Lmd), a transcription factor of the Gli superfamily that functions to transcriptionally regulate myoblast fusion (Duan et al., 2001) (Figure 20 C). Downstream of Lmd is Stick and stones (Sns), an immunoglobulin domain adhesion protein that mediates myoblast attachment (Gildor et al., 2012) (Figure 20D). Verprolin 1 (Vrp1) associates with Sns and is responsible for actin polymerisation required at the later stage of myoblasts fusion (Massarwa et al., 2007) (Figure 20E). Expression of *vrp1* in particular seemed to be restricted to the somatic muscle population.

Expression of *bin* and *bap* was used to identify the visceral mesoderm. Bin is expressed throughout the visceral mesoderm (Zaffran et al., 2001) and as such, appeared to be expressed in both visceral muscle populations (Figure 20F). Expression of *bap* was found to be strongest early during visceral mesoderm differentiation but appeared to be restricted at later stages to the one visceral muscle population (Figure 20G); this is in line with published results that show that longitudinal visceral muscle founder cells does not express Bap (Zaffran et al., 2001). Expression of Connectin (con), an adhesion molecule expressed specifically by circular visceral founder cells, confirmed that this branch was indeed the circular visceral muscles (Martin et al., 2001; Meadows et al., 1994) (Figure 20H).

The longitudinal visceral muscle was identified by expression of longitudinal muscle founder cell markers. Helix-loop-helix transcription factor HLH54F and Teyrha-Meyrha (Tey) are both required for migration of the longitudinal muscle founder cells and subsequent differentiation

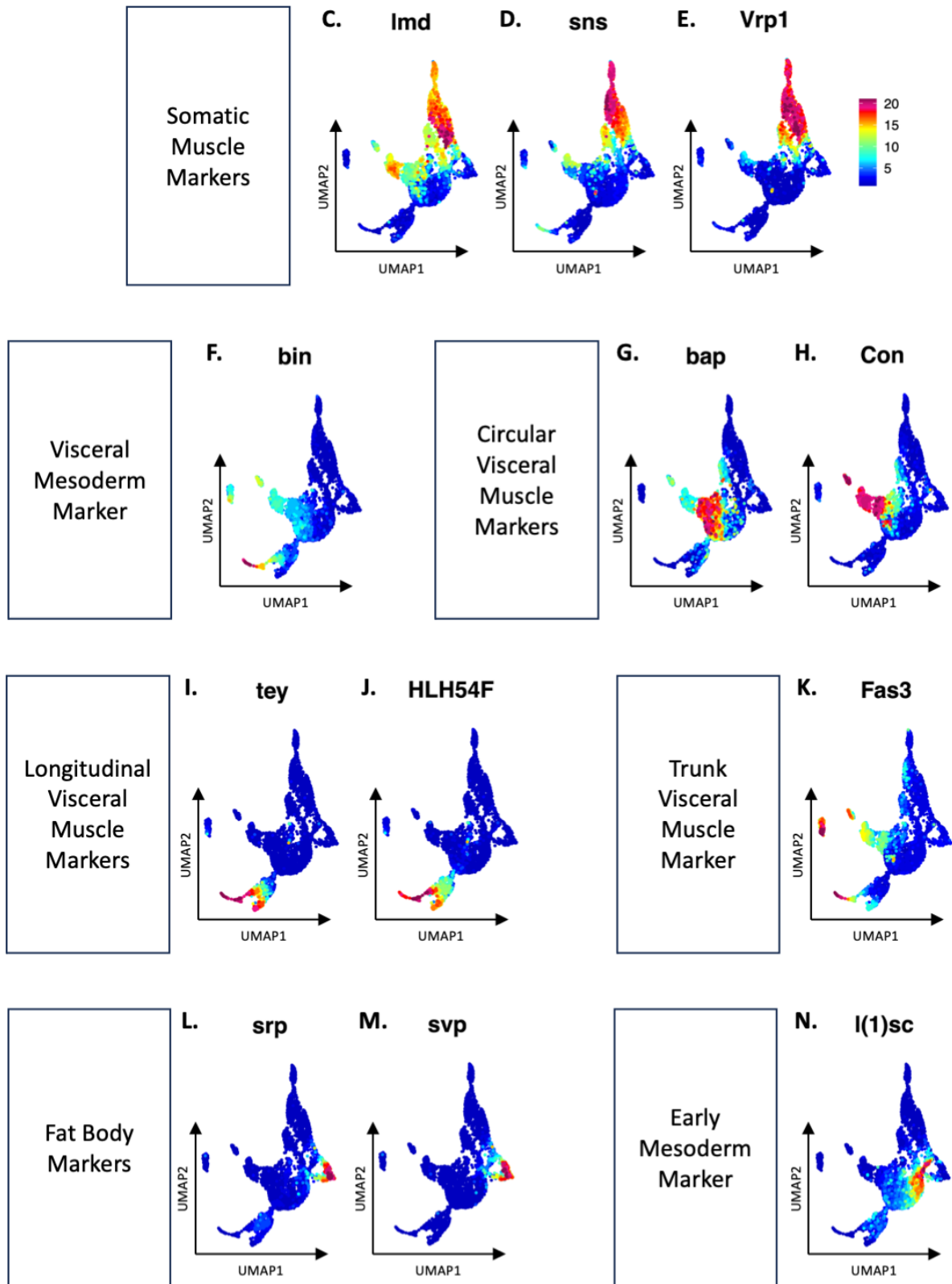into longitudinal visceral muscles (Frasch et al., 2022; Ismat et al., 2010). Expression of both of these genes appeared to be highly restricted to the *bap*-negative visceral muscle populations. As such, it was likely that this branch was the longitudinal muscle lineage (Figure 20I,J). Finally, expression of FasIII appeared to be expressed in both the circular and longitudinal visceral muscle (Figure 20K); this was expected as FasIII marks both visceral muscles in the trunk mesoderm. UMAP region for Fat body markers also indicated that these were present in the dissected material.

In addition to identifying differentiated muscles, the single cell data also appears accurately captures the transcriptional changes that occur throughout differentiation. For example, expression of *l'sc*, which marks muscle progenitor cells, is detected. Furthermore, this is restricted to a population corresponding to cells sampled at timepoint 1 (Figure 20N, compare with Figure 20A), indicating that the data also captures early mesoderm development. Additionally, it has been previously observed that *bap* is expressed at stage 10 before downregulation at late stage 11 (Martin et al., 2001). The UMAP appears to reflect this; expression of *bap* is strongest in population corresponding to the visceral mesoderm but drops off in the branch corresponding to the circular visceral muscle (Figure 20G). These observations indicate that the single cell data also captures changes in expression levels that occur throughout mesoderm differentiation.

Put together, the above data shows that the single cell sequencing data of the dissected midgut also accurately captures mesoderm development. The data captures four unique lineages including the circular visceral muscle and the somatic muscle. I therefore next used the scRNA-seq data of the different muscle populations to investigate the potential mechanisms underlying their distinct roles in mediating midgut migration and MET.

Figure 20. Mesoderm populations branch into 4 distinct populations.

A. UMAP of the mesodermal population coloured according to the timepoints at which the embryos were sampled.

B. Dotplot of the mesodermal population, based on expression within Seurat clusters.
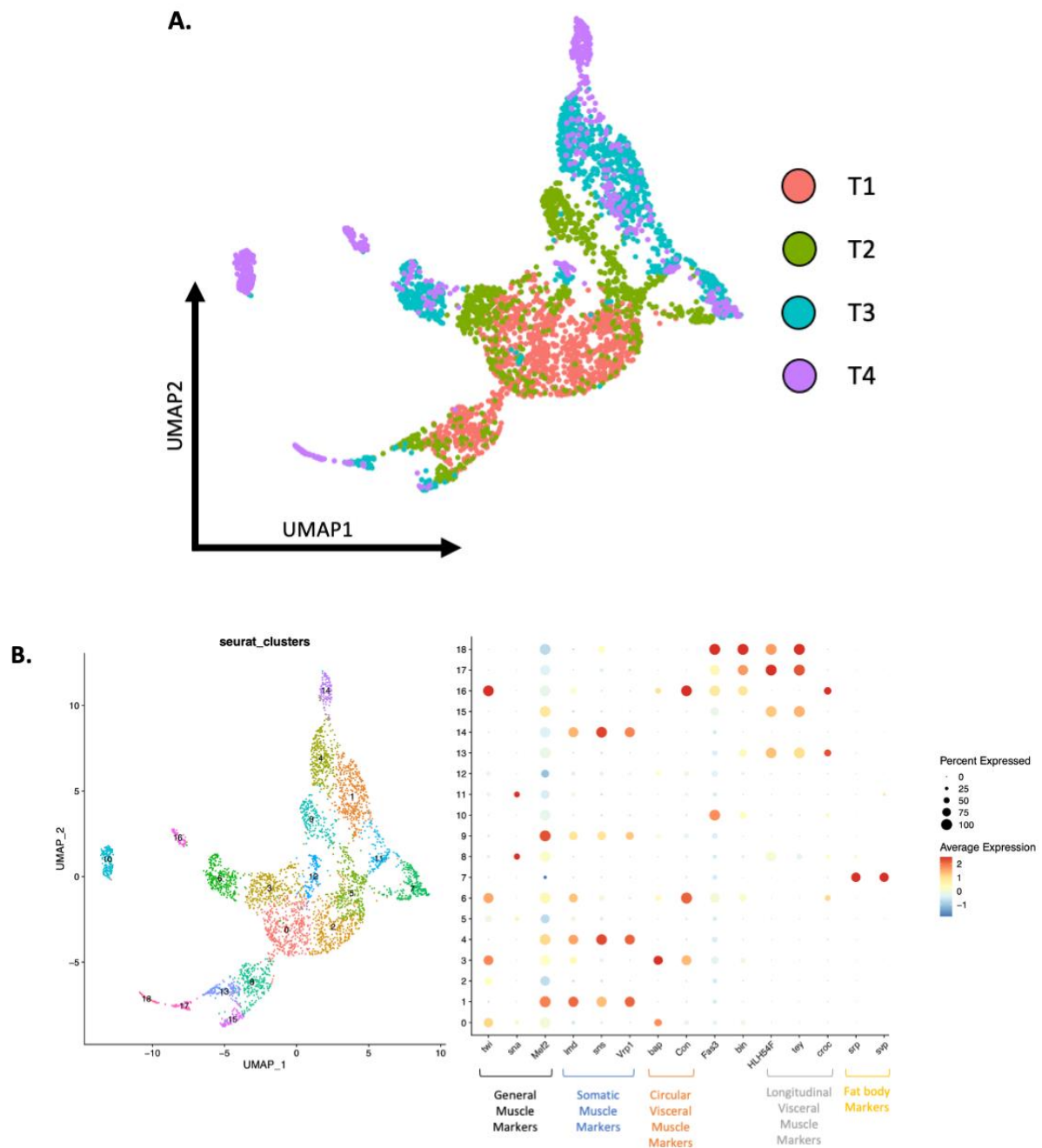
Figure 20. Mesoderm populations branch into 4 distinct populations.

C ~ I. UMAPs coloured by relative expression level of each gene. Labelling with various mesoderm markers reveal distinct populations arising from the mesoderm.

3.1.3 Examining laminin and integrin expression patterns in midgut and the mesoderm.

One surprising aspect about the *bin* phenotype, described in the previous chapter, was the presence of basal Wb between the midgut and the somatic muscle. This came as a surprise as it was previously suggested that the visceral mesoderm is the major source of Wb at the basal interface of the midgut in wildtype embryos (Pitsidianaki et al., 2021). Given this observation, I wanted to examine gene expression of laminins in the midgut and muscle to clarify which tissues expressed each gene.

Wb expression in the muscle appears to be strongest early in development. Given that both the circular visceral muscle and somatic muscle express similar levels of *wb* (Figure 21A), this supports my finding that the somatic muscle appears sufficient to provide the Wb found at the basal interface of the midgut in *bin* mutants. In contrast, there appears to be stronger expression of *lanA* in the circular visceral muscle compared to the somatic muscle (Figure 21B).

In contrast to the muscle, both Laminin α-chains appeared to show similar expression patterns within PMECs (Figure 21C & D). Both Laminin α -chains are upregulated during migration and MET and are downregulated at late stages of PMEC differentiation. One minor difference is that expression of *wb* is upregulated earlier than *lanA* (compare Figure 21C and 21D), which corresponds with its earlier role in driving epithelialisation (Pitsidianaki et al., 2021).

In summary, expression of *wb* does not appear to be significantly different between the somatic and circular visceral muscle. This is in line with observations of *bin* mutants, in which Wb at the interface between the midgut and the somatic muscle appears to be sufficient to mediate adhesion. Instead, expression of *lanA* appears to be a major distinguishing factor between the circular visceral muscle and the somatic muscle.
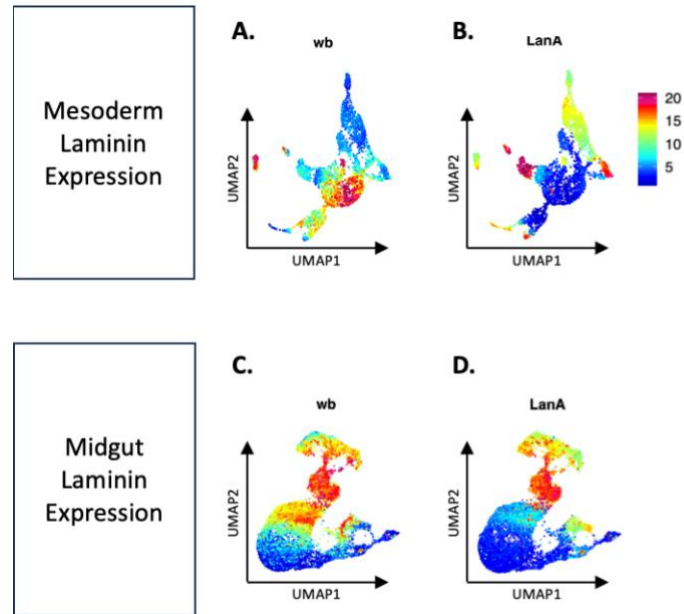
Figure 21. Relative expression levels of laminins in the mesoderm and midgut.

**A & B.** Mesoderm UMAPs coloured by relative expression level of Laminin α chains

C & D. Midgut UMAPs coloured by relative expression level of Laminin α chains.

3.1.4 Examining differentially expressed genes between the circular visceral muscle and the somatic muscle.

As discussed in the previous chapter, the circular visceral muscle appears to specifically drive MET; observations of *bin* mutants suggests that the somatic muscle is able to support early migration but is unable to drive MET. While it has been shown in *bin* mutants that Wb is present at the interface between the midgut and the somatic muscle, it is also plausible that Wb at this interface, while sufficient to mediate adhesion, fails to play a functional role to organise the basal domain. In support of this, partial mislocalisation of Talin can be observed in *bin* mutants. Regardless, basal localisation of Cher, which has been shown to be independent of adhesion (Devenport and Brown, 2004), is also lost in *bin* mutants, clearly implicating the visceral muscle in midgut MET.

Thus, I assumed that the genes responsible for driving MET would be expressed in the circular visceral muscle and not the somatic muscle. To find these genes, I examined a list of differentially expressed genes between the clusters reflecting the two muscle populations at T3 and T4, which reflected the differentiated populations (Figure 22A). This was done in R based on datasets generated by Camille. *Con* and *Fas3* were both present in the list of top 15 differentially expressed genes for clusters 6 and 16, suggesting that the list accurately reflects genes specific to the circular visceral muscle (Figure 22B, left). Likewise, somatic muscle marker Vrp1 was present in the list of top 15 differentially expressed genes for cluster 1, 4, 14 (Figure 22B, right). *argk*, *sug*, *ab* and *eno* are also in published list of genes expressed by the somatic muscle, predicted based on differentially accessible ATAC peaks generated by scATAC-seq (Secchia et al., 2022). Thus, it appears that the two lists accurately reflect differences in gene expression between the circular visceral muscle and somatic muscle.

A. Seurat Clusters — Timepoint

Legend: T1, T2, T3, T4
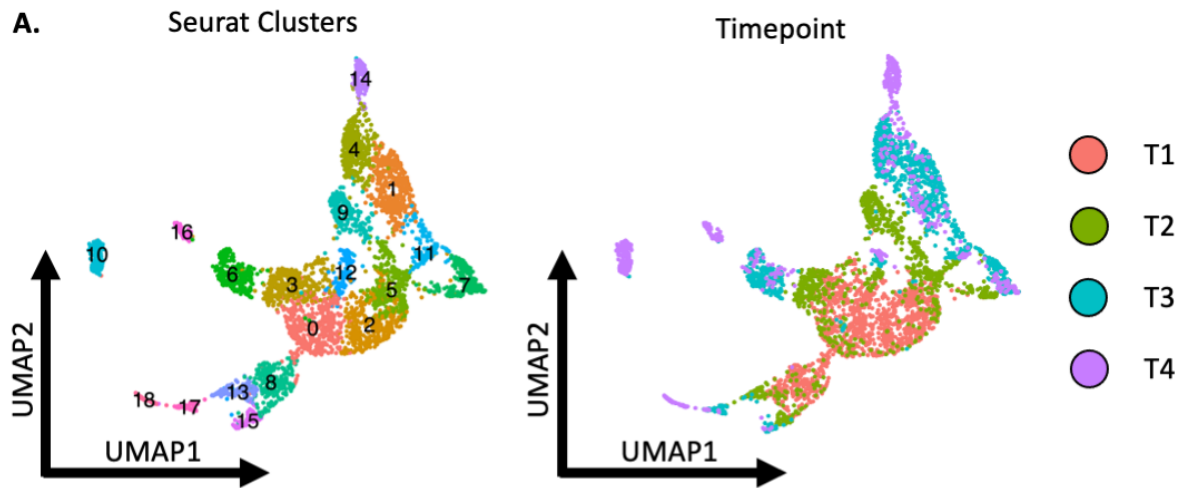
B.

Top 15 Differentially Expressed Genes			
Upregulated in T3, T4 Circular Visceral Muscle (Clusters 6, 16)		Upregulated in T3, T4 Somatic Muscle (Clusters 1, 4, 14)	
FBgn	**Gene**	**FBgn**	**Symbol**
FBgn0005775	**Con**	FBgn0000116	Argk
FBgn0000459	disco	FBgn0033988	pcs
FBgn0264001	bru3	FBgn0033782	sug
FBgn0000636	**Fas3**	FBgn0001235	hth
FBgn0085407	Pvf3	FBgn0264442	ab
FBgn0010453	Wnt4	**FBgn0243516**	**Vrp1**
FBgn0016797	fz2	FBgn0002735	E(spl)mgamma-HLH
FBgn0029002	miple2	FBgn0024238	Fim
FBgn0032297	CG17124	FBgn0011584	Trp1
FBgn0025682	scf	FBgn0003944	Ubx
FBgn0013718	nuf	FBgn0014011	Rac2
FBgn0023214	edl	FBgn0000591	E(spl)m8-HLH
FBgn0261648	salm	FBgn0002609	E(spl)m3-HLH
FBgn0004839	otk	FBgn0032731	Swip-1
FBgn0003900	twi	FBgn0000579	Eno

Figure 22. Using single cell data to identify circular visceral muscle-specific gene expression.
A. UMAP of the mesodermal cells. Unsupervised clusters were generated using Seurat. Clusters 1, 4 and 14 correspond to somatic muscles from T3 and T4 sample windows. Clusters 6 and 16 correspond to visceral muscles from T3 and T4 sample windows. **B.** Top 15 genes differentially expressed between the visceral muscle and somatic muscle. Con and Fas3, in bold, are known specific markers of the circular visceral muscle that were strongly differentially expressed. Vrp1, also in bold, is a known marker of somatic fusion competent myoblasts.

3.1.5 Identifying midgut-circular visceral muscle interactions.

In order to identify cues from the circular visceral muscle that contribute to midgut morphogenesis, the cross talk between the two tissues must be considered. The manner in which the two tissues can interact can be broadly divided in to three types. These include interactions mediated by the ECM, ligands secreted by the circular visceral muscle and transmembrane ligands expressed on the circular visceral muscle. Examples of the first two have been discussed. It is difficult to rule out the possibility of interactions mediated by transmembrane ligands expressed on the circular visceral muscle; at stage 13, the ECM between the midgut and the visceral muscle is punctate (Wolfstetter et al., 2009) and thus could allow for transmembrane ligands expressed on the surface of midgut cells to interact with the visceral muscle. Only at stage 14 onwards upon flattening of the visceral muscle does the ECM form a continuous layer at the interface between the midgut and visceral muscle (Wolfstetter et al., 2009). Thus, all three types of interactions were considered for candidate genes mediating signalling between the two tissues.

In an attempt to find receptor-ligand interactions, I started with the genes differentially upregulated in the circular visceral muscle compared to somatic muscle at timepoints 3 and 4. From this list, I made a list of cognate genes based on a curated list of ligand-receptor interactions provided by FlyPhoneDB (Liu et al., 2021). The expression of each of the cognate genes in the midgut were manually checked using the single cell data using the Loupe cell Browser and the Berkeley Drosophila Genome Project *in situ* expression database (Hammonds et al., 2013; Tomancak et al., 2007, 2002) (Figure 23A). The list of ligand-receptor pairs that fulfilled the above requirements are listed in Figure 23B. With respect to the cognate genes, genes expressed across the midgut at both timepoint 3 and 4 were included to cast a wide net for possible interactions.

Sema1a - Otk was identified in the list of possible interactions mediated by CVM receptors. Although typically characterised as a ligand, Sema1a can mediate bi-directional signalling with Otk as its cognate receptor during motor axon guidance (Jeong et al., 2017; Nguyen et al., 2022). Its cognate receptor *otk* is one of the most differentially upregulated genes in the circular visceral muscle. PlexA was also added to the list of candidate genes as a potential

receptor for Sema1a. PlexA can function as a receptor for Sema1a signalling during axon guidance (Cho et al., 2012; Winberg et al., 1998) and has been suggested to have some interaction with Sema1a – Otk signalling as well.

Wnt4, which is involved in MET during nephrogenesis (Carroll et al., 2005), was identified as one of the most differentially upregulated genes in the circular visceral muscle. It has been suggested that it can potentially acts as a ligand for Otk (Peradziryi et al., 2011), which is also expressed in the midgut. It should be noted that this has been called into question, with another paper suggesting Wnt2 to be a ligand for Otk (Linnemannstöns et al., 2014). Regardless, the presence of Wnt4 and the expression of various possible receptors in the midgut pointed towards a possible conserved role for Wnt4 to drive MET and thus was added to the list of candidate genes.

Various BMP signalling receptors also appear to be expressed in the midgut and muscle. For example, Babo, associated with Activin signalling, appears to be uniquely expressed in the midgut. Two different Mad/BMP ligands, *mav* and *gbb* were shown to be expressed in the circular visceral muscle, which may mediate the signalling from the visceral muscle to the midgut mediated by BMP signalling. It should be noted that the visceral muscle also expresses BMP signalling receptors, and thus could simply reflect the dual roles that BMP signalling can play in the development of muscle and the midgut (Upadhyay et al., 2017). One known interaction mediated between the visceral muscle and the midgut mediated by BMP signalling is the expression of *lab.* However, as expression of *mothers against decapentaplegic (mad)*, the key downstream mediator of BMP signalling, occurs much earlier than *lab,* Mad probably plays other roles during PMEC development (Figure 24). Similarly, the expression of BMP signalling receptors throughout development point towards a role for BMP signalling. Thus, Mad was added to the list as of genes to screen as a potential downstream mediator for various BMP receptors.

A.

CVM vs Somatic	FlyPhone Ligand-Receptor Interactions
Differential expression between Cluster 1, 4, 14 vs cluster 6, 16 Filter: • $\log_2 FC < 0$ • $p < 0.05$	Check: • Gene expressed in midgut according to UMAPs • Prioritise genes to look at based on in-situ database
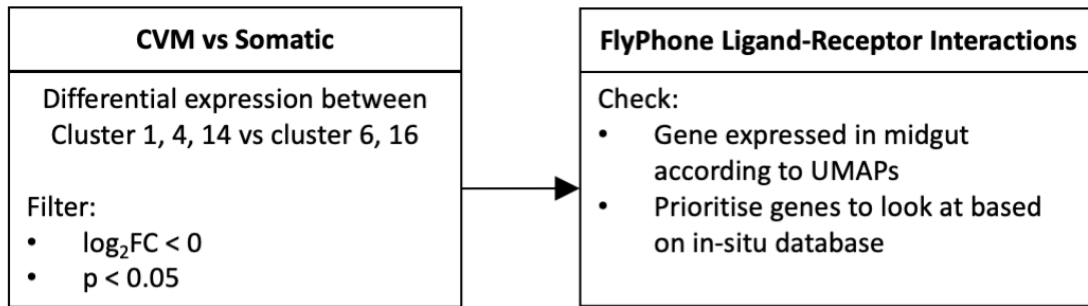
B.

CVM Receptors		Cognate Ligands expressed in midgut	
FBgn	Symbol	FBgn	Symbol
FBgn0010389	htl	FBgn0033649	pyr
FBgn0004647	N	FBgn0000463	Dl
FBgn0030766	mthl1	FBgn0000719	fog
FBgn0025936	Eph	FBgn0040324	Ephrin
FBgn0025741	PlexA	**FBgn0011259**, FBgn0011260, FBgn0284221	**Sema1a**, Sema2a, Sema5c
FBgn0004839	otk	**FBgn0011259**, FBgn0010453	**Sema1a**, Wnt4
FBgn0003391	shg	FBgn0003391	shg
FBgn0003169	put	FBgn0024234, FBgn0026199	gbb, myo
FBgn0003317	sax	FBgn0024234	gbb
FBgn0003716	tkv	FBgn0024234, FBgn0026199	gbb, myo
FBgn0263930	dally	FBgn0041604	dlp
FBgn0001085	fz	FBgn0010453, FBgn0010194, FBgn0031902	Wnt4, Wnt5, Wnt6
FBgn0016797	fz2	FBgn0010453, FBgn0010194, FBgn0031902	Wnt4, Wnt5, Wnt6

CVM Ligands		Cognate Receptor expressed in midgut	
FBgn	Symbol	FBgn	Symbol
FBgn0004569	aos	FBgn0003731	Egfr
FBgn0005672	spi	FBgn0003731	Egfr
FBgn0003984	vn	FBgn0003731	Egfr
FBgn0000463	Dl	FBgn0004647	N
FBgn0010194	Wnt5	FBgn0015380, FBgn0000119, FBgn0001085, FBgn0016797, FBgn0027342	drl, arr, fz, fz2, fz4
FBgn0010453	Wnt4	FBgn0004839, FBgn0000119, FBgn0001085, FBgn0016797, FBgn0027342	otk, arr, fz, fz2, fz4
FBgn0003391	shg	FBgn0003391	shg
FBgn0085407	Pvf3	FBgn0032006	Pvr
FBgn0024234	gbb	FBgn0011300, FBgn0003169, FBgn0003317, FBgn0003716	babo, put, sax, tkv
FBgn0039914	mav	FBgn0011300, FBgn0003169, FBgn0003317, FBgn0003716	babo, put, sax, tkv
FBgn0041604	dlp	FBgn0263930	dally

Figure 23. Examining receptor-ligand interactions between the midgut and the circular visceral muscle interactions to identify candidate genes for functional screens.

A. Schematic showing the process taken to examine receptor-ligand interactions. **B.** Receptor-ligand interactions between the midgut and circular visceral muscle. In red are the genes within the list of top 15 upregulated genes in the circular visceral muscle.
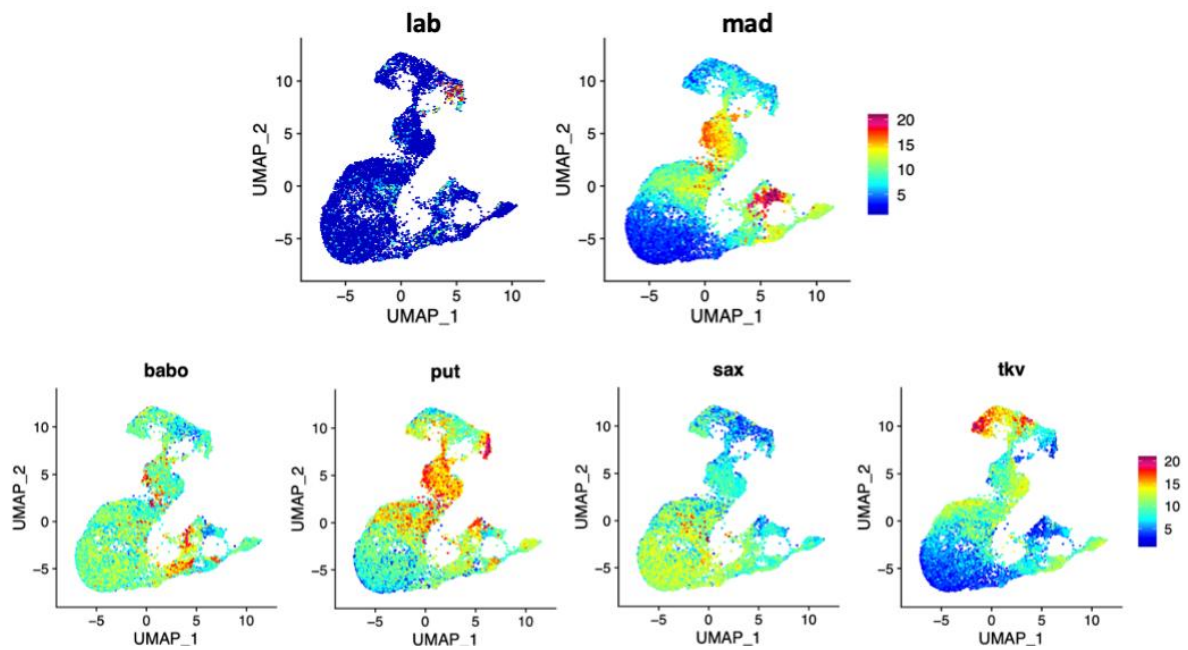
Figure 24. Midgut UMAPs showing expression of *lab*, *mad* and BMP signalling receptors.

Expression of *lab* is strictly in terminal stage of PMEC and ICP specification. BMP signalling receptors including *baboon* (*babo*)*, put* (*punt*)*, sax* (*saxophone*) and *tkv* (*thickveins*) are expressed throughout PMEC development. BMP Type 2 Receptor *wishful thinking* (*wit*) was not in the expression matrix. However, the *in situ* database indicates that *wit* is not expressed in the embryo (Hammonds et al., 2013; Tomancak et al., 2007, 2002).

3.2 Discussion

In this chapter, I used the scRNA-seq data to examine midgut gene expression throughout midgut morphogenesis. I first examined the changes in gene expression between the midgut epithelia that forms pre-EMT and the midgut epithelial that forms post-MET to explore both common and distinct mechanisms associated with an epithelial state. I also examined mesoderm gene expression to look at the genes expressed in the circular visceral muscle, which has been shown to be specifically required for midgut MET. Given this key role for the circular visceral muscle, I used the midgut and mesoderm scRNA-deq data to identify potential ligand-receptor pairs that mediate the interaction between the circular visceral muscle and the midgut to drive midgut MET.

Examining gene expression patterns within PMECs showed that expression of polarity proteins *sas* was downregulated early during PMEC differentiation, suggesting that it does not play any role during MET. This is in line with published results that indicate SAS is not expressed post-EMT (Campbell et al., 2011). Expression of *crb* also appeared to be downregulated prior to migration. Given this finding, it was likely that the mechanisms governing polarity pre-EMT were distinct from those governing polarity post-MET.

To examine this further, I looked for genes in PMECs that were upregulated during both epithelial stages. Surprisingly, very few genes were identified. One of the genes conserved in both epithelial states encoded the polarity protein Lgl. Lgl is a basolateral polarity protein, that antagonise apical proteins including members of the Par protein complex (Buckley and St Johnston, 2022; Chalmers et al., 2005). It is tempting to suggest that apical localisation of Baz is regulated by transcription of *lgl*. However, this is unlikely to be the case; maternal contribution of Lgl in wildtype is sufficient for normal embryogenesis (Manfruelli et al., 1996). Furthermore, it is also noted that midgut MET occurs normally in the absence of Lgl function (Manfruelli et al., 1996). Regardless, there appears to be very few genes that are upregulated specifically when PMECs are epithelial.

One possible explanation for this is that the re-epithelialisation of PMEC cells post-MET is distinct from the mechanisms underlying formation of the epithelia pre-EMT. This would not

be a surprise given the difference in morphological changes that occur; the process of epithelial folding that occurs early during the development of the posterior midgut (Lengyel and Liu, 1998) is a distinct process from MET. Alternatively, it could also suggest that epithelialisation during midgut MET is regulated by additional mechanisms separate from transcriptional regulation. For example, expression of *baz* is downregulated during PMEC differentiation but is still retained apically in the midgut epithelia post-MET. In contrast, the expression pattern of *itgbn*, encoding βv, suggests that some aspects of polarity are controlled by regulation of protein expression at the transcription level. Thus, while it is likely that some aspects of MET are regulated by transcription, some appear to be determined by other mechanisms. One such mechanism may involve post-translational modifications; post-translation modifications are known to affect the localisation and stability of tight junction proteins in vertebrates (Reiche and Huber, 2020). This idea that transcription does not fully capture the mechanisms underlying epithelial organisation is one that has slowly gained traction within the field of EMT (Yang et al., 2020). This is of particular relevance given the widespread use of biomarker expression levels as an indicator of an epithelial state and highlights the importance of functional studies examining localisation of proteins.

Examining scRNA-seq of the mesoderm revealed that expression of *lanA* in the circular visceral muscle is much greater than the somatic muscle. This suggests that the midgut in *bin* mutants lack a major source of basal LanA. Despite this, the midgut retains the capacity to migrate in *bin* mutants. Together with the fact that migration in LanA mutants is slowed (Pitsidianaki et al., 2021), this suggests that LanA from the underlying muscle is not required for migration, but rather that LanA secreted by the midgut cells themselves is important for normal midgut migration. This is in line with previous work suggesting LanA secreted by midgut plays a key role in midgut migration (Pitsidianaki et al., 2021).

With regards to MET, it appears that adhesion and basal localisation of βPS is not disrupted in *bin* mutants despite loss of LanA. This is in line with observations that indicate that the *lanA* mutant remains adherent to the muscle and maintains basal localisation of βPS (Pitsidianaki et al., 2021), confirming that LanA from the visceral muscle does not play a role in adhesion or basal localisation of βPS. The phenotypes of the *lanA* mutants are distinct from *bin* in that the PMECs form a monolayer of columnar cells and retain apically localised Ecad and Baz,

albeit in a dispersed manner compared to wildtype (Pitsidianaki et al., 2021). In contrast, my results show that *bin* mutants fail to form a monolayer and lose Ecad and Baz localisation. Thus, it appears that the phenotypes observed in *lanA* mutants are milder than that of *bin* mutants, indicating that loss of basal LanA is likely not the cause of phenotypes observed in *bin* mutants. Furthermore, it is thought that organisation of the apical domain mediated by LanA is driven by apical secretion of LanA from the midgut (Pitsidianaki et al., 2021), rather than a function of LanA from the underlying the visceral muscle. Thus, while LanA does play roles in MET at later stages, the loss of LanA from the visceral muscle does not explain the phenotype observed in *bin* mutants. Put together, it appears that LanA expressed in the visceral muscle does not affects midgut migration or MET.

Finally, I examined genes expressed in the visceral muscle that were differentially upregulated in the somatic muscle to identify candidate genes that might play a role in driving midgut MET. For this, I used a curated list of high confidence ligand-receptor interactions from FlyPhone DB (Liu et al., 2021). It should be noted that Fra and Netrins, a receptor-ligand interaction between the midgut and visceral muscle that contributes to MET (Pert et al., 2015), was not part of the list of curated receptor-ligand interactions from FlyPhone. While this does suggest that the list may not comprehensive, both Netrin A and B were identified as genes specifically upregulated in the visceral muscle and thus would have been picked up had Fra-Netrin interactions been on the list of possible interactions. Thus, this does not take away from the validity of this methods; using this method, I have examined an extensive list of receptor-ligand interactions for possible interactions between the visceral muscle and midgut that play a role in MET. Although Sema1a and Mad-related genes were prioritised for further investigation, the other possible receptor-ligand interactions include candidates that may be worth exploring in the future.

Chapter 4. Phenotypic Screen for signals from the circular visceral muscle that drive midgut MET

4.0 Introduction

As described in Chapter 1, examining midgut MET in *bin* mutants showed that adhesion to the somatic muscle is not sufficient for MET and that the circular visceral muscle, the basal substrate for the midgut during wildtype MET, is specifically required to provides cues that is critical for midgut MET. By leveraging scRNA-seq data, I compared the transcriptome of visceral mesoderm and the somatic muscle to identify genes expressed specifically by the circular visceral muscle. Using this list, I identified a number of potential receptor-ligand interactions that might mediate signalling between the midgut and the visceral muscle that drives midgut MET. In this chapter I will focus on characterising embryos mutant for the genes that potentially mediate the mechanisms that drives midgut MET. In the following section, I will describe the literature surrounding BMP signalling and genes related to Sema1a, both of which were identified as possible mediators of receptor-ligand interactions driving midgut MET.

BMP signalling

BMP signalling, one of the two Transforming growth factor β (TGF-β) family signalling pathways in *Drosophila*, is a well characterised signalling pathway that plays roles in a wide range of developmental processes in *Drosophila*, including embryonic patterning and axon guidance (Upadhyay et al., 2017).

The downstream activities of BMP signalling are mediated by a single central transcription factor called Mothers against dpp (Mad). The signalling cascade that leads to the phosphorylation of Mad is initiated by extracellular BMP ligands that promote the dimerization of Type I and type II BMP receptor kinases. Constitutively active type II BMP receptor kinases phosphorylate Type I BMP receptor kinase, which in turn phosphorylates Mad. Upon phosphorylation, Mad forms a complex with Medea (Upadhyay et al., 2017). This Mad-Med complex moves to the nucleus, where it is able to regulate gene expression with other transcription cofactors (Hamaratoglu et al., 2014).

BMP signalling also plays roles in midgut morphogenesis. The activation of BMP signalling in the midgut is dependent on expression of BMP signalling ligand Dpp in the visceral muscle. Dpp is expressed in the visceral muscle in parasegment 7, corresponding the middle region of the midgut. Downstream signalling BMP signalling in the midgut is mediated by the binding of Dpp to Type I receptor Thickvein (Tkv) (Casas-Tinto et al., 2008). Phosphorylation of Mad by Tkv is thought to drive expression of D-Fos, a member of the AP-1 family of transcription factors (Riese et al., 1997) and FoxK, a member of the Fox family of transcription factors (Casas-Tinto et al., 2008), which together promote the expression of Lab in the midgut corresponding to parasegment 7. Lab is itself a transcription factor of Hox gene family required for embryonic midgut constrictions (Casas-Tinto et al., 2008), as well as the specification copper cells in the adult midgut. (Dubreuil et al., 2001; Hoppler and Bienz, 1994).

This mechanism of BMP signalling between the visceral muscle and midgut is particularly interesting given the expression of other BMP ligands and receptors in PMECs and the visceral muscle (see Figures 23 and 24); given that BMP signalling occurs between the visceral muscle and the midgut, other ligands or receptors may play a role in coordinating MET. Whether there is a role for BMP signalling earlier than midgut constriction is not clear. Phospho-Mad stains of stage 13 wildtype embryos indicated that Mad signalling was active in parasegment 7 in both the visceral muscle and midgut, corresponding to the region populated by the ICPs (Shirinian et al., 2007).

A possible role for BMP signalling during MET was suggested in a study looking at mutants for Anaplastic Lymphoma Kinase (Alk) (Shirinian et al., 2007). Alk is a receptor expressed in visceral muscle for the ligand Jelly belly (Jeb) which is produced by the somatic muscle. This Jeb-Alk signalling is critical for expression of dumbfounded (duf), which defines specification of visceral muscle founders. In the absence of Alk and Jeb, there is an absence of visceral muscle founders, resulting in aberrant myoblast fusion between visceral fusion competent myoblasts to somatic founder cells and thus, failure to form visceral muscles (Lee et al., 2003). These mutants are thought to be distinct from *bin* mutants in that they are able to define the visceral mesoderm and form visceral fusion competent myoblasts. In these mutants, no migration or midgut fusion defects were reported. However, a failure of dorsal-ventral

spreading of the midgut was noted, such that the midgut fails to enclose the yolk. Although speculative, this could be a consequence resulting from a failure to undergo MET. Crucially, BMP signalling in the midgut is disrupted in *alk* mutants, leading to loss of *lab* expression in the midgut (Shirinian et al., 2007). Furthermore, the disruption of BMP signalling in these *alk* mutants was shown to be independent of myoblast fusion (Shirinian et al., 2007); migration of the midgut and BMP signalling are unperturbed in *sns* mutants, in which founder cells are specified but fail to fuse with fusion competent myoblasts. Thus, this suggested the possibility that the failure of dorsal-ventral spreading observed in *alk* mutants were the result of aberrant BMP signalling between the visceral muscle and midgut.

Sema1a

Semaphorins are a widely conserved family of proteins, defined by the presence of an extracellular Sema domain (Goodman et al., 1999). They function in a wide range of processes including cell morphology and motility (Alto and Terman, 2017). Members of the Semaphorin family can be secreted, transmembrane or glycosylphosphatidylinositol-linked (GPI) proteins (Goodman et al., 1999), which function to anchor the protein to the exterior of the cell.

The majority of binding partners for Semaphorins belong to the Plexin family of receptors. Plexins are unique among cell surface receptors in that they have GTPase activating protein (GAP) domains (Pascoe et al., 2015). These GAP domains can activate small GTPase, which are responsible for a variety of molecular functions including cytoskeleton dynamics (Dent et al., 2004; Driessens et al., 2001). Interestingly, Plexins also have a Sema domain, despite the fact that Plexins are evolutionarily distant from Semaphorins (Goodman et al., 1999).

A key characteristic of transmembrane Semaphorins, such as Sema1a, is its ability to mediate bidirectional signalling. This means that it can function as a ligand during forward signalling, such that it mediates activation of a signalling cascade in the opposing cells, but also as an receptor during reverse signalling, such that binding of a ligand to the transmembrane Semaphorin will activate a signalling cascade through its cytoplasmic domain (Battistini and Tamagnone, 2016; Hernandez-Fleming et al., 2017; Hsieh et al., 2014; Jeong et al., 2017, 2012).

Early studies examining Semaphorins in *Drosophila* characterised Sema1a as a repulsive axon guidance cue in *Drosophila*. During the development of motor neurons, fasciculated bundles of axons grow together and segregate at their respective destinations to innervate the correct muscle. Ectopic expression of Sema1a in muscle prevented innervation of the motor axon, indicative of its repulsive function (Yu et al., 1998). This function of Sema1a as a repulsive axon guidance was shown to be mediated by its binding to Plexin A (PlexA); motor axon defects observed upon ectopic expression of Sema1a in muscles could be rescued upon loss of PlexA in the neuron (Winberg et al., 1998). PlexA is one of two Plexins in *Drosophila (Yu and Kolodkin, 1999).* In addition to its role in the axon guidance, PlexA has also been associated with coordinating migration of follicular epithelial cells; expression of PlexA at the trailing edge and transmembrane Semaphorin Sema5C at the leading edge suppresses the formation of leading-edge protrusion into neighbouring cells (Stedden et al., 2019).

Notably, in the context of motor axon guidance, PlexA does not mediate Sema1a reverse signalling (Jeong et al., 2012). This is particularly relevant in the context of the potential ligand-receptor interactions between the midgut and circular visceral muscle, as Sema1a was identified as a potential binding partner expressed in the midgut for PlexA, which was found to be enriched in the circular visceral muscle compared to the somatic muscle (Figure 23). If the assumption that PlexA also does not mediate reverse signalling holds true in the midgut, it is likely that any function for Sema1a as it relates to midgut MET is mediated by Otk, the other Sema1a-binding protein enriched in the circular visceral muscle.

Off-track (Otk) mediates Sema1a reverse signalling in motor axons (Nguyen et al., 2022; Rozbesky et al., 2020). Otk is a ortholog of vertebrate protein tyrosine kinase 7 (Ptk7), which functions as a regulator of planar cell polarity during neural tube closure (Lu et al., 2004). The extracellular domain of Otk is composed of five immunoglobulin-like domains and, in addition to Sema1a, can also bind to Wnt4 and the glycosaminoglycans heparan and heparin sulfate (Rozbesky et al., 2020).

Like Plexins, Sema1a reverse signalling is associated with cytoskeleton remodelling (Jeong et al., 2017, 2012). During motor axon guidance, the intracellular domain of Sema1a is able to recruit Pebble (Peb), a Rho GEF, and RhoGAPp190. These are likely to act upon Rho1 (Jeong

et al., 2017), which can mediate cytoskeleton remodelling required during axonal growth (Bodakuntla et al., 2021). Interestingly, it has been proposed that Cher and Varicose are also recruited to the intracellular domain of Sema1a (Jeong et al., 2017). Varicose is a membrane associated guanylate kinase (MAGUK) that is also associated with smooth septate junctions (Bachmann et al., 2008), and likely functions as a scaffold to organise various signalling complexes at the axon-axon contact sites (Jeong et al., 2017). It has been proposed that Cher and Varicose function to coordinate localised cytoskeleton remodelling by anchoring Peb to both Sema1a and the actin cytoskeleton (Jeong et al., 2017). This is interaction between Sema1a and Cher is of particular interest given that the mechanisms driving Cher localisation in the midgut has not been fully characterised (Devenport and Brown, 2004; Pert et al., 2015). It has also been shown that Sema1a reverse signalling drives activation of Moesin in photoreceptor axons, but whether this is dependent on Otk has not been shown (Hsieh et al., 2014). This represents an alternative mechanism that might play a role in mediating MET; Moesin has been shown to be basally localised in midgut cells post-MET (Pert et al., 2015).

Otk is also expressed in the midgut as well (Figure 23) and as such may mediate signalling that affects midgut morphology. Wnt4, a binding partner for Otk (Peradziryi et al., 2011; Rozbesky et al., 2020), is also highly enriched in the circular visceral muscle (Figure 23), and as such could act as a ligand for Otk expressed in the midgut. It has been shown in the context of wing patterning that Otk can function as a co-receptor with Frizzled to bind Wnt4. Upon binding with Wnt4, Otk recruits Dishevelled (Dsh) to the cell membrane via its cytoplasmic domain, which inhibits canonical Wnt signalling (Peradziryi et al., 2011).

Given the expression patterns of Sema1a, PlexA, Otk, and Wnt4 in the midgut and muscle, and their links to mechanisms related to midgut MET, mutants for Sema1a, PlexA, Otk, and Wnt4 were selected as candidates to screen for MET phenotypes.

4.1 Results

4.1.1 Phenotypic Screen of Mad

Given the expression of various Mad-related ligands and receptors in the visceral muscle and midgut, the *Mad^{12}* allele, that functions as a null mutant specifically for the BMP pathway (Eivers et al., 2009), was used to examine the possible role for Mad signalling between the visceral muscle and midgut to drive midgut MET. Examination of stage 13 *Mad^{12}* mutant embryos revealed no obvious defects in dorsal-ventral spreading, with the midgut fusing and enclosing the yolk in a similar manner to wildtype (Figure 25A). ICP localisation and basal localisation of βPS and Cher appeared normal.

It should be noted that maternal contribution of Mad may be playing a functional role in the *Mad^{12}* mutant. Mad is maternally expressed as indicated by the *in situ* database (Hammonds et al., 2013; Tomancak et al., 2007, 2002) (Figure 25B). While maternal contribution of Mad appears to be restricted to early stages, it is also possible that the protein persists until later stages. Thus, examination of the *Mad^{12}* mutant does not entirely rule out a role for Mad signalling in midgut MET. One possible phenotype from the *Mad^{12}* mutants was the aberrant Cher expression in the foregut, but this was not explored further.
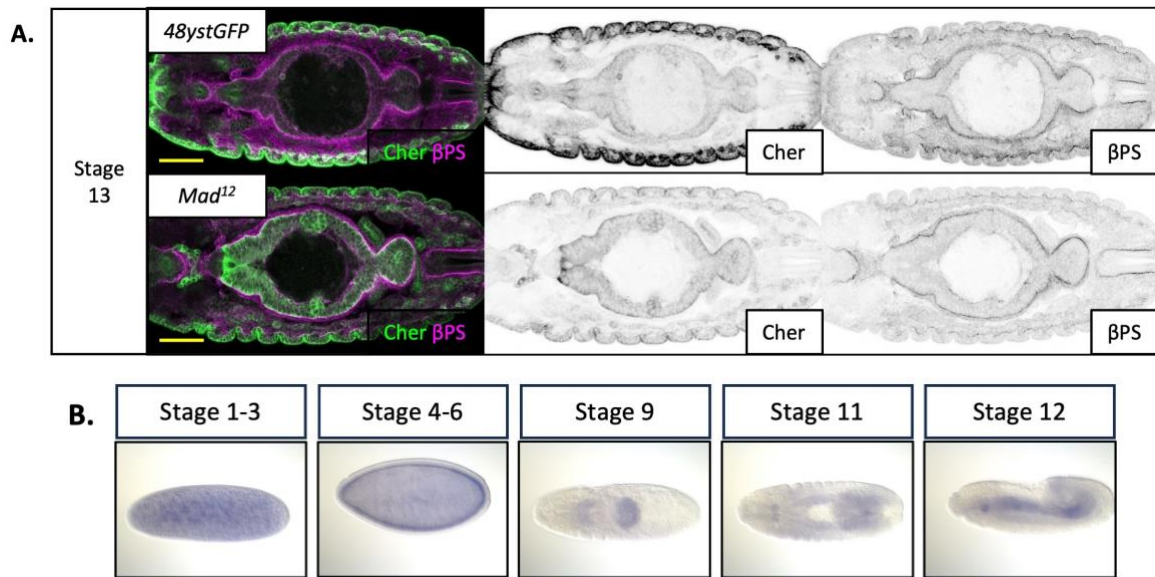
Figure 25. Examination of Mad¹² mutants.

A. Dorsal-ventral view of stage 13 embryos. Basal Cher (Green) and βPS (Magenta) are maintained in *mad¹²* mutants. ICP localisation also appears normal. Cher expression is possibly aberrant in the foregut; a clear distinction in Cher expression between the midgut and the foregut could be observed. N = 48ystGFP, N = 18 embryos. *Mad12*, N = 4 embryos.

B. In-situ hybridisation staining for Mad shows maternal contribution of Mad. Mad appears to be expressed by the midgut after stage 9. Images taken from the Berkeley Drosophila Genome Project in situ database (Hammonds et al., 2013; Tomancak et al., 2007, 2002).

4.1.2 Phenotypic Screen of Wnt4 and PlexA

Given the analysis presented in the previous chapter showing Sema1a expression in the midgut and enriched Otk expression in the visceral muscle respectively (Figure 23), Otk-Sema1a reverse signalling was thought to be the most likely to be mediating interactions between the visceral muscle and the midgut. Wnt4 and PlexA were implicated in Otk-Sema1a signalling and thus mutants for Wnt4 and PlexA were also initially examined.

PlexA^MB09499 (Bellen et al., 2011) is a previously characterised loss of function mutation (Jeong et al., 2012) that disrupts all four isoforms of PlexA. Homozygous *plexA ^MB09499* mutants showed a defect in visceral muscle formation, with staining for the visceral muscle marker FasIII showing only sparse patches of staining where the visceral muscle should be (Figure 26, white arrowhead). Despite this, both Wb and βPS appeared to be basally localised (Figure 26, grey arrowheads). The loss of continuous FasIII was indicative of aberrant visceral muscle development. Thus, the *PlexA* mutant was not further examined for any MET phenotypes as any phenotype observed could be the result of aberrant muscle development rather than the specific loss of *PlexA*.

I next examined *wnt4^EMS23* mutants, a previously characterised amorphic mutation for the *wnt4* gene (Cohen et al., 2002), with a premature stop codon. Examination of *wnt4* mutants for the lateral midgut cell marker FasII did not reveal any significant phenotypes in midgut cell shape. Furthermore, Ecad appears to localise apically in midgut cells, as in wildtype, indicating that the apical domain forms normally (Figure 27, grey arrowheads).
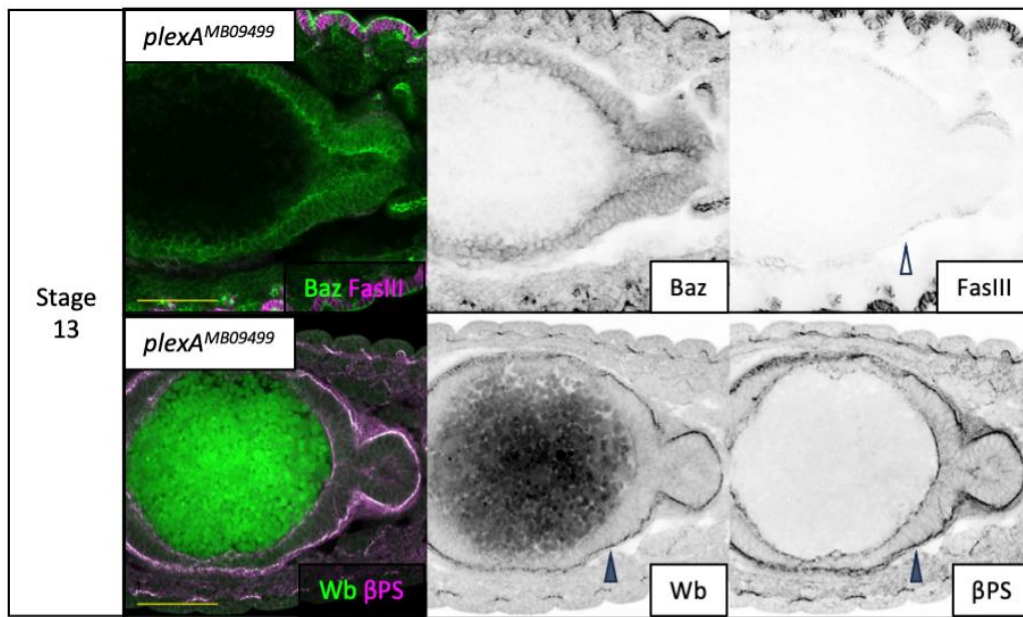
Figure 26 Visceral muscle in *plexA^MB09499* mutants appears to be intact but shows weak expression of FasIII.

Ventral view of *plexA^MB09499* embryos White arrowheads show weak expression of FasIII (Magenta). Wb stains show that Wb is present at the interface between the visceral muscle and the midgut, suggesting that the visceral muscle is present (Grey arrowheads). In support of this, βPS appears to be localised to the basal membrane of the midgut. All scale bars 50μm. Baz, FasIII stain, N = 2 embryos. Wb, βPS stain, N = 4 embryos.
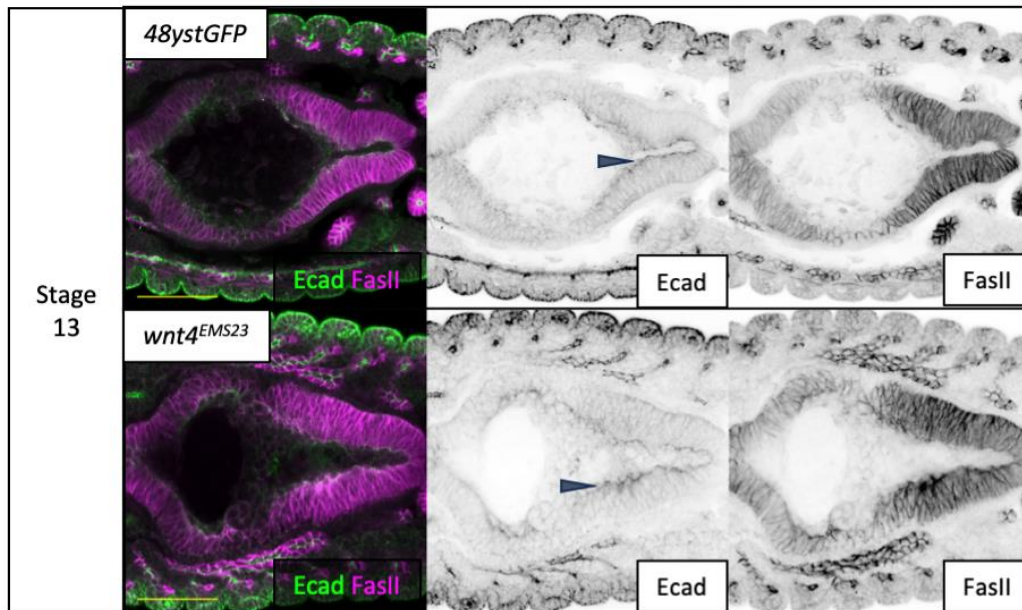
Figure 27 Apical Ecad is maintained in wnt4[EMS23], indicative of an organised apical domain.

Ventral view of stage 13 embryos. Upper panels are wildtype. Lower Panels are wnt4[EMS23] mutants. Grey arrowheads point to apical Ecad in PMEC, which can be seen in both WT and *wnt4* mutants. All scale bars 50µm. 48ystGFP, N = 15 embryos. *wnt4,* N = 6 embryos.

<u>4.1.3 Mutants for Sema1a and Otk demonstrate phenotypes indicative of MET failure.</u>

To investigate a potential role for Sema1a in MET, I first wanted to characterise its expression pattern in wildtype and confirm that the previously characterised *Sema1a^{P1}* was indeed mutant for Sema1a. *Sema1a^{P1},* also known as Sema1a^{k13702}, is a loss of function mutant (Komiyama et al., 2007; Yu et al., 1998) with an insertion within the 5' untranslated region (UTR) of *sema1a*; homozygous mutants of *sema1a* have defects in motor axon and central nervous system axons formation (Yu et al., 1998).

First, I examined Sema1a expression in wildtype to check for Sema1a expression in the midgut. Staining wildtype embryos for Sema1a revealed that Sema1a was expressed throughout the embryo, including in the midgut (Figure 28A). At stage 13, Sema1a appeared to be localised to the basal and apical domains of the midgut (Figure 28A, arrowheads). I next wanted to confirm that the *sema1a^{P1}* mutants were indeed mutants. In stage 13 *sema1a^{P1}* mutants, Sema1a was lost from the midgut (Figure 28A, red outline).

Expression of Sema1a across the embryo is likely due to maternal contribution of *sema1a* mRNA, as indicated by the *in situ* database (Hammonds et al., 2013; Tomancak et al., 2007, 2002) (Figure 28B). However, reduction and mislocalisation of Sema1a from the apical and basal domains of the midgut in *sema1a^{P1}* mutants suggests that the majority of Sema1a in the midgut is not maternally contributed. As such, while maternally contributed *sema1a* mRNA may play a partial role, any function Sema1a may play in the midgut is likely greatly impaired in *sema1a^{P1}* mutants.

Single cell sequencing data suggests that *sema1a* is expressed in the midgut at early stages before being downregulated (Figure 28C). Although *sema1a* RNA is downregulated during late PMEC differentiation, protein expression as maintained throughout the stages in which the cells undergo MET. This is similar to Baz*,* suggesting that Sema1 protein may also persist in the midgut to play a role during MET. In the mesoderm, the differentiated longitudinal visceral muscle appears to express Sema1a (Figure 28D); Otk, thought to be expressed in the circular visceral muscle, may also interact with the longitudinal muscle via Sema1a.
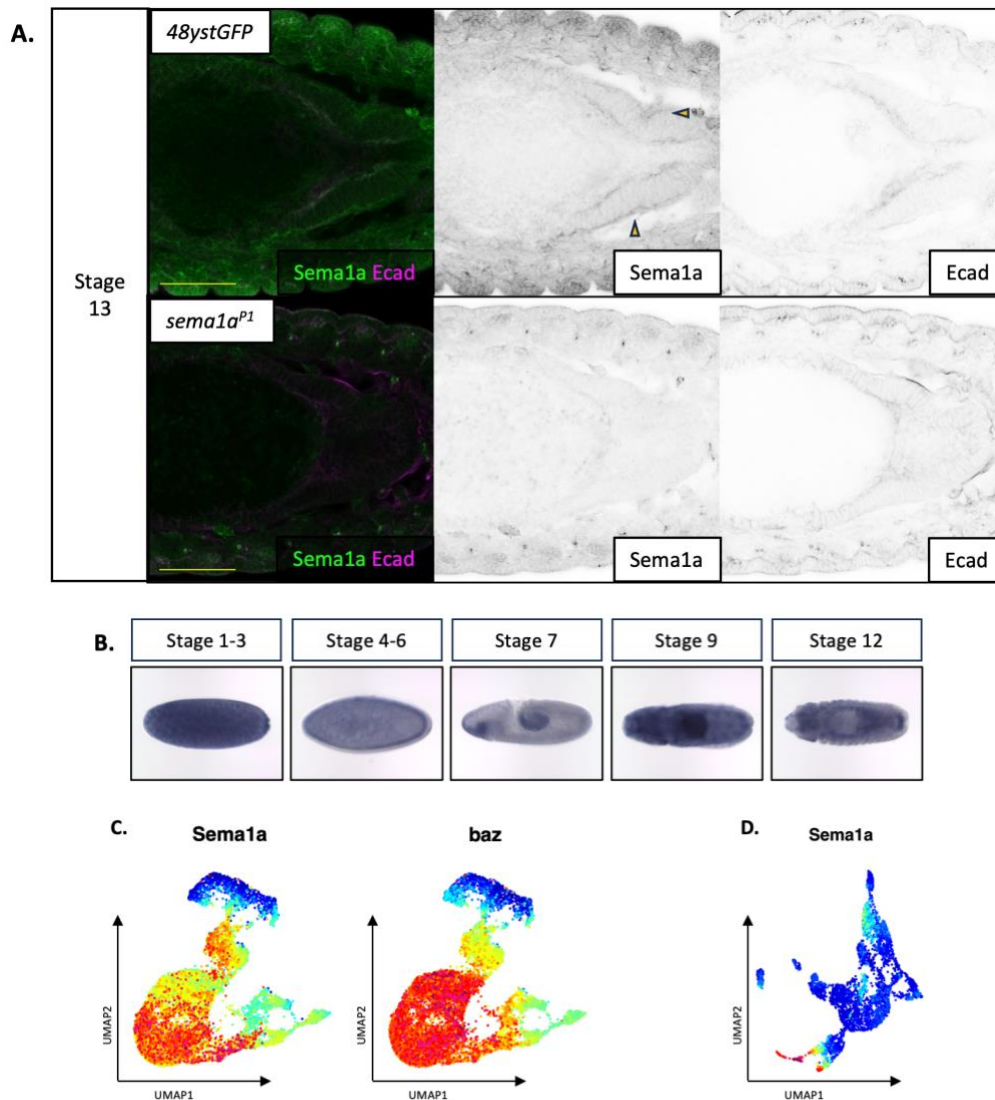
Figure 28. Sema1a expression in wildtype and *sema1aP1* mutant embryos.

A. Ventral view of stage 13 embryos. Upper Panels: In wildtype embryos, Sema1a is found throughout the embryo. Sema1a can also be found at the apical and basal sides of the midgut (arrowhead). Lower Panels: Levels of Sema1a at the apical and basal domains of the midgut is reduced in *sema1a^{P1}* embryos. Thus, the midgut in homozygous *sema1a^{P1}* embryos likely represent a mutant in which Sema1a function is impaired. Note that for the contrast of images have not been adjusted for the images used to examine the presence of Sema1a. All scale bars 50µm. 48ystGFP, N = 17 embryos. *sema1a,* N = 5 embryos.

B. In-situ hybridisation staining for Sema1a shows maternal contribution of Sema1a. Sema1a appears to be expressed by the midgut after stage 9. Images taken from the Berkeley Drosophila Genome Project in situ database (Hammonds et al., 2013; Tomancak et al., 2007, 2002).

C. UMAP of the midgut. Sema1a and Baz show similar expression patterns.

D. UMAP of the mesoderm. Sema1a expression is largely restricted to the longitudinal visceral muscle.

I next wanted to look at Otk, the binding partner for Sema1a which has previously been demonstrated to mediate Sema1a reverse signalling (Nguyen et al., 2022). Staining wildtype embryos revealed expression of Otk in the middle midgut and the posterior midgut (Figure 29A, grey arrowheads). Otk was also expressed throughout the visceral muscle (Figure 29A, black arrowheads), but is stronger in the regions corresponding to Otk expression in the midgut. This is in line with the scRNAseq data, which suggests that *otk* expression is enriched in the circular visceral muscle compared to the visceral muscle (Figure 29B) and expressed in a subset of the PMECs (Figure 29C).

I next examined Otk expression in *otk^{MI14316}* mutant to confirm that these were indeed mutant prior to subsequent analysis. *Otk^{MI14316}* contains a MIMC insertion (Nagarkar-Jaiswal et al., 2015; Venken et al., 2011) within the first intron of *otk*. MIMIC cassettes contain a splice acceptor site and stop codons, and likely results in truncated proteins. The position of the MIMIC cassette suggests that it would disrupt both isoforms of Otk. In line with this, Otk was absent from both the midgut and visceral muscle in *otk^{MI14316}* (Figure 29A, red outline), indicating that the MIMIC insertion in *otk^{MI14316}* likely caused the formation of truncated proteins. Given that the Otk antibody used targets the extracellular domain of Otk (Linnemannstöns et al., 2014), the loss of detectable Otk in *otk^{MI14316}* mutants suggests that any truncated proteins are likely null for any extracellular receptor-ligand function.

Given the failure to undergo MET in *bin* mutants, it was shown that the visceral muscle was specifically required for midgut MET. It was further shown that the somatic muscle was not sufficient. Thus, it was hypothesized that the basal cues driving midgut MET would be enriched in the circular visceral muscle compared to somatic muscle. The expression pattern of Otk fits this description. Furthermore, Sema1a appears to be localised to the basal membrane, which suggests that it could be interacting with Otk to mediate signalling with the underlying visceral muscle. It should be noted that Otk is also expressed in a subset of the midgut and that Sema1a is universally expressed, and therefore may be involved in processes other than midgut MET. Regardless, it appears that Sema1a and Otk expression follow a spatial and temporal pattern that would fit with a role to mediate midgut MET.
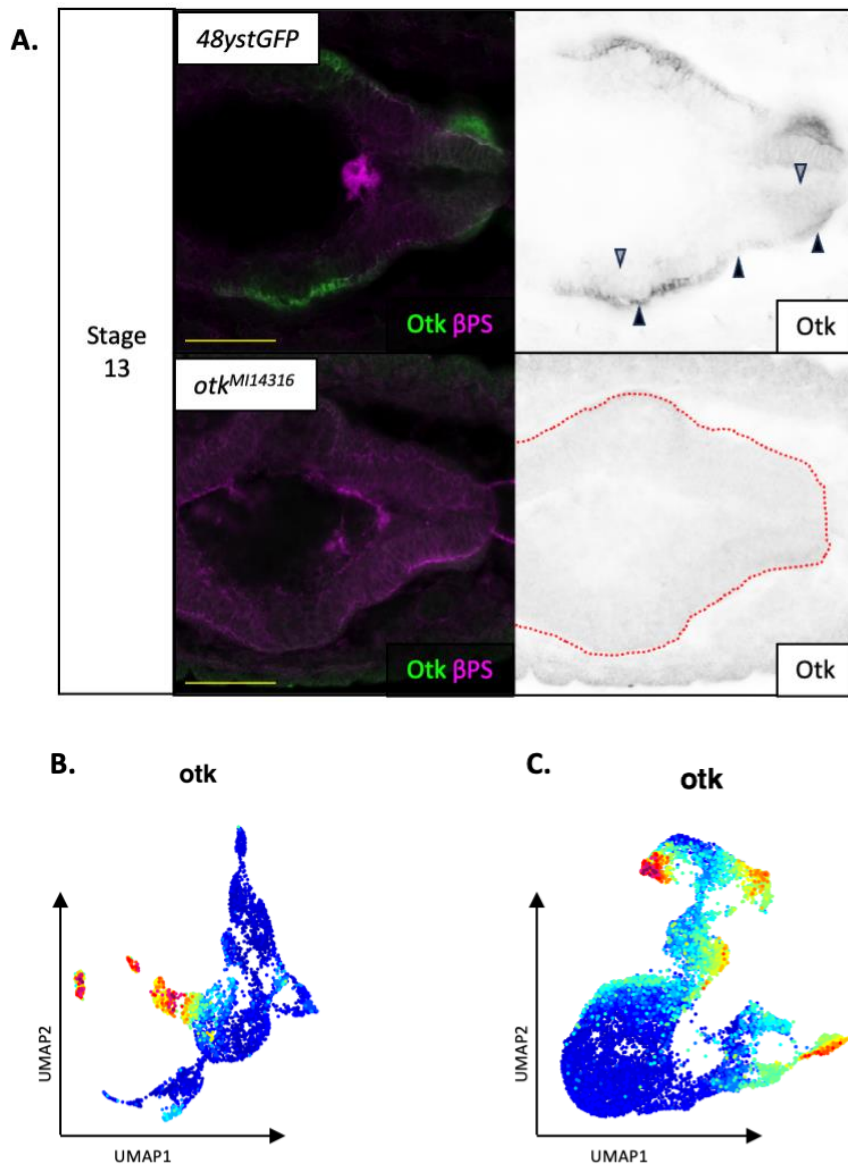
Figure 29. Otk expression in wildtype and *otk^MI14316^* mutant embryos.

A. Ventral view of stage 13 embryos. Upper Panels: In wildtype embryos, Otk is found along the visceral muscle in wildtype. Otk is also expressed in the middle midgut and posterior portion of the posterior midgut. Lower Panels: Otk expression is lost in *otk^MI14316^* embryos. Thus, homozygous *otk^MI14316^* embryos are mutants for Otk. Note that for the contrast of images have not been adjusted for the images used to examine the presence of Otk. All scale bars 50μm. 48ystGFP, N = 5 embryos. *otk,* N = 6 embryos.

B. UMAP of the mesoderm. Otk expression is largely restricted to the circular visceral muscle.

C. UMAP of the midgut. Otk expression is restricted to subpopulations of PMECs.

In stage 12 wildtype embryos, the PMECs within the midgut start to undergo MET during which the cells establish apicobasal polarity. During this stage, midgut cells localise integrins to their basal surface and localise Baz and Ecad apically (Pitsidianaki et al., 2021). I therefore used apical Baz as a marker for organisation of the apical domain; mis-localisation of Baz would indicate a failure to establish an apical domain correctly and failure to undergo proper MET. In this regard, the apical domain is severely affected in *bin* mutants, with almost no apical Baz staining in midgut cells. I therefore looked at Baz localisation in stage 12 embryos of *sema1a^{P1}* and *otk^{MI14316}* mutants to investigate whether Sema1a and Otk affected MET in a similar fashion to loss of contact with the visceral muscle.

Baz in stage 12 wildtype embryos appear as puncta along the apical membrane of the midgut cells (Figure 30A, blue arrowhead). Upon examining Baz localisation in stage 12 *sema1a^{P1}* mutants, Baz appears to maintain an apical bias but appears more diffuse compared to wildtype (Figure 30A, white arrowhead). Examining Baz localisation in stage 12 *otk^{MI14316}* mutants suggested that Baz expression in the midgut was weaker (Figure 30A, compare blue arrowhead to blue arrow).
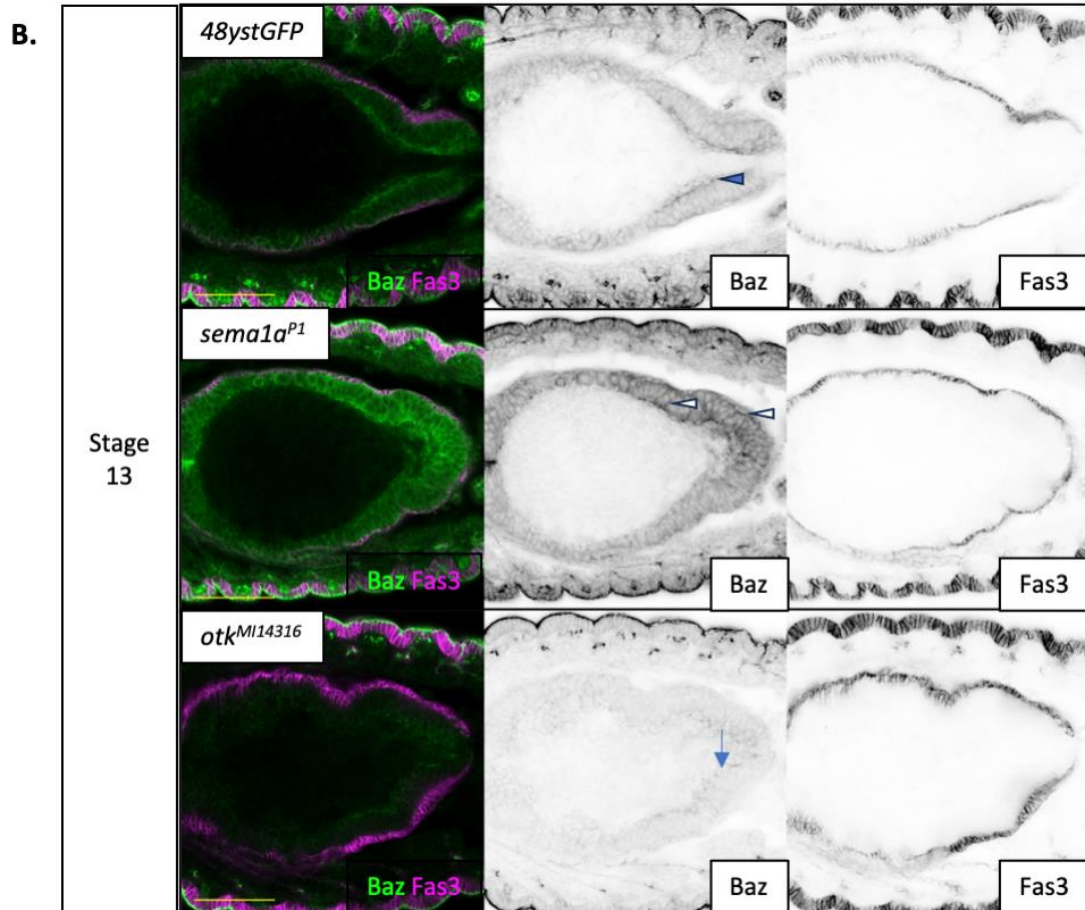
In stage 13 wildtype embryos, Baz localises along the apical membrane of the midgut cells (Figure 30B, blue arrowhead). In stage 13 *sema1a^{P1}* mutants, Baz appeared to be diffuse throughout the cell (Figure 30B, white arrowhead). Like in stage 12, Baz signal appeared to be weaker than wild type in stage 13 *otk^{MI14316}* mutants (Figure 30B, compare blue arrowhead to blue arrow). FasIII stains suggested that the visceral muscle is unperturbed in both mutants; striated patterns typical of the visceral muscle appear wildtype. Put together, although *sema1a^{P1}* and *otk^{MI14316}* appear to show different phenotypes, both fail to organise apical Baz, indicative of some role in MET. In both mutants, adhesion between the midgut and visceral muscle is not disrupted, suggesting that they do not play a role in adhesion.
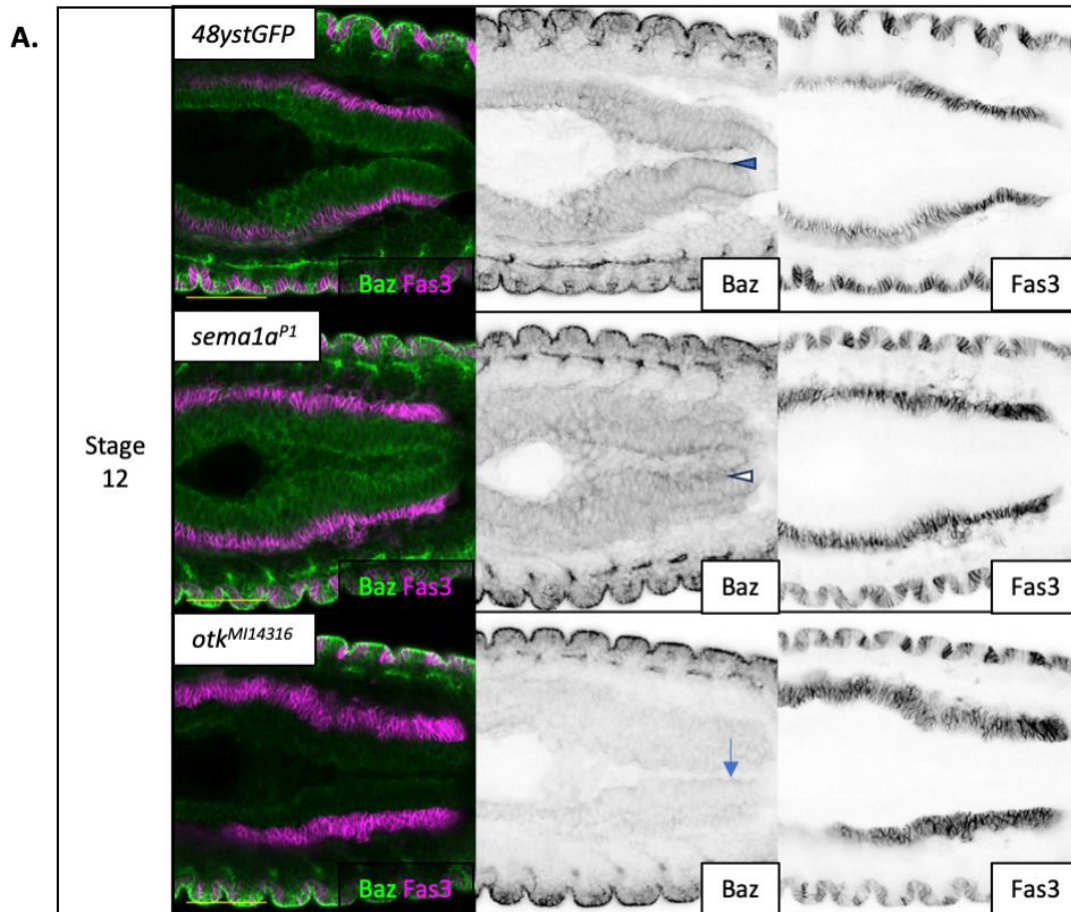
Figure 30. Apical localisation of Baz disrupted in *sema1a^{P1}* and *otk^{MI14316}* mutants.

A. Ventral view of stage 12 embryos. Baz localisation is restricted to the apical membrane in wildtype (Blue arrowhead). Baz localisation is apical but diffuse in *sema1a^{P1}* mutants (white arrowhead). Baz signal is weak in otk^{MI14316} mutants (blue arrow). All scale bars 50μm. 48ystGFP, N = 10. *sema1a,* N = 3. *otk,* N = 4.

Figure 30. Apical localisation of Baz is disrupted in *sema1a^P1* and *otk^MI14316* mutants.

B. Ventral view of stage 13 embryos. Baz localisation is apical in wildtype (Blue arrowhead). Baz localisation is diffuse in *sema1a^P1* mutants, and can be seen along the apical, lateral and basal membranes (white arrowhead)*.* Baz signal is weak in otk^MI14316 mutants (blue arrow). All scale bars 50µm. 48ystGFP, N = 18 embryos. *sema1a,* N = 5 embryos. *otk,* N = 5.

The fact that MET is disrupted in both *sema1aP1* and *otk^MI14316* mutants supported the hypothesis that they interact to drive midgut MET. Based on literature and the observation that Sema1a is basally localised, I hypothesized that Otk from the visceral muscle drives Sema1a to localise to the basal membrane, upon which the intracellular domain of Sema1a mediates Sema1a reverse signalling and recruit Cher.

To test this hypothesis, I examined localisation of Sema1a in wildtype, and homozygous *otk^MI14316 and bin^R22* mutants. I was not able to for Baz as a marker of apical localisation alongside Sema1a as they were both rabbit antibodies. Instead, I examined at Ecad localisation, as Ecad has previously been shown to be apically localised during MET and function as an apical marker similar to Baz (Pitsidianaki et al., 2021). Furthermore, I have shown that apical Ecad is also lost in *bin* mutants, demonstrating that localisation of Ecad is lost upon failure to undergo MET. As such, using Ecad as an apical marker, I wanted to examine whether mislocalisation of Sema1a was linked with aberrant apical polarity.

In stage 13 wildtype embryos, Sema1a is found at both the basal membrane of the midgut (Figure 31A, yellow arrowheads), and at slightly lower levels at the apical membrane (Figure 31A, blue arrowhead). It appears that Sema1a is occluded from the lateral membranes. Ecad is apically localised in these embryos (Figure 31A, blue arrowhead), showing that the apical domain is organised in the wildtype midgut at this stage. In stage 13 *bin^R22* mutants, Sema1a is dispersed around the membranes of cells with disrupted polarity, as indicated by loss of Ecad localisation (Figure 31A, white arrowhead). This suggests that contact with the visceral mesoderm is required for localisation of Sema1a. In stage 13 *otk^MI14316* mutants, Ecad is not restricted to the apical domain (Figure 31A, white arrowhead), indicating that polarity is disrupted. While some Sema1a is maintained at the basal membrane (Figure 31A, yellow arrowhead) it also appears to be dispersed along the lateral membrane (Figure 31A, white arrowheads). Together, this supports a role for Otk in mediating the localisation of Sema1a.

In light of the fact that Sema1a is downregulated at later stages of PMEC differentiation, I wanted to examine whether the phenotypes caused by loss of Sema1a persisted at later stages. In stage 14 wildtype embryos, Sema1a is restricted to the apical and basal domain (Figure 31B, blue and yellow arrowheads). Ecad is apically localised at this stage, indicative of

normal MET. In contrast, apical localisation of Ecad is disrupted in stage 14 *otk^MI14316* mutant embryos. Sema1a appears dispersed throughout the midgut of these *otk* mutants but is also found along lateral membranes (Figure 31B, white arrowheads). Intriguingly, Sema1a appears to be maintained along the basal membrane (Figure 31B, yellow arrowheads).

Put together, the results show that Sema1a is mislocalised in the absence of the visceral muscle and in the absence of Otk. Basal localisation of Sema1a is lost in *bin* mutants, suggesting that basal localisation of Sema1a specifically requires the visceral muscle. In *otk* mutants, Sema1a is found along the basal membrane but is mislocalised to the lateral membranes. This suggests that Otk has a partial role in localising Sema1a, but also suggests that the other signalling cues from the visceral muscle may function to drive localisation of Sema1a. PlexA is expressed in the circular visceral muscle and could contribute to the localisation of Sema1a. This could have been answered by staining for Sema1a in either *plexA^MB09499* mutants or *plexA^MB09499*, *otk^MI14316* double mutants but this has not been examined.
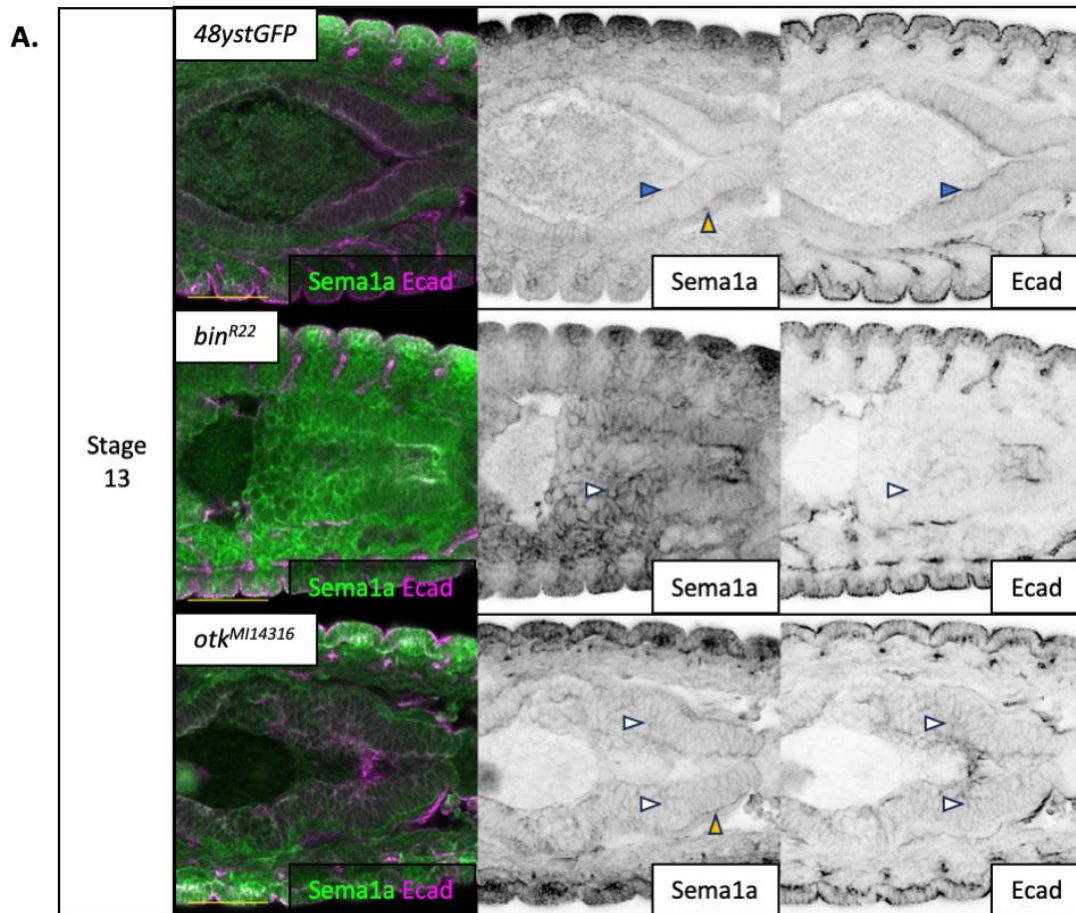
Figure 31. Disruption of Sema1a localisation in *bin^R22* and *otk^MI14316* suggests that Otk plays a role in localisation of Sema1a.

A. Ventral view of stage 13 embryos. In wildtype embryos, Sema1a is found at the apical and basal membrane of the midgut (blue and yellow arrowhead respectively). Ecad is predominantly apically localised (blue arrowhead). In *bin* mutants, Sema1a appears to be dispersed around the membrane in unpolarised cells, as indicated by loss of Ecad (white arrowheads). In *otk^MI14316* mutants, Sema1a appears to be present along the lateral membrane, but is also maintained along the basal membrane. Ecad is no longer apically localised, indicating a loss of polarity. All scale bars 50μm. 48ystGFP, N = 17 embryos. *bin*, N = 6 embryos. *otk*, N= 7 embryos.
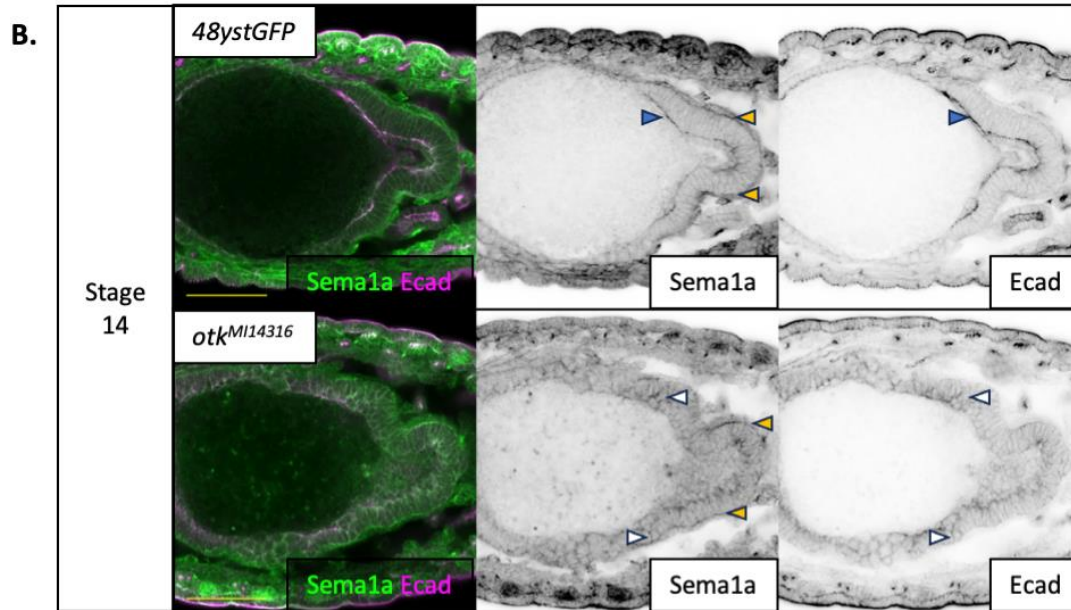
Figure 31. Disruption of Sema1a localisation in *bin^R22* and *otk^MI14316* suggests that Otk plays a role in localisation of Sema1a.

B. Ventral view of stage 14 embryos. In wildtype embryos, Sema1a is found at the apical and basal membrane of the midgut (blue and yellow arrowhead respectively). Ecad is predominantly apically localised (blue arrowhead). In *otk^MI14316* mutants, Sema1a is dispersed throughout the midgut but is also present along lateral membranes. Despite mislocalisation of Sema1a, it appears that Sema1a is still maintained along the basal membrane. Ecad is no longer apically localised, indicating a loss of polarity. All scale bars 50µm. 48ystGFP, N = 5 embryos. *otk*, N= 5 embryos.

During Sema1a reverse signalling in motor axons, Sema1a recruits Pebble (Pbl), a Guanine Exchange Factor that regulates small GTPase Rho1, which is associated with actin remodelling (Jeong et al., 2017). Sema1a also recruits Cher directly to its intracellular domain. In this context, Cher is thought to function as an anchor, physically linking the actin cytoskeleton and Pbl, to spatially restrict localised actin remodelling mediated by Rho1 (Jeong et al., 2017). In light of this, I hypothesized that Sema1a recruits Cher to the basal membrane of the midgut.

Before examining a role for Sema1a in recruiting Cher, I wanted to examine whether Cher is required for MET. It has previously been shown that Cher is localised along the basement membrane (Devenport and Brown, 2004). However, it has never been shown what basal Cher does in the context of MET. Therefore, I examined whether MET occurs normally in *cher^MI07480* mutants by staining for Baz localisation.

There are ten different isoforms of Cher, which can be classified as either full length Cher240 isoforms or short Cher90 isoforms (Külshammer et al., 2022). *cher^MI07480* contains a MIMC insertion (Nagarkar-Jaiswal et al., 2015; Venken et al., 2011) such that the position of the MIMIC cassette likely disrupt all six isoforms of Cher240, but not the other four isoforms of Cher90. Crucially, the long form of Cher contains the F-actin binding domain. Thus, any function for Cher to anchor the actin cytoskeleton to Sema1a should be disrupted in the *cher^MI07480* mutant.

Staining for Baz in homozygous *cher^MI07480* mutants revealed a loss of Baz at the apical domain (Figure 32A). Instead, Baz appears to be mislocalised to the basal domain (Figure 32A, white arrowheads). This may suggest a role for Cher to restrict Baz from the basal domain. It is unlikely that this phenotype is caused by any defects to visceral muscle development; FasIII staining in *cher^MI07480* mutants did not show any visceral muscle phenotypes. This is further supported by single cell sequencing data, which indicates that Cher expression only occurs late during muscle development (Figure 32B). Together these results indicate that the Cher plays a key role in mediating midgut MET. In light of this, if Sema1a does indeed play a role in Cher localisation, the mislocalisation of Cher should lead to the mislocalisation of Baz. The fact that Baz is mislocalised in *sema1aP1* mutants appears to support a role for Cher localisation by Sema1a.
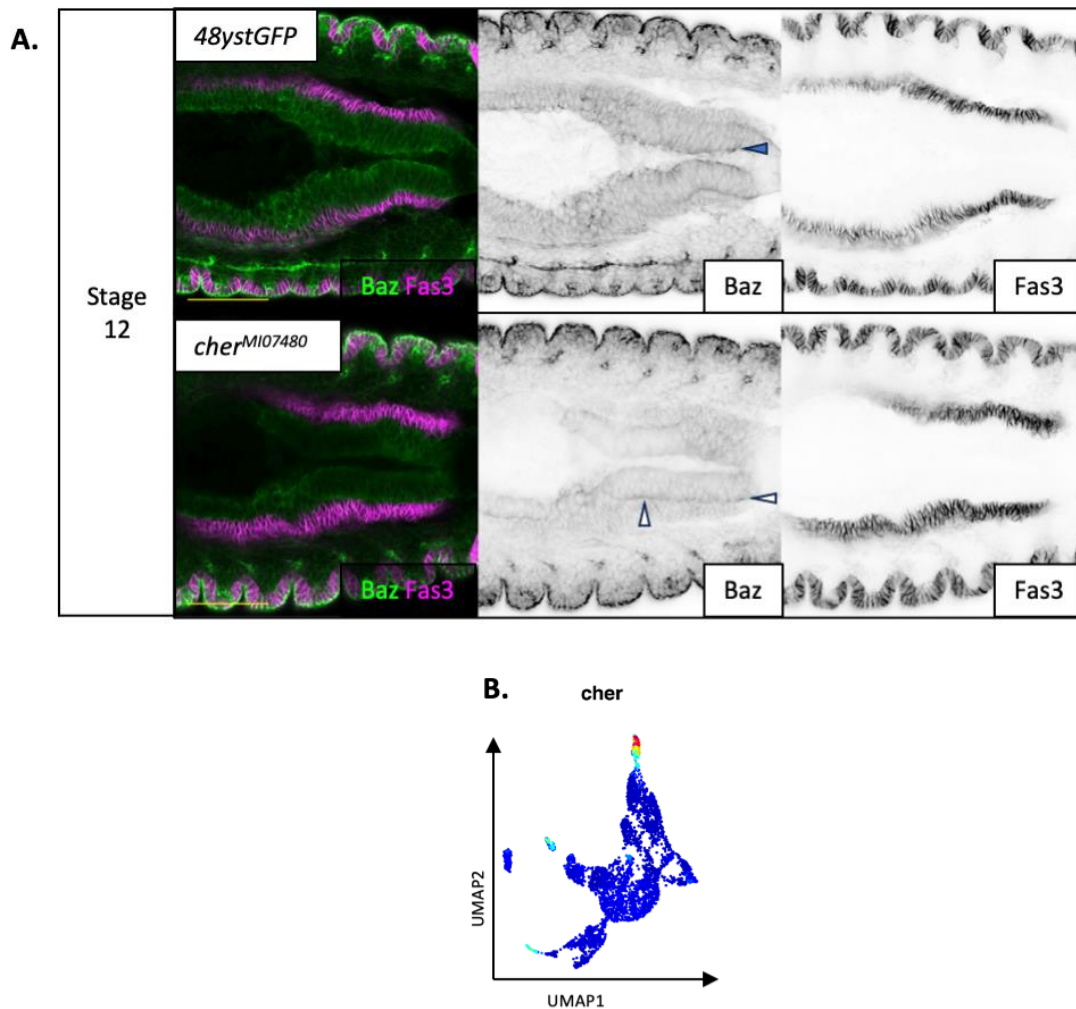
Figure 32. Apical localisation of Baz is lost in *cher^MI07480*.

A. Ventral view of stage 12 embryos. Baz localisation is restricted to the apical membrane in wildtype (Blue arrowhead). Baz localisation in homozygous *cher^MI07480* mutants is more basal than apical. All scale bars 50μm.

B. UMAP of the mesoderm. Expression of *cher* is restricted to late stages of mesoderm development, suggesting that there are no mesoderm phenotypes at stage 12.

48ystGFP, N = 10 embryos. *cher*, N= 3 embryos.

4.1.4 Examining βPS and Cher localisation in *sema1a*^{P1} and *otk*^{MI14316} mutants.

I next wanted to examine whether interactions between the visceral muscle and midgut mediated by Otk and Sema1a play a role in driving Cher localisation. Given the hypothesis that Otk expressed on the surface of the visceral muscle provides a basal cue, I quantified localisation of βPS and Cher in wildtype and in homozygous mutants of *bin*^{R22}, *Sema1a*^{P1}, *otk*^{MI14316} respectively to examine whether the distribution of basally localised proteins was disrupted.

To examine this, I stained each genotype for βPS and Cher at stage 13. βPS in wildtype embryos at this stage is restricted to the basal membrane (Figure 33). In the mutants, βPS can be seen along the basal membrane (Figure 33, yellow arrowheads) but also appears dispersed laterally (Figure 33, white arrowheads). Basal localisation of Cher appears to be largely lost in *bin* mutants. (Figure 33, blue arrow). In *sema1a*^{P1} mutants, basal localisation of Cher was maintained but appears to express at higher levels throughout the midgut (Figure 33, red arrow). In *otk*^{MI14316} mutants, basal Cher was largely lost in a similar manner to *bin* mutants.

Contrary to my hypothesis, these observations appeared to indicate that *sema1a*^{P1} does not affect Cher localisation but instead may have an effect on level of Cher expression. Furthermore, *sema1a*^{P1} and *otk*^{MI14316} mutants have distinct phenotypes, which suggests that they may not be interacting with one another. However, similarity between *otk* and *bin* mutants suggests that Otk may mediate signalling between the midgut and visceral muscle.
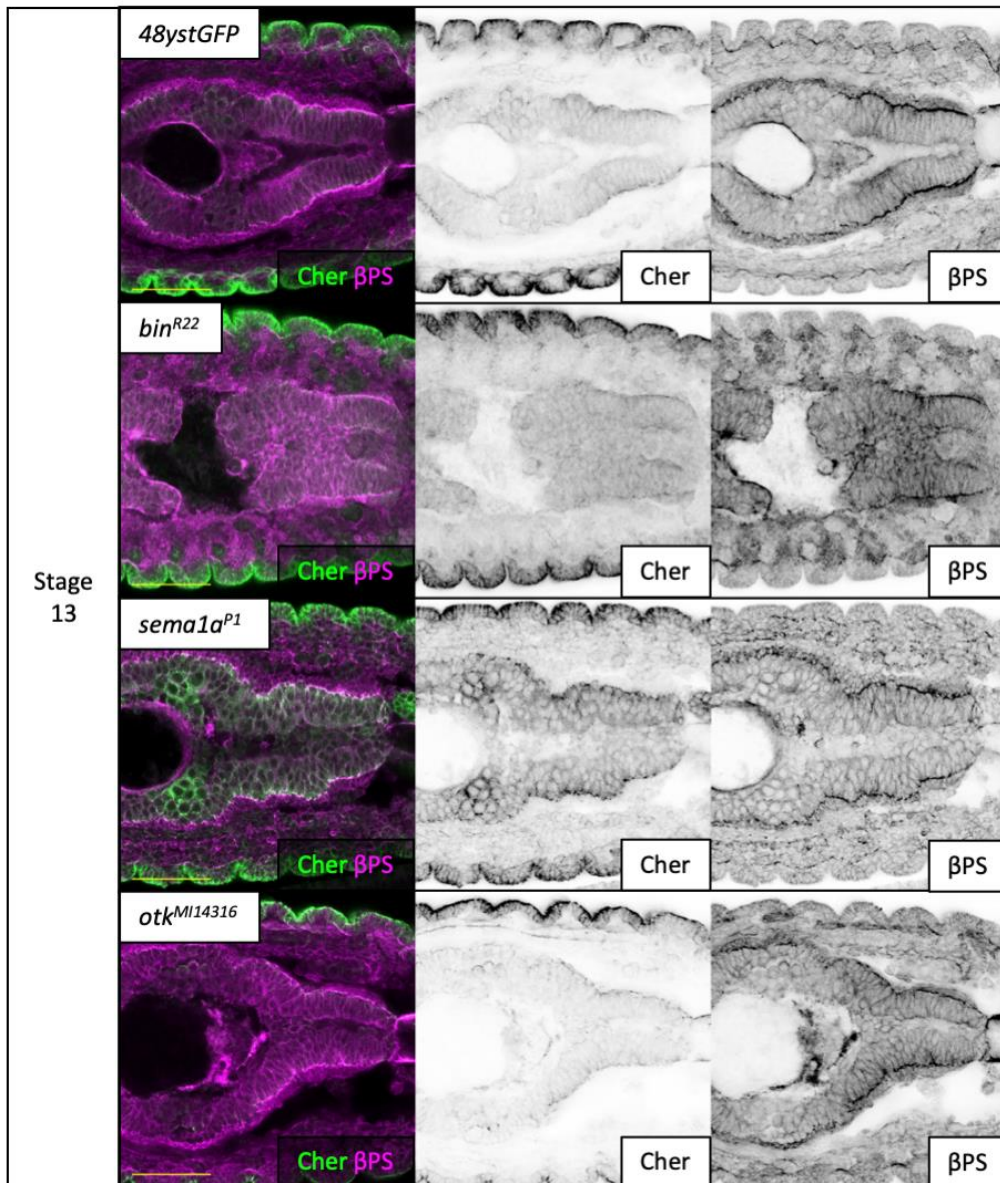
Figure 33. Distribution of βPS and Cher in *bin^{R22}*, *sema1a^{P1}*, *otk^{MI14316}* mutant midguts.

Ventral view of stage 13 embryos. Basal localisation of βPS is retained in all four genotypes. Lateral βPS appears stronger in *bin^{R22}* and *otk^{MI14316}* compared to *sema1a^{P1}* mutant embryos. Basal Cher appears to be maintained in *sema1a^{P1}* but looks to be expressed at a greater level throughout. Basal Cher is largely lost in *bin^{R22}* and *otk^{MI14316}* mutants. All scale bars 50μm.

48ystGFP, N = 19 embryos. *bin*, N= 14 embryos. *sema1a*, N = 11 embryos. *otk*, N = 15 embryos.

Given these findings, I next aimed to quantify these changes. To quantify the distribution of proteins across the apical-basal axis of the midgut, 40-pixel wide lines of various lengths were drawn perpendicular to the interface between the underlying muscle and midgut. The average grey values across the width of each line were used as a readout of protein distribution across the length of each line. For this, peaks in βPS staining were used to identify the basal membrane of the midgut. 5 regions of interests (ROIs) were measured per embryo. 5 embryos were measured per genotype.

However, given the difficulties in getting consistent antibody penetrance within the embryo, the laser power I used to image the cells varied between slides. Given this difference in laser power, I was unable to directly compare grey values as a readout of protein levels. Thus, I instead normalised these readings relative to the minimum and maximum grey values measured in each region of interest. These normalised relative values allow for the relative distribution of protein across the midgut to be compared but not the amount, i.e. the shape of graphs can be compared but not the height of the peaks. Calculations for relative values are outlined in the method section.

Plots showing relative distribution of βPS showed a strong peak of βPS at the basal membrane in all genotypes (Figure 34A). Plots showing distribution of Cher indicated that localisation of Cher to the basement membrane in *bin* and *otk* mutants were disrupted. Distribution of Cher in *sema1a^{P1}* mutants appeared to similar to wildtype (Figure 34B).

Using these relative measurements, I calculated full width at half maximum (FWHM) of the maximum peak. Methods used to calculate FWHM are outlined in the method section. However, there was no significant difference between any genotype in the distribution of βPS or Cher. For βPS, this indicated that βPS peak at the basal membrane was comparable between all four genotypes (Figure 34C). While measurements of FWHM indicates that Cher distribution is unchanged (Figure 34D), it is tempting to suggest, given the shape of the graphs in Figure 34B, that anchoring to the membrane is lost in *otk* and *bin* mutants.

I next calculated the ratio between the area under the curve (AUC) for the basal half of the measured region against the AUC for the full measured region. Comparing the AUC between

the regions allowed for relative distribution across the region in the adjacent to the basal membrane and the region distant from the basal membrane to be compared; epithelia with even distribution of protein should have a lower ratio compared to epithelia with basally biased distribution. This was dubbed AUC Ratio. Methods used to calculate AUC Ratio are outlined in the method section.

In line with observations, AUC Ratios under 1 indicated that βPS was biased towards the basal domain in all genotypes. Compared to wildtype, there was a statistically significant difference in the distribution of βPS of *bin* mutants and *otk* mutants (Figure 34E). *sema1a* appeared have a lower ratio than wildtype but Wilcox rank sum tests indicated that the difference between wildtype and *sema1a* was not statistically significant (p = 0.11). Finally, although Cher was basally biased, the measurement of AUC Ratios failed to show any statistically significant difference in the distribution of Cher between genotypes (Figure 34D). It is likely that the phenotype observed were not strong enough for measurable differences in AUC Ratio.

In conclusion, the quantification of relative distribution suggests that *bin* and *otk* mutants have comparable phenotypes with regards to Cher and βPS localisation. In both mutants, βPS localisation appears to be maintained at the basal membrane but is also dispersed laterally. This is in line with observations of the phenotype. In contrast, relative distribution of βPS and Cher in *sema1a^{P1}* mutants appear to be largely comparable to wildtype, which suggests that Sema1a does not play role in localisation of Cher. It should be noted that these quantifications only looked at relative distribution and does not describe the levels of expression. Stains of *sema1a^{P1}* mutants suggest that Cher expression is elevated, but this will need to be confirmed with methods other than immunofluorescent staining of fixed embryos. For this, live imaging of embryos expressing GFP-tagged Cher should help resolve difficulties with varying antibody penetrance.
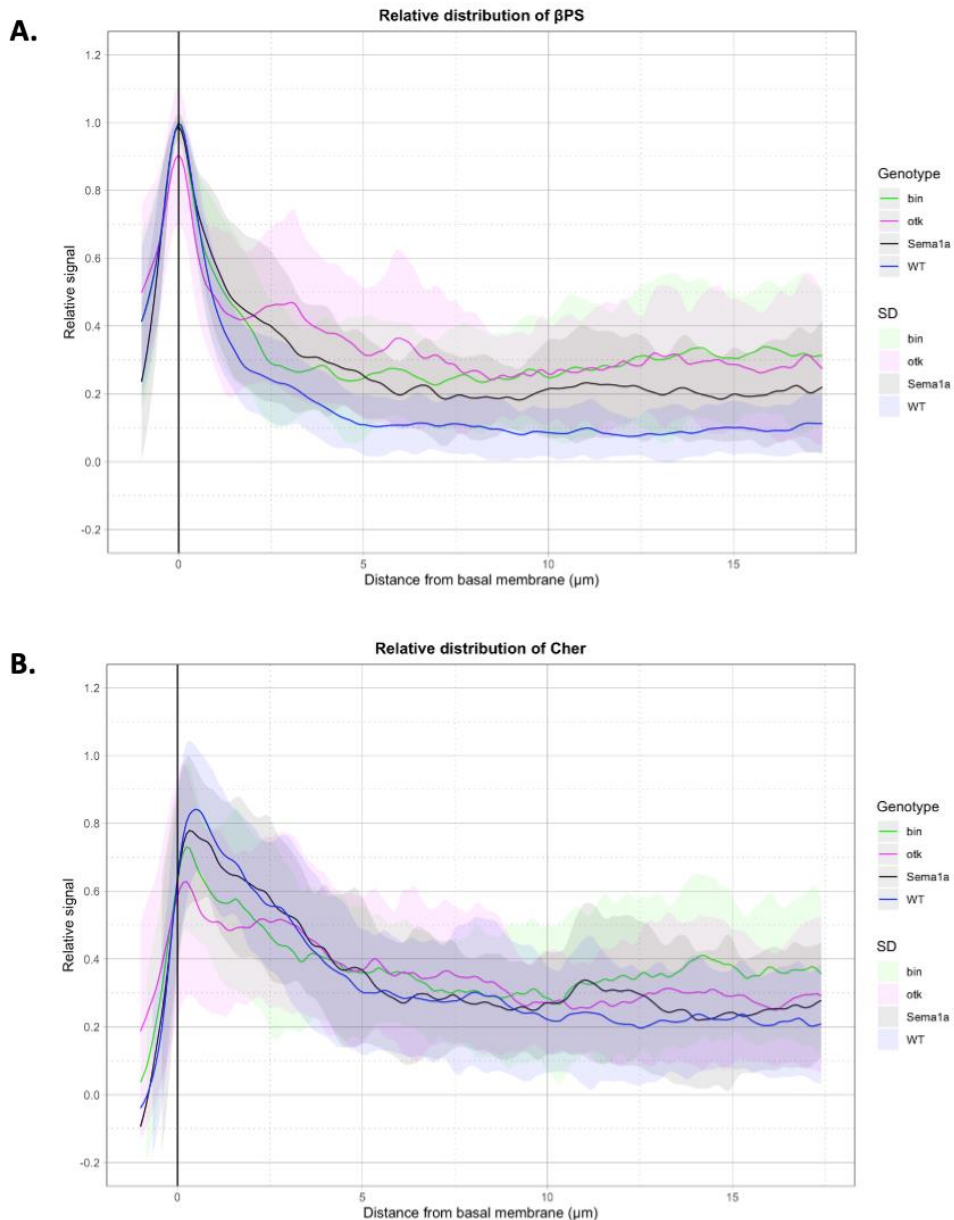
Figure 34. Quantifications of βPS and Cher Distribution in wildtype and *binR22, sema1a^{P1}*, *otk^{MI14316}* mutant midguts.

Solid line corresponds to the average distributions from 5 embryos, each of which were the average of 5 ROIs. Error bars corresponds to the standard deviation of the 5 embryos.

A. Relative distribution of βPS according to distance from the basal membrane of the midgut. βPS peaks were used to identify the position of the basal membrane. Peaks of βPS at the basal membrane appeared relatively consistent in all genotypes.

B. Relative distribution of Cher according to distance from the basal membrane of the midgut. Wildtype and *sema1a^{P1}* mutants showed comparable distribution of Cher. Both *bin^{R22}* and *otk^{MI14316}* mutants appeared to lose localisation of Cher adjacent to the basal membrane.
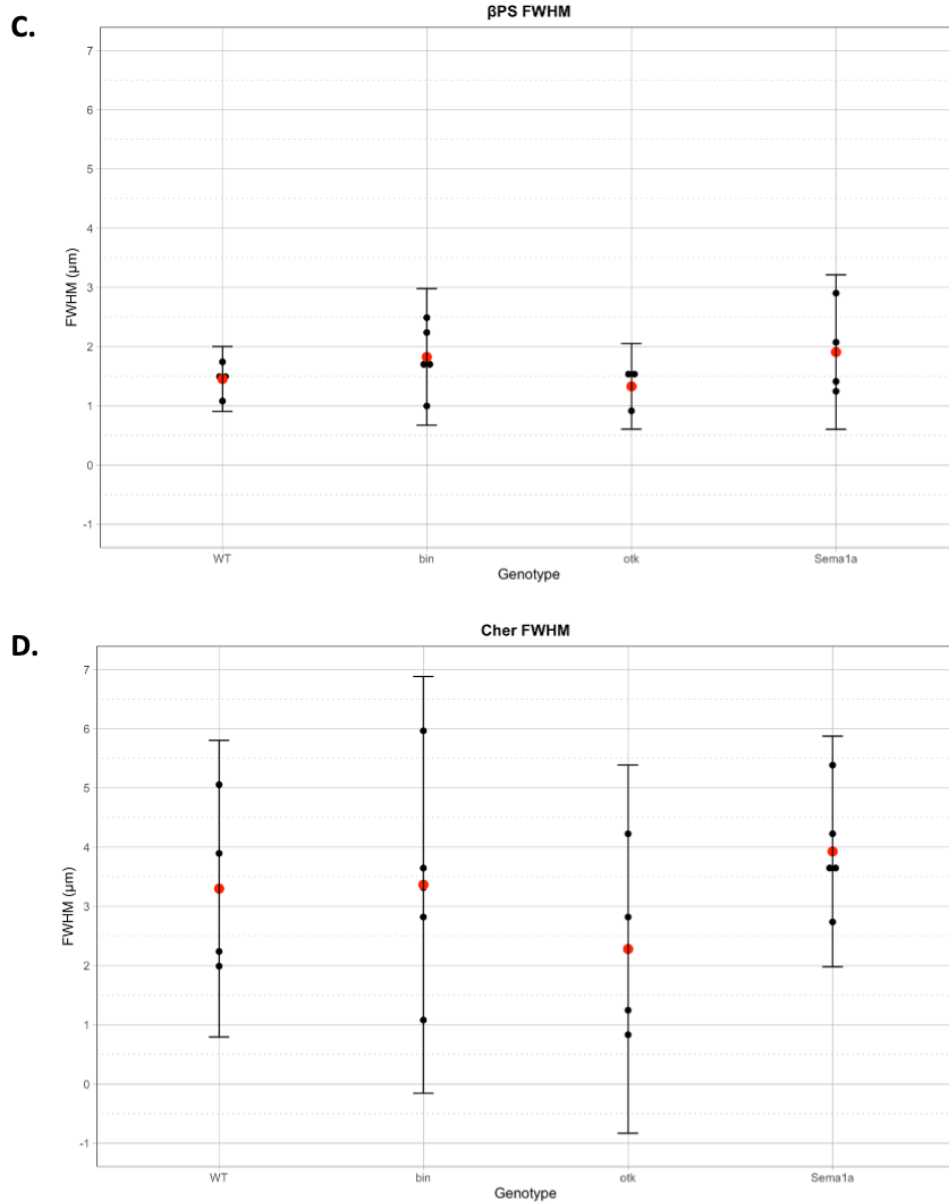
Figure 34. Quantifications of βPS and Cher Distribution in wildtype and *binR22, sema1a^P1^,*

***otk^MI14316^ mutant midguts.**

C and D. Black dots correspond to the average Full width at half maximum **(**FWHM) of one embryo, each an average of ROIs. It should be noted that the FWHM could not be measured from some curves. ROIs in which FWMH could not be measured were not included in the analysis. Embryos missing ROIs were excluded from the calculations. Red dots correspond to the average of readings from the embryos included in the calculations. Error bars are standard deviation.

C and D. FWMH calculated from graphs showing relative βPS and Cher distribution. There is no significant difference between genotypes.
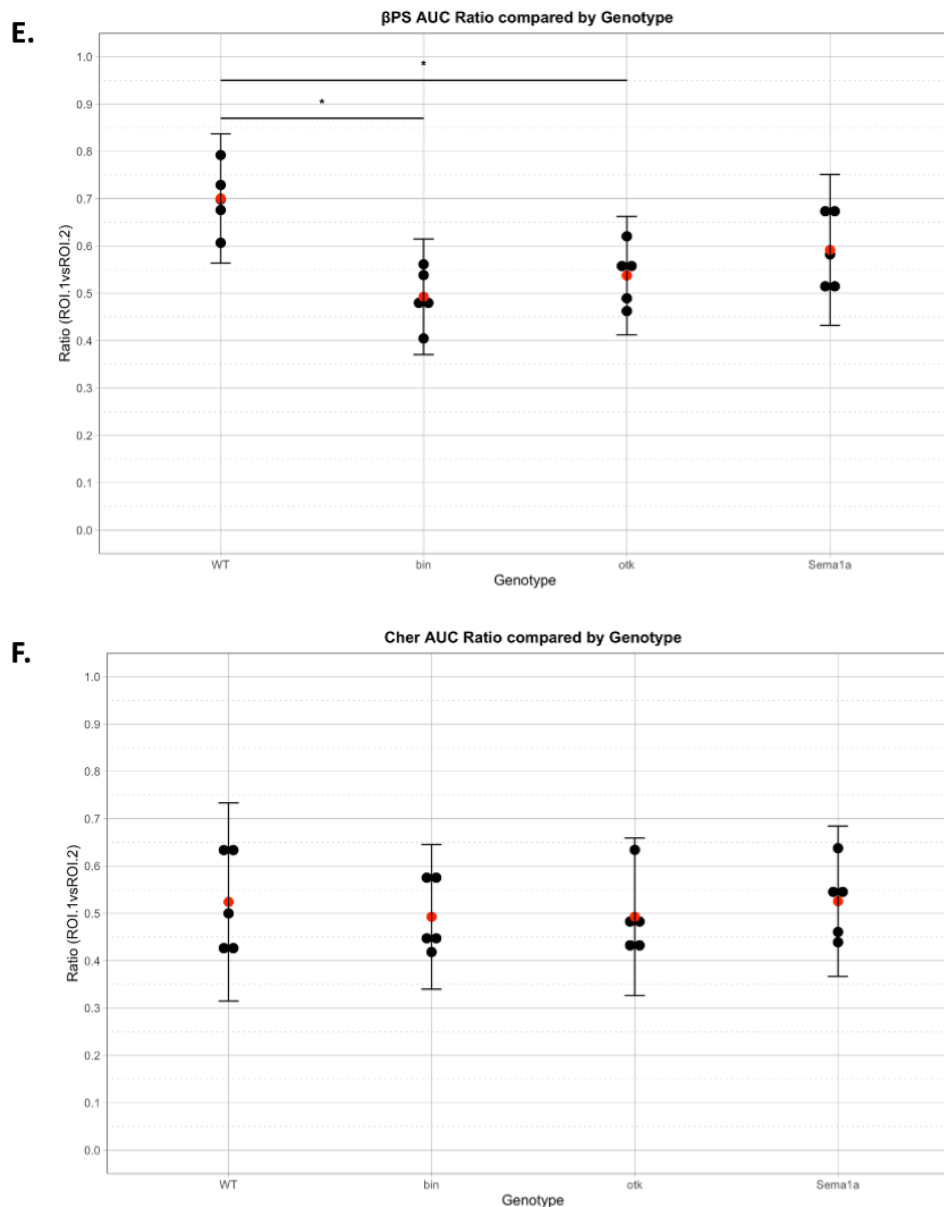
Figure 34. Quantifications of βPS and Cher Distribution in wildtype and *binR22, sema1a^{P1}*,

***otk^{MI14316}* mutant midguts.**

E &F. Black dots correspond to the average AUC Ratio of one embryo, each an average of 5 ROIs. Red dots correspond to the average of the 5 embryos. Error bars are standard deviation.

E. Wildtype βPS is strongly biased to the basal domain. Bias to the basal domain is decreased in *bin* and *otk* mutants, indicating a greater distribution of βPS across the rest of the cell. Bias to the basal domain is decreased in *sema1a* mutants but is not significant.

F. Wildtype Cher is biased to the basal domain. There is no significant difference in distribution of Cher across the genotypes.

4.2. Discussion

In this chapter, I have largely focused on characterising *sema1a^P1* and *otk^MI14316* mutants to explore the potential roles for Otk and Sema1a to mediate midgut MET via signalling interactions between the visceral muscle and the midgut. Given that there is a strong phenotype in the shape and polarity of midgut cells in mutants which lack visceral muscle, this suggested that the visceral muscle provides a specific cue to the midgut, and it is loss of this cue that underlies these cellular phenotypes. Using scRNAseq data, I explored potential ligand-receptor interactions that might be mediating this interaction. Among these genes, mutants for *sema1a* and *otk* showed mislocalisation of the apical protein Baz, indicative of a failure to undergo MET. A number of studies supported a role for Otk in mediating Sema1a reverse signalling (Nguyen et al., 2022). Furthermore, Sema1a reverse signalling, which drives cytoskeleton remodelling, was associated with the recruitment of Cher to the intracellular domain of Sema1a. Together with the fact that Cher is basally localised in the midgut (Devenport and Brown, 2004), I hypothesized that Otk from the visceral muscle could mediate Sema1a reverse signalling in the midgut to drive basal localisation of Cher and cytoskeleton remodelling during MET.

Examination of Sema1a and Otk protein expression and localisation showed that the expression patterns of Otk and Sema1a aligned with their potential role to mediate interactions between the visceral muscle and midgut. At stage 13, Sema1a was localised in the midgut to the basal membrane while Otk was expressed throughout the visceral muscle. Crucially, both *sema1a^P1* and *otk^MI14316* mutants showed mislocalisation of Baz, indicative of failure to undergo MET. It should be noted, however, that although MET appeared to be disrupted in both mutants, phenotypes for Baz mislocalisation were distinct from one another.

In support of interactions between the Sema1a and Otk, localisation of Sema1a appeared to be perturbed in *otk* mutants. In contrast, Sema1a appeared to show a mis-localisation to the lateral membrane in the midgut of *otk* mutants. Interestingly, basal localisation of Sema1a was completely lost in *bin* mutants. This suggested that the visceral muscle was required for basal localisation of Sema1a and that Otk plays at least a partial role in localisation of Sema1a.

Next, given the role of Cher as downstream mediator in Sema1a reverse signalling, I examined *cher^MI07480* to investigate whether failure to undergo MET could be explained by disrupting Cher function. Baz localisation was indeed disrupted in the absence of Cher. This result suggested that Cher localisation mediated by Sema1a could play a role in MET. However, this was not supported by the relative distribution of Cher in *sema1a^P1* and *otk^MI14316* mutants, which indicate that Cher localisation is not dependent on Sema1a. Instead, levels of Cher expression appeared to be greater in *sema1a^P1* mutants, although this remains to be confirmed and needs to be quantified. Interestingly, increased levels of Cher throughout the midgut could explain the dispersed Baz observed in *sema1a^P1* mutants; if Cher acts to restrict Baz from the basal domain, increased Cher throughout the midgut would likely lead to loss of Baz localisation.

Crucially, there are differences in relative distribution of Cher localisation between the *sema1a^P1* and *otk^MI14316* mutants, indicating that they are phenotypically distinct and that they are unlikely to interact with one another. These results could suggest one of two possibilities. First, although I have shown that Sema1a is not detectable in *sema1a^P1* mutants, it is possible that maternal contribution of Sema1a is able to mediate signalling sufficiently such that basal localisation of Cher is not disrupted. A second possibility is that Otk and Sema1a do not interact with one another in this system. Although I have shown that Sema1a localisation is disrupted in *otk^MI14316* mutants, it is possible that the loss of Sema1a localisation observed in *otk* mutants is in fact a consequence of a general loss disruption of polarity, rather than due to the specific loss interactions between Sema1a and Otk. This is plausible given basal localisation of βPS and Cher is also disrupted in *otk^MI14316* mutants.

It remains unclear whether Otk interacts with Sema1a at the basal membrane. A key experiment that might resolve this question would involve driving ectopic expression of Otk in the somatic muscle in a *bin* mutant background. In this background, the midgut should be adherent to a somatic muscle expressing Otk. Thus, if Sema1a is indeed basally localised by Otk, Sema1a should be localised to the basal membrane upon contact with somatic muscle expressing Otk. The absence of Sema1a at the basal membrane would indicate that Sema1a and Otk do not interact. If an interaction between Sema1a and Otk is shown, this can be

followed by generation of mutant clones of homozygous *sema1a^{P1}* mutant germ cells to examine maternal-zygotic mutants for Sema1a.

Regardless of whether Sema1a mediates signalling with Otk, results from the *otk* mutants suggests that Otk plays a role in MET. Loss of basal βPS and Cher in *otk* mutants appears to be comparable to *bin* mutants, despite the fact that the midgut in *otk* mutants is adherent to the visceral muscle. This suggests that Otk is crucial to organise the basal domain. Furthermore, Ecad and Baz localisation are both disrupted in *otk* mutants, clearly indicating that MET is disrupted. Together, this suggests that Otk plays an important role in mediating MET. Given that gaps between the visceral muscle and the midgut were not found in *otk* mutants, a role for adhesion can be ruled out. Importantly, the phenotypes do not appear to be limited to the region in which Otk is expressed in the midgut cells, and thus it is unlikely that the phenotypes observed in the *otk* mutants are due to the loss of Otk from the midgut.

Similarly, Sema1a also appears to be required for midgut MET to take place. Despite normal relative distribution of βPS and Cher in *sema1a* mutants, a disruption of Baz localisation indicates a failure to organise the apical domain. Thus, regardless of whether or not there are low levels of maternal Sema1a in *sema1a^{P1}* mutants, reducing Sema1a function appears to be sufficient to disrupt organisation of the apical domain. While my work so far has focused on Cher as a downstream mediator of Sema1a reverse signalling, phosphorylation of Moesin (Moe) has been shown to occur downstream of Sema1a reverse signalling in photoreceptor axons (Hsieh et al., 2014). In light of the fact that Moe is also basally localised during midgut MET (Pert et al., 2015), it would be interesting to examine basal Moe in the future, as this may reveal a link between Sema1a function and organisation of the basal domain.

While further experiments are required to examine whether the specific interaction between Sema1a and Otk mediates signals between the visceral muscle and the midgut, recent evidence suggests signalling by Otk-Sema1a may not require direct contact between the two tissues. It has been shown in the adult *Drosophila* intestinal epithelium that injury-induced expression of Matrix Metalloproteinase 1 (MMP1) can cleave the extracellular domain of Otk. Crucially, although the exact mechanisms underlying this has not been made clear, dispersal of this extracellular domain of Otk appears to be sufficient to drive migration of intestinal

stem cells to sites of injury (Hu et al., 2021). This is particularly interesting given the evidence indicative of adhesion-independent cues that polarise the midgut (Devenport and Brown, 2004).

In conclusion, my data supports role for both Otk and Sema1a in mediating midgut-MET. While it is likely that both Otk and Sema1a act on the basal side of midgut cells, their activity appears to be somehow required for the localisation of Baz to the opposing apical surface. While the importance of basal cues in establishing polarity in epithelial cells is well established, how crosstalk between basal and apical domains translate into organisation of the apical domain and cell shape change remains poorly understood (Barrera-Velázquez and Ríos-Barrera, 2021). Further examination of precisely how loss of either Otk or Sema1a leads to a failure to localise Baz may help uncover these mechanisms.

Chapter 5. Discussion and Conclusions

During development, cells require the ability to transition between epithelial and mesenchymal cells to organise themselves into functional tissues and organs. While the molecular mechanisms by which mesenchymal cells reepithelialise are poorly understood, it has been shown in a number of developmental contexts that contact with external tissues is required. For example, the overlying ectoderm is required for the formation of epithelial somites (Correia and Conlon, 2000). Additionally, signals from the ureteric bud have been shown to be required for the formation of epithelial renal vesicles during nephrogenesis (Yang et al., 2013). In *Drosophila*, the visceral muscle has been shown to be required during embryonic midgut morphogenesis. In this thesis, I have investigated the role of external cues during midgut morphogenesis.

A number of studies examining *Drosophila* midgut morphogenesis have demonstrated that the surrounding visceral muscle is required. Firstly, given that the posterior midgut makes contact with the underlying visceral muscle during migration (Wolfstetter et al., 2009), it was suggested that the visceral muscle functions as a guiding tract for migration (Reuter et al., 1993). Secondly, they suggested that the re-epithelialisation of midgut cells after migration is also dependent on contact with the visceral muscle (Tepass and Hartenstein, 1994b). Although a few players mediating migration and MET have been identified (Pert et al., 2015; Pitsidianaki et al., 2021), the interactions between the midgut and muscle during MET have not yet been thoroughly explored. In this thesis, I have presented a characterisation of wildtype midgut throughout MET. I have also examined *bin* mutants, which lack all visceral muscle, to examine the role of the underlying visceral muscle in both migration and MET. Surprisingly, I showed that both the somatic and visceral muscle are capable of supporting midgut migration. In contrast, contact with the visceral muscle is specifically required for midgut cells to undergo a full MET. In embryos that lack the visceral muscle, reestablishment of apicobasal polarity, tubulin remodelling, and the cell shape changes required to form a columnar monolayer are disrupted. Finally, by leveraging scRNAseq, I have identified Sema1a and Otk as potential mediators of the midgut and visceral muscle interactions.

5.1 The role of Muscle in Midgut Migration.

During midgut migration in wildtype, the midgut makes contact with the underlying circular visceral muscle (Wolfstetter et al., 2009) and is considered an important basal substrate for midgut migration (Devenport and Brown, 2004; Pitsidianaki et al., 2021). In examining midgut migration in wildtype and *bin* mutants which lack all visceral muscle, I have shown that early midgut migration does not specifically require the visceral muscle and that the somatic muscle is sufficient to drive the early stages of migration. While this is contrary to published work that indicates netrins from the circular visceral muscle play a role in migration and midgut fusion (Pert et al., 2015), my results indicate that the somatic muscle is sufficient to support migration at early stages.

5.2 The role of Visceral Muscle in MET.

Although migration was unperturbed in *bin* mutants, there was a failure to undergo MET in the absence of the underlying visceral muscle. This indicated that phenotypes observed in *bin* mutants were not the result of aberrant migration preceding MET. More importantly, this finding allowed for a clear distinction to be made between the cues mediating MET and migration; the basal cues driving MET are likely to be found in the visceral muscle but not the somatic muscle. In light of this, I focused on investigating the role of the visceral muscle in driving MET.

Laminins and integrins have previously been shown to play an important role during midgut-MET (Devenport and Brown, 2004; Pitsidianaki et al., 2021). Crucially, *bin* mutant embryos appear to retain Wb at the basal interface of the midgut, mediating adhesion to the somatic muscle. Furthermore, this basal Wb was shown to be sufficient to drive basal localisation of βPS integrin. Basal localisation of βPS has previously been shown to be an early step during midgut MET and crucial to organise the basal domain (Pitsidianaki et al., 2021). Despite this, *bin* mutants are unable to undergo MET; apical localisation of Baz and Ecad found in wildtype embryos is lost in *bin* mutants. This result highlights that integrins are not sufficient to drive MET. Importantly, this result also show that the *bin* mutant phenotype is a result of visceral muscle-specific cues; the failure to undergo MET despite the fact that the midgut is adherent to the somatic muscle indicates that the visceral muscle provides cues critical for MET. This

demonstrated that *bin* mutants can be used to investigate the cues specific to the visceral muscle that drive MET.

My work has shown that the cues specific to visceral muscle is required for various aspects of midgut morphology including apical polarity, microtubule remodelling, and for coordinated cell shape changes. Loss of apical Baz and Ecad observed in *bin* mutants suggested that the visceral muscle is required to organise the apical domain. Polarised microtubule bundles were also lost in the absence of the visceral muscle, indicative of its role to organise microtubules. Finally, I showed that *bin* mutants do not undergo the cell shape changes that occur in wildtype. In wildtype embryos, the midgut transition between a pseudostratified epithelium to a columnar monolayer, indicative of a mechanism driving coordinated cell shape changes across the midgut.

These changes in midgut morphology are thought to be caused by the loss of specific basal cues from the visceral muscle. This raises the question how basal cues translate into organisation of the apical domain and the formation of polarised microtubules. Although it is not possible from my results to tell whether these are sequential or concurrent processes, published work suggests that apical localisation of microtubule organising centres are dependent on apical polarity proteins such as Baz/Par3, indicating that these processes are closely linked (Feldman and Priess, 2012; Sanchez and Feldman, 2017). This relationship between polarised microtubules and organisation of the apical domain can be tested by ectopic expression of microtubule severing proteins in the midgut. Uncovering this would provide a better insight into the sequence of events that occur during MET downstream of the basal cues that initiate the process.

Leveraging scRNAseq data, I identified Sema1a and Otk as potential mediators of this basal cue. Although I have not been able to prove that they interact with one another, they are both likely play a role to organise the basal domain during midgut MET. Importantly, organisation of the apical domain is disrupted in both *sema1a^{P1}* and *otk^{MI14316}* mutant. As such, investigating the downstream mediators of Sema1a and Otk will likely reveal the mechanisms by which basal cues establish apicobasal polarity.

5.3 Modes of MET regulation

Unlike EMT, there does not appear to be a conserved transcription factor that drives MET. Instead, it appears that external cues are required to drive MET. The role of external cues during MET appears to be conserved in the context of both cancer and development (Esposito et al., 2019; Gao et al., 2012; Plygawko et al., 2020). My work has confirmed that in the context of the embryonic midgut, the visceral muscle provides a specific basal cue required for MET. This specificity between the external cue and cells undergoing MET appears to be conserved in other developmental systems. For example, the tail mesoderm specifically requires the tail ectoderm for expression of Paraxis, which was shown to be required for subsequent formation of epithelial somites in the tail mesoderm; recombining different sources of ectoderm or mesoderm disrupted somite development (Correia and Conlon, 2000). This specificity between external cues and cells undergoing MET might indicate that developmental METs are strictly regulated by the local environmental.

Regulation of MET is likely a complex process involving a number of external cues. In this work, I have focused on examining the role of the underlying visceral muscle on PMECs throughout the midgut. However, it is likely there are other external cues that help mediate midgut MET. For example, apical ECM has been shown to play a role in cell morphology in the tracheal tube and the pupal wing disc (Barrera-Velázquez and Ríos-Barrera, 2021). Although apical ECM has not been studied extensively in the midgut, apical secretion of LanA by the midgut has been previously suggested to reinforce polarity (Pitsidianaki et al., 2021). Thus, it is likely that apical ECM also plays a role to dictate aspects of MET. Furthermore, the synchronous manner in which cell shape changes that occur during MET suggests that there is signalling between the lateral domains midgut cells to coordinate cell shape changes. The role of external cues as a driver of MET is poorly understood and as such, warrants further investigation.

To conclude, the *Drosophila* embryonic midgut is an excellent developmental model to analyse MET. The scRNAseq atlas of the embryonic wildtype midgut has enabled analysis of the transcription changes underlying midgut MET. In combination with imaging techniques, a phenotypic screen of mutants has identified a potential mechanism by which Otk expressed on the surface of the visceral muscle provides a basal cue to induce midgut MET via Sema1a

reverse signalling. Future experiments are needed to confirm this interaction and to investigating the downstream mechanisms by which these basal cues drive midgut MET.

Chapter 6. Material and Methods

6.1 Fly Stocks

Fly stocks were maintained at room temperature. Crosses to balance or recombine stocks were carried out at 25° C. Details for all genotypes and transgenes can be found in Flybase (http://flybase.org) or in references listed here. The genotypes of the flies used and where they were obtained can be found in the table below.

Description	Source
48y-Gal4	Bloomington #4935
UAS-stGFP	Bloomington #84277
bin^{R22}	Gift from Manfred Frasch
sna^{18} twi^{3}	Bloomington #3299
ush^{2}	Bloomington #2508
wb^{PZ09437}	Bloomington #12362
ResilleGFP, SpiderGFP	Gift from Claire Lye from the lab of Bénédicte Sanson
Mad^{12}	Bloomington #58785
plex^{AMB09499}	Bloomington #61741
wnt4^{EMS23}	Bloomington #6650
sema1a^{k13702}	Bloomington #11097
otk^{MI14316}	Bloomington #59688
cher^{MI07480}	Bloomington #43714

6.2 Embryo collection and staining

Flies were kept at 25° C for a minimum of 36 hours before collecting embryos.

Live confocal microscopy

Embryos were dechorionated in a solution of 50% bleach. Dechorionated embryos were placed on to an agar plate. These were staged, selected and oriented under a Zeiss fluorescent dissecting microscope. The embryos were then transferred to a coverslip coated with heptane glue and covered in Voltalef 10S oil. Embryos were imaged using an inverted Zeiss LSM880.

Fixing

Embryos fixed for alpha-Tubulin were fixed as described in (Gomez et al., 2016) using a 1:1 10% paraformaldehyde solution in PBS:Heptane at 20 mins at room temperature. Otherwise, embryos were fixed in a 1:1 Heptane and a solution of 4% paraformaldehyde solution in PBS with 0.05% Tween-20 for 20 min at room temperature. Fixed embryos were stained and mounted using standard procedures. Slides were mounted in Fluoromount-G mounting medium (eBiosciences). Embryos were staged according to developmental stages described in the Atlas of Drosophila Development (Hartenstein, 1993). Antibodies used include mouse anti-αTubulin 1:1000 (T6199, Sigma); rabbit anti-Baz (1:400; gift from Andreas Wodarz); rabbit anti-Cher (1:400; gift from Lynn Cooley); rat anti-Ecad (DCAD2; 1:40; Hybridoma Bank); mouse anti-Fas3 (7G10; 1:10; Hybridoma Bank); goat anti-GFP (AB6673; 1:500; Abcam); rabbit anti-GFP (PABG1; 1:1000; ChromoTek); mouse anti-Hnt (1G9; 1:20; Hybridoma Bank); guinea pig anti-Otk (1:500; gift from Andreas Wodarz); rabbit anti-Sema1a (1:400; gift from Alex Kolodkin); mouse anti-Talin A22A (1:10; Hybridoma Bank); mouse anti-Talin E16B(1:10; Hybridoma Bank).

Polyclonal Sema1a antibody was diluted to 1:10 concentration before pre-adsorption using fixed embryos at 4˚C overnight. This was then used at a 1:40 concentration.

Secondary antibodies used were all made in donkey and used at a dilution of 1:100. The following antibodies were used: anti-rabbit 488+ (A32790; Invitrogen), anti-goat 488 (A11055; Invitrogen); anti-goat 488+ (A32814; Invitrogen); anti-rabbit 555 (A31572; Invitrogen); anti-mouse 555 (A31570; Invitrogen); anti-rat 555+ (A48270; Invitrogen); anti-mouse 647 (A31571; Invitrogen); anti-mouse 647+ (A32787; Invitrogen); anti-rabbit 647 (A-31573; Invitrogen); and anti-rat 647+ (A48272; Invitrogen); anti-guinea pig Cy3 (AB_2340460; Jackson Immunoresearch).

6.2 Imaging setup

Confocal images were acquired using a Zeiss LSM880 with either the internal GaAsP detectors or an Airyscan detector. A Plan-Apochromat 25×/0.8 multi-immersion lens with oil or a Plan-Apochromat 63×/1.40 oil-immersion lens was used for fixed images. Images taken at 63x

using the Airyscan detector were processed using Zen software. All images presented are of a single selected Z-stack. Homozygous mutants were identified using fluorescent balancers.

For live imaging, the Plan-Apochromat 40×/1.3 oil immersion lens was used. Embryos were imaged with a Chameleon Discovery dual output multiphoton laser, with the spectral laser tuned to 890-nm wavelength.

All images presented were set to a contrast in which the top 5% of pixels were saturated with the exception of images in Figure 28 and 29. These images were used to illustrate the presence of Sema1a and Otk respectively; enhancing images pixels in the absence of signal leads to increased noise. Images were converted to 8-bit without adjusting contrast for images showing both wildtype and mutant were not changed. Any adjustments made to contrast were linear adjustments and made across the entire image.

6.3 Imaging set up for nuclear tracking.

For timelapses used to image nuclear migration, stacks of 20–25 μm and a z-depth of 1.5 μm were acquired at 2-min intervals over a period of over 60 min. A minimum of five videos per condition were selected for analysis. *48ystGFP* embryos or *48ystGFP;bin^{R22}* expressing nuclear GFP in the midgut were imaged to examined nuclear migration. Homozygous *bin* mutants were identified using the fluorescent balancers.

Germband was labelled by inducing photodamage using a laser focused a small region distal to the midgut at the central Z-stack. Lasers were focused on a 10x10 pixel square. Pixel dwell was set to a speed of 1 (65.43μsec) and averaging was set to 16. The spectral laser was tuned to 700-nm wavelength. After one round of laser-induced photodamage, embryos were checked for fluorescence before starting the timelapse. Tracking germband retraction speed using the anterior portion of the hindgut in unlabelled wildtype embryos showed no difference compared to labelled wildtype embryos. Similarly, wildtype midgut migration was comparable between unlabelled and labelled embryos. Germband migration was consistent across both genotypes at a speed of 1.6μm/2 mins at 25˚ C.

Live movies of nuclear migration were pre-processed and quantified using ImageJ Fiji following a protocol previously used in the lab (Tosi and Campbell, 2019).

6.4 Quantification of cell shape

ResilleGFP;SpiderGFP or *ResilleGFP;bin^{R22}/TTG* were imaged to examined cell shape. Overall embryo morphology was imaged using 25x lens; images used to quantify cells were captured using the 63x lens. Cell shape was quantified by manually drawing masks. A minimum of 6 cells were quantified from each embryo. Masks were drawn with help from Noah Landgraf.

6.5 Quantification of nuclear shape

Images of *48ystGFP* embryos expressing nuclear GFP in the midgut were captured at stages 8, 10 and 13. Non-PMEC cells were cropped out from the image before running the ImageJ/Fiji plugin for ImageJ. The masks generated were confirmed visually before running quantifications. Nuclear shape was quantified using in-built ImageJ Circularity calculations.

6.4 Methods for scRNAseq analysis

Protocols for scRNAseq sample preparation are described in Plygawko et. al, 2023 (under review). An excerpt from the methods section of the paper is provided below:

Alignment and read count

Fastq files were processed with the 10x Genomics software Cellranger (v4-0.0) using the Drosophila melanogaster reference transcriptome built with genome version r6.32 for data from collection windows 1 and 2. For collection windows 3 and 4, Cellranger (v3.0.2) and reference 6.29 was used. Default values were used for all parameters.

Normalization

Count matrices were read into R (v4.1.3) (R Core Team, 2021) and merged into a single Seurat (v4.1.1) object (Butler et al., 2018). All following functions belong to the Seurat package unless specified. Ribosomal genes were excluded from the count matrix and

cells with less than 2500 read counts were discarded. After applying quality filters, this resulted in the gene expression profiles of 21796 cells, with an average of 10886 counts and 3919 genes detected per cell. Cell cycle phase scores were computed using the function CellCycleScoring with the homologs of the human gene sets included in the Seurat package. Expression was normalized with the SCT_transform function, regressing out the S and G2M scores and the percent of mitochondrial reads per cell.

Normalization of the Midgut compartment

We selected cells is the connected component containing Midgut and Malpighian tubules and normalized them following the same procedure as in the whole dataset. To generate two dimensional maps of midgut cells only, we recalculated the UMAP representation after removing all Malpighian tubule cells.

Dimensionality reduction and clustering

Dimensionality reduction was performed through the function RunPCA, followed by the calculation of the Uniform Manifold Approximation and Projection (UMAP) using the first 12 principal components. Unsupervised clustering was found with the functions FindNeighbors, with 12 components, and FindClusters with resolution 1.2.

Gene expression imputation and smoothing and marker identification

Gene expression was imputed and smoothed using MAGIC (Rmagic v2.0.3) (59). For the Midgut compartment we used 9 principal components for finding clusters. MAGIC expression scores were used for all expression plots. Population markers were found using the function FindMarkers with default parameters. Gene set scores were computed as the mean of the Magic expression of the corresponding genes.

Annotation of cell populations

Differential expression of unsupervised clusters against the rest of the cells were found and compared to markers of known populations.

Pseudotime computation

Monocle (v 3_1.0.0) (Trapnell et al., 2014) was used to compute pseudotimes. For the whole dataset the number of centres for the learn_graph function was set to the default value (300 for the midgut subset).

In addition to the above except, two dimensional maps of mesoderm cells were generated in a similar manner to midgut populations.

6.4 PMEC Trajectory analysis

PMEC trajectory analysis was analysed using R based on a dataset showing differentially expressed genes between timepoint 1 and 3; and timepoint 3 and 4.

6.5 Quantification of relative distribution

Localisation of Cher and βPS in stage 13 embryos were calculated using ImageJ Fiji. Single z-stack of two-colour images were selected and split by colour channels. Contrast adjusted to set so 5% of pixels were saturated before converting to inverted 8-bit gray scale images, such that there was a white background. The straight-line tool was used to draw a 40-pixel wide line across the cells in an basal to apical direction. Lines were drawn such that lines started 1μm below the basal membrane of the midgut. Given that βPS was basal in all genotypes, βPS peaks were used to identify the basal membrane of the midgut. Data frames containing gray values were imported into RStudio for subsequent calculations. All measurements were trimmed to match the shortest measurement made, and as such represent the distance from the visceral muscle, rather than measurements relative to cell size.

Relative Values

Relative values were calculated for each ROI. Calculations for Relative values are as follows:

$$\text{Relative Value}_x = \text{Gray value}_x - \text{Gray value}_{max}/\text{Gray value}_{max}-\text{Gray Value}_{min}.$$

Where the Relative Value$_x$ is the relative value at any given x; Gray value$_x$ is the gray value at any given x; Gray value$_{max}$ is the maximum gray value within the midgut; and Gray value$_{min}$ is the minimum gray value within the midgut.

Full width at half Max

Full width at half maximum (FWHM) was calculated for each ROI. ROIs in which FWHM could not be measured were dropped. The embryos missing any ROIs were dropped from the graph. The uncertainty for FWHM measurements is ± 0.16µM. This corresponding to a margin of error from calculating X at half max at both sides of the peak.

AUC Ratio

Area under the curve was calculated using the R package DescTools (v. 0.99.50) (Signorell et al., 2023). Area under the curve was calculated using the trapezoid rule. Calculations for AUC Ratio are as follows:

$$\text{AUC Ratio} = \text{AUC}_{1/2ROI} \div \text{AUC}_{ROI}$$

Where the $\text{AUC}_{1/2ROI}$ is the area under the curve across half of the ROI adjacent to the basal domain; and AUC_{ROI} is the area under the curve across the entire ROI.

6.6 Preparation of figures, graphs and statistics

Figures were prepared in ImageJ Fiji and Microsoft Powerpoint. All images of fixed samples were converted to 8-bit. Graphs were generated using the R package ggplot (Wickham H, 2016). Significance between pairs of data were calculated using Wilcox Rank sum tests using the False discovery rate (fdr) correction for multiple testing.

Chapter 7. Bibliography

Abe, K., Takeichi, M., 2008. EPLIN mediates linkage of the cadherin–catenin complex to F-actin and stabilizes the circumferential actin belt. Proc. Natl. Acad. Sci. 105, 13–19. https://doi.org/10.1073/pnas.0710504105

Aigner, K., Dampier, B., Descovich, L., Mikula, M., Sultan, A., Schreiber, M., Mikulits, W., Brabletz, T., Strand, D., Obrist, P., Sommergruber, W., Schweifer, N., Wernitznig, A., Beug, H., Foisner, R., Eger, A., 2007. The transcription factor ZEB1 (deltaEF1) promotes tumour cell dedifferentiation by repressing master regulators of epithelial polarity. Oncogene 26, 6979–6988. https://doi.org/10.1038/sj.onc.1210508

Al-Sadi, R., Khatib, K., Guo, S., Ye, D., Youssef, M., Ma, T., 2011. Occludin regulates macromolecule flux across the intestinal epithelial tight junction barrier. Am. J. Physiol. Gastrointest. Liver Physiol. 300, G1054-1064. https://doi.org/10.1152/ajpgi.00055.2011

Alto, L.T., Terman, J.R., 2017. Semaphorins and their Signaling Mechanisms, in: Terman, J.R. (Ed.), Semaphorin Signaling: Methods and Protocols, Methods in Molecular Biology. Springer, New York, NY, pp. 1–25. https://doi.org/10.1007/978-1-4939-6448-2_1

Angelow, S., Ahlstrom, R., Yu, A.S.L., 2008. Biology of claudins. Am. J. Physiol. - Ren. Physiol. 295, F867–F876. https://doi.org/10.1152/ajprenal.90264.2008

Antony, J., Thiery, J.P., Huang, R.Y.-J., 2019. Epithelial-to-mesenchymal transition: lessons from development, insights into cancer and the potential of EMT-subtype based therapeutic intervention. Phys. Biol. 16, 041004. https://doi.org/10.1088/1478-3975/ab157a

Asada, M., Irie, K., Morimoto, K., Yamada, A., Ikeda, W., Takeuchi, M., Takai, Y., 2003. ADIP, a Novel Afadin- and α-Actinin-Binding Protein Localized at Cell-Cell Adherens Junctions*. J. Biol. Chem. 278, 4103–4111. https://doi.org/10.1074/jbc.M209832200

Bachmann, A., Draga, M., Grawe, F., Knust, E., 2008. On the role of the MAGUK proteins encoded by Drosophila varicose during embryonic and postembryonic development. BMC Dev. Biol. 8, 55. https://doi.org/10.1186/1471-213X-8-55

Bae, G.-Y., Choi, S.-J., Lee, J.-S., Jo, J., Lee, J., Kim, J., Cha, H.-J., 2013. Loss of E-cadherin activates EGFR-MEK/ERK signaling, which promotes invasion via the ZEB1/MMP2 axis in non-small cell lung cancer. Oncotarget 4, 2512–2522. https://doi.org/10.18632/oncotarget.1463

Bailey, M.J., Prehoda, K.E., 2015. Establishment of Par-Polarized Cortical Domains via Phosphoregulated Membrane Motifs. Dev. Cell 35, 199–210. https://doi.org/10.1016/j.devcel.2015.09.016

Baker, R.E., Schnell, S., Maini, P.K., 2006. A clock and wavefront mechanism for somite formation. Dev. Biol. 293, 116–126. https://doi.org/10.1016/j.ydbio.2006.01.018

Bamforth, S.D., Kniesel, U., Wolburg, H., Engelhardt, B., Risau, W., 1999. A dominant mutant of occludin disrupts tight junction structure and function. J. Cell Sci. 112 (Pt 12), 1879–1888. https://doi.org/10.1242/jcs.112.12.1879

Barnes, G.L., Hsu, C.W., Mariani, B.D., Tuan, R.S., 1996. Chicken Pax-1 gene: structure and expression during embryonic somite development. Differentiation 61, 13–23. https://doi.org/10.1046/j.1432-0436.1996.6110013.x

Barrera-Velázquez, M., Ríos-Barrera, L.D., 2021. Crosstalk between basal extracellular matrix adhesion and building of apical architecture during morphogenesis. Biol. Open 10, bio058760. https://doi.org/10.1242/bio.058760

Batlle, E., Sancho, E., Francí, C., Domínguez, D., Monfar, M., Baulida, J., García De Herreros, A., 2000. The transcription factor Snail is a repressor of E-cadherin gene expression in epithelial tumour cells. Nat. Cell Biol. 2, 84–89. https://doi.org/10.1038/35000034

Battistini, C., Tamagnone, L., 2016. Transmembrane semaphorins, forward and reverse signaling: have a look both ways. Cell. Mol. Life Sci. 73, 1609–1622. https://doi.org/10.1007/s00018-016-2137-x

Beerling, E., Seinstra, D., de Wit, E., Kester, L., van der Velden, D., Maynard, C., Schäfer, R., van Diest, P., Voest, E., van Oudenaarden, A., Vrisekoop, N., van Rheenen, J., 2016. Plasticity between Epithelial and Mesenchymal States Unlinks EMT from Metastasis-Enhancing Stem Cell Capacity. Cell Rep. 14, 2281–2288. https://doi.org/10.1016/j.celrep.2016.02.034

Bellen, H.J., Levis, R.W., He, Y., Carlson, J.W., Evans-Holm, M., Bae, E., Kim, J., Metaxakis, A., Savakis, C., Schulze, K.L., Hoskins, R.A., Spradling, A.C., 2011. The Drosophila gene disruption project: progress using transposons with distinctive site specificities. Genetics 188, 731–743. https://doi.org/10.1534/genetics.111.126995

Beutel, O., Maraspini, R., Pombo-García, K., Martin-Lemaitre, C., Honigmann, A., 2019. Phase Separation of Zonula Occludens Proteins Drives Formation of Tight Junctions. Cell 179, 923-936.e11. https://doi.org/10.1016/j.cell.2019.10.011

Beyenbach, K.W., Schöne, F., Breitsprecher, L.F., Tiburcy, F., Furuse, M., Izumi, Y., Meyer, H., Jonusaite, S., Rodan, A.R., Paululat, A., 2020. The septate junction protein Tetraspanin 2A is critical to the structure and function of Malpighian tubules in Drosophila melanogaster. Am. J. Physiol. Cell Physiol. 318, C1107–C1122. https://doi.org/10.1152/ajpcell.00061.2020

Bienz, M., 2005. β-Catenin: A Pivot between Cell Adhesion and Wnt Signalling. Curr. Biol. 15, R64–R67. https://doi.org/10.1016/j.cub.2004.12.058

Bilder, D., Perrimon, N., 2000. Localization of apical epithelial determinants by the basolateral PDZ protein Scribble. Nature 403, 676–680. https://doi.org/10.1038/35001108

Bilder, D., Schober, M., Perrimon, N., 2003. Integrated activity of PDZ protein complexes regulates epithelial polarity. Nat. Cell Biol. 5, 53–58. https://doi.org/10.1038/ncb897

Bodakuntla, S., Nedozralova, H., Basnet, N., Mizuno, N., 2021. Cytoskeleton and Membrane Organization at Axon Branches. Front. Cell Dev. Biol. 9, 707486. https://doi.org/10.3389/fcell.2021.707486

Boutet, A., De Frutos, C.A., Maxwell, P.H., Mayol, M.J., Romero, J., Nieto, M.A., 2006. Snail activation disrupts tissue homeostasis and induces fibrosis in the adult kidney. EMBO J. 25, 5603–5613. https://doi.org/10.1038/sj.emboj.7601421

Brown, N.H., Gregory, S.L., Rickoll, W.L., Fessler, L.I., Prout, M., White, R.A.H., Fristrom, J.W., 2002. Talin is essential for integrin function in Drosophila. Dev. Cell 3, 569–579. https://doi.org/10.1016/s1534-5807(02)00290-3

Buckley, C.E., St Johnston, D., 2022. Apical–basal polarity and the control of epithelial form and function. Nat. Rev. Mol. Cell Biol. 23, 559–577. https://doi.org/10.1038/s41580-022-00465-y

Butler, A., Hoffman, P., Smibert, P., Papalexi, E., Satija, R., 2018. Integrating single-cell transcriptomic data across different conditions, technologies, and species. Nat. Biotechnol. 36, 411–420. https://doi.org/10.1038/nbt.4096

Campbell, I.D., Humphries, M.J., 2011. Integrin structure, activation, and interactions. Cold Spring Harb. Perspect. Biol. 3, a004994. https://doi.org/10.1101/cshperspect.a004994

Campbell, K., Casanova, J., 2015. A role for E-cadherin in ensuring cohesive migration of a heterogeneous population of non-epithelial cells. Nat. Commun. 6, 7998. https://doi.org/10.1038/ncomms8998

Campbell, K., Rossi, F., Adams, J., Pitsidianaki, I., Barriga, F.M., Garcia-Gerique, L., Batlle, E., Casanova, J., Casali, A., 2019. Collective cell migration and metastases induced by an epithelial-to-mesenchymal transition in Drosophila intestinal tumors. Nat. Commun. 10, 2311. https://doi.org/10.1038/s41467-019-10269-y

Campbell, K., Whissell, G., Franch-Marro, X., Batlle, E., Casanova, J., 2011. Specific GATA Factors Act as Conserved Inducers of an Endodermal-EMT. Dev. Cell 21, 1051–1061. https://doi.org/10.1016/j.devcel.2011.10.005

Cano, A., Pérez-Moreno, M.A., Rodrigo, I., Locascio, A., Blanco, M.J., Del Barrio, M.G., Portillo, F., Nieto, M.A., 2000. The transcription factor Snail controls epithelial–mesenchymal transitions by repressing E-cadherin expression. Nat. Cell Biol. 2, 76–83. https://doi.org/10.1038/35000025

Carroll, T.J., Park, J.-S., Hayashi, S., Majumdar, A., McMahon, A.P., 2005. Wnt9b Plays a Central Role in the Regulation of Mesenchymal to Epithelial Transitions Underlying Organogenesis of the Mammalian Urogenital System. Dev. Cell 9, 283–292. https://doi.org/10.1016/j.devcel.2005.05.016

Carver, E.A., Jiang, R., Lan, Y., Oram, K.F., Gridley, T., 2001. The Mouse Snail Gene Encodes a Key Regulator of the Epithelial-Mesenchymal Transition. Mol. Cell. Biol. 21, 8184–8188. https://doi.org/10.1128/MCB.21.23.8184-8188.2001

Casas-Tinto, S., Gomez-Velazquez, M., Granadino, B., Fernandez-Funez, P., 2008. FoxK mediates TGF-β signalling during midgut differentiation in flies. J. Cell Biol. 183, 1049–1060. https://doi.org/10.1083/jcb.200808149

Chaffer, C.L., Weinberg, R.A., 2011. A Perspective on Cancer Cell Metastasis. Science 331, 1559–1564. https://doi.org/10.1126/science.1203543

Chalmers, A.D., Pambos, M., Mason, J., Lang, S., Wylie, C., Papalopulu, N., 2005. aPKC, Crumbs3 and Lgl2 control apicobasal polarity in early vertebrate development. Development 132, 977–986. https://doi.org/10.1242/dev.01645

Chambers, J.M., Wingert, R.A., 2020. Advances in understanding vertebrate nephrogenesis. Tissue Barriers 8, 1832844. https://doi.org/10.1080/21688370.2020.1832844

Chen, H., Li, Q., Nirala, N.K., Ip, Y.T., 2020. The Snakeskin-Mesh Complex of Smooth Septate Junction Restricts Yorkie to Regulate Intestinal Homeostasis in Drosophila. Stem Cell Rep. 14, 828–844. https://doi.org/10.1016/j.stemcr.2020.03.021

Chen, J., Sayadian, A.-C., Lowe, N., Lovegrove, H.E., St Johnston, D., 2018. An alternative mode of epithelial polarity in the Drosophila midgut. PLOS Biol. 16, e3000041. https://doi.org/10.1371/journal.pbio.3000041

Chen, J., St Johnston, D., 2022. Epithelial Cell Polarity During Drosophila Midgut Development. Front. Cell Dev. Biol. 10, 886773. https://doi.org/10.3389/fcell.2022.886773

Chen, Y., Gridley, T., 2013. Compensatory regulation of the Snai1 and Snai2 genes during chondrogenesis. J. Bone Miner. Res. Off. J. Am. Soc. Bone Miner. Res. 28, 1412–1421. https://doi.org/10.1002/jbmr.1871

Chen, Z.F., Behringer, R.R., 1995. twist is required in head mesenchyme for cranial neural tube morphogenesis. Genes Dev. 9, 686–699. https://doi.org/10.1101/gad.9.6.686

Chng, Z., Teo, A., Pedersen, R.A., Vallier, L., 2010. SIP1 Mediates Cell-Fate Decisions between Neuroectoderm and Mesendoderm in Human Pluripotent Stem Cells. Cell Stem Cell 6, 59–70. https://doi.org/10.1016/j.stem.2009.11.015

Cho, J.Y., Chak, K., Andreone, B.J., Wooley, J.R., Kolodkin, A.L., 2012. The extracellular matrix proteoglycan perlecan facilitates transmembrane semaphorin-mediated repulsive guidance. Genes Dev. 26, 2222–2235. https://doi.org/10.1101/gad.193136.112

Choi, J., Troyanovsky, R.B., Indra, I., Mitchell, B.J., Troyanovsky, S.M., 2019. Scribble, Erbin, and Lano redundantly regulate epithelial polarity and apical adhesion complex. J. Cell Biol. 218, 2277–2293. https://doi.org/10.1083/jcb.201804201

Cohen, E.D., Mariol, M.-C., Wallace, R.M.H., Weyers, J., Kamberov, Y.G., Pradel, J., Wilder, E.L., 2002. DWnt4 Regulates Cell Movement and Focal Adhesion Kinase during Drosophila Ovarian Morphogenesis. Dev. Cell 2, 437–448. https://doi.org/10.1016/S1534-5807(02)00142-9

Comijn, J., Berx, G., Vermassen, P., Verschueren, K., van Grunsven, L., Bruyneel, E., Mareel, M., Huylebroeck, D., van Roy, F., 2001. The two-handed E box binding zinc finger protein SIP1 downregulates E-cadherin and induces invasion. Mol. Cell 7, 1267–1278. https://doi.org/10.1016/s1097-2765(01)00260-x

Correia, K.M., Conlon, R.A., 2000. Surface ectoderm is necessary for the morphogenesis of somites. Mech. Dev. 91, 19–30. https://doi.org/10.1016/S0925-4773(99)00260-9

Costa, G., Harrington, K.I., Lovegrove, H.E., Page, D.J., Chakravartula, S., Bentley, K., Herbert, S.P., 2016. Asymmetric division coordinates collective cell migration in angiogenesis. Nat. Cell Biol. 18, 1292–1301. https://doi.org/10.1038/ncb3443

Dale, J.K., Malapert, P., Chal, J., Vilhais-Neto, G., Maroto, M., Johnson, T., Jayasinghe, S., Trainor, P., Herrmann, B., Pourquié, O., 2006. Oscillations of the Snail Genes in the Presomitic Mesoderm Coordinate Segmental Patterning and Morphogenesis in Vertebrate Somitogenesis. Dev. Cell 10, 355–366. https://doi.org/10.1016/j.devcel.2006.02.011

De Franceschi, N., Arjonen, A., Elkhatib, N., Denessiouk, K., Wrobel, A.G., Wilson, T.A., Pouwels, J., Montagnac, G., Owen, D.J., Ivaska, J., 2016. Selective integrin endocytosis is driven by interactions between the integrin α-chain and AP2. Nat. Struct. Mol. Biol. 23, 172–179. https://doi.org/10.1038/nsmb.3161

Delon, I., Brown, N.H., 2007. Integrins and the actin cytoskeleton. Curr. Opin. Cell Biol., Cell structure and dynamics 19, 43–50. https://doi.org/10.1016/j.ceb.2006.12.013

Dent, E.W., Barnes, A.M., Tang, F., Kalil, K., 2004. Netrin-1 and semaphorin 3A promote or inhibit cortical axon branching, respectively, by reorganization of the cytoskeleton. J. Neurosci. Off. J. Soc. Neurosci. 24, 3002–3012. https://doi.org/10.1523/JNEUROSCI.4963-03.2004

Derynck, R., Weinberg, R.A., 2019. EMT and Cancer: More Than Meets the Eye. Dev. Cell 49, 313–316. https://doi.org/10.1016/j.devcel.2019.04.026

Desai, R., Sarpal, R., Ishiyama, N., Pellikka, M., Ikura, M., Tepass, U., 2013. Monomeric α-catenin links cadherin to the actin cytoskeleton. Nat. Cell Biol. 15, 261–273. https://doi.org/10.1038/ncb2685

Devenport, D., Brown, N.H., 2004. Morphogenesis in the absence of integrins: mutation of both Drosophila β subunits prevents midgut migration. Development 131, 5405–5415. https://doi.org/10.1242/dev.01427

Dongre, A., Weinberg, R.A., 2019. New insights into the mechanisms of epithelial–mesenchymal transition and implications for cancer. Nat. Rev. Mol. Cell Biol. 20, 69–84. https://doi.org/10.1038/s41580-018-0080-4

Drees, F., Pokutta, S., Yamada, S., Nelson, W.J., Weis, W.I., 2005. α-Catenin Is a Molecular Switch that Binds E-Cadherin-β-Catenin and Regulates Actin-Filament Assembly. Cell 123, 903–915. https://doi.org/10.1016/j.cell.2005.09.021

Driessens, M.H., Hu, H., Nobes, C.D., Self, A., Jordens, I., Goodman, C.S., Hall, A., 2001. Plexin-B semaphorin receptors interact directly with active Rac and regulate the actin cytoskeleton by activating Rho. Curr. Biol. CB 11, 339–344. https://doi.org/10.1016/s0960-9822(01)00092-6

Duan, H., Skeath, J.B., Nguyen, H.T., 2001. Drosophila Lame duck, a novel member of the Gli superfamily, acts as a key regulator of myogenesis by controlling fusion-competent myoblast development. Development 128, 4489–4500. https://doi.org/10.1242/dev.128.22.4489

Dubreuil, R.R., Grushko, T., Baumann, O., 2001. Differential effects of a labial mutation on the development, structure, and function of stomach acid-secreting cells in Drosophila melanogaster larvae and adults. Cell Tissue Res. 306, 167–178. https://doi.org/10.1007/s004410100422

Eivers, E., Fuentealba, L.C., Sander, V., Clemens, J.C., Hartnett, L., Robertis, E.M.D., 2009. Mad Is Required for Wingless Signaling in Wing Development and Segment Patterning in Drosophila. PLOS ONE 4, e6543. https://doi.org/10.1371/journal.pone.0006543

Esposito, M., Mondal, N., Greco, T.M., Wei, Y., Spadazzi, C., Lin, S.-C., Zheng, H., Cheung, C., Magnani, J.L., Lin, S.-H., Cristea, I.M., Sackstein, R., Kang, Y., 2019. Bone vascular niche E-selectin induces mesenchymal–epithelial transition and Wnt activation in cancer cells to promote bone metastasis. Nat. Cell Biol. 21, 627–639. https://doi.org/10.1038/s41556-019-0309-2

Fanning, A.S., Jameson, B.J., Jesaitis, L.A., Anderson, J.M., 1998. The Tight Junction Protein ZO-1 Establishes a Link between the Transmembrane Protein Occludin and the Actin Cytoskeleton*. J. Biol. Chem. 273, 29745–29753. https://doi.org/10.1074/jbc.273.45.29745

Feldman, J.L., Priess, J.R., 2012. A role for the centrosome and PAR-3 in the hand-off of MTOC function during epithelial polarization. Curr. Biol. CB 22, 575–582. https://doi.org/10.1016/j.cub.2012.02.044

Fessler, L.I., Campbell, A.G., Ducan, K.G., Fessler, J.H., 1987. Drosophila laminin: characterization and localization. J. Cell Biol. 105, 2383–2391.

Frasch, M., Ismat, A., Reim, I., Raufer, J., 2022. The RNF220 domain nuclear factor Teyrha-Meyrha (Tey) regulates the migration and differentiation of specific visceral and somatic muscles in Drosophila. https://doi.org/10.1101/2022.11.18.517102

Furuse, M., Izumi, Y., 2017. Molecular dissection of smooth septate junctions: understanding their roles in arthropod physiology. Ann. N. Y. Acad. Sci. 1397, 17–24. https://doi.org/10.1111/nyas.13366

Furuse, M., Takai, Y., 2021. Recent advances in understanding tight junctions. Fac. Rev. 10, 18. https://doi.org/10.12703/r/10-18

Galli, R., Uckermann, O., Andresen, E.F., Geiger, K.D., Koch, E., Schackert, G., Steiner, G., Kirsch, M., 2014. Intrinsic Indicator of Photodamage during Label-Free Multiphoton

Microscopy of Cells and Tissues. PLOS ONE 9, e110295.
https://doi.org/10.1371/journal.pone.0110295

Gammons, M., Bienz, M., 2018. Multiprotein complexes governing Wnt signal transduction. Curr. Opin. Cell Biol., Cell Signalling 51, 42–49. https://doi.org/10.1016/j.ceb.2017.10.008

Gao, D., Joshi, N., Choi, H., Ryu, S., Hahn, M., Catena, R., Sadik, H., Argani, P., Wagner, P., Vahdat, L.T., Port, J.L., Stiles, B., Sukumar, S., Altorki, N.K., Rafii, S., Mittal, V., 2012. Myeloid Progenitor Cells in the Premetastatic Lung Promote Metastases by Inducing Mesenchymal to Epithelial Transition. Cancer Res. 72, 1384–1394. https://doi.org/10.1158/0008-5472.CAN-11-2905

Garcia, M.A., Nelson, W.J., Chavez, N., 2018. Cell-Cell Junctions Organize Structural and Signaling Networks. Cold Spring Harb. Perspect. Biol. 10, a029181. https://doi.org/10.1101/cshperspect.a029181

Gildor, B., Schejter, E.D., Shilo, B.-Z., 2012. Bidirectional Notch activation represses fusion competence in swarming adult Drosophila myoblasts. Development 139, 4040–4050. https://doi.org/10.1242/dev.077495

Gomez, J.M., Chumakova, L., Bulgakova, N.A., Brown, N.H., 2016. Microtubule organization is determined by the shape of epithelial cells. Nat. Commun. 7, 13172. https://doi.org/10.1038/ncomms13172

Goodman, C.S., Kolodkin, A.L., Luo, Y., Püschel, A.W., Raper, J.A., 1999. Unified Nomenclature for the Semaphorins/Collapsins. Cell 97, 551–552. https://doi.org/10.1016/S0092-8674(00)80766-7

Gramates, L.S., Agapite, J., Attrill, H., Calvi, B.R., Crosby, M.A., Dos Santos, Gilberto, Goodman, J.L., Goutte-Gattat, D., Jenkins, V.K., Kaufman, T., Larkin, A., Matthews, B.B., Millburn, G., Strelets, V.B., the FlyBase Consortium, Perrimon, N., Gelbart, S.R., Agapite, J., Broll, K., Crosby, L., Dos Santos, Gil, Falls, K., Gramates, L.S., Jenkins, V., Longden, I., Matthews, B., Seme, J., Tabone, C.J., Zhou, P., Zytkovicz, M., Brown, N., Antonazzo, G., Attrill, H., Garapati, P., Goutte-Gattat, D., Larkin, A., Marygold, S., McLachlan, A., Millburn, G., Öztürk-Çolak, A., Pilgrim, C., Trovisco, V., Calvi, B., Kaufman, T., Goodman, J., Krishna, P., Strelets, V., Thurmond, J., Cripps, R., Lovato, T., 2022. FlyBase: a guided tour of highlighted features. Genetics 220, iyac035. https://doi.org/10.1093/genetics/iyac035

Greenburg, G., Hay, E.D., 1982. Epithelia suspended in collagen gels can lose polarity and express characteristics of migrating mesenchymal cells. J. Cell Biol. 95, 333–339. https://doi.org/10.1083/jcb.95.1.333

Hajra, K.M., Chen, D.Y.-S., Fearon, E.R., 2002. The SLUG Zinc-Finger Protein Represses E-Cadherin in Breast Cancer1. Cancer Res. 62, 1613–1618.

Hamaratoglu, F., Affolter, M., Pyrowolakis, G., 2014. Dpp/BMP signaling in flies: From molecules to biology. Semin. Cell Dev. Biol., RNA biogenesis & TGFβ signalling in embryonic development 32, 128–136. https://doi.org/10.1016/j.semcdb.2014.04.036

Hammonds, A.S., Bristow, C.A., Fisher, W.W., Weiszmann, R., Wu, S., Hartenstein, V., Kellis, M., Yu, B., Frise, E., Celniker, S.E., 2013. Spatial expression of transcription factors in Drosophilaembryonic organ development. Genome Biol. 14, R140. https://doi.org/10.1186/gb-2013-14-12-r140

Harris, T.J.C., Peifer, M., 2004. Adherens junction-dependent and -independent steps in the establishment of epithelial cell polarity in Drosophila. J. Cell Biol. 167, 135–147. https://doi.org/10.1083/jcb.200406024

Hartenstein, V., 1993. Atlas of Drosophila Development. Cold Spring Harbor Laboratory Press.

Hay, E.D., Zuk, A., 1995. Transformations between epithelium and mesenchyme: Normal, pathological, and experimentally induced. Am. J. Kidney Dis. 26, 678–690. https://doi.org/10.1016/0272-6386(95)90610-X

Hernandez-Fleming, M., Rohrbach, E.W., Bashaw, G.J., 2017. Sema-1a Reverse Signaling Promotes Midline Crossing in Response to Secreted Semaphorins. Cell Rep. 18, 174–184. https://doi.org/10.1016/j.celrep.2016.12.027

Honda, T., Shimizu, K., Kawakatsu, T., Yasumi, M., Shingai, T., Fukuhara, A., Ozaki-Kuroda, K., Irie, K., Nakanishi, H., Takai, Y., 2003. Antagonistic and agonistic effects of an extracellular fragment of nectin on formation of E-cadherin-based cell-cell adhesion. Genes Cells 8, 51–63. https://doi.org/10.1046/j.1365-2443.2003.00616.x

Hong, Y., 2018. aPKC: the Kinase that Phosphorylates Cell Polarity. https://doi.org/10.12688/f1000research.14427.1

Hoppler, S., Bienz, M., 1994. Specification of a single cell type by a Drosophila homeotic gene. Cell 76, 689–702. https://doi.org/10.1016/0092-8674(94)90508-8

Hough, C.D., Woods, D.F., Park, S., Bryant, P.J., 1997. Organizing a functional junctional complex requires specific domains of the Drosophila MAGUK Discs large. Genes Dev. 11, 3242–3253. https://doi.org/10.1101/gad.11.23.3242

Hsieh, H.-H., Chang, W.-T., Yu, L., Rao, Y., 2014. Control of axon–axon attraction by Semaphorin reverse signaling. Proc. Natl. Acad. Sci. U. S. A. 111, 11383–11388. https://doi.org/10.1073/pnas.1321433111

Hu, D.J.-K., Yun, J., Elstrott, J., Jasper, H., 2021. Non-canonical Wnt signaling promotes directed migration of intestinal stem cells to sites of injury. Nat. Commun. 12, 7150. https://doi.org/10.1038/s41467-021-27384-4

Hung, R.-J., Hu, Y., Kirchner, R., Liu, Y., Xu, C., Comjean, A., Tattikota, S.G., Li, F., Song, W., Ho Sui, S., Perrimon, N., 2020. A cell atlas of the adult Drosophila midgut. Proc. Natl. Acad. Sci. 117, 1514–1523. https://doi.org/10.1073/pnas.1916820117

Hung, T.-J., Kemphues, K.J., 1999. PAR-6 is a conserved PDZ domain-containing protein that colocalizes with PAR-3 in *Caenorhabditis elegans* embryos. Development 126, 127–135. https://doi.org/10.1242/dev.126.1.127

Huveneers, S., van den Bout, I., Sonneveld, P., Sancho, A., Sonnenberg, A., Danen, E.H.J., 2007. Integrin αvβ3 Controls Activity and Oncogenic Potential of Primed c-Src. Cancer Res. 67, 2693–2700. https://doi.org/10.1158/0008-5472.CAN-06-3654

Ismat, A., Schaub, C., Reim, I., Kirchner, K., Schultheis, D., Frasch, M., 2010. HLH54F is required for the specification and migration of longitudinal gut muscle founders from the caudal mesoderm of Drosophila. Development 137, 3107–3117. https://doi.org/10.1242/dev.046573

Izumi, Y., Furuse, K., Furuse, M., 2021. The novel membrane protein Hoka regulates septate junction organization and stem cell homeostasis in the *Drosophila* gut. J. Cell Sci. 134, jcs257022. https://doi.org/10.1242/jcs.257022

Izumi, Y., Hirose, T., Tamai, Y., Hirai, S., Nagashima, Y., Fujimoto, T., Tabuse, Y., Kemphues, K.J., Ohno, S., 1998. An Atypical PKC Directly Associates and Colocalizes at the Epithelial

Tight Junction with ASIP, a Mammalian Homologue of Caenorhabditis elegans Polarity Protein PAR-3. J. Cell Biol. 143, 95–106. https://doi.org/10.1083/jcb.143.1.95

Izumi, Y., Motoishi, M., Furuse, K., Furuse, M., 2016. A tetraspanin regulates septate junction formation in Drosophila midgut. J. Cell Sci. 129, 1155–1164. https://doi.org/10.1242/jcs.180448

Izumi, Y., Yanagihashi, Y., Furuse, M., 2012. A novel protein complex, Mesh–Ssk, is required for septate junction formation in the Drosophila midgut. J. Cell Sci. 125, 4923–4933. https://doi.org/10.1242/jcs.112243

Jakobsen, J.S., Braun, M., Astorga, J., Gustafson, E.H., Sandmann, T., Karzynski, M., Carlsson, P., Furlong, E.E.M., 2007. Temporal ChIP-on-chip reveals Biniou as a universal regulator of the visceral muscle transcriptional network. Genes Dev. 21, 2448–2460. https://doi.org/10.1101/gad.437607

Janda, E., Nevolo, M., Lehmann, K., Downward, J., Beug, H., Grieco, M., 2006. Raf plus TGFβ-dependent EMT is initiated by endocytosis and lysosomal degradation of E-cadherin. Oncogene 25, 7117–7130. https://doi.org/10.1038/sj.onc.1209701

Jeong, S., Juhaszova, K., Kolodkin, A.L., 2012. The Control of Semaphorin-1a-Mediated Reverse Signaling by Opposing Pebble and RhoGAPp190 Functions in Drosophila. Neuron 76, 721–734. https://doi.org/10.1016/j.neuron.2012.09.018

Jeong, S., Yang, D., Hong, Y.G., Mitchell, S.P., Brown, M.P., Kolodkin, A.L., 2017. Varicose and cheerio collaborate with pebble to mediate semaphorin-1a reverse signaling in *Drosophila*. Proc. Natl. Acad. Sci. 114. https://doi.org/10.1073/pnas.1713010114

Jonusaite, S., Beyenbach, K.W., Meyer, H., Paululat, A., Izumi, Y., Furuse, M., Rodan, A.R., 2020. The septate junction protein Mesh is required for epithelial morphogenesis, ion transport, and paracellular permeability in the Drosophila Malpighian tubule. Am. J. Physiol. Cell Physiol. 318, C675–C694. https://doi.org/10.1152/ajpcell.00492.2019

Jonusaite, S., Donini, A., Kelly, S.P., 2016. Occluding junctions of invertebrate epithelia. J. Comp. Physiol. B 186, 17–43. https://doi.org/10.1007/s00360-015-0937-1

Jordà, M., Olmeda, D., Vinyals, A., Valero, E., Cubillo, E., Llorens, A., Cano, A., Fabra, À., 2005. Upregulation of MMP-9 in MDCK epithelial cell line in response to expression of the Snail transcription factor. J. Cell Sci. 118, 3371–3385. https://doi.org/10.1242/jcs.02465

Joseph, M.J., Dangi-Garimella, S., Shields, M.A., Diamond, M.E., Sun, L., Koblinski, J.E., Munshi, H.G., 2009. Slug is a downstream mediator of transforming growth factor-β1-induced matrix metalloproteinase-9 expression and invasion of oral cancer cells. J. Cell. Biochem. 108, 726–736. https://doi.org/10.1002/jcb.22309

Jung, H.-Y., Fattet, L., Tsai, J.H., Kajimoto, T., Chang, Q., Newton, A.C., Yang, J., 2019. Apical–basal polarity inhibits epithelial–mesenchymal transition and tumour metastasis by PAR-complex-mediated SNAI1 degradation. Nat. Cell Biol. 21, 359–371. https://doi.org/10.1038/s41556-019-0291-8

Kalluri, R., Weinberg, R.A., 2009. The basics of epithelial-mesenchymal transition. J. Clin. Invest. 119, 1420–1428. https://doi.org/10.1172/JCI39104

Kechagia, J.Z., Ivaska, J., Roca-Cusachs, P., 2019. Integrins as biomechanical sensors of the microenvironment. Nat. Rev. Mol. Cell Biol. 20, 457–473. https://doi.org/10.1038/s41580-019-0134-2

Khales, S.A., Abbaszadegan, M.R., Majd, A., Forghanifard, M.M., 2020. TWIST1 upregulates matrix metalloproteinase (MMP) genes family in esophageal squamous carcinoma cells. Gene Expr. Patterns 37, 119127. https://doi.org/10.1016/j.gep.2020.119127

Kim, W.K., Kwon, Y., Jang, M., Park, M., Kim, J., Cho, S., Jang, D.G., Lee, W.-B., Jung, S.H., Choi, H.J., Min, B.S., Il Kim, T., Hong, S.P., Paik, Y.-K., Kim, H., 2019. β-catenin activation down-regulates cell-cell junction-related genes and induces epithelial-to-mesenchymal transition in colorectal cancers. Sci. Rep. 9, 18440. https://doi.org/10.1038/s41598-019-54890-9

Klapholz, B., Brown, N.H., 2017. Talin – the master of integrin adhesions. J. Cell Sci. 130, 2435–2446. https://doi.org/10.1242/jcs.190991

Klapper, R., Stute, C., Schomaker, O., Strasser, T., Janning, W., Renkawitz-Pohl, R., Holz, A., 2002. The formation of syncytia within the visceral musculature of the Drosophila midgut is dependent on duf, sns and mbc. Mech. Dev. 110, 85–96. https://doi.org/10.1016/S0925-4773(01)00567-6

Kobayashi, A., Valerius, M.T., Mugford, J.W., Carroll, T.J., Self, M., Oliver, G., McMahon, A.P., 2008. Six2 Defines and Regulates a Multipotent Self-Renewing Nephron Progenitor Population throughout Mammalian Kidney Development. Cell Stem Cell 3, 169–181. https://doi.org/10.1016/j.stem.2008.05.020

Kobielak, A., Pasolli, H.A., Fuchs, E., 2004. Mammalian formin-1 participates in adherens junctions and polymerization of linear actin cables. Nat. Cell Biol. 6, 21–30. https://doi.org/10.1038/ncb1075

Kolberg, L., Raudvere, U., Kuzmin, I., Adler, P., Vilo, J., Peterson, H., 2023. g:Profiler— interoperable web service for functional enrichment analysis and gene identifier mapping (2023 update). Nucleic Acids Res. 51, W207–W212. https://doi.org/10.1093/nar/gkad347

Komiyama, T., Sweeney, L.B., Schuldiner, O., Garcia, K.C., Luo, L., 2007. Graded Expression of Semaphorin-1a Cell-Autonomously Directs Dendritic Targeting of Olfactory Projection Neurons. Cell 128, 399–410. https://doi.org/10.1016/j.cell.2006.12.028

Külshammer, E., Kilinc, M., Csordás, G., Bresser, T., Nolte, H., Uhlirova, M., 2022. The mechanosensor Filamin A/Cheerio promotes tumourigenesis via specific interactions with components of the cell cortex. FEBS J. 289, 4497–4517. https://doi.org/10.1111/febs.16408

Kuure, S., Vuolteenaho, R., Vainio, S., 2000. Kidney morphogenesis: cellular and molecular regulation. Mech. Dev. 92, 31–45. https://doi.org/10.1016/S0925-4773(99)00323-8

Laprise, P., Lau, K.M., Harris, K.P., Silva-Gagliardi, N.F., Paul, S.M., Beronja, S., Beitel, G.J., McGlade, C.J., Tepass, U., 2009. Yurt, Coracle, Neurexin IV and the Na+,K+-ATPase form a novel group of epithelial polarity proteins. Nature 459, 1141–1145. https://doi.org/10.1038/nature08067

Lee, H.-H., Norris, A., Weiss, J.B., Frasch, M., 2003. Jelly belly protein activates the receptor tyrosine kinase Alk to specify visceral muscle pioneers. Nature 425, 507–512. https://doi.org/10.1038/nature01916

Lee, J.L., Streuli, C.H., 2014. Integrins and epithelial cell polarity. J. Cell Sci. 127, 3217–3225. https://doi.org/10.1242/jcs.146142

Leggett, S.E., Sim, J.Y., Rubins, J.E., Neronha, Z.J., Williams, E.K., Wong, I.Y., 2016. Morphological single cell profiling of the epithelial–mesenchymal transition. Integr. Biol. 8, 1133–1144. https://doi.org/10.1039/c6ib00139d

Leimeister, C., Schumacher, N., Steidl, C., Gessler, M., 2000. Analysis of HeyL expression in wild-type and Notch pathway mutant mouse embryos. Mech. Dev. 98, 175–178. https://doi.org/10.1016/S0925-4773(00)00459-7

Lengyel, J.A., Liu, X.J., 1998. Posterior gut development in Drosophila: a model system for identifying genes controlling epithelial morphogenesis. Cell Res. 8, 273–284. https://doi.org/10.1038/cr.1998.27

Leptin, M., 1991. twist and snail as positive and negative regulators during Drosophila mesoderm development. Genes Dev. 5, 1568–1576. https://doi.org/10.1101/gad.5.9.1568

Li, Q., Shi, J., Liu, W., 2020. The role of Wnt/β-catenin-lin28a/let-7 axis in embryo implantation competency and epithelial-mesenchymal transition (EMT). Cell Commun. Signal. 18, 108. https://doi.org/10.1186/s12964-020-00562-5

Liebner, S., Cattelino, A., Gallini, R., Rudini, N., Iurlaro, M., Piccolo, S., Dejana, E., 2004. β-Catenin is required for endothelial-mesenchymal transformation during heart cushion development in the mouse. J. Cell Biol. 166, 359–367. https://doi.org/10.1083/jcb.200403050

Lim, J., Thiery, J.P., 2012. Epithelial-mesenchymal transitions: insights from development. Development 139, 3471–3486. https://doi.org/10.1242/dev.071209

Lin, D., Edwards, A.S., Fawcett, J.P., Mbamalu, G., Scott, J.D., Pawson, T., 2000. A mammalian PAR-3–PAR-6 complex implicated in Cdc42/Rac1 and aPKC signalling and cell polarity. Nat. Cell Biol. 2, 540–547. https://doi.org/10.1038/35019582

Linker, C., Lesbros, C., Gros, J., Burrus, L.W., Rawls, A., Marcelle, C., 2005. β-Catenin-dependent Wnt signalling controls the epithelial organisation of somites through the activation of *paraxis*. Development 132, 3895–3905. https://doi.org/10.1242/dev.01961

Linnemannstöns, K., Ripp, C., Honemann-Capito, M., Brechtel-Curth, K., Hedderich, M., Wodarz, A., 2014. The PTK7-Related Transmembrane Proteins Off-track and Off-track 2 Are Co-receptors for Drosophila Wnt2 Required for Male Fertility. PLOS Genet. 10, e1004443. https://doi.org/10.1371/journal.pgen.1004443

Liu, Y., Hu, Y., Li, J.S.S., Rodiger, J., Comjean, A., Attrill, H., Antonazzo, G., Brown, N.H., Perrimon, N., 2021. FlyPhoneDB: An integrated web-based resource for cell-cell communication prediction in Drosophila. https://doi.org/10.1101/2021.06.14.448430

Lohia, M., Qin, Y., Macara, I.G., 2012. The Scribble Polarity Protein Stabilizes E-Cadherin/p120-Catenin Binding and Blocks Retrieval of E-Cadherin to the Golgi. PLoS ONE 7, e51130. https://doi.org/10.1371/journal.pone.0051130

Lu, F., Zhu, L., Bromberger, T., Yang, J., Yang, Q., Liu, J., Plow, E.F., Moser, M., Qin, J., 2022. Mechanism of integrin activation by talin and its cooperation with kindlin. Nat. Commun. 13, 2362. https://doi.org/10.1038/s41467-022-30117-w

Lu, X., Borchers, A.G.M., Jolicoeur, C., Rayburn, H., Baker, J.C., Tessier-Lavigne, M., 2004. PTK7/CCK-4 is a novel regulator of planar cell polarity in vertebrates. Nature 430, 93–98. https://doi.org/10.1038/nature02677

Lynch, H.E., Crews, S.M., Rosenthal, B., Kim, E., Gish, R., Echiverri, K., Hutson, M.S., 2013. Cellular Mechanics of Germ Band Retraction in Drosophila. Dev. Biol. 384, 10.1016/j.ydbio.2013.10.005. https://doi.org/10.1016/j.ydbio.2013.10.005

Macabenta, F., Stathopoulos, A., 2019. Migrating cells control morphogenesis of substratum serving as track to promote directional movement of the collective. Development 146, dev177295. https://doi.org/10.1242/dev.177295

Manfruelli, P., Arquier, N., Hanratty, W.P., Sémériva, M., 1996. The tumor suppressor gene, lethal(2)giant larvae (l(2)gl), is required for cell shape change of epithelial cells during Drosophila development. Development 122, 2283–2294. https://doi.org/10.1242/dev.122.7.2283

Martin, B.S., Ruiz-Gómez, M., Landgraf, M., Bate, M., 2001. A distinct set of founders and fusion-competent myoblasts make visceral muscles in the *Drosophila* embryo. Development 128, 3331–3338. https://doi.org/10.1242/dev.128.17.3331

Martin, D., Zusman, S., Li, X., Williams, E.L., Khare, N., DaRocha, S., Chiquet-Ehrismann, R., Baumgartner, S., 1999. wing blister, A New Drosophila Laminin α Chain Required for Cell Adhesion and Migration during Embryonic and Imaginal Development. J. Cell Biol. 145, 191–201. https://doi.org/10.1083/jcb.145.1.191

Martin-Belmonte, F., Perez-Moreno, M., 2012. Epithelial cell polarity, stem cells and cancer. Nat. Rev. Cancer 12, 23–38. https://doi.org/10.1038/nrc3169

Martin-Bermudo, M.D., Alvarez-Garcia, I., Brown, N.H., 1999. Migration of the *Drosophila* primordial midgut cells requires coordination of diverse PS integrin functions. Development 126, 5161–5169. https://doi.org/10.1242/dev.126.22.5161

Martin-Bermudo, M.D., Brown, N.H., 1999. Uncoupling integrin adhesion and signaling: the ^{N}LPS cytoplasmic domain is sufficient to regulate gene expression in the Drosophila embryo. Genes Dev. 729–739. https://doi.org/10.1101/gad.13.6.729

Massarwa, R., Carmon, S., Shilo, B.-Z., Schejter, E.D., 2007. WIP/WASp-based actin-polymerization machinery is essential for myoblast fusion in Drosophila. Dev. Cell 12, 557–569. https://doi.org/10.1016/j.devcel.2007.01.016

Mateos, C.S.-C., Valencia-Expósito, A., Palacios, I.M., Martín-Bermudo, M.D., 2020. Integrins regulate epithelial cell shape by controlling the architecture and mechanical properties of basal actomyosin networks. PLOS Genet. 16, e1008717. https://doi.org/10.1371/journal.pgen.1008717

McGill, M.A., McKinley, R.F.A., Harris, T.J.C., 2009. Independent cadherin–catenin and Bazooka clusters interact to assemble adherens junctions. J. Cell Biol. 185, 787–796. https://doi.org/10.1083/jcb.200812146

Meadows, L.A., Gell, D., Broadie, K., Gould, A.P., White, R.A.H., 1994. The cell adhesion molecule, connectin, and the development of the Drosophila neuromuscular system. J. Cell Sci. 107, 321–328. https://doi.org/10.1242/jcs.107.1.321

Meng, W., Takeichi, M., 2009. Adherens Junction: Molecular Architecture and Regulation. Cold Spring Harb. Perspect. Biol. 1, a002899. https://doi.org/10.1101/cshperspect.a002899

Miyoshi, A., Kitajima, Y., Sumi, K., Sato, K., Hagiwara, A., Koga, Y., Miyazaki, K., 2004. Snail and SIP1 increase cancer invasion by upregulating MMP family in hepatocellular carcinoma cells. Br. J. Cancer 90, 1265–1273. https://doi.org/10.1038/sj.bjc.6601685

Morais-de-Sá, E., Mirouse, V., St Johnston, D., 2010. aPKC Phosphorylation of Bazooka Defines the Apical/Lateral Border in Drosophila Epithelial Cells. Cell 141, 509–523. https://doi.org/10.1016/j.cell.2010.02.040

Moreno-Layseca, P., Streuli, C.H., 2014. Signalling pathways linking integrins with cell cycle progression. Matrix Biol. 34, 144–153. https://doi.org/10.1016/j.matbio.2013.10.011

Morgan, M.R., Byron, A., Humphries, M.J., Bass, M.D., 2009. Giving off mixed signals—Distinct functions of α5β1 and αvβ3 integrins in regulating cell behaviour. IUBMB Life 61, 731–738. https://doi.org/10.1002/iub.200

Müsch, A., 2004. Microtubule Organization and Function in Epithelial Cells. Traffic 5, 1–9. https://doi.org/10.1111/j.1600-0854.2003.00149.x

Mylavarapu, S., Kumar, H., Kumari, S., Sravanthi, L.S., Jain, M., Basu, A., Biswas, M., Mylavarapu, S.V.S., Das, A., Roy, M., 2019. Activation of Epithelial-Mesenchymal Transition and Altered β-Catenin Signaling in a Novel Indian Colorectal Carcinoma Cell Line. Front. Oncol. 9.

Myllymäki, S.M., Teräväinen, T.P., Manninen, A., 2011. Two Distinct Integrin-Mediated Mechanisms Contribute to Apical Lumen Formation in Epithelial Cells. PLOS ONE 6, e19453. https://doi.org/10.1371/journal.pone.0019453

Nagarkar-Jaiswal, S., Lee, P.-T., Campbell, M.E., Chen, K., Anguiano-Zarate, S., Cantu Gutierrez, M., Busby, T., Lin, W.-W., He, Y., Schulze, K.L., Booth, B.W., Evans-Holm, M., Venken, K.J., Levis, R.W., Spradling, A.C., Hoskins, R.A., Bellen, H.J., 2015. A library of MiMICs allows tagging of genes and reversible, spatial and temporal knockdown of proteins in Drosophila. eLife 4, e05338. https://doi.org/10.7554/eLife.05338

Nance, J., Zallen, J.A., 2011. Elaborating polarity: PAR proteins and the cytoskeleton. Dev. Camb. Engl. 138, 799–809. https://doi.org/10.1242/dev.053538

Nguyen, C.T., Nguyen, V.M., Jeong, S., 2022. Regulation of Off-track bidirectional signaling by Semaphorin-1a and Wnt signaling in the Drosophila motor axon guidance. Insect Biochem. Mol. Biol. 150, 103857. https://doi.org/10.1016/j.ibmb.2022.103857

Nieto, M.A., Huang, R.Y.-J., Jackson, R.A., Thiery, J.P., 2016. EMT: 2016. Cell 166, 21–45. https://doi.org/10.1016/j.cell.2016.06.028

Nishimura, G., Manabe, I., Tsushima, K., Fujiu, K., Oishi, Y., Imai, Y., Maemura, K., Miyagishi, M., Higashi, Y., Kondoh, H., Nagai, R., 2006. δEF1 Mediates TGF-β Signaling in Vascular Smooth Muscle Cell Differentiation. Dev. Cell 11, 93–104. https://doi.org/10.1016/j.devcel.2006.05.011

Niwa, Y., Shimojo, H., Isomura, A., González, A., Miyachi, H., Kageyama, R., 2011. Different types of oscillations in Notch and Fgf signaling regulate the spatiotemporal periodicity of somitogenesis. Genes Dev. 25, 1115–1120. https://doi.org/10.1101/gad.2035311

O'Brien, L.E., Jou, T.-S., Pollack, A.L., Zhang, Q., Hansen, S.H., Yurchenco, P., Mostov, K.E., 2001. Rac1 orientates epithelial apical polarity through effects on basolateral laminin assembly. Nat. Cell Biol. 3, 831–838. https://doi.org/10.1038/ncb0901-831

Ocaña, O.H., Córcoles, R., Fabra, Á., Moreno-Bueno, G., Acloque, H., Vega, S., Barrallo-Gimeno, A., Cano, A., Nieto, M.A., 2012. Metastatic Colonization Requires the Repression of the Epithelial-Mesenchymal Transition Inducer Prrx1. Cancer Cell 22, 709–724. https://doi.org/10.1016/j.ccr.2012.10.012

Ooshio, T., Irie, K., Morimoto, K., Fukuhara, A., Imai, T., Takai, Y., 2004. Involvement of LMO7 in the Association of Two Cell-Cell Adhesion Molecules, Nectin and E-cadherin, through Afadin and α-Actinin in Epithelial Cells*. J. Biol. Chem. 279, 31365–31373. https://doi.org/10.1074/jbc.M401957200

Page-McCaw, A., Ewald, A.J., Werb, Z., 2007. Matrix metalloproteinases and the regulation of tissue remodelling. Nat. Rev. Mol. Cell Biol. 8, 221–233. https://doi.org/10.1038/nrm2125

Pascoe, H.G., Wang, Y., Zhang, X., 2015. Structural mechanisms of plexin signaling. Prog. Biophys. Mol. Biol. 118, 161–168. https://doi.org/10.1016/j.pbiomolbio.2015.03.006

Patel, N.H., Snow, P.M., Goodman, C.S., 1987. Characterization and cloning of fasciclin III: A glycoprotein expressed on a subset of neurons and axon pathways in Drosophila. Cell 48, 975–988. https://doi.org/10.1016/0092-8674(87)90706-9

Pei, D., Shu, X., Gassama-Diagne, A., Thiery, J.P., 2019. Mesenchymal–epithelial transition in development and reprogramming. Nat. Cell Biol. 21, 44–53. https://doi.org/10.1038/s41556-018-0195-z

Peradziryi, H., Kaplan, N.A., Podleschny, M., Liu, X., Wehner, P., Borchers, A., Tolwinski, N.S., 2011. PTK7/Otk interacts with Wnts and inhibits canonical Wnt signalling: PTK7/Otk interacts with Wnts. EMBO J. 30, 3729–3740. https://doi.org/10.1038/emboj.2011.236

Perez, T.D., Nelson, W.J., 2004. Cadherin Adhesion: Mechanisms and Molecular Interactions. Handb. Exp. Pharmacol. 3–21. https://doi.org/10.1007/978-3-540-68170-0_1

Pert, M., Gan, M., Saint, R., Murray, M.J., 2015. Netrins and Frazzled/DCC promote the migration and mesenchymal to epithelial transition of *Drosophila* midgut cells. Biol. Open 4, 233–243. https://doi.org/10.1242/bio.201410827

Piontek, J., Krug, S.M., Protze, J., Krause, G., Fromm, M., 2020. Molecular architecture and assembly of the tight junction backbone. Biochim. Biophys. Acta BBA - Biomembr. 1862, 183279. https://doi.org/10.1016/j.bbamem.2020.183279

Pitsidianaki, I., Morgan, J., Adams, J., Campbell, K., 2021. Mesenchymal-to-epithelial transitions require tissue-specific interactions with distinct laminins. J. Cell Biol. 220, e202010154. https://doi.org/10.1083/jcb.202010154

Plygawko, A.T., Kan, S., Campbell, K., 2020. Epithelial–mesenchymal plasticity: emerging parallels between tissue morphogenesis and cancer metastasis. Philos. Trans. R. Soc. B Biol. Sci. 375, 20200087. https://doi.org/10.1098/rstb.2020.0087

Plygawko, A.T., Stephan-Otto Attolini, C., Pitsidianaki, I., Cook, D., Darby, A.C., Campbell, K., 2024. Drosophila intestinal stem cells arise through asymmetric divisions of neuroblast-like cells. Manuscript in submission.

Qiu, R.-G., Abo, A., Martin, G.S., 2000. A human homolog of the C. elegans polarity determinant Par-6 links Rac and Cdc42 to PKCζ signaling and cell transformation. Curr. Biol. 10, 697–707. https://doi.org/10.1016/S0960-9822(00)00535-2

R Core Team, 2021. R: The R Project for Statistical Computing.

Radisky, E.S., Radisky, D.C., 2010. Matrix Metalloproteinase-Induced Epithelial-Mesenchymal Transition in Breast Cancer. J. Mammary Gland Biol. Neoplasia 15, 201–212. https://doi.org/10.1007/s10911-010-9177-x

Razinia, Z., Mäkelä, T., Ylänne, J., Calderwood, D.A., 2012. Filamins in Mechanosensing and Signaling. Annu. Rev. Biophys. 41, 227–246. https://doi.org/10.1146/annurev-biophys-050511-102252

Reiche, J., Huber, O., 2020. Post-translational modifications of tight junction transmembrane proteins and their direct effect on barrier function. Biochim. Biophys. Acta BBA - Biomembr. 1862, 183330. https://doi.org/10.1016/j.bbamem.2020.183330

Reuter, R., Grunewald, B., Leptin, M., 1993. A role for the mesoderm in endodermal migration and morphogenesis in *Drosophila*. Development 119, 1135–1145. https://doi.org/10.1242/dev.119.4.1135

Reversi, A., Loeser, E., Subramanian, D., Schultz, C., De Renzis, S., 2014. Plasma membrane phosphoinositide balance regulates cell shape during Drosophila embryo morphogenesis. J. Cell Biol. 205, 395–408. https://doi.org/10.1083/jcb.201309079

Riese, J., Tremml, G., Bienz, M., 1997. *D-Fos* , a target gene of Decapentaplegic signalling with a critical role during *Drosophila* endoderm induction. Development 124, 3353–3361. https://doi.org/10.1242/dev.124.17.3353

Rodgers, L.S., Beam, M.T., Anderson, J.M., Fanning, A.S., 2013. Epithelial barrier assembly requires coordinated activity of multiple domains of the tight junction protein ZO-1. J. Cell Sci. 126, 1565–1575. https://doi.org/10.1242/jcs.113399

Rowton, M., Ramos, P., Anderson, D.M., Rhee, J.M., Cunliffe, H.E., Rawls, A., 2013. Regulation of mesenchymal-to-epithelial transition by PARAXIS during somitogenesis: Met Regulation by Paraxis. Dev. Dyn. 242, 1332–1344. https://doi.org/10.1002/dvdy.24033

Rozbesky, D., Monistrol, J., Jain, V., Hillier, J., Padilla-Parra, S., Jones, E.Y., 2020. Drosophila OTK Is a Glycosaminoglycan-Binding Protein with High Conformational Flexibility. Structure 28, 507-515.e5. https://doi.org/10.1016/j.str.2020.02.008

Saitou, M., Fujimoto, K., Doi, Y., Itoh, M., Fujimoto, T., Furuse, M., Takano, H., Noda, T., Tsukita, S., 1998. Occludin-deficient embryonic stem cells can differentiate into polarized epithelial cells bearing tight junctions. J. Cell Biol. 141, 397–408. https://doi.org/10.1083/jcb.141.2.397

Sanchez, A.D., Branon, T.C., Cote, L.E., Papagiannakis, A., Liang, X., Pickett, M.A., Shen, K., Jacobs-Wagner, C., Ting, A.Y., Feldman, J.L., 2021. Proximity labeling reveals non-centrosomal microtubule-organizing center components required for microtubule growth and localization. Curr. Biol. 31, 3586-3600.e11. https://doi.org/10.1016/j.cub.2021.06.021

Sanchez, A.D., Feldman, J.L., 2017. Microtubule-organizing centers: from the centrosome to non-centrosomal sites. Curr. Opin. Cell Biol. 44, 93–101. https://doi.org/10.1016/j.ceb.2016.09.003

Sato, T., Fujita, N., Yamada, A., Ooshio, T., Okamoto, R., Irie, K., Takai, Y., 2006. Regulation of the assembly and adhesion activity of E-cadherin by nectin and afadin for the formation of adherens junctions in Madin-Darby canine kidney cells. J. Biol. Chem. 281, 5288–5299. https://doi.org/10.1074/jbc.M510070200

Saxena, K., Jolly, M.K., Balamurugan, K., 2020. Hypoxia, partial EMT and collective migration: Emerging culprits in metastasis. Transl. Oncol. 13, 100845. https://doi.org/10.1016/j.tranon.2020.100845

Scarpa, E., Mayor, R., 2016. Collective cell migration in development. J. Cell Biol. 212, 143–155. https://doi.org/10.1083/jcb.201508047

Schmidt, C., Stoeckelhuber, M., McKinnell, I., Putz, R., Christ, B., Patel, K., 2004. Wnt 6 regulates the epithelialisation process of the segmental plate mesoderm leading to somite formation. Dev. Biol. 271, 198–209. https://doi.org/10.1016/j.ydbio.2004.03.016

Schmidt, U., Weigert, M., Broaddus, C., Myers, G., 2018. Cell Detection with Star-Convex Polygons, in: Frangi, A.F., Schnabel, J.A., Davatzikos, C., Alberola-López, C., Fichtinger, G. (Eds.), Medical Image Computing and Computer Assisted Intervention – MICCAI 2018, Lecture Notes in Computer Science. Springer International Publishing, Cham, pp. 265–273. https://doi.org/10.1007/978-3-030-00934-2_30

Scott, L.E., Weinberg, S.H., Lemmon, C.A., 2019. Mechanochemical Signaling of the Extracellular Matrix in Epithelial-Mesenchymal Transition. Front. Cell Dev. Biol. 7.

Secchia, S., Forneris, M., Heinen, T., Stegle, O., Furlong, E.E.M., 2022. Simultaneous cellular and molecular phenotyping of embryonic mutants using single-cell regulatory trajectories. Dev. Cell 57, 496-511.e8. https://doi.org/10.1016/j.devcel.2022.01.016

Self, M., Lagutin, O.V., Bowling, B., Hendrix, J., Cai, Y., Dressler, G.R., Oliver, G., 2006. Six2 is required for suppression of nephrogenesis and progenitor renewal in the developing kidney. EMBO J. 25, 5214–5228. https://doi.org/10.1038/sj.emboj.7601381

Shaw, T.J., Martin, P., 2016. Wound repair: a showcase for cell plasticity and migration. Curr. Opin. Cell Biol. 42, 29–37. https://doi.org/10.1016/j.ceb.2016.04.001

Shibue, T., Weinberg, R.A., 2017. EMT, CSCs, and drug resistance: the mechanistic link and clinical implications. Nat. Rev. Clin. Oncol. 14, 611–629. https://doi.org/10.1038/nrclinonc.2017.44

Shirinian, M., Varshney, G., Lorén, C.E., Grabbe, C., Palmer, R.H., 2007. Drosophila Anaplastic Lymphoma Kinase regulates Dpp signalling in the developing embryonic gut. Differentiation 75, 418–426. https://doi.org/10.1111/j.1432-0436.2006.00148.x

Shtutman, M., Levina, E., Ohouo, P., Baig, M., Roninson, I.B., 2006. Cell adhesion molecule L1 disrupts E-cadherin-containing adherens junctions and increases scattering and motility of MCF7 breast carcinoma cells. Cancer Res. 66, 11370–11380. https://doi.org/10.1158/0008-5472.CAN-06-2106

Signorell, A., Aho, K., Alfons, A., Anderegg, N., Aragon, T., Arachchige, C., Arppe, A., Baddeley, A., Barton, K., Bolker, B., Borchers, H.W., Caeiro, F., Champely, S., Chessel, D., Chhay, L., Cooper, N., Cummins, C., Dewey, M., Doran, H.C., Dray, S., Dupont, C., Eddelbuettel, D., Ekstrom, C., Elff, M., Enos, J., Farebrother, R.W., Fox, J., Francois, R., Friendly, M., Galili, T., Gamer, M., Gastwirth, J.L., Gegzna, V., Gel, Y.R., Graber, S., Gross, J., Grothendieck, G., Jr, F.E.H., Heiberger, R., Hoehle, M., Hoffmann, C.W., Hojsgaard, S., Hothorn, T., Huerzeler, M., Hui, W.W., Hurd, P., Hyndman, R.J., Jackson, C., Kohl, M., Korpela, M., Kuhn, M., Labes, D., Leisch, F., Lemon, J., Li, D., Maechler, M., Magnusson, A., Mainwaring, B., Malter, D., Marsaglia, G., Marsaglia, J., Matei, A., Meyer, D., Miao, W., Millo, G., Min, Y., Mitchell, D., Mueller, F., Naepflin, M., Navarro, D., Nilsson, H., Nordhausen, K., Ogle, D., Ooi, H., Parsons, N., Pavoine, S., Plate, T., Prendergast, L., Rapold, R., Revelle, W., Rinker, T., Ripley, B.D., Rodriguez, C., Russell, N., Sabbe, N., Scherer, R., Seshan, V.E., Smithson, M., Snow, G., Soetaert, K., Stahel, W.A., Stephenson, A., Stevenson, M., Stubner, R., Templ, M., Lang, D.T., Therneau, T., Tille, Y., Torgo, L., Trapletti, A., Ulrich, J., Ushey, K., VanDerWal, J., Venables, B., Verzani, J., Iglesias, P.J.V., Warnes, G.R., Wellek, S., Wickham, H., Wilcox, R.R., Wolf, P., Wollschlaeger, D., Wood, J., Wu, Y., Yee, T., Zeileis, A., 2023. DescTools: Tools for Descriptive Statistics.

Stark, K., Vainio, S., Vassileva, G., McMahon, A.P., 1994. Epithelial transformation of metanephric mesenchyme in the developing kidney regulated by Wnt-4. Nature 372, 679–683. https://doi.org/10.1038/372679a0

Stedden, C.G., Menegas, W., Zajac, A.L., Williams, A.M., Cheng, S., Özkan, E., Horne-Badovinac, S., 2019. Planar-Polarized Semaphorin-5c and Plexin A Promote the Collective Migration of Epithelial Cells in Drosophila. Curr. Biol. 29, 908-920.e6. https://doi.org/10.1016/j.cub.2019.01.049

Stemmler, M.P., Eccles, R.L., Brabletz, S., Brabletz, T., 2019. Non-redundant functions of EMT transcription factors. Nat. Cell Biol. 21, 102–112. https://doi.org/10.1038/s41556-018-0196-y

Stringer, C., Wang, T., Michaelos, M., Pachitariu, M., 2021. Cellpose: a generalist algorithm for cellular segmentation. Nat. Methods 18, 100–106. https://doi.org/10.1038/s41592-020-01018-x

Takagi, T., Moribe, H., Kondoh, H., Higashi, Y., 1998. δEF1, a zinc finger and homeodomain transcription factor, is required for skeleton patterning in multiple lineages. Development 125, 21–31. https://doi.org/10.1242/dev.125.1.21

Takahashi, Y., Sato, Y., Suetsugu, R., Nakaya, Y., 2005. Mesenchymal-to-Epithelial Transition during Somitic Segmentation: A Novel Approach to Studying the Roles of Rho Family GTPases in Morphogenesis. Cells Tissues Organs 179, 36–42. https://doi.org/10.1159/000084507

Takekuni, K., Ikeda, W., Fujito, T., Morimoto, K., Takeuchi, M., Monden, M., Takai, Y., 2003. Direct Binding of Cell Polarity Protein PAR-3 to Cell-Cell Adhesion Molecule Nectin at Neuroepithelial Cells of Developing Mouse*. J. Biol. Chem. 278, 5497–5500. https://doi.org/10.1074/jbc.C200707200

Tanentzapf, G., Smith, C., McGlade, J., Tepass, U., 2000. Apical, Lateral, and Basal Polarization Cues Contribute to the Development of the Follicular Epithelium during Drosophila Oogenesis. J. Cell Biol. 151, 891–904. https://doi.org/10.1083/jcb.151.4.891

Tepass, U., 1996. Crumbs, a Component of the Apical Membrane, Is Required for Zonula Adherens Formation in Primary Epithelia ofDrosophila. Dev. Biol. 177, 217–225. https://doi.org/10.1006/dbio.1996.0157

Tepass, U., Hartenstein, V., 1995. Neurogenic and proneural genes control cell fate specification in the *Drosophila* endoderm. Development 121, 393–405. https://doi.org/10.1242/dev.121.2.393

Tepass, U., Hartenstein, V., 1994a. The Development of Cellular Junctions in the Drosophila Embryo. Dev. Biol. 161, 563–596. https://doi.org/10.1006/dbio.1994.1054

Tepass, U., Hartenstein, V., 1994b. Epithelium formation in the *Drosophila* midgut depends on the interaction of endoderm and mesoderm. Development 120, 579–590. https://doi.org/10.1242/dev.120.3.579

Tepass, U., Knust, E., 1993. crumbs and stardust Act in a Genetic Pathway That Controls the Organization of Epithelia in Drosophila melanogaster. Dev. Biol. 159, 311–326. https://doi.org/10.1006/dbio.1993.1243

Theveneau, E., Mayor, R., 2012. Neural crest delamination and migration: From epithelium-to-mesenchyme transition to collective cell migration. Dev. Biol., Neural Crest 366, 34–54. https://doi.org/10.1016/j.ydbio.2011.12.041

Thiery, J.P., Acloque, H., Huang, R.Y.J., Nieto, M.A., 2009. Epithelial-Mesenchymal Transitions in Development and Disease. Cell 139, 871–890. https://doi.org/10.1016/j.cell.2009.11.007

Tomancak, P., Beaton, A., Weiszmann, R., Kwan, E., Shu, S., Lewis, S.E., Richards, S., Ashburner, M., Hartenstein, V., Celniker, S.E., Rubin, G.M., 2002. Systematic determination of patterns of gene expression during Drosophila embryogenesis. Genome Biol. 3, research0088.1. https://doi.org/10.1186/gb-2002-3-12-research0088

Tomancak, P., Berman, B.P., Beaton, A., Weiszmann, R., Kwan, E., Hartenstein, V., Celniker, S.E., Rubin, G.M., 2007. Global analysis of patterns of gene expression during

Drosophilaembryogenesis. Genome Biol. 8, R145. https://doi.org/10.1186/gb-2007-8-7-r145

Tosi, S., Campbell, K., 2019. 3D Tracking of Migrating Cells from Live Microscopy Time-Lapses, in: Rebollo, E., Bosch, M. (Eds.), Computer Optimized Microscopy, Methods in Molecular Biology. Springer New York, New York, NY, pp. 385–395. https://doi.org/10.1007/978-1-4939-9686-5_18

Tran, H.D., Luitel, K., Kim, M., Zhang, K., Longmore, G.D., Tran, D.D., 2014. Transient SNAIL1 Expression Is Necessary for Metastatic Competence in Breast Cancer. Cancer Res. 74, 6330–6340. https://doi.org/10.1158/0008-5472.CAN-14-0923

Trapnell, C., Cacchiarelli, D., Grimsby, J., Pokharel, P., Li, S., Morse, M., Lennon, N.J., Livak, K.J., Mikkelsen, T.S., Rinn, J.L., 2014. The dynamics and regulators of cell fate decisions are revealed by pseudotemporal ordering of single cells. Nat. Biotechnol. 32, 381–386. https://doi.org/10.1038/nbt.2859

Tsai, J.H., Donaher, J.L., Murphy, D.A., Chau, S., Yang, J., 2012. Spatiotemporal Regulation of Epithelial-Mesenchymal Transition Is Essential for Squamous Cell Carcinoma Metastasis. Cancer Cell 22, 725–736. https://doi.org/10.1016/j.ccr.2012.09.022

Upadhyay, A., Moss-Taylor, L., Kim, M.-J., Ghosh, A.C., O'Connor, M.B., 2017. TGF-β Family Signaling in Drosophila. Cold Spring Harb. Perspect. Biol. 9, a022152. https://doi.org/10.1101/cshperspect.a022152

Urbano, J.M., Domínguez-Giménez, P., Estrada, B., Martín-Bermudo, M.D., 2011. PS Integrins and Laminins: Key Regulators of Cell Migration during Drosophila Embryogenesis. PLoS ONE 6, e23893. https://doi.org/10.1371/journal.pone.0023893

Urbano, J.M., Torgler, C.N., Molnar, C., Tepass, U., López-Varea, A., Brown, N.H., De Celis, J.F., Martín-Bermudo, M.D., 2009. *Drosophila* laminins act as key regulators of basement membrane assembly and morphogenesis. Development 136, 4165–4176. https://doi.org/10.1242/dev.044263

Vasioukhin, V., Bauer, C., Yin, M., Fuchs, E., 2000. Directed Actin Polymerization Is the Driving Force for Epithelial Cell–Cell Adhesion. Cell 100, 209–219. https://doi.org/10.1016/S0092-8674(00)81559-7

Venken, K.J.T., Schulze, K.L., Haelterman, N.A., Pan, H., He, Y., Evans-Holm, M., Carlson, J.W., Levis, R.W., Spradling, A.C., Hoskins, R.A., Bellen, H.J., 2011. MiMIC: a highly versatile transposon insertion resource for engineering Drosophila melanogaster genes. Nat. Methods 8, 737–743. https://doi.org/10.1038/nmeth.1662

Walko, G., Castañón, M.J., Wiche, G., 2015. Molecular architecture and function of the hemidesmosome. Cell Tissue Res. 360, 529–544. https://doi.org/10.1007/s00441-015-2216-6

Wang, C.-A., Drasin, D., Pham, C., Jedlicka, P., Zaberezhnyy, V., Guney, M., Li, H., Nemenoff, R., Costello, J.C., Tan, A.-C., Ford, H.L., 2014. Homeoprotein Six2 Promotes Breast Cancer Metastasis via Transcriptional and Epigenetic Control of E-Cadherin Expression. Cancer Res. 74, 7357–7370. https://doi.org/10.1158/0008-5472.CAN-14-0666

Wang, H., Luo, X., Leighton, J., 2015. Extracellular Matrix and Integrins in Embryonic Stem Cell Differentiation. Biochem. Insights 8, 15–21. https://doi.org/10.4137/BCI.S30377

Wang, X., Dong, B., Zhang, K., Ji, Z., Cheng, C., Zhao, H., Sheng, Y., Li, X., Fan, L., Xue, W., Gao, W.-Q., Zhu, H.H., 2018. E-cadherin bridges cell polarity and spindle orientation to ensure prostate epithelial integrity and prevent carcinogenesis in vivo. PLoS Genet. 14, e1007609. https://doi.org/10.1371/journal.pgen.1007609

Weng, M., Wieschaus, E., 2016. Myosin-dependent remodeling of adherens junctions protects junctions from Snail-dependent disassembly. J. Cell Biol. 212, 219–229. https://doi.org/10.1083/jcb.201508056

Whiteman, E., Liu, C.-J., Fearon, E., Margolis, B., 2008. The transcription factor snail represses Crumbs3 expression and disrupts apico-basal polarity complexes. Oncogene 27, 3875–3879. https://doi.org/doi:10.1038/onc.2008.9

Wickham H, 2016. ggplot2: Elegant Graphics for Data Analysis. Springer-Verlag New York.

Williams, E., Villar-Prados, A., Bowser, J., Broaddus, R., Gladden, A.B., 2017. Loss of polarity alters proliferation and differentiation in low-grade endometrial cancers by disrupting Notch signaling. PLOS ONE 12, e0189081. https://doi.org/10.1371/journal.pone.0189081

Williams, E.D., Gao, D., Redfern, A., Thompson, E.W., 2019. Controversies around epithelial–mesenchymal plasticity in cancer metastasis. Nat. Rev. Cancer 19, 716–732. https://doi.org/10.1038/s41568-019-0213-x

Winberg, M.L., Noordermeer, J.N., Tamagnone, L., Comoglio, P.M., Spriggs, M.K., Tessier-Lavigne, M., Goodman, C.S., 1998. Plexin A is a neuronal semaphorin receptor that controls axon guidance. Cell 95, 903–916. https://doi.org/10.1016/s0092-8674(00)81715-8

Wolfstetter, G., Shirinian, M., Stute, C., Grabbe, C., Hummel, T., Baumgartner, S., Palmer, R.H., Holz, A., 2009. Fusion of circular and longitudinal muscles in Drosophila is independent of the endoderm but further visceral muscle differentiation requires a close contact between mesoderm and endoderm. Mech. Dev. 126, 721–736. https://doi.org/10.1016/j.mod.2009.05.001

Wu, S.-Y., McClay, D.R., 2007. The Snail repressor is required for PMC ingression in the sea urchin embryo. Development 134, 1061–1070. https://doi.org/10.1242/dev.02805

Yalim-Camci, I., Balcik-Ercin, P., Cetin, M., Odabas, G., Tokay, N., Sayan, A.E., Yagci, T., 2019. ETS1 is coexpressed with ZEB2 and mediates ZEB2-induced epithelial-mesenchymal transition in human tumors. Mol. Carcinog. 58, 1068–1081. https://doi.org/10.1002/mc.22994

Yamada, S., Pokutta, S., Drees, F., Weis, W.I., Nelson, W.J., 2005. Deconstructing the Cadherin-Catenin-Actin Complex. Cell 123, 889–901. https://doi.org/10.1016/j.cell.2005.09.020

Yanagihashi, Y., Usui, T., Izumi, Y., Yonemura, S., Sumida, M., Tsukita, S., Uemura, T., Furuse, M., 2012. Snakeskin, a membrane protein associated with smooth septate junctions, is required for intestinal barrier function in Drosophila. J. Cell Sci. 125, 1980–1990. https://doi.org/10.1242/jcs.096800

Yang, J., Antin, P., Berx, G., Blanpain, C., Brabletz, T., Bronner, M., Campbell, K., Cano, A., Casanova, J., Christofori, G., Dedhar, S., Derynck, R., Ford, H.L., Fuxe, J., García de Herreros, A., Goodall, G.J., Hadjantonakis, A.-K., Huang, R.Y.J., Kalcheim, C., Kalluri, R., Kang, Y., Khew-Goodall, Y., Levine, H., Liu, J., Longmore, G.D., Mani, S.A., Massagué, J., Mayor, R., McClay, D., Mostov, K.E., Newgreen, D.F., Nieto, M.A., Puisieux, A., Runyan, R., Savagner, P., Stanger, B., Stemmler, M.P., Takahashi, Y., Takeichi, M., Theveneau, E., Thiery, J.P., Thompson, E.W., Weinberg, R.A., Williams, E.D., Xing, J., Zhou, B.P., Sheng, G., On behalf of the EMT International Association (TEMTIA), 2020. Guidelines and definitions for research on epithelial–mesenchymal transition. Nat. Rev. Mol. Cell Biol. 21, 341–352. https://doi.org/10.1038/s41580-020-0237-9

Yang, J., Mani, S.A., Donaher, J.L., Ramaswamy, S., Itzykson, R.A., Come, C., Savagner, P., Gitelman, I., Richardson, A., Weinberg, R.A., 2004. Twist, a Master Regulator of Morphogenesis, Plays an Essential Role in Tumor Metastasis. Cell 117, 927–939. https://doi.org/10.1016/j.cell.2004.06.006

Yang, X., Zhu, L.-C., Wang, Y.-J., Li, Y.-Y., Wang, D., 2019. Current Advance of Therapeutic Agents in Clinical Trials Potentially Targeting Tumor Plasticity. Front. Oncol. 9, 887. https://doi.org/10.3389/fonc.2019.00887

Yang, Z., Zimmerman, S., Brakeman, P.R., Beaudoin, G.M., Reichardt, L.F., Marciano, D.K., 2013. *De novo* lumen formation and elongation in the developing nephron: a central role for afadin in apical polarity. Development 140, 1774–1784. https://doi.org/10.1242/dev.087957

Yano, T., Torisawa, T., Oiwa, K., Tsukita, S., 2018. AMPK-dependent phosphorylation of cingulin reversibly regulates its binding to actin filaments and microtubules. Sci. Rep. 8, 15550. https://doi.org/10.1038/s41598-018-33418-7

Yip, M.L.R., Lamka, M.L., Lipshitz, H.D., 1997. Control of germ-band retraction in *Drosophila* by the zinc-finger protein HINDSIGHT. Development 124, 2129–2141. https://doi.org/10.1242/dev.124.11.2129

Yokoyama, S., Tachibana, K., Nakanishi, H., Yamamoto, Y., Irie, K., Mandai, K., Nagafuchi, A., Monden, M., Takai, Y., 2001. alpha-catenin-independent recruitment of ZO-1 to nectin-based cell-cell adhesion sites through afadin. Mol. Biol. Cell 12, 1595–1609. https://doi.org/10.1091/mbc.12.6.1595

Yu, H.-H., Araj, H.H., Ralls, S.A., Kolodkin, A.L., 1998. The Transmembrane Semaphorin Sema I Is Required in Drosophila for Embryonic Motor and CNS Axon Guidance. Neuron 20, 207–220. https://doi.org/10.1016/S0896-6273(00)80450-X

Yu, H.-H., Kolodkin, A.L., 1999. Semaphorin Signaling: A Little Less Per-Plexin. Neuron 22, 11–14. https://doi.org/10.1016/S0896-6273(00)80672-8

Yu, W., Datta, A., Leroy, P., O'Brien, L.E., Mak, G., Jou, T.-S., Matlin, K.S., Mostov, K.E., Zegers, M.M.P., 2005. β1-Integrin Orients Epithelial Polarity via Rac1 and Laminin. Mol. Biol. Cell 16, 433–445. https://doi.org/10.1091/mbc.e04-05-0435

Zaffran, S., Küchler, A., Lee, H.-H., Frasch, M., 2001. *biniou* (*FoxF*), a central component in a regulatory network controlling visceral mesoderm development and midgut morphogenesis in *Drosophila*. Genes Dev. 15, 2900–2915. https://doi.org/10.1101/gad.917101